UNIVERSITÀ DEGLI STUDI DI TORINO

Department of Life Sciences and Systems Biology

PhD Programme in Experimental Medicine and Therapy

XXXV° Cycle

TARGETING VIRUSES USING A NOVEL *h*DHODH INHIBITOR

Thesis' author: Giulia Sibille   Supervisors: Dr. Paola Costelli

Dr. Anna Luganini

PhD Programme Coordinator: Dr. Pasquale Pagliaro

Academic Years of enrolment 2019-2023

Code of scientific discipline: BIO-19 (general microbiology)

UNIVERSITÀ DEGLI STUDI DI TORINO

Department of Life Sciences and Systems Biology

PhD Programme in Experimental Medicine and Therapy

XXXV° Cycle

TARGETING VIRUSES USING A NOVEL *h*DHODH INHIBITOR

Thesis' author: Giulia Sibille

Supervisors: Dr. Paola Costelli

Dr. Anna Luganini

PhD Programme Coordinator: Dr. Pasquale Pagliaro

Academic Years of enrolment 2019-2023

Code of scientific discipline: BIO-19 (general microbiology)

TABLE OF CONTENTS

1. INTRODUCTION

1.1 Viruses: a worldwide problem

In recent years, there has been a significant increase in the emergence of emerging or re-emerging viruses, representing a growing threat to public health security and causing substantial global economic losses. Currently, the World Health Organization (WHO) has declared six international public health emergencies, including the H1N1 Influenza pandemic in 2009, the Polio epidemic in 2014, the Ebola epidemic in West Africa in 2014, the Zika epidemic in 2015-2016, the Ebola epidemic in the Democratic Republic of Congo (announced in July 2019, but began in 2018), and the pandemic of Severe Acute Respiratory Syndrome Coronavirus 2 (SARS-CoV-2) pneumonia that began at the end of 2019 (WHO; Sepulveda *et al.* 2022; Zheng *et al.* 2022).

In particular, this latest pandemic has had a profound impact on cultures, economies, and healthcare systems worldwide. The devastating impact of the COVID-19 pandemic, the exponential increase in cases and mortality rates related to SARS-CoV-2, has exposed vulnerabilities in public health infrastructure, revealing deficiencies in pandemic preparedness and international collaboration. The unprecedented scale of the pandemic has overwhelmed healthcare systems, resulting in shortages of essential medical supplies, hospital beds, and personnel. Furthermore, the economic and social disruptions caused by the pandemic underscore the need for effective strategies to curb the spread of infectious diseases and ensure rapid and equitable vaccine distribution. The emergence of new viral variants, often with increased transmissibility or immune system evasion capabilities, has added another layer of complexity to the issue. The constant evolution of SARS-CoV-2, and indeed all viruses, poses ongoing challenges in vaccine development and public health maintenance. This underscores the need for continuous research, surveillance, and collaboration among scientists, healthcare professionals, and governments to keep up with viral mutations (WHO; Chitalia *et al.* 2020; Xiong *et al.* 2020)

Previous epidemics like SARS and MERS demonstrated that SARS-CoV-2 was not the first zoonotic coronavirus capable of infecting humans, and it likely won't be the last. Viral zoonotic diseases originating from wildlife could pose the most significant future threat to global public health, given that 75% of known human viruses to date (e.g., rabies, yellow fever, HIV, Ebola, SARS coronaviruses, MERS, and SARS-CoV-2, Influenza) are derived from animals, and 60% of emerging diseases have been transmitted by wildlife (Taveira 2023; Chitalia *et al.* 2020).

The 2019-2020 pandemic serves as a tangible example of the far-reaching consequences of viral outbreaks, highlighting the critical importance of robust public health systems and international collaboration (Maffei *et al.* 2022; Chitalia *et al.* 2020).

However, viruses are not just a problem during pandemics; they are a daily global concern. For instance, the Hepatitis C Virus (HCV), while now curable, still infects over 185 million people annually, leading to up to 500,000 deaths. The age-standardized incidence rate of acute hepatitis did not significantly change from 1990 to 2017, suggesting that more proactive global initiatives are important, particularly with respect to vaccine coverage and cost-effective access to hepatitis C curative treatments (GBD 2017 Disease and Injury Incidence and Prevalence Collaborators 2018).

Other viruses like the Dengue Virus (DENV) and Zika Virus (ZIKV) collectively infect approximately 390 million individuals worldwide, with 4 million cases in Brazil alone. The lack of specific antiviral drugs and vaccines for newly emerging viruses, including DENV and ZIKV, places a significant social burden on related diseases GBD 2017 Disease and Injury Incidence and Prevalence Collaborators 2018).

According to the WHO, there are some viruses that deserve a special surveillance program that provides reports every 3, 6 or 12 months based on the incidence of infection. Among these viruses, there are respiratory viruses such as Influenza Virus, Respiratory Syncytial Virus, Coronaviruses, which spread rapidly within the population, furthermore, these are also the viruses that lead to new outbreaks every few years. But not only that, among the most popular health topics the WHO also includes the Herpes Simplex Virus and the Human Immunodeficiency Virus, as they are also very widespread viruses, but have no treatments available, in particular: in the first case they were developed various antivirals, but due to the onset of resistance due to the high mutagenicity of the virus they are no longer usable; in the second case there are drugs that allow to live a good life, but they do not eliminate the infection, so the therapy can never be interrupted, these cocktails of drugs will have to be taken for the entire duration of the individual's life (WHO).

1.1.1   Respiratory Viruses

Acute infections of the upper and lower respiratory tract (RT) represent a serious public health problem and one of the leading causes of morbidity and mortality worldwide. Morbidity related to RTIs is associated with loss of productivity and medical expenses, thus generating a significant economic burden. Lower respiratory tract infections have remained the deadliest communicable infectious disease in the world, ranked as the fourth leading cause of death (WHO).

The most severe diseases develop in specific populations, including newborns, the elderly, chronically ill individuals with underlying comorbidities (e.g., those with chronic heart or lung diseases, diabetes, kidney or liver diseases, or blood disorders), malnourished individuals, and those with compromised immune systems. In immunocompromised individuals, respiratory viruses seem to be acquired at the same frequency as immunocompetent individuals but are associated with prolonged infections, a higher progression to lower respiratory tract infections, and higher mortality rates. Recipients of hematopoietic stem cell transplants (HSCT) and solid organ transplants (SOT) receiving immunosuppressive drugs, immunosuppressed cancer patients on chemotherapy, children with primary immunodeficiencies, and individuals infected with the Human Immunodeficiency Virus (HIV) are particularly vulnerable to severe and sometimes fatal infections with common respiratory viruses. The progression of respiratory disease from the upper to the lower respiratory tract can occur in 5% to 50% of patients receiving chemotherapy for leukemia or undergoing HSCT, with mortality rates that can reach 10% to 50% (Hodinka 2016).

Each year in the United States, nearly 29 to 59 million people contract Influenza virus infections; over 200,000 are hospitalized, and about 36,000 die. In addition, nearly 500 million people in the United States experience two or more non-Influenza viral respiratory tract infections each year. The economic burden of these annual Influenza epidemics and non-Influenza viral respiratory tract infections approaches $87.1 billion and $40 billion, respectively (Hodinka 2016; Cheung *et al.* 2017).

The definite diagnosis of viral respiratory tract infection is not straightforward, as the signs and symptoms are often very similar, not specific to a particular virus, so a laboratory test is required, incurring additional costs for global healthcare. Infections can also vary in severity, from simple colds and sore throats to more severe laryngeal and tracheobronchial infections, bronchiolitis, and full-blown pneumonia. Common complications can include secondary bacterial infections leading to otitis media, sinusitis, or pneumonia. Each virus has a predilection for specific parts of the respiratory tract, and while some viruses are often associated with specific syndromes, each virus can cause a variety of respiratory illnesses, and each syndrome can be caused by more than one respiratory virus. Lower respiratory tract infections account for most hospitalizations for infectious diseases, constituting 34% of the 4.5 million bed-days attributed to a primary diagnosis of infectious disease every year (Hodinka 2016; Cheung *et al.* 2017).

The common viruses that cause most RTIs include Influenza A Virus (IAV), Influenza B Virus (IBV), Coronaviruses (CoV), Respiratory Syncytial Virus (RSV), human Rhinovirus (HRV), and some Enteroviruses, such as Enterovirus A71 (EV-A71) (WHO).

European Centre for Disease Prevention and Control (ECDC) and WHO Regional Office for Europe have jointly developed the European Respiratory Virus Surveillance Summary (ERVISS), an interactive surveillance data dashboard for Influenza, Respiratory Syncytial Virus (RSV), and Severe Acute Respiratory Syndrome Coronavirus 2 (SARS-CoV-2) that also features a weekly epidemiological summary. The primary aim of the platform is to serve as a tool for the early detection and communication of signals of respiratory virus circulation in the EU/EEA and WHO European region. (ECDC; WHO)

1.1.1.1 Coronavirus

Among the respiratory viruses, it must be included coronaviruses, belonging to the family of enveloped, positive-sense, single-stranded RNA viruses. There are seven known coronaviruses that can infect humans. CoV-229E and NL63 belong to the Alphacoronavirus genus, while OC43, HKU1, SARS-CoV-1 and SARS-CoV-2 and Middle East Respiratory Syndrome (MERS)-CoV are part of the β-Coronavirus genus (Hodinka 2016; Haake *et al.* 2020).

All coronaviruses have a distinctive appearance with petal- or club-shaped spikes on their surface, giving them the appearance of a solar corona or crown. The Coronavirus RNA genome encodes two nonstructural replicase polyproteins and four structural proteins, including spike (S), envelope (E), membrane (M) glycoproteins, and the nucleocapsid (N) protein. β-Coronaviruses also possess a fifth structural protein known as hemagglutinin esterase (HE), which is responsible for binding to and cleaving neuraminic acid on the host cell surface (Hodinka 2016; Haake *et al.* 2020).

The S protein is responsible for binding to receptors on the host cell, while E and M are integral membrane proteins for virus assembly. The N protein is an internal protein that binds to viral RNA to form ribonucleoprotein complexes. The replicase polyproteins are directly translated from the viral genome and play a crucial role in viral transcription and replication (Hodinka 2016; Haake *et al.* 2020).

The symptoms of coronavirus can range from mild to severe and may appear 2 to 14 days after exposure to the virus. Common symptoms include:

1. Fever: An increase in body temperature.
2. Dry cough: A cough without mucus production.
3. Difficulty breathing: Breathing problems, such as shortness of breath or breathlessness.

4. Sore throat: Pain or irritation in the throat.

5. Sneezing and runny nose: Cold or flu-like symptoms.

6. Fatigue: Feeling tired and weak.

7. Headache: Pain in the head area.

8. Muscle or joint pain: Joint or muscle aches.

9. Loss of smell or taste: Some people report a loss of smell or taste.

10. Nasal congestion: Blocked or congested nose.

Not all infected patients have all these symptoms, and in some cases, they may be asymptomatic (without symptoms), depending on both the specific coronavirus that has infected them and the individual. For example, *h*CoV-229E primarily causes a simple cold, while SARS-CoV-2 can lead to severe symptoms, such as pneumonia, respiratory failure, and other serious problems (ECDC; WHO).

People with underlying health conditions are at greater risk when they contract COVID-19. These include individuals taking immunosuppressive medications, those with chronic heart, lung, liver, or rheumatological issues, individuals with HIV, diabetes, cancer, obesity, or dementia. People with severe illness and those requiring hospital care should receive treatment as soon as possible. Severe COVID-19 consequences include death, respiratory failure, sepsis, thromboembolism (blood clots), and multiorgan dysfunction, including heart, liver, or kidney injury. In rare situations, children can develop a severe inflammatory syndrome a few weeks after infection (ECDC; WHO).

Some individuals who have had COVID-19, whether they needed hospitalization or not, continue to experience symptoms. These long-term effects are known as long COVID (or post-COVID-19 condition). The most common symptoms associated with long COVID include fatigue, shortness of breath, and cognitive dysfunction (e.g., confusion, forgetfulness, or a lack of mental focus or clarity). Long COVID can impact a person's ability to perform daily activities like work or household tasks (ECDC; WHO).

SARS-CoV-2 has recorded a total of 771,549,718 cases worldwide, of which 6,974,473 deaths, in particular in Italy there were 26,202,253 cases with 192,210 deaths (ECDC; WHO).

Since April 2020, the Access to COVID-19 Tools (ACT) accelerator, launched by WHO and its partners, has supported the fastest, most coordinated and successful global effort in history to develop tools to fight a disease. COVAX, the vaccines pillar of ACT-Accelerator, is an innovative global collaboration to accelerate the development, production and equitable access of COVID-19 tests, treatments and vaccines.

In fact, less than 2 years after the first case of COVID-19, the first vaccines began to circulate. Some of them were obtained using the same vaccine technology currently in use, others were made using new approaches or recently used in the development of vaccines against SARS and Ebola. The aim of all these vaccines was obviously to produce an immune response in order to neutralize the virus and prevent infection of the cells. The main vaccine technology used are the following:

- inactivated viral vaccines: produced by growing the SARS-CoV-2 virus in cell cultures and chemically inactivating it (for example: Valneva vaccine);
- live attenuated vaccines: produced by generating a genetically weakened version of the virus that replicates to a limited extent, not causing disease but inducing immune responses similar to those induced by natural infection (for example: Codagenix Inc. vaccine that is ongoing Phase 3 efficacy study);
- recombinant protein vaccines: based on the spike protein, or on the receptor binding domain (RBD) or on virus-like particles (VLPs) (for example: Nuvaxovid and VidPrevtyn Beta vaccines);
- viral vector vaccines: typically based on an existing virus (usually a replication-incompetent adenovirus) that carries the genetic code sequence encoding the spike protein (for example: Astrazeneca and Johnson & Johnson vaccines);
- DNA vaccines: based on plasmids, modified to carry genes that typically code for the spike protein which is then produced in the vaccinated individual;
- RNA vaccines: based on messenger RNA (mRNA) or a self-replicating RNA that provides the genetic information for the spike protein (for example: Pfizer/BioNTech and Moderna vaccines)

Over 13 billion vaccine doses have been administered as of June 2023 (ECDC; WHO).

Thanks to vaccines, it has been possible to emerge from the state of emergency, but COVID-19 still remains a respiratory virus in the WHO surveillance program.

This is due to the limited number of FDA or EMA-approved medications now available for treatment against SARS-CoV-2; specifically, the most commonly used medications are Veklury (remdesivir), Evulshed and Paxlovid. Veklury (remdesivir) is an antiviral medicine used to treat the 2019 coronavirus (COVID-19). It is used in adults and children, from at least 4 weeks of age and weighing at least 3 kg, with pneumonia requiring supplemental oxygen (low- or high-flow oxygen or other non-invasive ventilation at the start of treatment). It's given through a needle in the skin (intravenously). The active substance, remdesivir, is a viral RNA polymerase inhibitor, so it interferes with the production of viral RNA by preventing SARS-CoV-2 from multiplying inside cells.

Paxlovid was approved as a treatment for emergencies in adult patients who do not require supplemental oxygen and who are at risk of developing the disease in a severe form (e.g., patients with oncological conditions, suffering from cardiovascular disease, uncompensated diabetes mellitus, chronic bronchopneumopathy, severe obesity). Administration is oral, in the form of two pills:

- one of nirmatrelvir, an antiviral propharmaceutical developed by Pfizer that inhibits the 3CL protease of SARS-CoV-2 by binding directly to its catalytic site and thus blocking viral replication;

- one of ritonavir, an antiviral drug that helps slow the degradation of nirmatrelvir by inhibiting the action of cytochrome P3A (CYP3A) (Pavan *et al.* 2021).

Finally, EMA approved the Evusheld, not currently authorized by FDA, a medicine used to treat COVID-19 in adults and adolescents who do not require supplemental oxygen and who are at increased risk of the disease becoming severe. This drug contains tixagevimab and cilgavimab, two monoclonal antibodies designed to bind to the spike protein of SARS-CoV-2 at two different sites (Ambrosio *et al.* 2023).

1.1.1.2 Influenza Virus

Human Influenza viruses (IV) are members of the family Orthomyxoviridae and belong to the four genera that contain single antigenically distinct species (types) of the same name, Influenza A virus (IAV), Influenza B virus (IBV), Influenza C virus (ICV) and Influenza D virus (IDV) (Hodinka 2016; Yamauchi 2018). All IVs possess a uniquely segmented, single-stranded, negative-sense RNA genome. Depending on the Influenza type, there are seven (ICV and IDV) or eight (IAV and IBV), the RNA-genome is subdivided into segments; each segment contains one or two genes that code for various proteins (Zhang *et al.* 2020). The viral genome is enclosed in a nucleocapsid that is surrounded by a lipid envelope. IAV contains eight genome-segments 11 genes on eight segments encoding for 11 proteins, including the surface glycoproteins hemagglutinin (HA) and neuraminidase (NA), a nucleoprotein (NP), the matrix proteins M1 and M2, the nonstructural proteins NS1 and NS2, and the core proteins PA, PB1 (polymerase basic 1), PB1-F2, and PB2. The HA glycoprotein mediates binding to sialic acid residues on the host cell surface and membrane fusion and virus entry, while NA functions to cleave sialic acid and release new virus particles from the surface of infected cells. The four IV types are distinguished by antigenic differences in their nucleoprotein and matrix protein. For IAV, based on the genetic and antigenic variability of the HA and NA proteins, IAV is divided into 18 distinct HA subtypes and 11 NA subtypes, as a result of frequent mutations (Hodinka 2016; Yamauchi 2018; Zhang *et al.* 2020).

IAV infects humans and many different animals and can undergo frequent genetic mutations, resulting in antigenic drift (the gradual modification of the sequence of amino acids that make up proteins is capable of stimulating an immune response) and consistent annual outbreaks and, less commonly, major reassortment events leading to antigenic shift (the emergence in humans of a new viral strain with a surface protein belonging to a subtype different from those commonly circulating in humans) and major worldwide pandemics. After emerging as a pandemic, strains of Influenza A Virus continue circulating in human populations for decades as seasonal epidemics and, some of these epidemic Influenza Viruses circulated in human populations for long enough to evolve into distinct genera (Yamauchi 2018).

The Influenza B Viruses cause annual seasonal human epidemics as well as occasionally infecting seals. In general, IBV and ICV infect primarily humans, are less genetically diverse than IAV, and consequently do not undergo antigenic shift and antigenic drift is far less frequent. IDV appear to cause only mild disease in cattle (Yamauchi 2018).

Influenza is a public health problem with a significant impact from an epidemiological, clinical, and economic perspective. This can be attributed to several factors: the ubiquity and contagiousness of the disease, the antigenic variability of the viruses, the epidemic (and periodically pandemic) and seasonal patterns, the potential for severe complications in certain groups of individuals (children, the elderly, people with comorbidities and chronic diseases), the management costs in case of complications, and the social costs (lost working days, loss of productivity, etc.) (WHO).

At the core of the epidemiology of Influenza is the marked tendency of Influenza viruses to mutate, meaning they undergo antigenic variations in the two glycoproteins HA and NA (antigenic drift). This allows them to evade the host's immune response from previous infections, leaving a significant portion of the population immunologically susceptible and capable of spreading widely and rapidly. These molecular variations need to be taken into account when preparing vaccines. The composition of vaccines must be updated every year by predicting the circulating strains. In fact, surveillance activities are essential for selecting specific strains based on their epidemiological and serological differences from what has circulated in previous seasons (Yamauchi 2018; Zhang *et al.* 2020; Krammer *et al.* 2018; Yamayoshi *et al.* 2019).

Most people recover within a week without requiring medical treatment, and in healthy individuals, Influenza rarely leads to complications. However, in some cases, severe complications or death can occur in high-risk individuals, including pregnant women, children aged 6 months to 5 years, the elderly, patients with chronic illnesses or those

undergoing immunosuppressive therapies, severely obese individuals, and healthcare personnel (WHO; Krammer *et al.* 2018; Yamayoshi *et al.* 2019).

In temperate climates, seasonal epidemics mainly occur during the winter, while in tropical regions, Influenza can manifest throughout the year, leading to more irregular epidemics.

Typically, during the two regular Influenza seasons in a year (one for each hemisphere), there are between 3-5 million cases of severe illness and up to 500,000 deaths worldwide, which, by some definitions, constitute an Influenza epidemic each year, although the incidence of the virus can vary widely (ECDC; WHO).

Pandemics occur at unpredictable intervals. For example, in the last century, pandemics occurred in 1918 (Spanish flu, subtype H1N1), 1957 (Asian flu, subtype H2N2), 1968 (Hong Kong flu, subtype H3N2), and 1977 (Russian flu, subtype H1N1). The most recent Influenza pandemic, caused by the A(H1N1)pdm09 virus, occurred in 2009 and was known as the swine flu. One of the most devastating pandemics in human history was the Spanish flu pandemic of 1918, which led to more than 20 million deaths in less than a year and a total of between 50 and 100 million deaths in three years, infecting approximately 500 million people (ECDC; WHO).

Seasonal vaccines are currently the most effective means of preventing and controlling infections caused by Influenza Viruses (IV). However, vaccines alone do not provide sufficient protection to mitigate the annual impact of IV infections. Therefore, current intervention strategies also rely on antiviral agents to reduce the burden of complications and case fatality rates (ECDC; WHO).

In this context, there are three classes of direct-acting antiviral (DAA) drugs that have been approved for the management of IV infections: amantadanes, neuraminidase inhibitors (NAIs), and RNA-dependent RNA polymerase (RdRp) complex inhibitors (Krammer *et al.* 2018; Yamayoshi *et al.* 2019).

Amantadanes function by blocking the IAV M2 ion channel. Unfortunately, due to widespread resistance among circulating IVs, they are no longer recommended for use.

Neuraminidase inhibitors (NAIs), on the other hand, such as peramivir, zanamivir, and especially oseltamivir, are considered the standard of care for the therapeutic management of IV infections. These NAIs have been successfully employed for two decades. However, during the period of 2007-2009, resistance to oseltamivir increased significantly among seasonal H1N1 IAV due to the emergence of the NA H275Y amino acid substitution. The subsequent global spread of the 2009 H1N1 IAV pandemic strain, which lacked this mutation at the time of its emergence, reduced the frequency of NAI resistance in seasonal IV to low levels (<2%), and it has remained low since then. Nevertheless, the rapid

emergence of IVs with reduced susceptibility to oseltamivir between 2007 and 2009 highlighted the potential for NAI resistance to develop and spread among circulating IVs. More recently, RdRp inhibitors have been licensed for the treatment of uncomplicated IV infections and those resistant to other antiviral drugs. These include baloxavir marboxil (baloxavir), which targets the PA subunit of RdRp, and favipiravir, an inhibitor of the PB1 subunit. Globally, IV variants with reduced susceptibility to baloxavir have been detected, albeit at a low frequency (Krammer *et al.* 2018; Yamayoshi *et al.* 2019).

However, available data suggest that the genetic barrier against viral resistance to some approved DAAs may be low, which poses challenges in the control of IV infections using a curative approach. Therefore, there is a clear need to develop alternative anti-IV agents with new mechanisms of action, reduced likelihood of selecting resistant strains, and efficacy against antigenically diverse IVs. These agents would be readily deployable against new zoonotic highly pathogenic IVs that may emerge in human populations in the future.

It's also important to consider that Influenza causes direct costs not only for medical treatments but also for the loss of productivity, along with indirect costs for preventive measures. In the United States alone, Influenza costs over $10 billion annually, and a pandemic could increase costs to hundreds of billions of dollars (White House Archive).

The costs of prevention are also high. The Influenza vaccine is the best way to prevent and combat this virus because it significantly reduces the likelihood of contracting the disease and, in the case of developing Influenza symptoms, they are much less severe and generally not followed by further complications. Furthermore, Influenza vaccination is an important protective measure not only for oneself but also for those around you. It reduces the likelihood of complications and decreases the burden on healthcare facilities during periods of high demand. For example, governments worldwide, from the American to the Vietnamese ones, have spent billions of dollars on preparing and planning for a potential avian Influenza pandemic (US AID).

1.1.1.3   *Respiratory Syncytial Virus*

Respiratory Syncytial Virus (RSV) is classified as a pneumovirus within the family Paramyxoviridae and possesses a linear single-stranded, negative-sense RNA genome contained within a helical nucleocapsid surrounded by a lipoprotein envelope. The genome has 10 genes encoding for two non-structural (NS1 and NS2) proteins and 9 structural proteins. Of the structural proteins, three are membrane glycoproteins and include G, F, and SH (small hydrophobic); the matrix (M) protein is involved in viral assembly; and the nucleocapsid protein (N), nucleocapsid phosphoprotein (P), and M2-1 and M2-2 proteins are involved in transcriptional activity and regulation. The two surface glycoproteins (F and

G) mediate attachment (G) and fusion (F) of the virus to the host cell surface. The F glycoprotein also mediates syncytium formation, and the name of the virus is derived from its ability to produce multinucleated cell syncytia through fusion of cell membranes of adjacent host cells. The virus contains an RNA-dependent RNA polymerase (L) for transcription and replication, and virus replication occurs in the cytoplasm of the host cell. The virus particle is pleomorphic in shape with spherical or filamentous forms (Hodinka 2016; Tripp *et al.* 2016).

There is a single antigenic type of RSV divided into two subgroups, A and B, one of which usually predominates in an epidemic. Subgroup A is thought to be associated with more severe disease, although the significance of the two variants is still not fully understood.

RSV is a widespread global cause of lower respiratory tract infections that affect individuals of all age groups. In infants and young children, RSV can lead to severe bronchiolitis, characterized by inflammation of the small airways in the lungs, and pneumonia, a lung infection that can be fatal in some cases. In children and adults without underlying health conditions, recurring upper respiratory tract infections are common, ranging from asymptomatic infections to symptomatic upper respiratory tract diseases (Hodinka 2016; Tripp *et al.* 2016; WHO).

Notably, RSV is increasingly recognized as a significant pathogen particularly in the elderly. RSV infections in this age group have resulted in increased hospitalization rates for those aged 65 and over, as well as elevated mortality rates among frail elderly individuals, approaching the levels observed with Influenza. The risk of severe disease in adults is further heightened by the presence of chronic pulmonary diseases, circulatory conditions, functional disability, and is associated with higher viral loads. RSV is also a nosocomial (hospital-acquired) threat to young infants and immunocompromised individuals, including those who have undergone bone marrow or lung transplantation (WHO).

The WHO has estimated that globally, RSV-associated lower respiratory tract infections result in around 64 million infections annually, leading to 3.2 million hospitalizations and 160,000 deaths.

In the United States alone, RSV has a significant impact, resulting in approximately:

- 2.1 million outpatient visits for children under the age of 5;
- 58,000-80,000 hospitalizations among children under the age of 5;
- 60,000-160,000 hospitalizations among adults aged 65 and older;
- 6,000-10,000 deaths among adults aged 65 and older;
- 100-300 deaths in children younger than 5 years old (CDC).

In developing countries, there are limited estimates of RSV incidence, but existing data indicate its significance as a cause of childhood diseases. A ten-country WHO study from the 1960s identified RSV in 19 percent of children under six years of age hospitalized with acute respiratory syndromes, accounting for approximately 80 percent of all respiratory infections of viral origin. The growing role of RSV as a cause of parainfluenza illnesses in older individuals has also been emphasized (WHO).

One complex aspect of RSV epidemiology is its seasonality. In temperate climate regions like Europe, the United States, Argentina, and Pakistan, RSV tends to cause winter or spring epidemics. In tropical countries, RSV appears to be more prevalent during rainy periods, although this pattern can vary significantly between neighboring countries.

Currently, antiviral medications are not routinely recommended for RSV infection, as most cases resolve on their own within a week or two. Hospitalization may be required for individuals experiencing severe symptoms, particularly older adults and infants under 6 months of age, who may struggle with breathing or dehydration. In severe cases, additional medical interventions like oxygen therapy, intravenous fluids, or mechanical ventilation with intubation may be necessary. However, hospitalization for RSV typically lasts only a few days.

At present, the prevention of RSV infections in adults is possible through the utilization of two recently approved RSV prefusion F protein-based vaccines in 2023, namely Abrysvo (manufactured by Pfizer) and Arexvy (developed by GSK) (Soni *et al.* 2023).

However, there is still no available RSV vaccine designed for infants and young children. The primary prophylactic measures for this age group continue to rely on neutralizing monoclonal antibodies (mAbs) directed against the F glycoprotein, such as Palivizumab, along with the recently sanctioned Nirsevimab (Simões *et al.* 2023). In contrast, the options for treating RSV infections are currently restricted to supportive care, including bronchodilators and supplemental oxygen. This is because the sole approved antiviral drug for RSV, ribavirin, is exclusively reserved for hospitalized infants and young children with severe Lower Respiratory Tract Infections (LRTIs). However, concerns about the safety and efficacy of ribavirin discourage its widespread clinical use (Jain *et al.* 2023).

Given the significant global public health impact of RSV infections and the limited array of interventions available, there is an urgent need to develop new and effective antiviral agents to alleviate or reduce the disease burden.

1.1.2 Other important viruses

According to the WHO, in addition to respiratory viruses, there are other viruses that deserve special surveillance, as they infect a very high number of people and the numbers are destined to grow over the years, such as Herpes Simplex Virus and Human Immunodeficiency Virus.

1.1.2.1 Herpes Simplex Virus

The Herpes Simplex Virus (HSV) refers to two virus species, Herpes alphaherpesvirus 1 and Herpes alphaherpesvirus 2 belonging to the family Herpesviridae, subfamily Alphaherpesvirinae, of the genus Simplexvirus (Whitley *et al.* 2001).

HSV are large Herpesviruses with a diameter of about 150 nm, equipped with a pericapsid. The capsid is icosadeltahedral in shape, consists of approximately 160 capsomeres and is separated from the pericapsid by a space called tegument containing certain viral enzymes essential for the initiation of replication. The capsid contains a genome consisting of linear double-stranded DNA coding for about 80 different proteins, half of which are involved in virus replication, including nucleotide recovery proteins (thymidine kinase, ribonucleotide reductase, deoxyribonuclease, various proteases), 11 are structural glycoproteins (gD, gH, etc.), others intervene in the immune system (gC, gE, gI), a fusion protein (gB), there is also a DNA-dependent DNA-polymerase. HSV-1 and HSV-2 are two viruses with a similar structure, in fact they possess almost the same antigenic determinants and a high degree of homology in the DNA (Whitley *et al.* 2001).

The Herpes Simplex virus, commonly referred to as Herpes, is a prevalent infection primarily transmitted through direct skin-to-skin contact. Many HSV infections go unnoticed or show no symptoms, but individuals with Herpes may experience painful blisters or sores that can recur over time (WHO).

HSV can be managed with medications, but it cannot be completely cured. Medications are often used to alleviate symptoms and reduce their duration and intensity, but they do not eliminate the infection, which remains with its host for life. Frequently prescribed antiviral drugs are nucleoside analogue inhibitors of viral DNA polymerase, such as acyclovir (guanosine analogue), famciclovir (adenosine analogue) and valaciclovir (the prodrug of acyclovir). However, due to the virus's high mutagenicity, many strains of HSV have developed resistance to these antivirals, rendering them less effective in numerous infections, without considering the adverse effects resulting mainly from long-term toxicity. As of 2016, approximately 67% of the global population under the age of 50, totaling 3.7 billion people, were infected with HSV-1, either orally or genitally. Most HSV-1 infections

are contracted during childhood. Genital Herpes, caused by HSV-2, affects around 13% of individuals aged 15 to 49 worldwide based on 2016 data, totaling about 491 million cases. HSV-2 infects women almost twice as often as men, mainly due to the more efficient transmission from men to women. The prevalence of HSV-2 increases with age, with the highest number of new infections occurring among adolescents (WHO; Whitley *et al.* 2001). In individuals with compromised immune systems, such as those with advanced HIV infection, Herpes can result in more severe symptoms and frequent recurrences. Rare complications of HSV-2 include meningoencephalitis (brain infection) and disseminated infection. HSV-1 infections, although rare, can lead to more serious complications like encephalitis (brain infection) or keratitis (eye infection). Neonatal Herpes can occur if a baby is exposed to HSV during childbirth, with an incidence of about 10 cases per 100,000 births globally. Although rare, it is a severe condition that can lead to lasting neurological damage or death. The risk of neonatal Herpes is highest when a mother contracts HSV for the first time late in pregnancy (WHO).

Furthermore, HSV-2 infection increases the risk of contracting HIV infection approximately threefold. People co-infected with both HIV and HSV-2 are more likely to transmit HIV to others. HSV-2 infection is one of the most common infections among people living with HIV (WHO).

1.1.2.2 *Human Immunodeficiency Virus*

The Human Immunodeficiency Virus (HIV) is a member of the Lentivirus genus within the Retroviridae family. Lentiviruses, sharing common morphologies and biological traits, often induce prolonged diseases with extended incubation periods across various species (Bekker *et al.* 2023).

These Lentiviruses, including HIV, are transmitted as enveloped single-stranded, positive-sense RNA viruses (mRNA). Specifically, HIV is a diploid virus, in that it contains two identical copies of mRNA (Bekker *et al.* 2023; Esposito *et al.* 2020).

According to current knowledge, HIV is divided into two strains: HIV-1 and HIV-2. HIV-1 is the virus that was initially discovered and referred to as both LAV and HTLV-III: it is more virulent, more infectious, and is the cause of most HIV infections worldwide. The former of the two is mostly located in Europe, America, and Central Africa; HIV-2, on the other hand, is mostly found in West Africa and Asia and results in a more clinically moderate syndrome than the former strain (Bekker *et al.* 2023).

Delving into the virus's structure, the HIV virion has a spherical structure about 100-120 nm in diameter, with two outer membranes: the capsid with a conoid shape and the pericapsid, which houses the viral membrane glycoproteins gp120 and gp41 (also named fusion

protein). These proteins play crucial roles in the virus's attachment to target cells and the fusion of viral and cellular membranes, facilitating virus entry. For this reason, knowledge of gp120 and gp41 is of particular importance in the fight against the virus: acting on them can slow or curb the infection of new cells. (Bekker *et al.* 2023).

The viral genome, however, is enclosed in a protective shell formed exclusively by the p24 protein, the core, that containing enzymes like reverse transcriptase (RNA-dependent DNA polymerase), integrase and protease, essential for the virus's replication process. Upon entry into the target cell, the viral RNA undergoes reverse transcription, converting into double-stranded DNA through a reverse transcriptase carried within the viral genome. The resulting viral DNA is then integrated into the cellular DNA by an integrase encoded by the virus. At this point, the virus can become dormant, allowing the virus and its host cell to avoid detection by the immune system. Alternatively, the virus can be transcribed, producing new RNA genomes and viral proteins that are packaged and released from the cell as new virus particles and have a way to begin a new replication cycle. (Bekker *et al.* 2023).

Finally, the last important characteristic of HIV is that between the core and the lipoprotein envelope of the virus there is a layer of electron-dense material made up entirely of the myristylated viral p17 protein. Myristylation is an important phenomenon for the subsequent interaction of p17 with the cell membrane in order to initiate the release of new viruses replicated inside the cell, with a budding process. (Bekker *et al.* 2023).

Human Immunodeficiency Virus infection continues to be a significant global public health challenge. This virus was initially identified in 1981 and has led to an ongoing pandemic, affecting approximately 40.4 million individuals worldwide, with cases reported in all countries. Furthermore, the prevalence of HIV infection is on the rise in many countries, despite previous years of decline. According to the WHO, by the end of 2022, an estimated 39.0 million people were living with HIV, with two-thirds of them (25.6 million) residing in the African region. In 2022, around 630,000 people lost their lives due to HIV-related causes, and 1.3 million people newly contracted the infection (WHO; Bekker *et al.* 2023).

HIV is primarily transmitted through contact with specific body fluids such as blood, semen, vaginal fluids, rectal fluids, and breast milk from an infected person. The most common modes of transmission include unprotected sexual intercourse, sharing of contaminated needles or syringes among intravenous drug users, and from an infected mother to her child during childbirth or breastfeeding (WHO; Bekker *et al.* 2023).

Once inside the body, HIV attacks the immune system, specifically the CD4 cells (T cells), which play a crucial role in the body's defense against infections. The progression of HIV infection occurs in stages, with the initial acute infection often presenting flu-like symptoms,

followed by a latency period where the virus remains relatively dormant. Without appropriate medical intervention, HIV can progress to Acquired Immunodeficiency Syndrome (AIDS), characterized by severe immunosuppression and the increased susceptibility to opportunistic infections and certain cancers (WHO; Bekker *et al.* 2023).

There is currently no known cure for HIV infection, that is, it cannot be cured by completely eliminating the virus from the infected individual. Thanks to antiretroviral treatments, people affected by HIV are able to lead long and healthy lives, but are forced to take cocktails of drugs every day to slow down the progression of the infection as much as possible.

Antiretroviral therapy is mainly aimed at reducing the plasma HIV RNA level to an undetectable level (i.e., < 20 to 50 copies/mL) and restoring the CD4 count to a normal level (> 200/mcl; immune restoration or reconstitution). These drug cocktails are composed of 2, 3, or 4 classes of antiretroviral drugs matched together based on the side effects observed on the patient, concomitant conditions that may develop (e.g., renal or hepatic dysfunctionality), other drugs the individual may need to take, simplicity of regimen, cost of therapy, etc.. There are numerous classes of antiretroviral drugs that act on different targets, for example: nucleoside reverse transcriptase inhibitors, protease inhibitors (PIs), entry inhibitors (EIs), integrase inhibitors, adhesion inhibitors, etc. (Cachay 2023). Furthermore, another major problem is the appearance of resistance against these antiretroviral drugs, so it is essential to identify new molecules with innovative mechanisms of action that can be effective against drug-resistant strains, the incidence of which is increasing among treated and naïve patients; for example antivirals that act as allosteric inhibitors by targeting two viral functions (double inhibitors): 5,6-dihydroxyindole-2-carboxylic acid (DHICA) derivatives act on both the activities of the integrase and the associated ribonuclease H to HIV reverse transcriptase (Esposito *et al.* 2020).

The WHO, the Global Fund, and UNAIDS have all developed global strategies with the aim of ending the HIV epidemic by 2030. Specifically, by 2025, the target is for 95% of all individuals living with HIV to be diagnosed, 95% of those diagnosed to be receiving life-saving antiretroviral treatment, and 95% of those receiving treatment to achieve a suppressed viral load for the benefit of the population (WHO).

1.2   Treatment: broad-spectrum antiviral agents and drug repurposing

Viral infections continue to pose a significant global public health concern. While it's known that hundreds of viruses are pathogenic, only fewer than ten of them can be clinically treated with available antiviral drugs. For some highly pathogenic viruses such as Zika (ZIKV), Ebola (EBOV), Severe Acute Respiratory Syndrome 1 and 2 (SARS-CoV-1 and -2), and many others, effective drugs are still not available on the market. Additionally, there are viruses that consistently infect the human population, such as the Influenza Viruses family (IAV), Herpesviruses family (HSV-1, VZV, CMV), and Norovirus, imposing a substantial burden on public health and the economy. Emerging and re-emerging viruses like EBOV, Marburg (MARV), Lassa (LASV), Chikungunya (CHIKV), ZIKV, Dengue (DENV), Rift Valley Fever (RVFV), Middle East Respiratory Syndrome Coronavirus (MERS-CoV), and SARS-CoV-1 and -2 regularly emerge from natural reservoirs, approximately one each year, posing global threats that often lead to epidemics or, worse, pandemics (Maffei *et al.* 2022; Sepulveda *et al.* 2022; Geraghty *et al.* 2021; Andersen *et al.* 2020; Ianevski *et al.* 2018).

According to the WHO, there is an urgent need for better control of these viruses, including immunity to drugs and vaccines that evade viral strains. Virus-specific vaccines and antiviral drugs are the most potent tools to combat viral diseases. Previously, the focus was on the "one drug, one virus" dogma, which targeted specific viral factors. A counterpoint to this is the "one drug, multiple viruses" paradigm, which emerged with the discovery of Broad-Spectrum Antiviral Agents (BSAA), small molecules that inhibit a wide range of human viruses. This paradigm was based on the observation that different viruses use similar host pathways and factors to replicate within a cell (**Figure 1**) (Maffei *et al.* 2022; Andersen *et al.* 2020; Ianevski *et al.* 2018).

While the concept of BSAA has been around for nearly 50 years, the field has received a new boost with recent epidemics of Ebola, Zika, Dengue, Influenza, and other viral infections, the discovery of new agents targeting the host, as well as drug repurposing methodology (Andersen *et al.* 2020; Mercorelli *et al.* 2018).

To overcome the time and cost challenges associated with developing virus-specific drugs and vaccines, priority should be given to the development of BSAA. Broad-spectrum antivirals can cover multiple viruses and genotypes, reducing the likelihood of resistance development. Therefore, some BSAA can be used for the treatment of viral coinfections, reducing the complexity of therapy, as a first-line treatment, or for the rapid management of

new or drug-resistant viral strains (Geraghty *et al.* 2021; Andersen *et al.* 2020; Mercorelli *et al.* 2018).
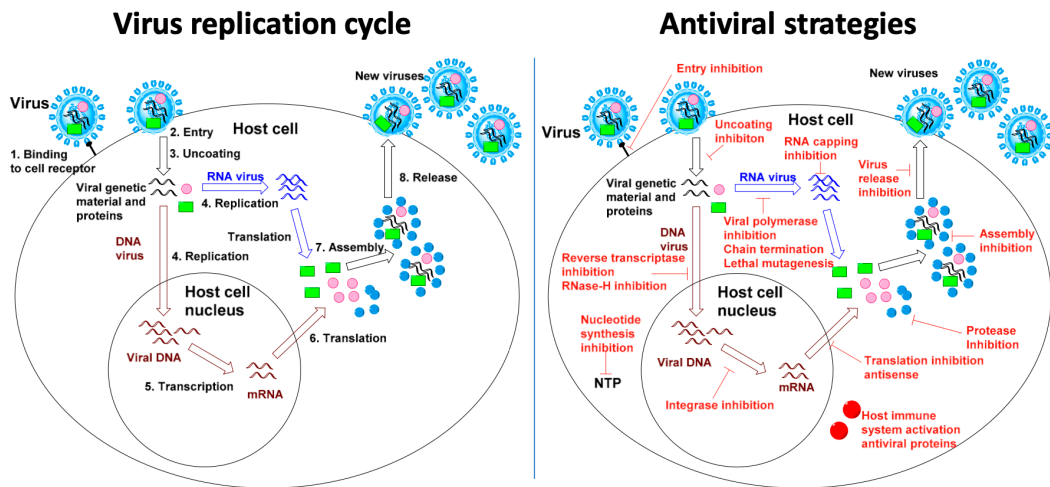

Figure 1. The image on the left depicts the stages of the viral replicative cycle, while in the image on the right all the possible cellular or viral targets that can be used to create antivirals are highlighted (Geraghty et al. 2021).

In BSAA research and development, the repositioning of existing antiviral agents, safe for humans, could be useful above all in the emergence of new pathogenic viral strains. Drug reuse, also known as repurposing, redirection, or reprofiling, is a strategy to generate additional value from an existing drug by targeting different diseases than originally intended. This presents significant advantages over discovering new drugs, as chemical synthesis stages, production processes, reliable safety, and pharmacokinetic properties in preclinical stages (animal models) and early clinical development (Phase 0, I, and IIa) are already available (**Figure 2**) (Geraghty *et al.* 2021; Andersen *et al.* 2020; Mercorelli *et al.* 2018).
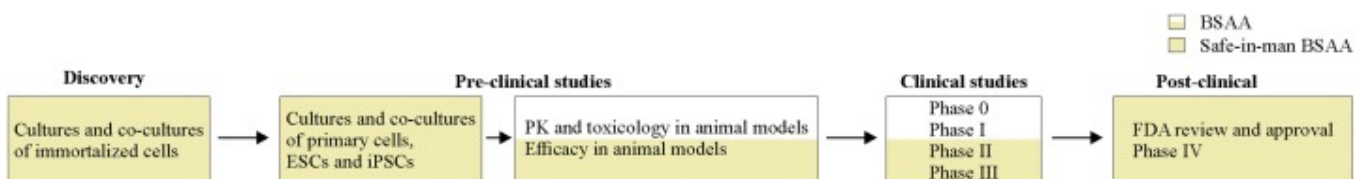

Figure 2. The exploration of new functionalities and the subsequent progression in creating all-encompassing antiviral substances. The highlighted yellow portion represents the process of uncovering and improving safe-for-human use broad-spectrum antiviral agents (BSAAs). These BSAAs have already been subjected to pharmacokinetic (PK) assessments during the preclinical stages, involving animal models, and the initial phases of clinical development (phase 0-IIa trials) (Andersen et al. 2020).

Therefore, repurposing existing drugs for viral diseases offers unique translational opportunities, including a substantially higher probability of market success compared to the development of new virus-specific drugs and vaccines, and significantly reduced costs and time to clinical availability (Geraghty *et al.* 2021; Andersen *et al.* 2020; Mercorelli *et al.* 2018).

One of the most unsettling lessons that the 2019 coronavirus (COVID-19) pandemic taught the world is its general unpreparedness in dealing with a new respiratory virus pandemic with a therapeutic approach. Despite the outbreaks of SARS-CoV-1 (2003) and MERS-CoV (2012) demonstrating the risk of emerging zoonotic coronaviruses, the lack of already available and effective broad-spectrum antivirals that could be rapidly deployed against the new SARS-CoV-2 made it initially difficult to reduce hospitalizations, deaths, and slow the spread of COVID-19. Therefore, new BSAA that can be rapidly employed against future emerging respiratory viruses in humans, such as coronaviruses and Influenza Viruses, are urgently needed. These BSAA could allow for the immediate onset of antiviral treatment upon the virus's emergence, gaining time for the development of new virus-specific vaccines and therapies (Maffei *et al.* 2022).

Existing direct-acting antiviral drugs (DAA) cannot be immediately applied to new viruses due to virus specificity, and the development of new DAAs from the start is not timely for epidemics. Broad-spectrum antivirals are clinically necessary for the effective control of emerging and re-emerging viral infections. However, despite the significant research efforts to discover therapeutic antiviral agents for these emergencies, rarely have specific and effective drugs with low toxicity been reported. Given the substantial diversity of viral structures and replication strategies, the development of effective BSAA has proven more challenging than that of the more approved antiviral drugs that inhibit only a specific virus-encoded target, such as a polymerase or protease. However, over the past two decades, the increasing number of new viral epidemics in humans has reaffirmed the fundamental need for molecules capable of implementing the "one drug, multiple viruses" paradigm, i.e., the inhibition of different virus families by the same molecule. Therefore, effective BSAA could be an essential weapon in the final arsenal of available antiviral options, as they could provide immediate therapeutic intervention against emerging and re-emerging viral threats. Future preclinical and ongoing clinical studies will increase the number of BSAA, expand their indications, and identify drug combinations for the treatment of emerging and re-emerging viral infections, as well as coinfections (Maffei *et al.* 2022; Ji *et al.* 2019; Ianevski *et al.* 2018).

As the development of effective BSAAs remains a challenging task in drug discovery, natural products have been considered as a unique source of chemical complexity and diversity within which antiviral activities can be identified. Indeed, a growing body of evidence, based on robust molecular, biochemical and pharmacological studies, indicates that a wide range of plant-derived natural products show inhibitory effects on the replication of many different viruses, thus having the potential to be used as BSAAs against current viruses and new emerging viral threats (El Sayed 2000). But synthetic molecules show additional advantages, as they are built with specific binding sites for the target they must inhibit; therefore, they tend to have higher affinities towards the target molecule (higher IC_{50}). Furthermore, the chemical strategies that are used to construct BSAAs also take into account the moieties that can induce greater or lesser toxicity on the host cell.

Based on the target, BSAA can be classified into two main types: (1) compounds that target viral structures or enzymatic activities and, therefore, belong to the broader category of DAAs; and (2) compounds that affect host factors or essential cellular biochemical pathways for viral replication, defined as Host-Targeted Antivirals (HTA) (Maffei *et al.* 2022; Geraghty *et al.* 2021; Chitalia *et al.* 2020; Ji *et al.* 2019; Debing *et al.* 2015).

Both families of broad-spectrum antiviral drugs (e.g., host-targeted or virus-targeted broad-spectrum antivirals) present advantages and disadvantages (**Table 1**).

Virus-Specific Antiviral Strategies	Broad-Spectrum Antiviral Strategies	
	Host-Targeted	Virus-Targeted
Pros: - Proven efficacy - Easier design, one viral target - Relative safety compared to other strategies Cons: - Narrow application - Low barrier to drug resistance development - Long development time	Pros: - Host proteins broadly required by viruses - Demonstrated antiviral effect - Higher barrier to drug resistance development Cons: - Not selective - Potential for toxicity	Pros: - Less potential for toxicity compared to host-targeted strategies. - Potential for repurposing Cons: - More complex design - Limited examples of broad-spectrum antiviral drugs

***Table 1.** Pros and cons of different antiviral strategies (Geraghty et al. 2021).*

Lately, to reduce the cons of both categories (reduce toxicities, reduce the occurrence of resistance, etc.), combinations of drugs are being studied. For example, it has been observed in the case of RNA viruses, such as the Junín virus that causes Argentine hemorrhagic fever, that the combination of A771726 (HTA), the active metabolite of leflunomide (hDHODH inhibitor) approved by the FDA for the treatment of arthritis rheumatoid and autoimmune diseases, combined with ribavirin (DAA) showed significantly more potent antiviral activity than either single drug treatment (Sepulveda *et al.* 2018).

It is therefore possible to hypothesize administering a DAA combined with an HTA that have a synergistic activity together, this brings a series of advantages:

- having synergistic activity, the doses of the drugs to be administered can be greatly reduced to obtain the same antiviral effect;
- the side effects induced by DAA drugs tend to be different from HTA drugs; therefore, the effects on humans are considerably more tolerable compared to the administration of the drug alone at higher doses which therefore causes much higher side effects to arise;
- the onset of resistance is reduced, because less drug is used, furthermore the strains resistant to DAA are still blocked by HTA.

Therefore, the study of the combination of the two drugs could be an aid for the therapeutic management of certain viruses, such as Herpesvirus or Influenza Virus which have a high rate of mutagenicity and easily develop resistance against DAAs.

1.2.1   Direct-Acting Antivirals

Most approved antiviral drugs are designed to target viral proteins to inhibit infections and are referred to as direct-acting antiviral agents. DAAs have proven to be very successful in the clinic in fighting viral infections and are generally considered very safe for human use because most of the viral target proteins do not have human homologs. However, these drugs currently have a number of shortcomings that still make them unclassifiable as broad-spectrum drugs and, in addition, greatly limit their use:

- Viral polymerases, one of the most important targets for antiviral design, share some structural similarities with their human counterparts, especially in the active sites, which is the main reason behind the toxicity observed with nucleoside-based antivirals. Thus, unfortunately, they are not low-toxicity antivirals.
- Viral proteins normally do not share structural similarities between different species or even genotypes of viruses, and thus an antiviral agent targeting one specific viral protein is unlikely to impart the same inhibitory effects against the other virus. As a result, commercially available antiviral drugs can hardly be used to treat newly emerging viruses and, therefore, can hardly be classified as BSAAs.
- The other inherent limitation of DAAs is that this category of antivirals, in most cases, has a low genetic barrier to drug resistance because they act directly on viral proteins, and the resulting selective pressure will facilitate virus mutations during replication, making the virus refractory to treatment with DAAs (Ji *et al.* 2020; Zheng *et al.* 2022; Sepulveda *et al.* 2022).

Overall, DAAs are the antivirals currently available to us to combat viruses, but unfortunately, they are a category of drugs with a number of problems, including the inability

to use them against emerging or re-emerging viruses because of their specificity or drug resistance that has arisen in viral strains.

An important first achievement to achieve a good DAA would be the development of molecules with broad antiviral activity within a specific family of viruses (pan-picornaviruses, pan-alphaviruses, etc.). Thus, to have a weapon against not just one virus, but against a category of viruses, for example, all RNA viruses or all envelope viruses.

Most DAAs currently approved for use in the clinic fall into two in two categories: nucleoside or nucleotide analogs and viral protease inhibitors (Debing *et al.* 2015; Geraghty *et al.* 2021; Ji *et al.* 2020).

Nucleoside and nucleotide analogues

Nucleoside and nucleotide analogues were among the earliest antiviral medications to become commercially accessible. Research into antiviral nucleosides commenced in the 1960s and 1970s but displayed their considerable potential in the 1980s and 1990s with the identification of multiple anti-HIV drugs like Abacavir, AZT, and others. Since then, their applications have extended to other viral pathogens. These Direct-Acting Antivirals (DAAs) now serve as the foundation of HIV therapy, including drugs like tenofovir, emtricitabine, and lamivudine. Nucleoside analogues also play a crucial role in treating Herpesvirus infections with medications such as acyclovir, ganciclovir, and cidofovir (Debing *et al.* 2015; Geraghty *et al.* 2021).

In contrast to non-nucleoside polymerase inhibitors, which frequently attach to non-conserved, mutation-tolerant allosteric sites, nucleoside and nucleotide analogs directly bind to the most universally preserved active site of the viral polymerase once they are converted into their active triphosphate form. While nucleoside/nucleotide antiviral analogs represent a vital category of antiviral medications, creating these antiviral inhibitors faces various challenges. The half-life and pharmacokinetics of these analogs significantly differ from those of natural nucleosides/nucleotides. These challenges primarily arise from the nature of these inhibitors, which inherently require activation by host kinases to form their active triphosphate state before becoming substrates for the viral polymerase. The effectiveness of antiviral nucleotide triphosphate formation can vary significantly among cell types due to varying kinase levels required for phosphorylation, and the concentration of antiviral nucleotide triphosphate in cells is a reliable indicator of antiviral activity that the drug can exert (Debing *et al.* 2015; Geraghty *et al.* 2021).

While the second phosphorylation step can be critical, the first phosphorylation is often the rate-limiting step for triphosphate formation for most nucleoside analogues. Consequently, nucleotide monophosphate prodrugs have been effectively developed to bypass the initial

phosphorylation hurdle, thereby enhancing antiviral efficacy. This is exemplified by the success of the anti-HCV drug Sofosbuvir, a nucleotide phosphoramidate prodrug that overcame initial challenges associated with less active nucleoside analogs. The nucleotide phosphoramidate prodrug can enter infected cells, where it is directly converted into monophosphate, thus bypassing the first phosphorylation step.

The concept of "broad-spectrum antiviral" which can be applied to this type of drug can take on a different meaning than usual: normally a BSAA drug is thought to be active against all viruses, but, more restrictively, it can be understood that a BSAA is active against all viruses within a specific family. Indeed, there are some direct-acting nucleoside/nucleotide analogues targeted at various virus families, therefore different from the classic DAAs directed against a specific virus, but unfortunately the number of those demonstrating broader-spectrum antiviral effects is limited. Ribavirin is probably the most renowned nucleoside antiviral with broad antiviral activity, used to treat chronic hepatitis C, E, respiratory syncytial virus (RSV) infections, and to some extent Lassa fever and Hantavirus infections. Additionally, favipiravir, also known as T-705, exhibits antiviral activity against both positive and negative-sense RNA viruses. This molecule is classified as a nucleobase and undergoes intracellular metabolism to become a nucleotide analog that inhibits the RNA-dependent RNA polymerase of Influenza. The compound has been approved in Japan for Influenza virus treatment. Similarly, the adenosine analog BCX4430 functions as a polymerase chain terminator for RNA viruses and demonstrates *in vitro* antiviral activity against most positive and negative-sense RNA viruses, with enhanced efficacy against filoviruses. Protective activity against filovirus infection has been demonstrated in primates. Nonetheless, these nucleoside and nucleotide drugs have associated toxicity, strong side effects, limited clinical efficacy against certain viruses, or are still in the experimental phase. Ultimately, their range of susceptible viral species is often too restricted to classify them as true Broad-Spectrum Antiviral Agents (BSAA) (Debing *et al.* 2015; Geraghty *et al.* 2021).

Despite the disadvantages and limitations of currently available nucleoside analogs, this class of compounds continues to hold great promise in the development of BSAA. Viral genome replication is a fundamental aspect of the viral life cycle, and most viruses encode polymerases that are markedly distinct from their mammalian counterparts. There is a level of conservation within each polymerase family, suggesting the possibility of creating BSAA that inhibit almost all polymerases of a particular type. To identify potential lead molecules for nucleoside/nucleotide-based BSAA, a customized screening approach may be essential. To date, a vast array of nucleoside and nucleotide analogs has been synthesized, making it crucial to meticulously select a high-quality library based on criteria like structural diversity,

drug-like properties, cell permeability, and solubility. This library can then be assessed using a specialized screening method. One approach could involve high-throughput polymerase enzymatic assays, where all selected compounds are tested against various representative viral polymerases of a certain type, seeking compounds that inhibit all tested enzymes. Alternatively, these libraries could be evaluated in cell-based phenotypic antiviral assays against a variety of viruses representative of specific genera, families, or groups. A third strategy involves the rational design of nucleoside/nucleotide analogs based on comparisons of available polymerase crystal structures, especially the conserved features within the catalytic site. The subsequent development of targeted compounds includes expanding the range of tested viruses, chemical modification of the initial hit (known as hit expansion) to increase antiviral potency and sensitivity, and to improve selectivity and pharmacokinetic properties. Given that certain nucleoside/nucleotide analogs targeting DNA viruses already exhibit relatively broad activity spectrums, these efforts should initially be directed toward RNA viruses (Debing *et al.* 2015; Geraghty *et al.* 2021).

The nucleoside/nucleotide analogs that stand out most in this category and are classified as broad-spectrum RNA virus inhibitors are remdesivir, to represent the nucleotide analogues categories, and ribavirin (as mentioned earlier), to represent the nucleoside analogues categories.

- *Remdesivir*

Remdesivir is a is a phosphoramidate prodrug of an adenosine C-nucleoside (AIFA; Geraghty *et al.* 2021).

The Ebola virus outbreak in West Africa in 2013 sparked increased research into antiviral drugs, leading to the discovery of several promising candidates. Research institutions initiated comprehensive studies, including experiments in non-human primates, ultimately resulting in the identification of Remdesivir. This broad-spectrum antiviral drug exhibited effectiveness against Ebola and Marburg viruses, as well as MERS-CoV and SARS-CoV-2. Remdesivir has received approval from the FDA for treating COVID-19 patients. Notably, Remdesivir displays an unusually wide-ranging antiviral effect, a rarity among molecules that operate through viral RNA chain termination (Geraghty *et al.* 2021).

Before functioning as a delayed chain terminator, the Remdesivir phosphate prodrug must enter infected cells, where it undergoes metabolic conversion by cellular kinases to its active triphosphate form. In its triphosphate form, Remdesivir becomes a substrate for the viral polymerase, a crucial and highly conserved protein in the viral replication process. Remdesivir triphosphate imitates the natural substrate nucleotide adenosine triphosphate. Delayed chain termination occurs after the incorporation of Remdesivir triphosphate into a

growing strand of viral RNA, leading to a stalling mechanism. It's worth noting that this delayed chain termination might shield Remdesivir from excision by viral proofreading proteins, thanks to the presence of an additional 3-5 natural nucleotides (Geraghty *et al.* 2021).

The delayed chain termination induced by Remdesivir compels the premature conclusion of viral RNA synthesis. A drawback of Remdesivir is its requirement for intravenous administration, which may be attributed to its limited oral bioavailability and short half-life. Consequently, there is a need for alternatives to Remdesivir or orally accessible formulations of the drug to enhance the practicality of treatment (AIFA; Geraghty *et al.* 2021).

- *Ribavirin*

Ribavirin, discovered during the 1970s, stands out as one of the most remarkable nucleoside antiviral agents due to its potent antiviral properties in both laboratory cell cultures and animal models. It exhibits effectiveness against a wide spectrum of viruses, including both DNA and RNA viruses. Ribavirin has gained approval as a medication for combating hepatitis C when used either in conjunction with alpha interferons or in combination with other drugs like sofosbuvir. Additionally, it has found applications in the treatment of various other viral infections (Geraghty *et al.* 2021; Ji *et al.* 2020).

In terms of its chemical structure, ribavirin consists of a ribose component linked to an aromatic triazole ring as its base, featuring an amide group that can rotate. This flexible amide group enables ribavirin to resemble either adenosine or guanosine as it undergoes rotation. Inside the confines of cellular environments, the nucleoside form of ribavirin undergoes a series of phosphorylation events, catalyzed by enzymes such as adenosine kinase, to transform it into its monophosphate and eventually into its triphosphate form.

The precise antiviral mechanisms of ribavirin remain a subject of ongoing research, likely comprising multiple facets. Originally viewed as a nucleoside analog targeting viruses directly, it has come to light that ribavirin also exerts its influence on the host's responses. This includes inhibiting inosine monophosphate dehydrogenase (IMPDH) when in its 5-monophosphate form, influencing the host's immune response, and affecting the virus itself by inhibiting viral polymerases, inducing lethal viral mutations, and hindering the capping of viral RNA (Geraghty *et al.* 2021; Ji *et al.* 2020).

The wide range of viruses susceptible to ribavirin can be attributed to the cumulative antiviral effects it provokes. For example, the vital role of IMPDH in the host, in controlling intracellular guanine nucleotide concentrations (GTP and dGTP), can explain ribavirin's efficacy against both DNA and RNA viruses. Furthermore, ribavirin possesses immunomodulatory qualities by altering the behavior of host T cells.

Concerning the virus-specific effects, ribavirin, behaving as a guanosine analog, can interact with enzymes responsible for capping RNA molecules. This is significant because capped RNAs possess a 7-methylguanosine cap structure crucial for RNA stability and translation. The disruption of viral RNA capping is of interest as it triggers the host's antiviral immune response by recognizing foreign viral RNA (Geraghty *et al.* 2021; Ji *et al.* 2020).

Ribavirin also exhibits virus-specific actions by inhibiting the viral RNA-dependent RNA polymerase (RdRp) and promoting lethal viral mutations. Although the precise mechanism by which ribavirin inhibits RdRp remains unclear, it is known to significantly reduce the catalytic efficiency of viral RNA synthesis when incorporated into the viral RNA. *In vitro* studies have shown that ribavirin triphosphate can inhibit the RNA polymerase of various viruses, including Influenza A Virus, Hepatitis C Virus, and Vesicular Stomatitis Virus. Finally, ribavirin elicits antiviral effects through lethal viral mutagenesis against a range of viruses, including Hepatitis C, *in vivo*. Most RNA viruses possess a high mutation rate, allowing them to adapt, evade host immune responses, and drug treatments. However, RNA viruses have a threshold beyond which genetic information cannot be sustained. Altering the viral mutation rate with ambiguous nucleoside analogs, termed lethal mutagenesis, has been proposed as a potential therapeutic approach against high-mutation-rate RNA viruses. Ribavirin increases the frequency of mutations in viral RNA to nonviable levels due to its ambiguous base-pairing capacity. As deleterious mutations accumulate in the viral genome, the virus can no longer maintain the necessary genetic information for survival. This process is referred to as lethal mutagenesis or error catastrophe (Geraghty *et al.* 2021; Ji *et al.* 2020). The understudied family of compounds that induce lethal viral mutagenesis offers a unique opportunity for broad-spectrum antiviral activity, theoretically impacting most high-mutation-rate RNA viruses. In summary, ribavirin's ability to mimic both adenosine and guanosine is advantageous as it enables ribavirin to interact with a variety of enzymes and biological mechanisms crucial to the replication cycle of many viruses. However, a drawback of ribavirin, similar to adenosine and guanosine, is its increased interaction with the host's cellular machinery, resulting in reduced selectivity and increased toxicity, which may lead to undesired side effects, such as severe anemia (Geraghty *et al.* 2021; Ji *et al.* 2020).

Viral protease inhibitors

In addition to the viral polymerase, the viral protease has garnered significant attention as one of the most extensively researched antiviral targets. Virus-specific protease inhibitors have proven to be effective in treating infections caused by HIV and HCV. Exploring the development of protease inhibitors that target multiple virus families represents an intriguing

strategy. Phylogenetic analysis suggests that picornaviruses, caliciviruses, and coronaviruses can be classified within the picornavirus-like supercluster. These viruses all share 3C or 3C-like (3CL) proteases with a characteristic chymotrypsin-like fold and a catalytic triad (or dyad) that includes a cysteine residue as a nucleophile, rendering them attractive targets for BSAA development (Debing *et al.* 2015).

For instance, Rupintrivir is an irreversible 3C and 3CL protease inhibitor initially designed to combat human Rhinovirus infections. It has also demonstrated antiviral activity against other picornaviruses, coronaviruses, and norovirus. Other inhibitors of 3C-like proteases have been identified with broad-spectrum antiviral activity against both feline coronaviruses and caliciviruses. Consequently, designing BSAA that target proteases across various virus families appears to be a feasible and promising strategy for the development of more comprehensive antiviral treatments (Debing *et al.* 2015).

As anticipated in the Coronaviruses paragraph, there is another 3CL protease inhibitor drug of SARS-CoV-2, also called M^{pro}, the nirmatrelvir. This drug is the only M^{pro} inhibitor used clinically in combination with ritonavir. Even in the presence of evolutionary mutations in the M^{pro}-gene, nirmatrelvir protects 90% of SARS-CoV-2 infected individuals from severe COVID-19 and hospitalization by binding the protease catalytic site and preventing viral multiplication. The significant time and costs required are detrimental for keeping up with the pandemic emergency of these last three years. For this reason, it is important to continue the search for a new potent BSAA by synthesizing new molecules or continuing to screen EMA-approved molecules for other disease treatment (drug repurposing) (Ambrosio *et al.* 2023).

1.2.2   Host-Targeting Antivirals

Direct-acting antiviral agents (DAAs), as previously described, have demonstrated a high degree of success in combating viral infections in clinical settings. However, DAAs suffer from several inherent limitations, including narrow-spectrum antiviral profiles and a tendency for drug resistance to develop. As a result, there are still many unmet needs in the treatment of viral infections, especially emerging viral infections.

The solution may lie in small molecules capable of inhibiting viral infection and replication by targeting specific host proteins necessary for the virus to complete its replicative cycle. These antivirals are known as host-targeting antivirals (HTAs) (Maffei *et al.* 2022; Zheng *et al.* 2022; Geraghty *et al.* 2021; Xiong *et al.* 2020).

HTAs work by inhibiting host factors widely exploited by infecting viruses during their replicative cycle, thereby overcoming both the limitations of DAAs. If the target is utilized

by various viruses, the candidate drug could have broad-spectrum activity against different types of viral infections, including emerging ones. Additionally, HTAs have the advantage of overcoming drug resistance (induced by DAAs), as host proteins are not under the genetic control of the viral genome. Therefore, HTAs could become an intriguing and innovative strategy for the development of new antiviral drugs, as it is well-known that viruses cannot complete their replication without the assistance of the host (Zheng *et al.* 2022).

In recent years, significant progress has been made in the development of HTAs, with the approval of the CCR5 chemokine receptor antagonist maraviroc for the treatment of Human Immunodeficiency Virus (HIV) and others in the pipeline for different viral infections (Ji *et al.* 2020).

Host-targeting antivirals (HTAs) complement DAAs and excel in several aspects. The primary advantage of HTAs over the current virus-specific DAAs, which may be inadequate for treating new emerging viruses, is their activity not only against viruses from different families but also against different genotypes of the same viral species. Therefore, HTAs are potentially effective against viruses that have not yet emerged in humans. For this reason, HTAs are suitable as first-line treatments for emerging respiratory virus epidemics or new sexually transmitted infections, thanks to their quick repositioning from one pandemic event to the next emerging one.

For instance, the heat shock protein 90 (Hsp90), a host chaperone responsible for the folding, assembly, and maturation of endogenous proteins, has also been found to be crucial for the maturation of many viral proteins. Hence, Hsp90 inhibitors possess broad-spectrum antiviral activity. Overall, targeting host factors is a highly promising strategy that offers the opportunity to address critical challenges not overcome by DAAs (Ji *et al.* 2020).

Host-targeting antiviral strategies encompass a wide range of host targets, including the inhibition of host proteases to limit viral entry, depletion of intracellular nucleotide pools, kinase inhibition, glycosidase inhibition, immune system activation, and more. Broad-spectrum antiviral strategies targeted at viruses have their challenges: the diversity of viral protein structures and sequences makes it particularly challenging to design compounds with broad action, often resulting in a limited range of antiviral applications. To date, only one class of compounds, nucleoside analogs, has shown promise for broad-spectrum antiviral applications in clinical practice, but they come with drug-induced toxicity and a tendency to select drug-resistant strains (Zheng *et al.* 2022; Geraghty *et al.* 2021; Xiong *et al.* 2020).

However, HTAs are also burdened with the potential for high cellular toxicity, as well as limited translatability from *in vitro* to *in vivo* due to the systemic compensation of the effects of blocking a specific cellular pathway. The feasibility of host-targeting antiviral strategies

will likely depend on which host factor is targeted and how viruses and cells rely on its functions. Clearly, the trade-offs, at least theoretically, of these disadvantages may be acceptable in the design of new intervention strategies based on HTAs, depending on the threat posed by an emerging viral infection, the characteristics of the causative agent, and the duration of treatment, with the ultimate goal of expanding the therapeutic window of HTAs. Furthermore, treatment of acute viral infections takes only a few days, greatly facilitating tolerance of the relevant toxicity by the target host pathway (Zheng *et al.* 2022; Geraghty *et al.* 2021; Xiong *et al.* 2020; Ji *et al.* 2020).

The most commonly used host targets for antiviral treatment are for example: dihydroorotate dehydrogenase (DHODH), chemokine receptor type 5, inosine monophosphate dehydrogenase, cyclophilins, eukaryotic initiation factor 2α, dihydrofolate reductase (Zheng *et al.* 2022).

Here are some examples of HTAs currently being approved: modulators of host lipid metabolism, nitazoxanide, cyclophilin inhibitors, and pyrimidine synthesis inhibitors.

Modulators of lipid metabolism

Many viruses rely heavily on the host's lipid metabolism to reproduce. As a result, lipid metabolism is considered a primary target for Broad-Spectrum Antiviral Agents (BSAA). One of the most commonly used categories of lipid regulators are the statins, which are known for reducing cholesterol levels. Statins inhibit the activity of the enzyme 3-hydroxy-3-methyl-glutaryl coenzyme A reductase, which is the rate-limiting step in cholesterol production in the liver. *In vitro* studies have shown that statins possess antiviral properties against a variety of viruses, including HCV, HIV, poliovirus, cytomegalovirus, dengue virus, and RSV. However, clinical studies on statins' antiviral effectiveness in patients have produced conflicting results. For example, when used as a monotherapy in HCV-infected patients, the antiviral effect of statins was modest or even absent. Yet, when combined with the previous standard of care, which included pegylated interferon-a and ribavirin, a significant increase in sustained virological response rates was observed. More research is needed to establish the *in vivo* antiviral efficacy of statins as BSAA (Debing *et al.* 2015; Ji *et al.* 2020).

Arbidol is another lipid regulator approved for prophylaxis and treatment of Influenza and other respiratory viral infections in China and Russia. This indole derivative also inhibits the replication of various enveloped and non-enveloped RNA and DNA viruses, including HBV, HCV, and chikungunya virus. Recent studies suggest that arbidol has a dual mechanism of action, involving binding to lipid membranes and interaction with aromatic amino acids in viral envelope glycoproteins. This interference disrupts viral entry and membrane fusion.

Arbidol offers good bioavailability and a safe patient usage record, making it a promising candidate for BSAA. However, there is a limited availability of *in vivo* studies confirming its antiviral effects (Debing *et al.* 2015; Ji *et al.* 2020).

LJ001 is a lipophilic thiazolidine derivative effective against several enveloped viruses, including Influenza, HIV, and Filoviruses. However, it has no impact on non-enveloped viruses. LJ001 targets the viral lipid envelope and impedes its role in virion-cell fusion. Recent research indicates that LJ001 induces lipid oxidation, negatively affecting membrane properties such as curvature and fluidity, which are necessary for viral fusion. Unfortunately, LJ001 itself is not suitable for further development due to its poor physiological stability and its reliance on light for its antiviral mechanism. New analogues have been developed to address these drawbacks, demonstrating improved antiviral activity, better pharmacokinetics, and altered light-absorbing properties. Nevertheless, when evaluated in a mouse infection model of Rift Valley fever virus, these molecules only delayed the time of death. While this specific class of molecules may be less suitable for clinical development, the viral membrane remains a potential target for BSAAs that disrupt viral-cell fusion.

Squalamine is another compound that targets host membranes, but its mechanism of action differs from LJ001 and its analogues. Squalamine is a compound derived from the dogfish shark and sea lamprey and inhibits both enveloped RNA and DNA viruses *in vitro* and *in vivo*. Its proposed mechanism of antiviral activity involves neutralizing the negative electrostatic surface charge of intracellular membranes, making the cellular environment less favorable for viral replication. This disruption of electrostatic potential does not result in structural damage to cellular membranes, as indicated by changes in cell permeability. Squalamine can be easily synthesized and has already been studied in humans in several phase 2 clinical trials for cancer and retinal vasculopathies without serious adverse events, making it a potential candidate for use as a BSAA (Debing *et al.* 2015; Ji *et al.* 2020).

Nitazoxanide

Nitazoxanide was originally formulated and brought to market as an antiprotozoal agent. In the United States, it gained approval as an orphan drug for the management of diarrhea induced by Cryptosporidium parvum and Giardia intestinalis. It is also widely employed in India and Latin America for treating parasitic infections affecting the intestines. Apart from its antiparasitic properties, nitazoxanide has the capability to inhibit a diverse array of unrelated RNA and DNA viruses. It hinders the maturation of the viral hemagglutinin in the Influenza virus at the post-translational stage. In cell cultures infected with HCV, nitazoxanide triggers protein kinase R, a crucial component of the innate immune system. Mercorelli et al. have shown that NTZ also inhibits the viral replication of hCMV: a block

of viral DNA synthesis and a reduction in the expression of viral proteins were observed following treatment with the molecule (Mercorelli *et al.* 2016).

Nitazoxanide's antiviral effectiveness has been assessed in patients as well. A clinical study in phase 2b/3, involving individuals with laboratory-confirmed Influenza, revealed that nitazoxanide shortened the duration of clinical symptoms and reduced viral shedding compared to a placebo. A substantial phase 3 trial is currently in progress. Phase 2 investigations have also illustrated that nitazoxanide notably lessened the duration of symptoms in patients infected with rotavirus or norovirus. In the case of HCV-infected patients, clinical studies demonstrated enhanced responses when nitazoxanide was combined with pegylated interferon; nevertheless, the clinical development for HCV treatment was halted due to the recent approval of direct-acting antivirals. Nitazoxanide's wide-ranging antiviral capabilities, coupled with its high resistance barrier and established *in vivo* effectiveness against certain viral infections, position it as an appealing candidate for development as a BSAA. The primary focus of the initial clinical development of this drug will center on viral respiratory infections and gastroenteritis. Nitazoxanide serves as the foundational structure for a novel class of medications known as thiazolides (Debing *et al.* 2015; Ji *et al.* 2020).

Cyclophilin antagonists

The cyclophilins are peptidyl-prolyl cis/trans isomerases that are necessary for the correct folding of specific host proteins and also play a crucial role in the life cycles of various viruses. Cyclosporine A and sanglifehrin A are immunosuppressive compounds that hinder cyclophilins. Through chemical alteration, analogs were created without immunosuppressive characteristics. These cyclophilin antagonists obstruct a wide array of RNA and DNA viruses, both *in vitro* and in animal models. The most advanced compounds are alisporivir and SCY-635. These substances exhibited therapeutic effectiveness in HCV-infected patients. Mechanistically, cyclophilin A (CypA) was demonstrated to interact with the HCV NS5A protein, and numerous mutations in NS5A were needed to convey *in vitro* resistance to alisporivir, implying a substantial hurdle to resistance. In the case of HIV, it was documented that CypA binds to the capsid protein p24. Although cyclophilin inhibitors vigorously repress HIV infection *in vitro* and, in most patients, naturally occurring capsid variations resistant to treatment were observed, which prevents the extensive therapeutic application of cyclophilin inhibitors against HIV. Nonetheless, since cyclophilins are indispensable for the replication of many viruses, these proteins may be intriguing targets within the host for the development of BSAA. Moreover, CypA knockout experiments in a human cell line and in mice indicated that CypA is not indispensable for fundamental cell

survival, mitigating concerns about associated cellular toxicity. Nevertheless, the *in vivo* efficacy of cyclophilin inhibitors will need to be established for other viruses (Debing *et al.* 2015; Ji *et al.* 2020).

1.2.2.1 Pyrimidine biosynthetic pathway and DHODH inhibitors

The development of broad-spectrum antiviral therapies that act on the host remains an important but elusive goal in anti-infective drug discovery. To replicate efficiently, viruses not only depend on their hosts for an adequate supply of pyrimidine nucleotides, but also regulate the biosynthesis of pyrimidine nucleotides in infected cells.

Pyrimidine nucleosides are heterocyclic aromatic metabolites that include uridine, cytidine and thymidine. In addition to their fundamental role in nucleic acid biosynthesis, they are required for carbohydrate and lipid metabolism (Zheng *et al.* 2022; Okesli *et al.* 2017).

Mammalian cells derive pyrimidine nucleotides through a combination of *de novo* biosynthesis and recovery. The pathway has been studied in detail in bacteria, fungi and mammals and appears to be universal. This pathway represents one of the earliest metabolic processes and all its steps have remained intact during evolution (**Figure 3**).
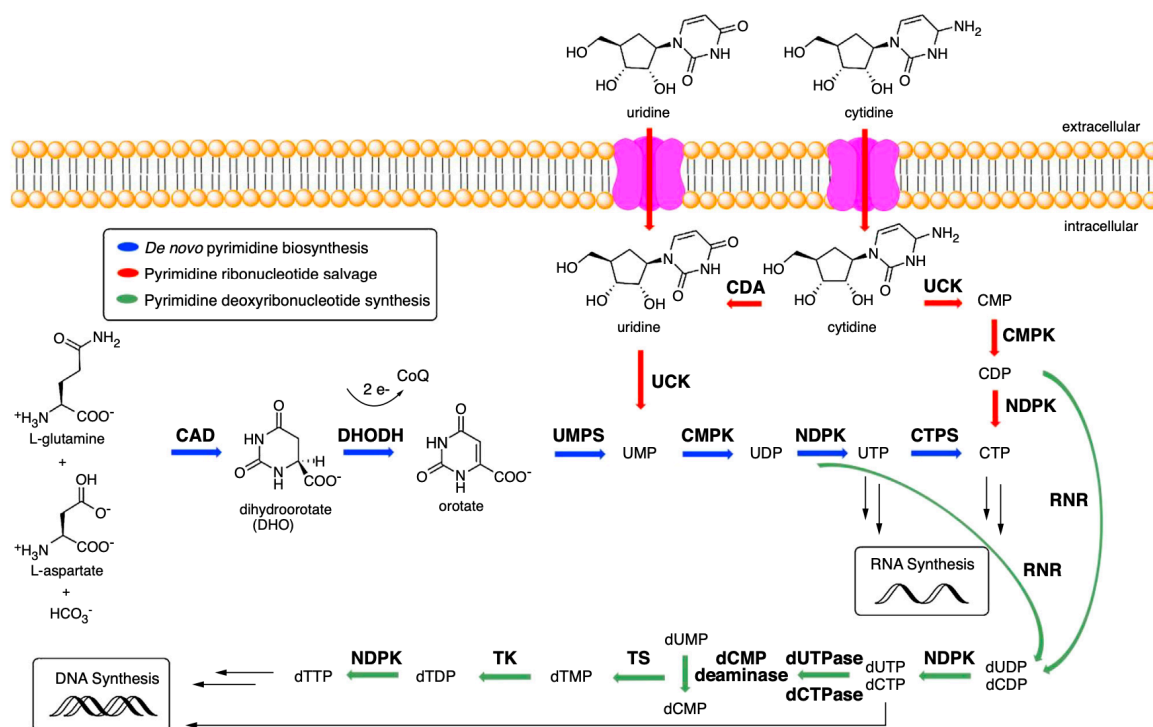
Figure 3. *Representation of pyrimidines synthesis: de novo pyrimidine biosynthetic pathway and salvage pathway (Okesli et al. 2017).*

The first three steps of the pyrimidine pathway are catalyzed by a large multifunctional enzyme complex called CAD, which acts as a carbamoyl phosphate synthase. It catalyzes the production of dihydroorotate (DHO) from carbamoyl phosphate, glutamine and aspartate

together with two ATP equivalents (Zheng *et al.* 2022; Boschi *et al.* 2019; Okesli *et al.* 2017).

In addition to energy metabolism, mitochondria are also important organelles for the *de novo* biosynthesis of pyrimidines, in fact the fourth step of pyrimidine biosynthesis occurs via a protein present in the inner mitochondrial membrane, the dihydroorotate dehydrogenase (DHODH), leading to the generation of uridine monophosphate (UMP) that can yield pyrimidines needed for biosynthesis of nucleic acids in proliferating cells. DHODH is the only redox enzyme of the six enzymes involved in the *de novo* biosynthesis pathway, which then oxidizes DHO to orotic acid (ORO) by transferring 2 electrons to coenzyme Q (CoQ, ubiquinone) in the respiratory mitochondrial chain (Zheng *et al.* 2022; Boschi *et al.* 2019; Okesli *et al.* 2017; Reis *et al.* 2017).

The fifth step in the pathway is the production of orotidine 5' monophosphate (OMP) from ORO and phosphoribosyl pyrophosphate (PRPP) by ORO phosphoribosyltransferase (OPT). Finally, decarboxylation of OMP into uracil monophosphate (UMP) by orotidine 50-phosphate decarboxylase (or uridine monophosphate synthase, UMPS) takes place.

UDP and UTP are synthesised by cytidine monophosphate kinase (CMPK) and nucleoside diphosphate kinase (NDPK), respectively. UTP is converted to CTP by CTP synthetase (CTPS) in an ATP-dependent reaction using glutamine as an amine donor. Alternatively, UDP and CDP are deoxygenated into deoxy-UDP (dUDP) and dCDP respectively by ribonucleotide reductase (RNR) and further phosphorylated by NDPK. To avoid misincorporation into DNA, dUTP is rapidly broken down by dUTPase into dUMP.

dUMP is a substrate of thymidylate synthase, which produces deoxy-TMP (dTMP) that can be phosphorylated into dTTP. Therefore, the *de novo* biosynthetic pathway in mammals is able to provide all pyrimidine ribonucleotides (CTP, UTP) and deoxyribonucleotides (dCTP, dTTP) for RNA and DNA biosynthesis, respectively. In addition to *de novo* biosynthesis, pyrimidine nucleotides can also be recovered from intracellular nucleic acid degradation or from extracellular nucleosides circulating in the bloodstream. The latter pathway depends on various nucleoside transport channels and pumps in mammalian cells. The relative importance of *de novo* biosynthesis and rescue varies from organ to organ and is also strongly dependent on the physiological state of the cells (Zheng *et al.* 2022; Boschi *et al.* 2019; Okesli *et al.* 2017).

Instead, regarding the salvage pathway by which the organism recycles pyrimidines, RNA catabolism produces UMP and CMP, which can be converted into the corresponding NTPs through the subsequent action of CMPK1 and NDPK. With a plasma concentration of 5 mM, uridine is the dominant circulating nucleoside in mammals; plasma concentrations of all

other pyrimidine nucleosides are at least an order of magnitude lower and are therefore insufficient to support the cellular demands for the corresponding nucleotides by direct rescue. Uridine/cytidine kinase (UCK) converts the transported pyrimidine nucleosides into the corresponding NMPs, which can be further phosphorylated and modified as discussed above. Since both *de novo* biosynthesis and intracellular and extracellular recovery require the activity of CMPK1, this enzyme is essential for pyrimidine utilization in all cells (Okesli *et al.* 2017).

The multifunctional protein CAD is the primary site for the regulation of *de novo* pyrimidine biosynthesis. Transcription factors such as Myc are known to induce its gene expression. The enzyme is activated by phosphorylation catalyzed by MAP kinase before the S-phase of the cell cycle and is inhibited by phosphorylation catalyzed by protein kinase A at a distinct site at the end of the S-phase. CAD is also activated by phosphorylation at a third site by the mammalian target of rapamycin complex 1 (mTORC1) or ribosomal protein S6 kinase 1 (p70S6K), thus enabling post-translational control in response to increase anabolic activity in the cell. The activity of KLA, which plays a key role in the recovery of pyrimidine nucleosides, is also subject to both negative regulation by CTP and UTP (i.e., the products of the final pathway) and positive regulation by ATP. This dual control is achieved through changes in the quaternary structure of KLA; CTP and UTP are competitive inhibitors (Ki 6 mM) that stabilize its inactive monomeric state, while ATP allosterically stabilizes KLA as an active tetramer. Finally, CMPK1, which lies at the intersection of *de novo* biosynthesis and intracellular/extracellular rescue, is subject to feedback regulation of its activity by CTP, UTP and dCTP, but not dTTP (Zheng *et al.* 2022; Okesli *et al.* 2017).

In addition, *in vitro* analysis revealed the need for reducing agents to maintain their catalytic activity, suggesting that intracellular redox potential may also play a significant role in controlling metabolic flux at this stage.

The pyrimidine synthesis pathway is a possible HTA target

Viruses are obligate parasites that rely entirely on the host's internal environment to produce viral progeny. Therefore, viruses usually must hijack the host machinery to replicate.

While most drugs that block the biosynthesis of pyrimidine nucleotides are targeted at chemotherapy or cancer immunosuppression, a deeper understanding of these metabolic pathways in humans could also be the basis for the design of new antiviral therapies. Pyrimidine is a heterocyclic compound and a vital component of cells. Therefore, antivirals targeting the pyrimidine synthesis pathway may be effective and have a broad spectrum of activity (Zheng *et al.* 2022; Okesli *et al.* 2017).

Pyrimidine participates in the synthesis not only of nucleotides but also of polysaccharides and phospholipids, which play an essential role in human metabolism. When cells become cancerous or infected by pathogenic microorganisms, the overall metabolic activity and demand for pyrimidines increase compared to those of quiescent cells. Munger et al. studied human fibroblasts infected with human Cytomegalovirus (HCMV) using liquid chromatography-tandem mass spectrometry and identified 167 differentially abundant metabolites (Zheng *et al.* 2022).

Among these metabolites, those linked to *de novo* pyrimidine biosynthetic pathways, such as carbamoyl-aspartic acid, cytidine triphosphate, uridine triphosphate and thymidine triphosphate, were significantly enriched compared to those in the uninfected group. Gribaudo et al. also showed that infection with cytomegalovirus in quiescent fibroblast cells stimulates thymidylate synthase expression (Gribaudo *et al.* 2002). These reports suggested that viruses would hijack the host pyrimidine synthesis pathway to promote their replication, as when viruses infect host cells, they increase the biosynthetic flux of nucleotides. Thus, not only would nucleotide biosynthesis inhibitors have the potential to neutralize a wide range of viruses, but their probability of eliciting drug-resistant mutants might also be lower than drugs targeting viral proteins (Zheng *et al.* 2022; Okesli *et al.* 2017).

However, due to the recycling of exogenous pyrimidines, inhibitors of uridine and cytidine synthesis (activated by the virus) lose their effectiveness *in vivo*. This opens up a new prospect of research into the combination of an inhibitor of pyrimidine synthesis and an inhibitor of exogenous uridine reuptake, such as dipyridamole, which inhibits ENT 1 and 2, as well as being an antiplatelet agent approved for the prophylaxis of thromboembolisms in cardiovascular diseases. Blocking the UCK-UCK2 isoenzyme strongly sensitizes cells to this class of inhibitors. This territory is currently very little explored *in vitro*, and *in vivo* even less so, so this could be an interesting new avenue of research to find an effective HTA. Another solution to the problem of pyrimidine reuptake could be the inhibition of CMPK1. Indeed, given its position at the convergence point of *de novo* biosynthesis and rescue, a CMPK1 inhibitor could be sufficiently effective *in vivo* even as a form of monotherapy. DHODH could be a perfect target for developing an HTA (Zheng et al. 2022).

Step 4 is the rate-limiting step in the *de novo* synthesis pathway, and dihydroorotate dehydrogenase (DHODH) is the only enzyme that oxidizes dihydroorotate acid (DHO) to orotate (ORO).

This specific role of DHODH, which is involved in the *de novo* synthesis of pyrimidine and links this pathway to the electron transport chain of aerobic respiration, makes DHODH the

most attractive pharmacological target in the pyrimidine synthesis pathway (Zheng *et al.* 2022).

DHODH inhibitors (DHODHi) are being developed to treat malignant tumors, autoimmune diseases, viral or bacterial infections, parasitic diseases and other diseases.

DHODHi inhibit viral infection by three mechanisms (**Figure 4**):

1. inhibiting viral replication
2. by promoting the expression of interferon-stimulated genes (ISGs)
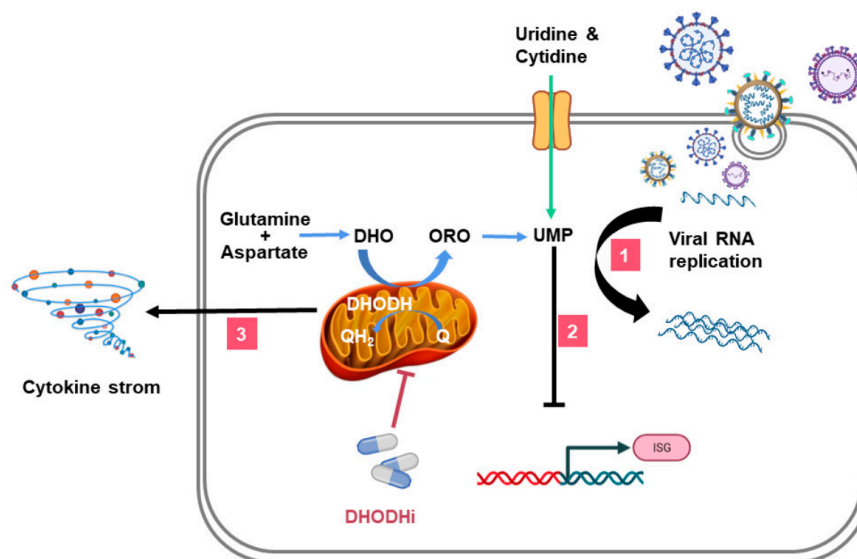3. by regulating inflammation.

Figure 4. Representation of the three mechanisms that an DHODHi could use to inhibit the viral replication (Zheng et al. 2022).

Regarding the first mechanism exerted by this class of inhibitors, it was observed that DHODHi inhibited the replication of RNA and DNA viruses from the early stages of the viral replication cycle. For example: in a Vero cell model infected with Junin virus (MOI = 0.1), teriflunomide 50 uM mainly inhibited viral replication in the early and intermediate phases (0-6 hours after infection). Interestingly, in Vero or A549 cell models infected with DENV serotype 2 (MOI = 2), brequinar inhibited not only the early and intermediate phases, but also the later phases (RNA synthesis, virion assembly or release) of the viral replication cycle. While in primary human embryonic lung fibroblasts infected with HCMV (Towne strain), treatment with a DHODH inhibitor called FK778 showed a potential antiviral effect with an EC50 of 1.97 uM. In the A549 cell model infected with human adenovirus 5 (MOI = 5), virus titers were reduced by 6 logarithms following treatment with a compound called A3 (Zheng *et al.* 2022; Okesli *et al.* 2017).

The second mechanism of action of DHODHi is the stimulation of ISGs: it was observed by Lucas-Hourani et al. that there was a link between pyrimidine biosynthesis and the

expression of ISGs, and they identified a DHODHi, DD264, which possessed ideal antiviral effects by enhancing the expression of ISGs. Supplementation with uridine abolished the amplification of ISG expression by DD264, thus confirming the link between these two mechanisms (Zheng *et al.* 2022).

However, it remains unclear whether DHODHi's induction of ISG expression depends on the classical JAK-STAT pathway. Jin et al. used the JAK inhibitor CP-690550 to block the JAK-STAT pathway in HEK293T cells infected with small ruminant plague virus (PPRV). Surprisingly, ISG transcription could still be upregulated by brequinar. This result indicated that the induction of ISGs by brequinar was independent of the JAK-STAT pathway. Furthermore, a study on Influenza virus suggested that leflunomide could still play an antiviral role after inhibiting tyrosine phosphorylation of JAK1 and JAK3. In contrast, the antiviral activity of FA-613 was based on stimulation of interferon-dependent ISGs. It appears that different DHODHi activate the expression of ISGs by triggering different pathways (Zheng *et al.* 2022).

Finally, the third mechanism of action of these inhibitors was confirmed to be the production of inflammatory cytokines. Cytokines and chemokines have long been thought to play an essential role in immunopathology during viral infection, as excessive virus-induced inflammation contributes to severe disease and death. DHODHi, such as leflunomide and teriflunomide, have been used clinically to treat autoimmune diseases and suppress cytokine production; thus, they could also regulate excessive virus-induced inflammation. Indeed, it has been shown that the combination of S312 and oseltamivir significantly reduced the levels of the pathogenic inflammatory cytokines IL6, MCP-1, IL5, KC/GRO (CXCL1), IL2, IFN-y, IP-10, IL9, TNF-a, GM -CSF, EPO, IL12p70, MIP3a and IL17A/F in Influenza A Virus-infected mice. Similarly, it has been reported that high levels of inflammatory factors are positively correlated with the severity of COVID-19, such as those of IL-2, IL-6, IL-7, IL-10, G-CSF, MCP, MIP1a, IFN -y, IP-10 and TNF-a. Preliminary studies indicated that leflunomide could regulate hyperinflammation reactions in people with severe SARS-CoV-2 infection by reducing the levels of pathogenic inflammatory cytokines and consequently reducing lung inflammation and serum C-reactive protein levels in patients with COVID-19 (Zheng *et al.* 2022; Okesli *et al.* 2017).

Furthermore, DHODHi would offer a dual effect in minimizing the immune overreaction induced by the viral infection. SARS-CoV-2 is believed to induce lung damage in two phases. The virus replicates directly in the lungs, causing lung tissue damage in the first phase. The second phase is characterized by the massive expression of cytokines and chemokines and the migration of immune cells to the lungs, resulting in an excessive

inflammatory response. The severity of tissue damage in the first stage determines the degree of inflammation in the second stage. Therefore, DHODHi could act in both stages to reduce lung damage by limiting viral replication in the first stage and further inhibit the overexpression of cytokines and chemokines from residual tissue damage in the second stage (Zheng *et al.* 2022).

Thus, a variety of DHODHi have been shown to inhibit viral infection *in vitro* and *in vivo*, several already have clinical applications and have therefore been approved for use, many are still in the experimental phase. Currently, all human DHODHi target the ubiquinone binding site in the N-terminal domain of DHODH (aa 30-68). Below is a description of some of the most promising DHODH inhibitors.

- *Leflunomide and Teriflunomide*

Leflunomide functions as a prodrug that can undergo metabolism to produce its active metabolite, teriflunomide. Teriflunomide, in turn, noncompetitively inhibits DHODH activity by binding to ubiquinone at an IC50 value of approximately 600 nM. The FDA has granted approval for the clinical treatment of rheumatoid arthritis and psoriatic arthritis for leflunomide, and for multiple sclerosis in the case of teriflunomide (Sanders *et al.* 2002).

Both compounds, leflunomide and teriflunomide, have demonstrated various antiviral activities *in vitro*. They exhibit inhibitory effects on the replication of various viruses, including SARS-CoV-2, Cytomegalovirus, Herpesvirus, BK Virus, Epstein-Barr Virus, RSV, and Influenza Virus. In an anti-Junin virus study, teriflunomide, when used in combination with the DAA drug ribavirin, exhibited superior antiviral activity compared to single-drug treatment. Leflunomide, in Influenza A Virus (H5N1 or H1N1)-infected mouse models, mitigated weight loss, reduced viral load in the lungs, and prolonged survival time. Teriflunomide, in the same study, inhibited H5N1 virus replication by blocking the activity of Janus kinase 1 (JAK1) and JAK3. Studies also indicated that both leflunomide and teriflunomide could prevent the reduction in alveolar fluid clearance post-RSV infection (Zheng *et al.* 2022; Sainas *et al.* 2021; Sainas *et al.* 2018; Okesli *et al.* 2017).

Moreover, leflunomide demonstrated strong anti-SARS-CoV-2 activity *in vitro*, with teriflunomide exhibiting approximately 2.6-fold higher antiviral activity than favipiravir, a DAA inhibiting viral RdRp. Leflunomide was also tested in a clinical trial for COVID-19 therapy at the People's Hospital of Wuhan University, China. Compassionate use results showed that patients taking leflunomide had a significantly shorter shedding time (median 5 days) compared to control patients (median 11 days). Additionally, C-reactive protein levels were reduced in leflunomide-treated patients, confirming its dual antiviral and anti-inflammatory functions (Zheng *et al.* 2022).

- *Brequinar*

Brequinar, a more potent DHODHi with an IC50 value of 10 nM for human DHODH compared to leflunomide or teriflunomide, has FDA approval for rheumatoid arthritis and multiple sclerosis. In contrast to the noncompetitive binding of leflunomide and teriflunomide, brequinar competitively binds to ubiquinone, disrupting the catalytic cycle of DHODH. Brequinar has demonstrated broad-spectrum antiviral activity against various viruses *in vitro*, including Flaviviruses, Western Equine Encephalitis Virus, EBOV, Influenza Virus, Enterovirus, Respiratory Syncytial Virus, Herpesvirus, and Vesicular Stomatitis Virus. Additionally, adding exogenous uridine could reverse the antiviral activity *in vitro*, indicating that the antiviral effect of brequinar may be attributed to affecting pyrimidine synthesis. Furthermore, a study by Li et al. demonstrated that brequinar exhibited antiviral efficacy in mice: brequinar significantly prolonged the survival time of infected mice and provided a 25% protection rate at 5 dpi (the virus-infected mice all died within 60 h). For SARS-CoV-2, Xiong et al. demonstrated that brequinar showed excellent anti-SARS-CoV-2 effect with CC_{50} = 231.30 uM, EC_{50} = 0.123 uM, and SI = 1880.49. Schultz et al. also found that, in a model of wildtype BALB/c mice infected with the SARS-CoV-2 Beta strain, combined treatment of brequinar and molnupiravir significantly reduced viral titers and pathology compared to using molnupiravir alone (Zheng *et al.* 2022; Sainas *et al.* 2021; Sainas *et al.* 2018; Okesli *et al.* 2017).

- *S312 and S416*

S312 and S416, identified by Zheng et al., represent potent DHODHi with a novel thiazole derivative scaffold, exhibiting IC50 values of 29.2 nM and 7.5 nM, respectively (Zheng *et al.* 2022).

In vitro experiments have proven the broad-spectrum antiviral activity of S312 and S416, including against Influenza A Virus (H1N1, H3N2, and H9N2), Zika virus, EBOV, and SARS-CoV-2. It was worth noting that S312 ($EC50$ = 1.56 uM, SI = 101.41) and S416 ($EC50$ = 0.017 uM, SI = 10,505.88) showed excellent anti-SARS-CoV-2 efficacy in Vero cells. *In vivo* experiments in Influenza-infected mice showed that S312 was superior to oseltamivir (the DAA targeting neuraminidase of Influenza Viruses) in treating the late infection phase and reducing cytokine and chemokine storms in Influenza Virus-infected mice because of its dual antiviral and immune regulation activities. In addition, combined with oseltamivir, S312 could confer an additional 16.7% survival in the severely late infection stage (Zheng *et al.* 2022).

- *PTC299*

PTC299 is an oral DHODHi displaying an IC50 value of 1 nM for human DHODH. It possesses favorable drug properties targeting hematological tumors and normalizes vascular endothelial growth factor levels in cancer patients. Research by Luban et al. revealed that PTC299 effectively inhibits SARS-CoV-2 replication with minimal cytotoxicity in Vero E6 cells (CC50 > 10,000 nM, EC50 = 2.6 nM, SI > 3800). The study also suggested its broad-spectrum antiviral activity against various viruses, including EBOV, poliovirus, hepatitis C virus genotype 1b, and Rift Valley fever virus. Additionally, PTC299 exhibits a dual mechanism by inhibiting viral replication and reducing the production of inflammatory cytokines such as interleukin (IL)-6, IL-17A, and IL-17F (Zheng *et al.* 2022; Luban *et al.* 2021).

- *IMU-838*

IMU-838, another oral selective immunomodulator, inhibits the intracellular metabolism of activated immune cells by blocking DHODH activity at an IC50 value of 160 nM. Its active moiety, vidofludimus, demonstrates broad-spectrum antiviral activity *in vitro*, including against SARS-CoV-2. Notably, the combination of IMU-838 and remdesivir (a DAA) significantly reduces viral yield in SARS-CoV-2-infected cells, highlighting the effectiveness of combining a DHODHi and DAA (Zheng *et al.* 2022).

- *Compound A3*

Compound A3, identified by Hoffmann et al., is an inhibitor of Influenza virus replication with low toxicity and high antiviral activity (CC50 = 268 uM, EC50 = 0.178 uM, SI = 1505). It exhibits broad-spectrum antiviral activity against retroviruses, RNA viruses, and DNA viruses. Inhibition of human DHODH at an IC50 of 1.13 uM, Compound A3 proves more effective in combination with ribavirin (an HTA, a guanosine analog) in anti-arenavirus studies, emphasizing the therapeutic benefits of combining a DHODHi and another HTA (Zheng *et al.* 2022; Hoffmann *et al.* 2011).

- *FA-613*

FA-613, discovered through screening compounds targeting Influenza Virus nucleoprotein, inhibits Influenza A Virus infection. It demonstrates broad-spectrum antiviral efficacy against various viruses, including Enterovirus A71, highly pathogenic Influenza A Virus (H5N1 and H7N9), RSV, SARS-CoV, MERS-CoV, and human Rhinovirus A. FA-613 exhibits almost no cytotoxicity at effective antiviral concentrations and shows promise in protecting mice from death when challenged with Influenza A/HK/415742Md/2009 (H1N1). Although FA-613's potential targeting of DHODH is suggested, direct inhibition remains uncertain (Zheng *et al.* 2022).

- *BAY2402234*

BAY2402234 is a novel potent selective DHODHi with an IC50 of 1.2 nM. Research by Mathieu et al. indicates that BAY2402234 blocks almost 100% of SARS-CoV-2 particle production at 0.6 uM. Furthermore, a combination of teriflunomide, IMU-838/vidofludimus, and BAY2402234 exhibits substantial inhibition of SARS-CoV-2 replication and significantly reduces viral yield in cells infected with wildtype, the Alpha variant, and the Beta variant of SARS-CoV-2 (Zheng *et al.* 2022; Sainas *et al.* 2021).

- *RYL-634*

RYL-634, a potent inhibitor targeting human DHODH with an IC50 of 60 nM, demonstrates excellent broad-spectrum antiviral activity against Hepatitis C Virus, DENV, Zika Virus, Chikungunya Virus, Enterovirus 71, Human Immunodeficiency Virus, RSV, and Influenza Virus. Recent research by Gong et al. highlights RYL-634's high antiviral activity (EC50 = 0.079 uM) in EBOV-infected Huh7 cells (MOI = 0.1) (Zheng et al. 2022).

1.2.2.1.1 MEDS433

Lolli et al. developed a novel class of hDHODH inhibitors, which are based on an unusual carboxylic group bioisostere 2-hydroxypyrazolo[1,5-a]pyridine, that has been designed starting from brequinar, one of the most potent hDHODH inhibitors (Sainas *et al.* 2018; Sainas *et al.* 2021).

To date they are extensively studied for the treatment of Acute Myeloid Leukemia (AML), restoring myeloid differentiation in AML cell lines (Sainas *et al.* 2021). Among the brequinar -derivatives hDHODH inhibitors, a combination of structure-based and ligand-based strategies produced compound 4, named MEDS433 (**Figure 5**), which shows brequinar-like *h*DHODH potency *in vitro* and is superior in terms of cytotoxicity (Sainas *et al.* 2018).
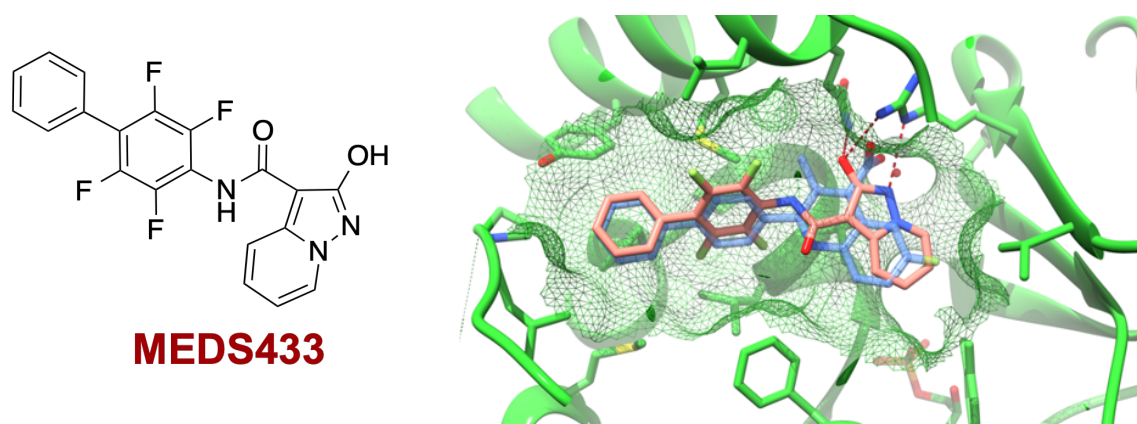
Figure 5. *On the left, the chemical structure of MEDS433; on the right, ubiquinone binding sites of hDHODH co-crystallized with* ***MEDS443*** *(blue) (PDB id: 6FMD), superimposed on the complex with brequinar analogue (pink) (PDB id:1D3G) (Sainas et al. 2021).*

MEDS433, as showed in figure 5, bind better than brequinar, the ubiquinone binding site showing IC_{50} 1.2 nM, compared to the 1.8 nM of the brequinar. MEDS433 had, also, 320 times higher activity when compared to teriflunomide ($IC_{50} = 388$ nM) (Sainas *et al.* 2018). Thus, this molecule seems to have a good chance of becoming a possible HTA with antiviral activity against a wide range of viruses.

In this regard, as a doctoral project, we verified the antiviral activity of MEDS433 against those viruses that still require surveillance due to the lack of adequate therapies or the possibility of new outbreaks, such as Coronaviruses, RSV, IV and HSV.

2. AIM OF THE STUDY

Viruses are one of the major causes of morbidity and mortality in the world against which antiviral drugs and vaccines have been developed to combat viral infections.

If in the past the dogma "one drug, one virus" was in force, often resulting in the emergence of viruses resistant to the drugs used, after the numerous outbreaks of emerging and re-emerging viruses, such as SARS-CoV-1, influenza virus, MERS, Ebola, Zika, SARS-CoV-2, the new paradigm of "one drug, more viruses" seems more appropriate.

If a true broad-spectrum antiviral agent (BSAA), was available, it would have an additional weapon to fight new viruses during a pandemic event.

Among BSAAs, Host-Targeting Antivirals (HTAs) acts by interfering with cellular biochemical pathways commonly used by different viruses for the replication, thus overcoming the problem of direct-acting antivirals, virus specificity and potential viral mutagenesis.

An example may be HTAs designed to target *de novo* biosynthesis of pyrimidines. When growing, mammalian cells demand the acquisition of pyrimidines necessary for DNA and RNA synthesis to *de novo* biosynthesis pathway (DNB), leaving the salvage pathway, in which intact pyrimidine are outsourced, to feed their resting state. In virus-infected cells, DNB is critical in supplying large intracellular nucleotide pools required for replication of viral genomes. Human dihydroorotate dehydrogenase (*h*DHODH) is a key enzyme of DNB that catalyzes the biosynthesis of orotate, precursor of uridine (U) and cytosine (C). It has been observed in different models that virus replication is largely restricted in cells where the *h*DHODH gene was inactivated or the *h*DHODH activity was blocked. By contrast, host cell growth was not affected by lack of *h*DHODH at all, thus indicating that *de novo* nucleotides biosynthesis is not required, at least for some days, in uninfected cells. Small molecules able to interfere with *h*DHODH enzymatic activity may therefore have a great potential in reducing viral replication.

The aim of this PhD project was to characterize a novel small molecule named MEDS433 with high potency toward *h*DHODH, representative of a novel class of *h*DHODH inhibitors based on a hydroxypyrazole-pyrimidine scaffold. MEDS433 could be a possible broad-spectrum antiviral compound, which will represent a valuable resource for future treatments of infections caused by several viruses. In fact, we decided to test this molecule in particular against the most common viruses that affect the world people, such as the Herpes Simplex Virus 1 and 2 (HSV-1 and -2), the Influenza A and B Viruses (IAV and IBV), the Respiratory Syncytial Virus A and B (RSV-A and -B), the α-Coronavirus 229E (hCoV-229E), the β-

Coronaviruses OC43 (hCoV-OC43) and Severe Acute Respiratory Syndrome Coronavirus 2 (SARS-CoV-2). All these viruses are classified by the WHO as viruses to be monitored annually due to their high mutagenicity which leads to resistance against the DAAs currently in use, as happens for HSV, due to the possible appearance of new highly contagious strains, as for IV and Coronavirus, or due to the lack of approved and clinically usable drugs, as for RSV.

3. RESULTS

Research paper

Effective deploying of a novel DHODH inhibitor against herpes simplex type 1 and type 2 replication

Anna Luganini [a,1], Giulia Sibille [a,1], Barbara Mognetti [a], Stefano Sainas [b],
Agnese Chiara Pippione [b], Marta Giorgis [b], Donatella Boschi [b], Marco L. Lolli [b],
Giorgio Gribaudo [a,*]

[a] *Department of Life Sciences and Systems Biology, 10123, Turin, Italy*
[b] *Department of Sciences and Drug Technology, University of Turin, 10125, Turin, Italy*

ARTICLE INFO

Keywords:
Herpes simplex virus type 1 and type 2
Antiviral activity
de novo pyrimidine biosynthesis
Dihydroorotate dehydrogenase
Salvage pathway
Combination treatment

ABSTRACT

Emergence of drug resistance and adverse effects often affect the efficacy of nucleoside analogues in the therapy of Herpes simplex type 1 (HSV-1) and type 2 (HSV-2) infections. Host-targeting antivirals could therefore be considered as an alternative or complementary strategy in the management of HSV infections. To contribute to this advancement, here we report on the ability of a new generation inhibitor of a key cellular enzyme of *de novo* pyrimidine biosynthesis, the dihydroorotate dehydrogenase (DHODH), to inhibit HSV-1 and HSV-2 in vitro replication, with a potency comparable to that of the reference drug acyclovir. Analysis of the HSV replication cycle in MEDS433-treated cells revealed that it prevented the accumulation of viral genomes and reduced late gene expression, thus suggesting an impairment at a stage prior to viral DNA replication consistent with the ability of MEDS433 to inhibit DHODH activity. In fact, the anti-HSV activity of MEDS433 was abrogated by the addition of exogenous uridine or of the product of DHODH, the orotate, thus confirming DHODH as the MEDS433 specific target in HSV-infected cells. A combination of MEDS433 with dipyridamole (DPY), an inhibitor of the pyrimidine salvage pathway, was then observed to be effective in inhibiting HSV replication even in the presence of exogenous uridine, thus mimicking *in vivo* conditions. Finally, when combined with acyclovir and DPY in checkerboard experiments, MEDS433 exhibited highly synergistic antiviral activity. Taken together, these findings suggest that MEDS433 is a promising candidate as either single agent or in combination regimens with existing direct-acting anti-HSV drugs to develop new strategies for treatment of HSV infections.

1. Introduction

The Herpes simplex virus (HSV) type 1 (HSV-1) and type 2 (HSV-2) causes lifelong infections characterized by periodic reactivations at the site of primary infection, and globally widespread among human populations with a seroprevalence of 50%–90% in adults. HSV-1 is traditionally associated with orofacial lesions and encephalitis, while HSV-2 is associated with genital diseases, although both oral HSV-2 infections and genital herpes caused by HSV-1 are recognized with increasing frequency. Following primary infection, HSV establishes latent infections in the neurons of the sensory ganglia from where they may, or may not, reactivate, causing recurrent infections (Roizman et al., 2013).

HSV infections are associated to a wide range of clinical

manifestations that diversify from asymptomatic infection or mild mucocutaneous lesions on the lips, cornea, genitals, or skin, to more severe diseases, such as encephalitis and recurrent keratitis, and up to even life-threatening systemic disseminate infections in immunocompromised patients or neonates after perinatal transmission (Roizman et al., 2013; Whitley, 2015; Samies and James, 2020).

Even if HSV infections are often subclinical, their incidence and the severity of diseases have increased over the past decades due mainly to the increasing number of transplant recipients. Concurrently, genital herpes has become one of the world's most prevalent sexually transmitted infections with evidence suggesting that HSV-2 infection increases the risk of acquiring HIV (Looker et al., 2017). Together the worldwide burden of HSV diseases is significant, as in 2016 3,7 billion of

HSV-1 infections and about half a billion of HSV-2 infections have been estimated by WHO (James et al., 2020).

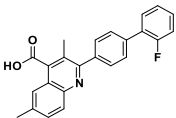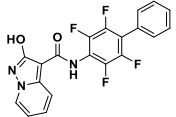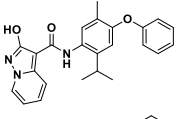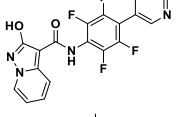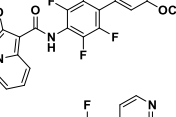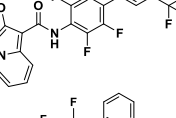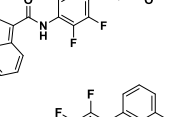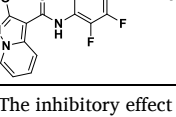Treatment of symptomatic primary or recurrent HSV infections with nucleoside analogues, such as acyclovir (ACV), famciclovir (FAM), and valacyclovir (VCV) that act as viral DNA polymerase inhibitors, ensure an effective therapeutic management of most HSV diseases. However, to date, none of these drugs can eliminate an established latent infection, and their extensive clinical use may lead to treatment failures due to the development of drug resistance, and to adverse effects mainly deriving from long-term toxicity (Whitley and Baines, 2018).

Taking into consideration both these limitations and the absence of efficacious vaccines, the treatment of HSV infections remains a high priority and highlights the need for the development of new antiviral agents directed against new targets. To this regard, host-targeted small molecules able to modulate virus-host interactions may be considered a compelling alternative to the *de novo* development of virally targeted agents, for which the typical timeline for approval can require more than 10 years.

Pyrimidines availability in infected cells is crucial for virus replication and thus compounds targeting the *de novo* pyrimidine biosynthetic pathway have the potential to be validated as host-acting antiviral (HTA) agents (Okesli et al., 2017). Furthermore, in addition to the advantage of overcoming viral drug resistance, inhibitors of pyrimidine biosynthesis, given the independence of the antiviral effects with respect to a specific virus replication strategy, may be broadly deployed against viruses belonging to different families, thus developed as

Table 1
The *h*DHODH inhibitors investigated as anti-HSV agents in the study.

Structure	Compound Code	hDHODH[a] IC$_{50}$ ± SE (nM)	Log D$^{7.4}$ ± SDc	Reference
	Brequinar	1.8 ± 0.3	1.83 ± 0.02	Peters (2018)
	MEDS433	1.2 ± 0.2	2.35 ± 0.02	Sainas et al. (2018)
	1 (MEDS548)	10.5 ± 0.16	3.18 ± 0.09	(unpublished results)
	2 (MEDS604)	6.23 ± 0.63	0.98 ± 0.03	Sainas et al. (2021)
	3 (MEDS605)	30 ± 2.8	2.51 ± 0.07	(unpublished results)
	4 (MEDS606)	2.75 ± 0.31	2.46 ± 0.04	Sainas et al. (2021)
	5 (MEDS608)	2.30 ± 0.33	3.27 ± 0.19	Sainas et al. (2021)
	6 (MEDS610)	150 ± 15	1.84 ± 0.06	Sainas et al. (2021)
	7 (MEDS613)	4.09 ± 0.62	3.28 ± 0.12	Sainas et al. (2021)
	8 (MEDS614)	2.78 ± 0.32	1.82 ± 0.09	Sainas et al. (2021)

[a] The inhibitory effect of the compounds (expressed as IC$_{50}$) on hDHODH *in vitro* assay.

broad-spectrum antivirals (BSAs) (Okesli et al., 2017). In the *de novo* pyrimidine biosynthesis pathway, the dihydroorotate dehydrogenase (DHODH) catalyzes the rate-limiting step of dehydrogenation of dihydroorotate (DHO) to orotate (ORO), essentially providing uridine and cytidine to fulfill cellular nucleotides demand (Reis et al., 2017; Loeffler et al., 2020). Therefore, due to its critical role in the biosynthetic pathway, DHODH is currently considered as a host target of choice for anti-infective drug development (Okesli et al., 2017; Boschi et al., 2019).

Recently, we have identified a novel class of human DHODH (*h*DHODH) inhibitors characterized by an unusual carboxylic group bioisostere 2-hydroxypyrazolo[1,5-a] pyridine (Sainas et al., 2018) that had been designed on the scaffold of brequinar, one of the most potent hDHODH inhibitors (Peters, 2018). These new *h*DHODH inhibitors showed little, if any, toxicity for human normal cells, while they induced myeloid differentiation in Acute Myeloid Leukemia (AML) cell lines through *h*DHODH inhibition, and therefore they are further being developed for treatment of AML (Sainas et al., 2018; Sainas et al., 2020).

The aim of this study was to investigate the potential of deploying this new class of *h*DHODH inhibitors against HSV-1 and HSV-2. We report on the ability of one of these small molecules, named MEDS433, to potently inhibit the *in vitro* replication of HSV-1 and HSV-2 via a mechanism that stems from selective blocking the DHODH enzymatic activity. These results indicate MEDS433 as a promising candidate as either single agent or as combination regimens, to develop new strategies for treatment of HSV infections.

2. Materials and methods

2.1. Compounds

MEDS433 and the small library of *h*DHODH inhibitors (Table 1) based on a hydroxyazole scaffold, were synthesized as described previously (Sainas et al., 2018; Sainas et al., 2021). Acyclovir (ACV), uridine (UR), orotic acid (ORO), dihydroorotic acid (DHO), and dipyridamole (DPY) were purchased from Sigma-Aldrich. All compounds were resuspended in DMSO.

2.2. Cells and viruses

African green monkey kidney cells (Vero) (ATCC CCL-81) and the human glioblastoma astrocytoma U-373 MG cell line (ATCC HTB-17) were purchased from the American Type Culture Collection (ATCC) and cultured in Dulbecco's Modified Eagle Medium (DMEM; Euroclone) supplemented with 10% fetal bovine serum (FBS, Euroclone), 2 mM glutamine, 1 mM sodium pyruvate, 100 U/ml penicillin, and 100 μg/ml streptomycin sulfate (P/S, both from Euroclone). Clinical isolates of HSV-1 (AS1 and AS2) and HSV-2 (AS3 and AS4) sensitive to ACV were a generous gift from V. Ghisetti, Amedeo di Savoia Hospital, Turin, Italy. They were propagated and titrated by plaque assay on Vero cells, as previously described (Luganini et al., 2011; Terlizzi et al., 2016).

2.3. Citotoxicity assay

Vero cells were seeded in 96-well plates (15000 cells/well) and after 24 h the cells were exposed to increasing concentrations of compounds or vehicle (DMSO), as control. After 72 h of incubation, the number of viable cells was determined using the CellTiter-Glo Luminescent assay (Promega) according to the specifications of the manufacturer.

2.4. Antiviral assays

To screen the mini-library of hDHODH inhibitors, plaque reduction assays (PRAs) were performed with Vero cells seeded in 24-well plate (50000 cells/well) and then treated with a single dose (0.5 μM) of the different compounds 1 h prior to and during infection with the clinical isolate of HSV-1 AS1 at 50 PFU/well. Following virus adsorption (2 h at

37 °C), viral inocula were removed, and cells were maintained in medium containing the corresponding compounds, 3% FBS, and 0.9% methylcellulose. After 48 h post-infection (p.i.) cell monolayers were fixed, stained with crystal violet, and viral plaques were microscopically counted; the mean plaque counts for each drug concentration were expressed as a percentage of the mean plaque counts of control virus (DMSO).

To evaluate the anti-HSV activity of selected compound, virus yield reduction assay (VRA) were performed on Vero cells, as previously described (Luganini et al., 2011; Terlizzi et al., 2016). For VRA, both untreated cells and those incubated with different concentrations of MEDS433 for 1 h before infection were infected with the clinical isolates HSV-1 and HSV-2 at a multiplicity of infection (MOI) of 0.01 or 1 PFU/cell. Following virus adsorption (2 h at 37 °C), cultures were maintained in medium containing compounds and then incubated for 48 h p.i. until control cultures displayed extensive cytopathology. Thereafter, the cells and supernatants from the antiviral assay were harvested and disrupted by sonication. The extent of virus replication was then assessed by titrating the infectivity of supernatants of cell suspensions on Vero cells. The mean plaque counts for compounds were expressed as a percentage of the mean plaque counts for the control virus (DMSO-treated), and the concentration that produced a 50% and 90% of reduction in plaque formation (EC_{50} and EC_{90}) was determined by GraphPad Prism software.

To evaluate the effect of uridine, DHO or ORO addition, PRAs were performed with Vero cells infected with HSV-1 AS1 or HSV-2 AS3 (50 PFU/well), and treated with increasing concentrations of uridine, ORO or DHO (10, or 100, or 1000 μM) in presence of 1 μM of MEDS433. After 48 h p.i., cell monolayers were fixed, stained with crystal violet, and plaques microscopically counted. To investigate the effect of blocking both the *de novo* biosynthesis and the salvage pathway of pyrimidines, Vero cells were infected with HSV-1 AS1 or HSV-2 AS3 (50 PFU/well) and treated throughout PRAs with different concentration of MEDS433 in combination with increasing concentrations of dipyridamole (0.5, 1.5 and 3 μM) in media supplemented with concentrations of uridine (20 μM) that exceed the physiological uridine plasma levels ranging from 2 to 6 μM (Pizzorno et al., 2002).

At 48 h p.i., cell monolayers were fixed, stained and plaques microscopically counted.

To assess the effects of the combination of MEDS433 and ACV or MEDS433, ACV and DPY on HSV-1 AS1 replication, PRAs were performed as described above. MEDS433 and ACV, as single agents or in combination, were added on Vero cells at equipotent ratio of 0.25 x, 0.5 x, 1 x, 2 x and 4 x the EC_{50} of each drug. For the three-drug combination, DPY (3 μM) was added to the MEDS433 and ACV concentrations used in the two-drug combination. The effect of the two- or three-drug combinations was then assessed using the Chou-Talalay method (Chou, 2006) based on the median-effect principle of the mass-action law computed in the CompuSyn software (http://www.combosyn.com)(Chou and Martin, 2005). With the Chou-Talalay method, a Combination Index (CI) = 1 represents an additive effect, a CI value > 1 means antagonism and a CI value < 1 indicates synergism.

2.5. Quantitative real-time PCR

Vero cells were seeded in a 6-well plate (600000 cells/well) and, after 24 h, treated with 5 μM MEDS433 1h prior to and during infection with the clinical isolate of HSV-1 AS1 at a multiplicity of infection (MOI) of 0.1 PFU/cell. At different times p.i., cells were harvested and DNA was extracted and purified using a DNA purification kit (Zymo Research). The levels of viral DNA were then evaluated by quantitative real-time PCR using a GENESIG standard kit (Primerdesign) to amplify a segment of the DNA polymerase UL30 gene. Briefly, 25 ng of DNA from each sample was amplified in triplicate using PrecisionPlus Low ROX qPCR master mix (Primerdesign), the oligonucleotide primers and the TaqMan UL30 probe, dually labeled (5′, fluorescein 6-
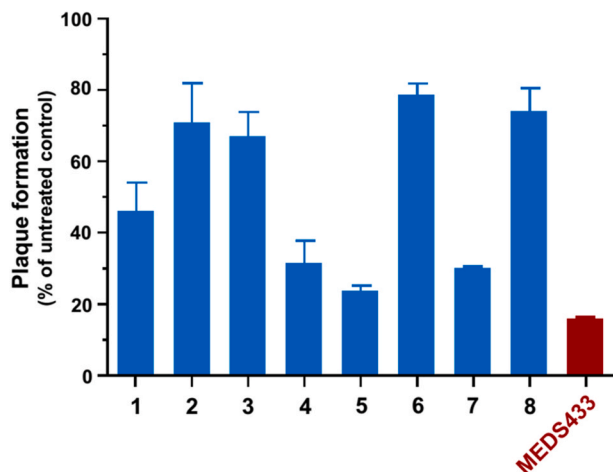
Fig. 1. Identification of *h*DHODH inhibitors with anti-HSV activity. Vero cells were pretreated and treated with 0.5 μM of the different DHODH inhibitors (Table 1) 1 h prior to, during infection with HSV-1 AS1 (50 PFU/well), and throughout the experiment. At 48 h post-infection, viral plaques were stained and the mean plaque number in treated culture determined compared to that of DMSO-treated and mock-infected control monolayers. The data shown represent means ± SD (error bars) of three independent experiments performed in triplicate.

carboxyfluorescein [FAM]; 3′, Iowa Black® dark quencher). After activation of Hot Start Taq DNA polymerase for 2 min at 95 °C, samples underwent 45 cycles of 10 s at 95 °C and 1 min at 60 °C in a Quant-Studio3 real-time PCR (Applied Biosystem). For HSV genome copy number determination, a serially diluted UL30-encoding plasmid (GENESIG standard kit) was used to determine a standard curve for mean Ct values and to calculate HSV genome copy numbers.

2.6. Immunoblotting

Vero cells were seeded in 6-well plates (600000 cells/well) and, after 24 h, were treated with 5 μM of MEDS433 1 h prior to and during infection with HSV-1 AS1 at a MOI of 1 PFU/cell. Whole-cell extracts were prepared at different times p.i., as previously described (Luganini et al., 2008; Mercorelli et al., 2016). An equal amount of the cell extracts was fractionated by 8% SDS-PAGE and then transferred to PVDF membranes (BioRad). Filters were blocked for 2 h at 37 °C in 5% non-fat dry milk in 10 mM Tris-HCl (pH 7.5), 100 mM NaCl, and 0.05% Tween 20 and immunostained with the mouse anti-HSV-1 ICP27 mAb (clone H1113; Virusys) (diluted 1:500), anti-HSV-1 ICP5 mAb (clone 3B6; Virusys) (diluted 1:500), or with anti-tubulin mAb (Chemicon International) (diluted 1:2000) as a control for protein loading. Immunocomplexes were detected with a goat anti-mouse Ig Ab conjugated to horseradish peroxidase (Life Technologies) and visualized by enhanced chemiluminescence (Western Blotting Luminol Reagent, Santa Cruz).

2.7. Statistical analysis

All statistical tests were performed using GraphPad Prism version 7.0. Antiviral assays data are presented as the means ± SDs of at least three experiments performed in triplicate. Differences were considered to be statistically significant for $p < 0.05$.

3. Results

3.1. Inhibition of HSV-1 and HSV-2 replication by the DHODH inhibitor MEDS433

To generate new *h*DHODH inhibitors, we have recently applied a

rational modulation to brequinar, one of the most potent *h*DHODH inhibitors so far discovered (Peters et al., 2018). A combination of structure-based and bioisosterism (Sainas et al., 2019) approaches resulted in a series of new 2-hydroxypyrazolo[1,5-a]pyridine derivatives of brequinar (Sainas et al., 2018; Sainas et al., 2021). Here, to investigate the feasibility of targeting DHODH activity to develop HTA aimed at inhibiting HSV replication, 9 of these new *h*DHODH inhibitors (Table 1) were selected using plaque reduction assays in which test compounds were present before, during and after virus infection. As shown in Fig. 1A, when tested at 0.5 μM, five compounds (**1**, **4**, **5**, **7**, and **MEDS433**) were able to decrease HSV-1 AS1 replication of more than 50%, while the remaining four compounds (**2**, **3**, **6** and **8**), reduced the virus replication of about 20–30%. Since MEDS433 was the most effective hDHODH inhibitor against HSV-1 replication (Fig. 1), it was selected for further analysis.

Virus yield reduction assays (VRAs) then confirmed a significant concentration-dependent inhibition of virus replication in Vero cells treated with MEDS433, and infected with the clinical isolates HSV-1 AS1 or HSV-2 AS3 at a multiplicity of infection (MOI) of 0.01 or 1 (Fig. 2). The EC_{50} and EC_{90} values against HSV-1 AS1 and HSV-2 AS3 (Table 2) also indicated that the inhibitory effect of MEDS433 cannot be overcome by infecting cells at higher multiplicities of infection.

To further strengthen these observations, a second pair of clinical isolates of HSV-1 and HSV-2, respectively HSV-1 AS2 and HSV-2 AS4, was examined by VRAs. As reported in Table 2, MEDS433 was effective also against HSV-1 AS2 and HSV-2 AS4, thus indicating that the anti-HSV activity of MEDS433 was independent from the viral strain used, and sustaining the view that indeed it targeted a host pathway in HSV-infected cells. Nevertheless, the antiviral activity of MEDS433 was not due to cytotoxicity of the target cells themselves, since the Cytotoxic Concentration (CC_{50}) determined in uninfected Vero cells was 234 ± 18.2 μM, with a favorable Selective Index (SI) on average greater than 2100 and 3000 for HSV-1 and HSV-2, respectively.

Noteworthy, MEDS433 showed an anti-HSV activity (Table 2) at least comparable to that of the reference drug ACV (EC_{50} 0.280 ± 0.080 and 0.120 ± 0.042 μM against HSV-1 AS1 and HSV-2 AS3, respectively), while it was more effective than the reference *h*DHODH inhibitor brequinar (EC_{50} 0.420 ± 0.124 μM against HSV-1 AS1 and 1.250 ± 0.276 μM against HSV-2 AS3, respectively).

Furthermore, in addition to being MOI-independent, the anti-HSV activity of MEDS433 was also cell-type independent, as it was observed in the human glioblastoma astrocytoma U-373 MG cell line permissive for HSV replication (Andrei et al., 1994). In these cells of neural origin, MEDS433 in fact inhibited HSV-1 AS1 replication with EC_{50} and EC_{90} values of 0.297 ± 0.080 and 1.881 ± 0.487 μM, respectively.

As a whole, these results indicate a potent anti-HSV activity of MEDS433 independent of the virus strain, the MOI, or the cell type used.

3.2. MEDS433 affects HSV DNA replication and late gene expression

To get more insights into the nature of the antiviral activity of MEDS433, we investigated its effects on HSV-1 DNA synthesis at different times p.i. As reported in Fig. 3, in untreated HSV-1-infected Vero cells, the qPCR analysis measured a progressive increase of viral DNA levels up to 48 h p.i. Conversely, the MEDS433 treatment determined an impairment of HSV-1 DNA synthesis starting from 16 h p.i. and for the entire time frame that was evaluated, thus suggesting that it can target the HSV replication cycle at a stage prior to the onset of viral DNA replication.

To further supporting this hypothesis, total protein extracts were prepared at various times p.i. from HSV-1-infected Vero cells treated with MEDS433 and the content of ICP27 and ICP5 proteins was evaluated to monitor the levels of representative immediate-early (IE) and late (L) HSV protein expression, respectively. As seen in Fig. 4, compared to cells treated with the vehicle DMSO, MEDS433 treatment did not
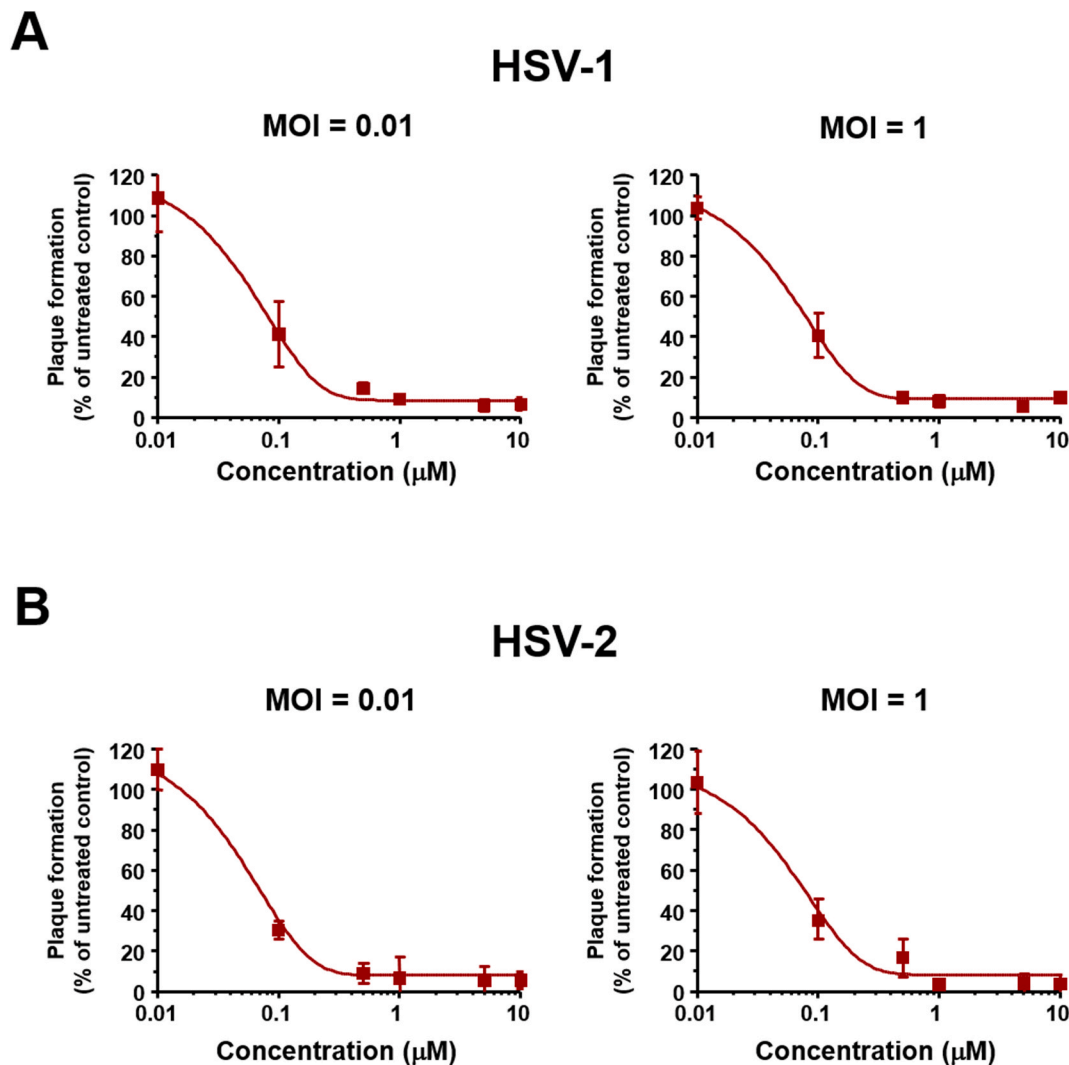
Fig. 2. Antiviral activity of MEDS433 against HSV-1 and HSV-2. Vero cell monolayers were infected with the clinical isolates of HSV-1 AS1 or HSV-2 AS3 at MOIs or 0.01 or 1, and, where indicated, the cells were treated with increasing concentrations of MEDS433 1 h before as well as during virus adsorption. MEDS433 remained in the culture medium throughout the experiment, until an extensive viral cytopathic effect was observed in the untreated controls. HSV replication was then quantified by titrating the infectivity of supernatants of Vero suspensions by standard plaque assay. The number of plaques was plotted as a function of MEDS433 and ACV concentrations, and the concentrations producing 50% and 90% reductions in plaque formation (EC_{50} and EC_{90}, respectively) were determined. The data shown represent means $\pm$ SD (error bars) of three independent experiments performed in triplicate.

affect noticeably the expression of ICP27 protein accumulation at any time analyzed. In contrast, it determined a clear reduction of the late ICP5 protein levels at 12 and 24 h p.i.

Together, these results suggest that MEDS433 targets HSV replication cycle after the expression of IE proteins and likely interferes with the viral DNA synthesis, since the MEDS433-mediated inhibition at this stage (Fig. 3) reduces late gene expression (Fig. 4).

3.3. The pyrimidine biosynthesis pathway is involved in the anti-HSV activity of MEDS433

The above results suggest a mechanism of the anti-HSV activity of MEDS433 consistent with its ability to inhibit DHODH activity. To verify this hypothesis, we investigated whether the antiviral HSV activity of MEDS433 could be overcome by the addition of increasing concentrations of exogenous uridine. As shown in Fig. 5, the inhibitory effect of 1 μM MEDS443 on both HSV-1 (Fig. 5A) and HSV-2 (Fig. 5B) replication was significantly reversed by a 10-fold excess of uridine relative to MEDS433 concentration and further decreased by greater uridine

concentrations that completely restored HSV replication, thus indicating that the pyrimidine pathway was affected by MEDS433. Then, to confirm that DHODH inhibition by MEDS433 was responsible of its anti-HSV effect, cell medium was supplemented with increasing concentrations of the substrate dihydroorotic acid (DHO) or the DHODH product, orotic acid (ORO). In HSV-infected Vero cell cultures treated with MEDS433 (1 μM), the addition of orotic acid reversed significantly the inhibitory effect of MEDS433 on HSV-1 and HSV-2 replication already at a concentration 10-fold that of MEDS433 (Fig. 5, lower panels). However, the reverting effect of orotic acid to MEDS433 was almost complete at the highest concentration (1000 x the MEDS433 concentration) evaluated. In contrast, the addition of DHO even at 1 mM (1000 times more than MED433) did not affect the anti-HSV activity of MEDS433 (Fig. 5, lower panels), thus indicating that MEDS433 inhibits a step in the *de novo* pyrimidine biosynthesis pathway downstream from DHO.

Together, these results confirm that MEDS433 selectively targets DHODH in HSV-infected cells and that the inhibition of DHODH is in charge of the overall anti-HSV activity of MEDS433.

Table 2
Antiviral activity of MEDS433 against different HSV strains.

HSV	EC$_{50}$ (μM)[a]	EC$_{90}$ (μM)[b]	CC$_{50}$ (μM)[c]	SI[d]
MOI of 0.01				
HSV-1 AS1	0.085 ± 0.021	0.765 ± 0.167	234 ± 18.2	2752
HSV-1 AS2	0.116 ± 0.014	0.678 ± 0.127	234 ± 18.2	2017
HSV-2 AS3	0.061 ± 0.019	0.840 ± 0.178	234 ± 18.2	3836
HSV-2 AS4	0.095 ± 0.027	0.778 ± 0.168	234 ± 18.2	2463
MOI of 1				
HSV-1 AS1	0.078 ± 0.024	0.702 ± 0.111	234 ± 18.2	3000
HSV-2 AS3	0.074 ± 0.023	0.731 ± 0.157	234 ± 18.2	3162

[a] EC$_{50}$, compound concentration that inhibits 50% of virus replication, as determined by VRAs against HSV-1 and HSV-2 in Vero cells. Reported values represent the means ± SD of data derived from three experiments in triplicate.

[b] EC$_{90}$, compound concentration that inhibits 90% of virus replication, as determined by VRAs.

[c] CC$_{50}$, compound concentration that produces 50% of cytotoxicity, as determined by cell viability assays in Vero cells. Reported values represent the means ± SD of data derived from three experiments in triplicate.

[d] SI, selectivity index (determined as the ratio between CC$_{50}$ and EC$_{50}$.
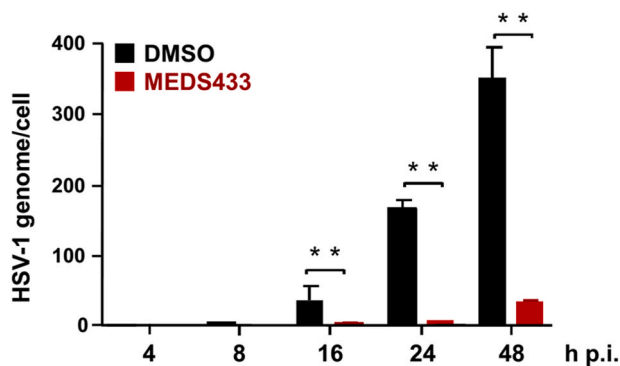
Fig. 3. MEDS433 inhibits HSV-1 viral DNA synthesis. Vero cell monolayers were infected with the clinical isolate of HSV-1 AS1 at an MOI of 0.1, and, where indicated, the cells were treated with 5 μM MEDS433, or 0.02% DMSO as a control. At 4, 8, 16, 24 and 48 h p.i., total DNA was purified and qPCR was performed with appropriate HSV primers. HSV-1 genomic copies were determined by interpolation from the standard curve, generated by a serially diluted UL30 plasmid and normalized to the number of cells. The data shown are the means ± SD of two independent experiments performed in triplicate and analyzed by unpaired *t*-test. ** (p < 0.0001) versus calibrator sample (DMSO).

3.4. The combination of MEDS433 with an inhibitor of the nucleoside salvage pathway enhances the antiviral activity

Despite useful in confirming the molecular target of MEDS433, the observation that uridine reversed the anti-HSV activity of MEDS433 may lead to hypothesize that, in the presence of physiological concentration of uridine as that occurring *in vivo*, the pyrimidine salvage pathway may reduce the antiviral efficacy of a DHODH inhibitor by importing extracellular nucleosides. To tackle this problem, we explored the effects of a combination treatment of MEDS433 with an inhibitor of the nucleoside transport, such as dipyridamole (DPY). To this end, a checkerboard analysis of MEDS433-DPY combination was carried by plaque reduction assay in HSV-1-infected Vero cells in culture medium supplemented even with 20 μM uridine to exceed physiological plasma conditions (Pizzorno et al., 2002). As depicted in Fig. 6A, the presence of 20 μM exogenous uridine abrogated, as expected, the inhibitory activity of MEDS433 at concentrations reducing HSV replication by 65–90% when it was tested as single agent (Fig. 2). In contrast, when the same MEDS433 concentrations were examined in the presence of increasing
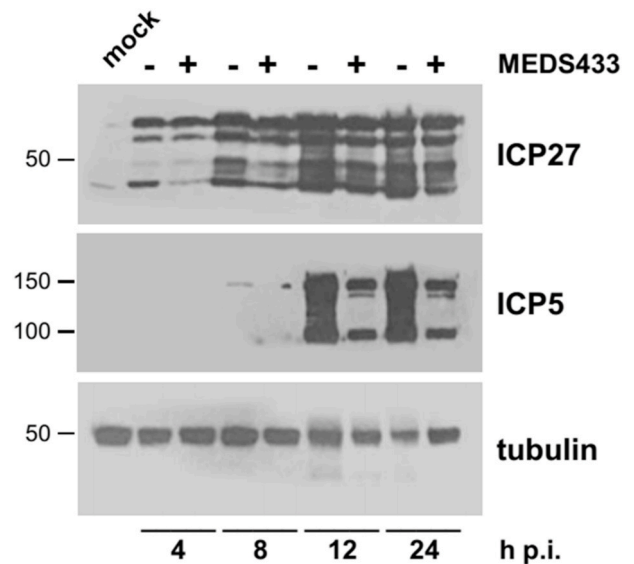

Fig. 4. MEDS433 reduces the expression of HSV L proteins. Vero cells were infected with HSV-1 AS1 at an MOI of 1, or mock infected (mock) and, where indicated, the cells were treated prior to and during infection with 5 μM MEDS433, or 0.02% DMSO as a control. Total cell extracts were prepared at the indicated times p.i., fractionated by 8% SDS-PAGE and analyzed by immunoblotting with anti-HSV ICP27 and anti-HSV ICP5 mAbs. Tubulin immunodetection was used as internal control.

amounts of dipyridamole, the combination of the two molecules successfully reduced HSV-1 replication despite the presence of exogenous uridine (Fig. 6A). At the used concentrations, DPY by itself did not exerted an inhibitory activity on HSV replication (data not shown), in accord to previous observations (Snoeck et al., 1994). Furthermore, the DPY-mediated enhancement of MEDS433 antiviral activity was not due to an aspecific cytotoxic effect, since none of the tested combinations affected Vero cell viability (Fig. 6B).

Taken together, these results sustain the feasibility of a combination of a DHODH inhibitor and a pyrimidine salvage inhibitor to determine an anti-HSV activity even in the presence of uridine concentrations that even exceed *in vivo* host conditions.

3.5. The combination of MEDS433, acyclovir and dipyridamole results in a synergistic effect on HSV-1 replication

Lastly, we investigated whether the antiviral activity of MEDS433 and the reference drug acyclovir would result in a synergistic, additive or antagonistic effect when tested in combination. To this end, the combined effects of 0.25-, 0.5-, 1-, 2-, or 4-fold of MEDS433 EC$_{50}$ to ACV EC$_{50}$ ratio were assessed by plaque reduction assays and then analyzed using the CompuSyn software. Results of MEDS433-ACV combinations are represented in Fig. 7A as a fractional effect analysis (Fa) plot in relation to the concentrations of drugs used, where Fa values closer to 1 indicate greater antiviral activity. The anti-HSV efficacy of ACV was clearly increased by the combination with MED433 as shown by the Fa values (blue triangles) closer to 1 than those of MEDS433 and ACV when used as single agent (Fig. 7A). The EC$_{50}$ of ACV (0.330 μM) was in fact decreased to 0.128 μM by the combination with MEDS433 (Fig. 7A). The calculated Combination Index (CI) values then indicated that combination of MEDS433 with ACV resulted in a synergistic effect at any of drug combinations tested, since all the CIs were <0.9 (Table 3) (Chou, 2006).

Then, to evaluate the efficacy of the MEDS433-ACV combination in the context of the inhibition of the pyrimidine salvage pathway, as that determined by DPY, the anti-HSV activity of the combination of the different MEDS433 EC$_{50}$ to ACV EC$_{50}$ relative rates was measured in the
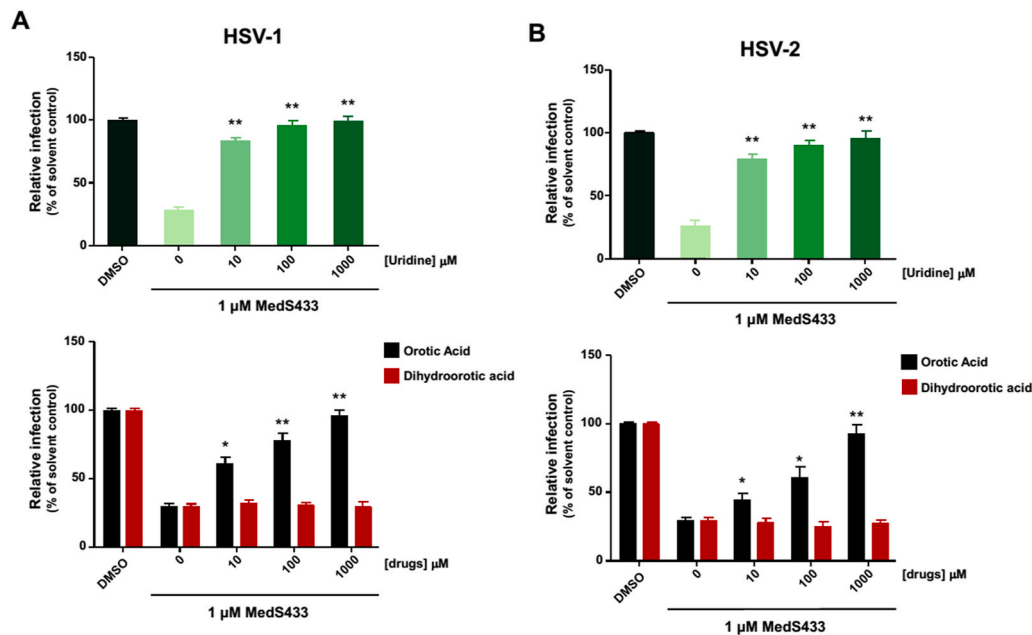
Fig. 5. Inhibition of HSV replication by MEDS433 is reversed by uridine and orotic acid. Vero cell monolayers were treated with 1 μM of MEDS433 in the presence or absence of increasing concentrations of uridine (upper panels), dihydroorotic acid or orotic acid (lower panels) before and during infection with HSV-1 AS1 (**A**) or HSV-2 AS3 (**B**) (50 PFU/well). Following virus adsorption, cells were incubated in the presence of compounds and viral plaques were then stained and were microscopically counted at 48 h p.i. The mean plaque counts for each drug concentration were expressed as a percent of the mean count of the control cultures treated with the DMSO vehicle. The data shown represent means ± SD (error bars) of three independent experiments performed in triplicate and analyzed by a one-way ANOVA followed by Dunnett's multiple comparison test. ** ($p < 0.0001$) and * ($p < 0.05$) compared to the calibrator sample (MEDS433 alone).
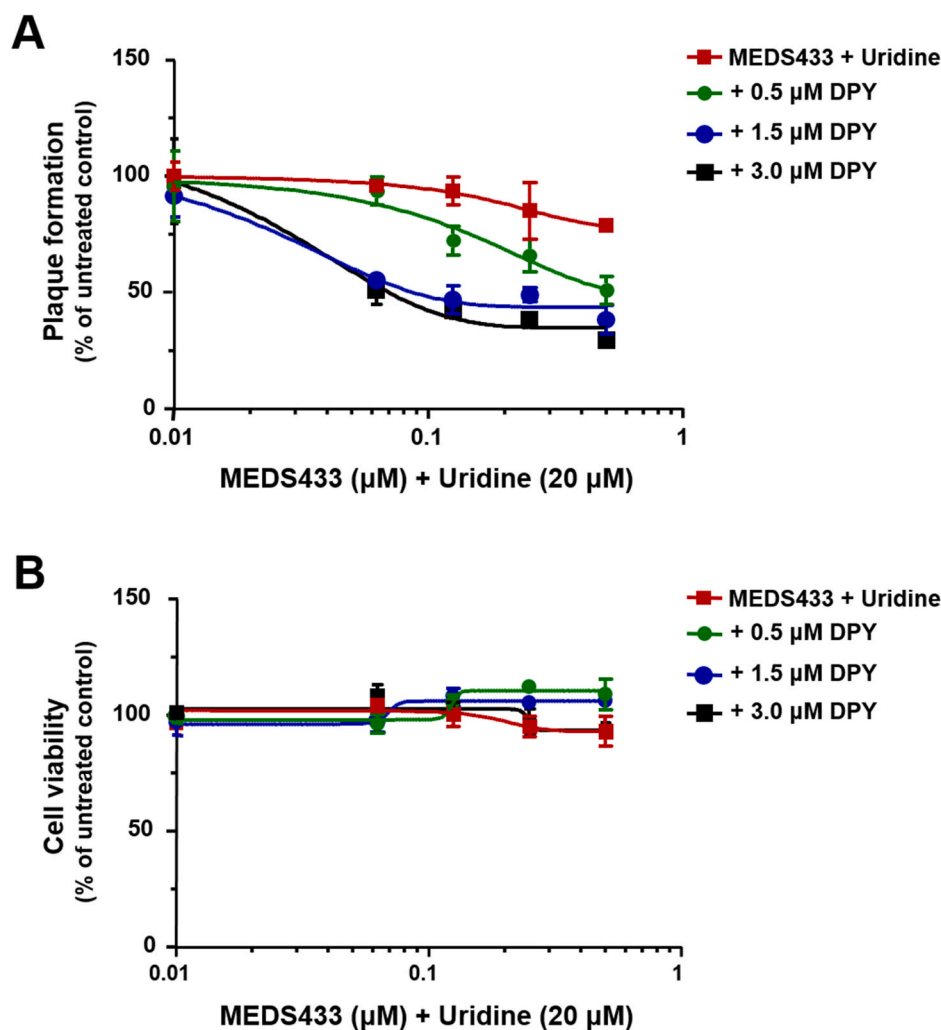
Fig. 6. A combination of modulators of pyrimidine metabolism inhibits HSV replication in the presence of exogenous uridine. A) Vero cell monolayers were treated with MEDS433 alone or in combination with different concentrations of DPY before and during HSV-1 AS1 infection (50 PFU/well). Following virus adsorption, cell monolayers were overlaid with 0.9% methylcellulose in the presence of compounds and viral plaques were then stained and counted at 48 h p.i. In all the assays, culture medium was supplemented with 20 μM uridine. The data shown represent means ± SD (error bars) of three independent experiments performed in triplicate. **B)** To determine cell viability, Vero cells were exposed to the different concentrations of MEDS433 alone or in combination with different amounts of DPY, or vehicle (DMSO), as control. After 72 h of incubation, the number of viable cells was determined by the CellTiter-Glo Luminescent assay. Results are shown as means ± SD (error bars) of three independent experiments performed in triplicate.
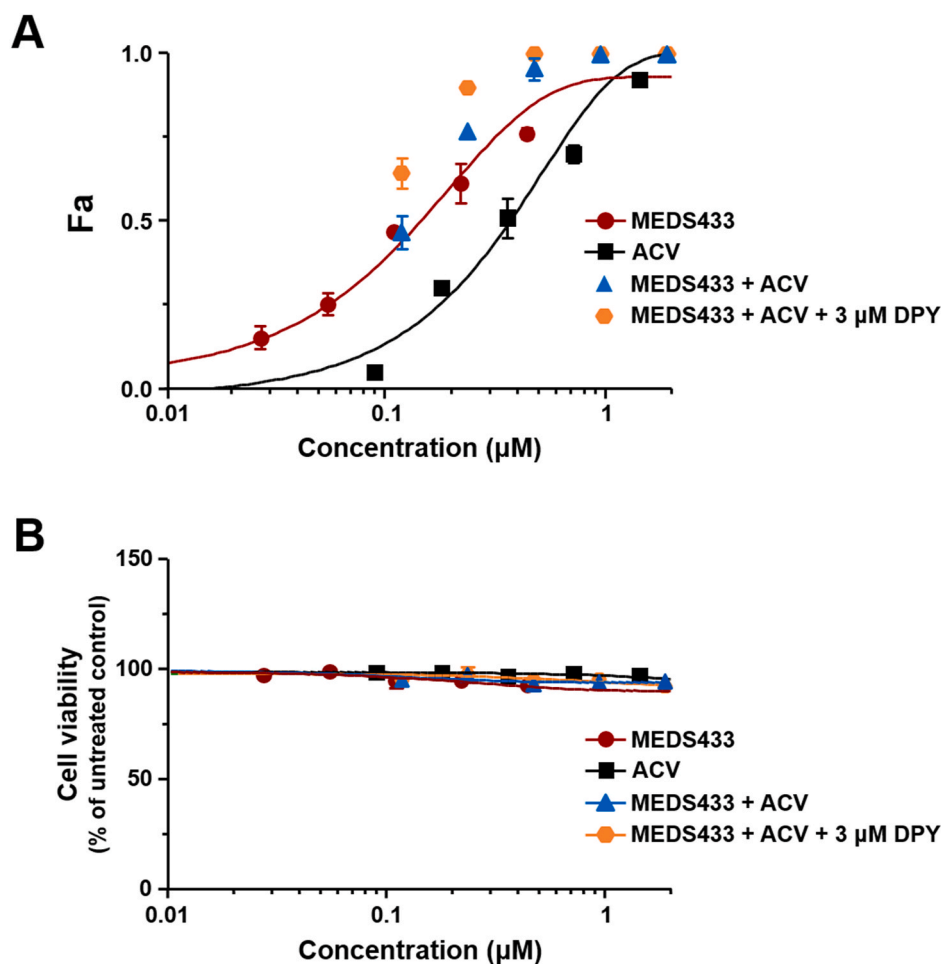
Fig. 7. Effects of the combination of MEDS433, acyclovir and dipyridamole on HSV replication. A) Plaque reduction assays were performed on Vero cell monolayers treated with different concentrations of MEDS433 and ACV as single agents, or in combination in the absence or presence of 3 μM of DPY prior to and during HSV-1 AS1 infection (50 PFU/well). After virus adsorption, cells were incubated in the presence of compounds and at 48 h p.i., viral plaques were stained and counted. Plaque numbers were analyzed with the CompuSyn software. The effects on HSV-1 replication of MEDS433 or ACV used as single agents are depicted by red and black Fa curve, respectively. The effect of MEDS433-ACV or MEDS433-ACV-DPY combinations are indicated by blue triangles and orange hexagons, respectively. The results are representative of three independent experiments performed in triplicate. **B)** To determine the cytotoxic effect of combinations, Vero cell monolayers were treated with the vehicle (DMSO), or with different concentrations of MEDS433 alone or in combination with different concentrations of ACV and in the absence or presence of 3 μM of DPY. At 72 h, Vero cell viability was assessed by the CellTiter-Glo Luminescent assay. Results are shown as means ± SD (error bars) of two independent experiments performed in triplicate.

presence of 3 μM DPY. As shown in Fig. 7A and Table 3, the antiviral strength of the MEDS433-ACV combination was further increased by the addition DPY, since Fa values of the triple combination (orange hexagons) were even more close to 1 than those of the MEDS433-ACV combination, and the EC_{50} of ACV further reduced to 0.089 μM. Furthermore, none of the MEDS433-ACV or MEDS433-ACV-DPY combinations exhibited significant cytotoxic effects against Vero cells (Fig. 7B), thus indicating that their synergistic anti-HSV activity was not the result of an increased cytotoxicity, which would have prevented the virus from replicating, but that it derived from the combined interference of different targets and mechanisms of action.

These results suggest that both combinations of MEDS433 and ACV and MEDS433, ACV and DPY might represent a new pharmacological strategy to be considered for the management of HSV infections.

4. Discussion

This study shows that the small molecule MEDS433 exerts a potent dose-dependent antiviral activity against clinical isolates of HSV-1 and HSV-2 with a mechanism that stems from the inhibition of the *de novo* synthesis of pyrimidines.

In a previous study, MEDS433 was shown to inhibit *h*DHODH activity with a potency similar to brequinar, while exerting a lower cell cytotoxicity and the ability to restores myeloid differentiation in AML cell lines at concentrations one log digit lower than those of brequinar (Sainas et al., 2018). Crystallographic studies of MEDS433 in complex with *h*DHODH then showed that it has a binding mode similar to that of brequinar, inside the ubiquinone binding site of the enzyme (Sainas et al., 2018).

Here, we have observed that even when tested for anti-HSV activity, MEDS433 results more active than brequinar and all other derivatives examined (Fig. 1). Among the tested *h*DHODH inhibitors, MEDS433 is in fact characterized by the highest inhibitory potency against hDHODH (IC_{50} 1.2 nM) and a favorable lipophilicity with a $logD^{7.4}$ value of 2.35 (Table 1). To this regard, a $logD^{7.4}$ value of 2.50 has been suggested for optimal inhibition of mitochondrial DHODH, since inhibitors with lower $logD^{7.4}$ are disadvantaged in reaching the mitochondrial membrane, while higher $logD^{7.4}$ values may reduce their cellular adsorption (Gradl et al., 2019). It is therefore reasonable that MEDS433 was more active as anti-HSV agent than either the most polar (low logD values) brequinar, **2, 6,** and **8** compounds, or the most lipophilic **5** and **7** derivatives ($logD^{7.4}$ 3.27 and 3.28, respectively).

Under normal physiological conditions, cells fulfill their requirement of pyrimidines mainly through the salvage pathways, therefore recycling pre-existing nucleosides from both degradation of intracellular nucleic acids and uptake of extracellular nucleosides. In contrast, in highly metabolically active virus-infected cells, the exceptional need for large pyrimidines pools associated to rapid viral replication cannot be supply sufficiently by nucleotide recycling. To keep up with the pyrimidine demand in infected cells, in fact, herpesviruses activate both the *de novo* pyrimidine biosynthetic gene expression and the metabolic flux to UTP (Gribaudo et al., 2002; Munger et al., 2008). It is therefore reasonable that *de novo* pyrimidine biosynthesis rather than its salvage pathway is more critical for herpesvirus replication, effectively making the rate-limiting DHODH enzyme activity crucial for maintaining high levels of viral DNA synthesis.

The observation that HSV replication was largely restricted when the DHODH activity was inhibited therefore confirms the dependence of

Table 3

Analysis of the effects of the combination of MEDS433, ACV and DPY against HSV-1 replication.

MEDS433/ACV combination at equipotent ratio	MEDS433/ACV	Drug combination effect of MEDS433/ACV[c]	MEDS433/ACV +3 μM DPY	Drug combination effect of MEDS433/ACV
(fold of EC$_{50}$[a])	CI[b]		CI[d]	+ 3 μM DPY[c]
4x	0.156 ± 0.051	**Strong synergism**	0.156 ± 0.096	**Strong synergism**
2x	0.082 ± 0.001	**Very strong synergism**	0.078 ± 0.033	**Very strong synergism**
1x	0.334 ± 0.039	**Synergism**	0.162 ± 0.043	**Strong synergism**
0.5x	0.419 ± 0.042	**Synergism**	0.299 ± 0.017	**Strong synergism**
0.25x	0.666 ± 0.152	**Moderate synergism**	0.306 ± 0.007	**Strong synergism**

[a] Fold of EC50 MED/EC50 ACV yielding an equipotent concentration ratio (approximately 1:0.31) between the two combined drugs. The EC50 values was determined by PRAs against HSV-1, as described in Material and Method. The ratio of the drugs was considered 1:0.31 from Fig. 2.

[b] Combination Index (CI), extrapolated by computational analysis with the CompuSyn software. Reported values represent means ± SD of data derived from n = 3 independent experiments in triplicate using MED/ACV concentration ratio showed in.

[c] Drug combination effect defined as: very strong synergism for CI < 0.1; strong synergism for 0.1 < CI < 0.3; synergism for 0.3 < CI < 0.7; moderate synergism for 0.7 < CI < 0.85, according to Chou (2006).

[d] Combination Index (CI), extrapolated by computational analysis with the CompuSyn software. Reported values represent means ± SD of data derived from n = 3 independent experiments in triplicate using MED/ACV concentration ratio showed in[a] added with 3 μM of DPY for each combination.

HSV on the host *de novo* pyrimidine biosynthesis for efficient replication, albeit, given the premises summarized above, this finding is not unexpected. In addition to this, with regard to herpesviruses infections, it has already been observed that a DHODH inhibitor can potently block the replication of the Human Cytomegalovirus (HCMV) with an *in vitro* EC$_{50}$ of 0.78 μM (Marschall et al., 2013). However, the present study is the first to report the antiviral efficacy of a low cell toxicity *h*DHODH inhibitor against HSV-1 and HSV-2 with a potency at least comparable to that of the reference drug acyclovir, thus suggesting that inhibition of DHODH activity by MEDS433 results in the reduction in the production of pyrimidines at an extent that restricts HSV replication but not cell growth.

However, it is worth noting that our study adds two new pieces of knowledge to the field of HTAs targeting the replenishment of nucleotides in virus-infected cells, that may be of interest to be considered to design new strategies for the management of HSV infections.

The first consists in the observation of the efficacy of a combined treatment between an inhibitor of the *de novo* pyrimidine biosynthesis, MEDS433, and dipyridamole, a broad nucleoside transporter inhibitor that blocks the nucleoside salvage from extracellular environment (Fitzgerald, 1987). In fact, when DPY was combined with concentrations of MEDS433 no longer effective against HSV due to the presence of extracellular uridine which mimics the physiological conditions in the infected host, it restored the antiviral activity of the *h*DHODH inhibitor. This observation is relevant as there is experimental evidence of the absence of inhibitory effects of pyrimidine biosynthesis inhibitors on the growth of some RNA viruses, in both rodents and non-human primate models despite their high efficacy *in vitro*, and likely due to the systemic pyrimidine salvage pathway that by importing extracellular nucleosides into virus-infected cells, may compensate DHODH inhibition (Wang et al., 2011; Smee et al., 2012; Grandin et al., 2016).

While the combination of DPY with inhibitors of *de novo* pyrimidine biosynthesis has been investigated previously in both *in vitro* studies and clinical trials to increase the anticancer effects of the latter, the potential of this combination against virus infections has not yet been thoroughly investigated. To this regard, it has been reported very recently the efficacy of a combination of a *h*DHODH inhibitor, GSK983, with a pyrimidine salvage inhibitor such as the cyclopentenyl uracil (CPU) in suppressing the *in vitro* replication of dengue virus, even in the presence of physiological concentrations of uridine (Liu et al., 2020). CPU is a uridine analogue able to block the activity of uridine/cytidine kinase 2 (Cysyk et., 1995), a cellular enzyme that phosphorylates uridine to UMP in the pyrimidine ribonucleotide salvage pathway, and therefore acting at a stage downstream from that targeted by DPY (Fitzgerald, 1987). DPY in fact is a pyrimido-pyrimidine derivative widely used as an oral agent in the prophylaxis of thromboembolism in cardiovascular disease,

because of its platelet antiaggregant and vasodilator activities due to the inhibition of the uptake of adenosine into platelets, endothelial cells and erythrocytes (Fitzgerald, 1987; Schaper, 2005). These cellular effects have been observed even after a single DPY dose at which the measured C$_{max}$ was of 2.2 μg/ml, corresponding to 4.4 μM (Gregov et al., 1987). This value is greater than the highest DPY concentration observed to be effective in combination with either MEDS433 (Fig. 6A) or MEDS433 and ACV (Fig. 7A), that therefore it could be clinically achievable in patients treated with DPY. The wide clinical experience of DPY could thus allow its rapid repositioning against viruses to be clinically useful in combination with HTAs and/or direct acting antivirals.

The second finding which deserves a further comment is the observation that several combinations of MEDS433 and ACV interact in a synergistic manner, each reinforcing the other's antiviral activity against HSV-1. To our knowledge, this is the first observation of a synergistic effect between a direct acting antiviral agent used to treat infections caused by DNA viruses and a DHODH inhibitor. While, in the case of RNA viruses, as the arenavirus Junín virus that causes the Argentine hemorrhagic fever, it has been reported that the combination of A771726, the active metabolite of the *h*DHODH inhibitor leflunomide approved by FDA for treatment of rheumatoid arthritis and autoimmune disorders (Sanders and Harisdangkul, 2002), and ribavirin showed a significantly more potent antiviral activity than each single drug treatment (Sepulveda et al., 2018).

Relevant to the possibility to exploit combinations between direct-acting antivirals and agents targeting the pyrimidine pathway against HSV infections, it is possible to have in view a regimen based on three different molecules: ACV, a DHODH inhibitor, and DPY. As we have observed in this study, indeed DPY not only restores the antiviral efficacy of the DHODH inhibitor that could be abolished by the uptake of exogenous pyrimidines from the bloodstream (Fig. 6A), but it also strengthens the synergism between ACV and MEDS433 against HSV replication (Fig. 7A). Obviously, one could argue that the addition of DPY to an ACV-DHODH combination could reduce the synergistic effect *in vivo* due to the inhibition of nucleoside transport and thus impairing the uptake of ACV from bloodstream. However, this would not seem to be the case, as it has been observed that DPY does not compromise the transport of ACV into cells (Mahony et al., 1988), as well as that of others nucleoside analogues, such as AZT and ddC (Szebeni et al., 1989). Therefore, our findings along with the reported ability of DPY to inhibit the intracellular transport of thymidine and dCTP which could compete with ACV for viral kinase-mediated phosphorylation, suggest that DPY actually may potentiate the antiviral efficacy of ACV. Although future investigations in animal models of HSV infection will be required to validate the *in vitro* observations, our results suggest that combinations of ACV and MEDS433 or ACV, MEDS433 and DPY might represent a new

therapeutic strategy for HSV infections.

In conclusion, the results of this study suggest MEDS433 as an attractive candidate as a novel HTA that might show advantageous features, such as an antiviral activity against a broad range of viruses since, in addition to HSV, we have observed MEDS433 effective against respiratory viruses, such as Influenza virus, Respiratory Syncytial Virus, and SARS-CoV-2 (unpublished results), and the low risk of emergence of drug-resistant strains.

Moreover, MEDS433 could also be considered for combinatorial drug treatment with nucleoside analogues and other anti-pyrimidines, such as ACV and DPY, for the therapeutic management of HSV infection. In light of the fact that no new anti-HSV agents have been introduced in nearly three decades, the potent *in vitro* anti-HSV activity of MEDS433 calls for further studies to be performed to evaluate their efficacy and safety in animal models, in order to validate its development as novel agent for the treatment of HSV infection.

Declaration of competing interest

The authors declare that they have no known competing financial interests or personal relationships that could have appeared to influence the work reported in this paper.

Acknowledgements

References

Andrei, G., Snoeck, R., De Clercq, E., 1994. Human brain tumour cell lines as cell substrate to demonstrate sensitivity/resistance of herpes simplex virus types 1 and 2 to nucleoside analogues. Antiviral Chem. Chemother. 5, 263–270. https://doi.org/10.1177/095632029400500408.

Boschi, D., Pippione, A.C., Sainas, S., Lolli, M.L., 2019. Dihydroorotate dehydrogenase inhibitors in anti-infective drug research. Eur. J. Med. Chem. 183, 111681. https://doi.org/10.1016/j.ejmech.2019.111681.

Chou, T.C., 2006. Theoretical basis, experimental design, and computerized simulation of synergism and antagonism in drug combination studies. Pharmacol. Rev. 58, 621–681.

Chou, T.C., Martin, N., 2005. CompuSyn for Drug Combinations: PC Software and User's Guide: A Computer Program for Quantitation of Synergism and Antagonism in Drug Combinations, and the Determination of IC50 and ED50 and LD50 Values. ComboSyn, Paramus, NJ.

Cysyk, R.L., Malinowski, N., Marquez, V., Zaharevitz, D., August, E.M., Moyer, J.D., 1995. Cyclopentenyl uracil: an effective inhibitor of uridine salvage in vivo. Biochem. Pharmacol. 49, 203-207. https://doi.org/10.1016/0006-2952(94)00470-6.

Fitzgerald, G.A., 1987. Dipyridamole. N. Engl. J. Med. 316, 1247–1257.

Gradl, S.N., Mueller, T., Ferrara, S., Sheikh, S.E., Janzer, A., Zhou, H.-J., Friberg, A., Guenther, J., Schaefer, M., Stellfeld, T., Eis, K., Kroeber, M., Nguyen, D., Merz, C., Niehues, M., Stoeckigt, D., Christian, S., Zimmermann, K., Lejeune, P., Bruening, M., Meyer, H., Puetter, V., Scadden, D.T., Sykes, D.B., Seidel, H., Eheim, A., Michels, M., Haegebarth, A., Bauser, M., 2019. Discovery of BAY 2402234 by phenotypic screening: a human dihydroorotate dehydrogenase (DHODH) inhibitor in clinical trials for the treatment of myeloid malignancies. Atlanta, GA. Philadelphia (PA). In: Proceedings of the American Association for Cancer Research Annual Meeting 2019; 2019 Mar 29-Apr 3, vol. 79, 13 Suppl. l), Abstr. 2.

Grandin, C., Lucas-Hourani, M., Janin, Y.L., Dauzonne, D., Munier-Lehmann, H., Paturet, A., Taborik, F., Vabret, A., Contamin, H., Tangy, F., Vidalain, P.-O., 2016. Respiratory syncytial virus infection in macaques is not suppressed by intranasal sprays of pyrimidine biosynthesis inhibitors. Antivir. Res. 125, 58–62.

Gregov, D., Jenkins, A., Duncan, E., Siebert, D., Rodgers, S., Duncan, B., Bochner, F., Lloyd, J., 1987. Dipyridamole: pharmacokinetics and effects on aspects of platelet function in man. Br. J. Clin. Pharmacol. 24, 425–434.

Gribaudo, G., Riera, L., Rudge, T.L., Caposio, P., Johnson, L.F., Landolfo, S., 2002. Human cytomegalovirus infection induces cellular thymidylate synthase gene expression in quiescent fibroblasts. J. Gen. Virol. 83, 2983–2993.

James, C., Harfouche, M., Welton, N.J., Turner, K.M.E., Abu-Raddad, L.J., Gottliebd, S.L., Looker, K.J., 2020. Herpes Simplex Virus: Global Infection Prevalence and Incidence

estimates. Bull. World Health Organ. 98, 315–329. https://doi.org/10.2471/BLT.19.237149, 2016.

Liu, Q., Gupta, A., Okesli-Armlovich, A., Qiao, W., Fischer, C.R., Smith, M., Carette, J.E., Bassik, M.C., Khosla, C., 2020. Enhancing the antiviral efficacy of RNA-dependent RNA polymerase inhibition by combination with modulators of pyrimidine metabolism. Cell Chem. Biol. 27, 668–677. https://doi.org/10.1016/j.chembiol.2020.05.002 e9.

Loeffler, M., Carrey, E.A., Knecht, W., 2020. The pathway to pyrimidines: the essential focus on dihydroorotate dehydrogenase, the mitochondrial enzyme coupled to the respiratory chain. Nucleos Nucleot. Nucleic Acids 11, 1–25. https://doi.org/10.1080/15257770.2020.1723625.

Looker, K.J., Elmes, J.A.R., Gottlieb, S.L., Schiffer, J.T., Vickerman, P., Turner, K.M.E., Boily, M.C., 2017. Effect of HSV-2 infection on subsequent HIV acquisition: an updated systematic review and meta-analysis. Lancet Infect. Dis. 11, 1303–1316. https://doi.org/10.1016/S1473-3099(17)30405-X.

Luganini, A., Caposio, P., Mondini, M., Landolfo, S., Gribaudo, G., 2008. New cell-based indicator assays for the detection of human cytomegalovirus infection and screening of inhibitors of viral immediate-early 2 protein activity. J. Appl. Microbiol. 105, 1791–1801. https://doi.org/10.1111/j.1365-2672.2008.03927.x.

Luganini, A., Fabiole Nicoletto, S., Pizzuto, L., Pirri, G., Giuliani, A., Landolfo, S., Gribaudo, G., 2011. Inhibition of Herpes Simplex Virus Type 1 and Type 2 Infections by peptide-derivatized dendrimers. Antimicrob. Agents Chemother. 55, 3231–3239.

Mahony, W.B., Domin, B., McConnells, R.T., Zimmerman, T., 1988. Acyclovir transport into human erythrocytes. J. Biol. Chem. 263, 9285–9291.

Marschall, M., Niemann, I., Kosulin, K., Bootz, A., Wagner, S., Dobner, T., Herz, T., Kramer, B., Leban, J., Vitt, D., Stamminger, T., Hutterer, C., Strobl, S., 2013. Assessment of drug candidates for broad-spectrum antiviral therapy targeting cellular pyrimidine biosynthesis. Antivir. Res. 100, 640–648. https://doi.org/10.1016/j.antiviral.2013.10.003.

Mercorelli, B., Luganini, A., Nannetti, G., Tabarrini, O., Palù, G., Gribaudo, G., Loregian, A., 2016. Drug repurposing approach identifies inhibitors of the prototypic vira transcription factor IE2 that block human cytomegalovirus replication. Cell Chem Biol 23, 340–351.

Munger, J., Bennett, B., Parikh, A., Feng, X.-J., McArdle, J., Rabitz, H.A., Shenk, T., Rabinowitz, J.D., 2008. Systems-level metabolic flux profiling identifies fatty acid synthesis as a target for antiviral therapy. Nat. Biotechnol. 26, 1179–1186. https://doi.org/10.1038/nbt.1500.

Okesli, A., Khosla, C., Bassik, M.C., 2017. Human pyrimidine nucleotide biosynthesis as a target for antiviral chemotherapy. Curr. Opin. Biotechnol. 48, 127–134. https://doi.org/10.1016/j.copbio.2017.03.010.

Peters, G.J., 2018. Re-evaluation of Brequinar sodium, a dihydroorotate dehydrogenase inhibitor. Nucleos Nucleot. Nucleic Acids 37, 666–678. https://doi.org/10.1080/15257770.2018.1508692.

Pizzorno, G., Cao, D., Leffert, J.J., Russell, R.L., Zhang, D., Handschumacher, R.E., 2002. Homeostatic control of uridine and the role of uridine phosphorylase: a biological and clinical update. Biochim. Biophys. Acta 1587, 133–144. https://doi.org/10.1016/S0925-4439(02)00076-5.

Reis, R.A.G., Calil, F.A., Feliciano, P.R., Pinheiro, M.P., Nonato, M.C., 2017. The dihydroorotate dehydrogenases: past and present. Arch. Biochem. Biophys. 632, 175–191. https://doi.org/10.1016/j.abb.2017.06.019.

Roizman, B., Knipe, D.M., Whitley, R.J., 2013. Herpes simplex viruses. Philadelphia, PA. In: Knipe, D.M., Howley, P.M. (Eds.), Fields Virology, sixth ed., vol. 2, pp. 1823–1897.

Sainas, S., Pippione, A.C., Lupino, E., Giorgis, M., Circosta, P., Gaidano, V., Goyal, P., Bonanni, D., Rolando, B., Cignetti, A., Ducime, A., Andersson, M., Järvå, M., Friemann, R., Piccinini, M., Ramondetti, C., Buccinnà, B., Al-Karadaghi, S., Boschi, D., Saglio, G., Lolli, M.L., 2018. Targeting myeloid differentiation using potent 2-Hydroxypyrazolo [1,5-α] pyridine scaffold-based human dihydroorotate dehydrogenase inhibitors. J. Med. Chem. 61, 6034–6055. https://doi.org/10.1021/acs.jmedchem.8b00373.

Sainas, S., Temperini, P., Farnsworth, J., Yi, F., Møllerud, S., Jensen, A.A., Nielsen, B., Passoni, A., Kastrup, J.S., Hansen, K.B., Boschi, D., Pickering, D.S., Clausen, R.P., Lolli, M.L., 2019. Use of the 4-hydroxy-triazole moiety as a bioisosteric tool in the development of ionotropic glutamate receptor ligands. J. Med. Chem. 62, 4467–4482.

Sainas, S., Giorgis, M., Circosta, P., Gaidano, V., Bonanni, D., Pippione, A.C., Bagnati, R., Passoni, A., Qiu, Y., Cojocaru, C.F., Canepa, B., Bona, A., Rolando, B., Mishina, M., Ramondetti, R., Buccinnà, B., Piccinini, M., Houshmand, M., Cignetti, A., Giraudo, E., Al-Karadaghi, S., Boschi, B., Saglio, G., Lolli, M.L., 2021. Targeting acute myelogenous leukemia using potent human dihydroorotate dehydrogenase inhibitors based on the 2-hydroxypyrazolo[1,5-a]pyridine scaffold: SAR of the biphenyl moiety. J. Med. Chem. (in press).

Samies, N.L., James, S.H., 2020. Prevention and treatment of neonatal herpes simplex virus infection. Antivir. Res. 176, 104721. https://doi.org/10.1016/j.antiviral.2020.104721.

Sanders, S., Harisdangkul, V., 2002. Leflunomide for the treatment of rheumatoid arthritis and autoimmunity. Am. J. Med. Sci. 323, 190–193.

Schaper, W., 2005. Dipyridamole, an underestimated vascular protective drug. Cardiovasc. Drugs Ther. 19, 357–363. https://doi.org/10.1007/s10557-005-4659-6.

Sepùlveda, C.S., Garcia, C.C., Damonte, E.B., 2018. Antiviral activity of A771726, the active metabolite of leflunomide, against Junín virus. J. Med. Virol. 90, 819–827. https://doi.org/10.1002/jmv.25024.

Smee, D.F., Hurst, B.L., Day, C.W., 2012. D282, a non-nucleoside inhibitor of influenza virus infection that interferes with de novo pyrimidine biosynthesis. Antivir. Chem. Chemother. 22, 263–272.

Snoeck, R., Andrei, G., Balzarini, J., Reymen, D., DeClercq, E., 1994. Dipyridamole potentiates the activity of various acyclicnucleoside phosphonates against varicella-zoster virus, herpes simplex virus and human cytomegalovirus. Antiviral Chem. Chemother. 5, 312–321. https://doi.org/10.1177/095632029400500505.

Szebeni, J., Wahl, S.M., Popovic, M., Wahl, L.M., Gartner, S., Fine, R.L., Skaleric, U., Friedman, R.M., Weinstein, J.N., 1989. Dipyridamole potentiates the inhibition by 3-azido-3-deoxythymidine and other dideoxynucleosides of human immunodeficiency virus replication in monocyte-macrophages. Proc. Natl. Acad. Sci. U.S.A. 86, 3842–3846.

Terlizzi, M.E., Occhipinti, A., Luganini, A., Maffei, M.E., Gribaudo, G., 2016. Inhibition of herpes simplex type 1 and type 2 infections by Oximacro®, a cranberry extract with a high content of A-type proanthocyanidins (PACs-A). Antivir. Res. 132, 154–164. https://doi.org/10.1016/j.antiviral.2016.06.006.

Wang, Q.Y., Bushell, S., Qing, M., Xu, H.Y., Bonavia, A., Nunes, S., Zhou, J., Poh, M.K., Florez de Sessions, P., Niyomrattanakit, P., Dong, H., Hoffmaster, K., Goh, A., Nilar, S., Schul, W., Jones, S., Kramer, L., Compton, T., Shi, P.Y., 2011. Inhibition of dengue virus through suppression of host pyrimidine biosynthesis. J. Virol. 85, 6548–6556.

Whitley, R.J., 2015. Herpes simplex virus infections of the central nervous system. Neuroinfectious Dis 21, 1704–1713. https://doi.org/10.1212/CON.0000000000000243.

Whitley, R.J., Baines, J., 2018. Clinical management of herpes simplex virus infections: past, present, and future [version 1; peer review: 2 approved]. F1000Research 7, 1726. https://doi.org/10.12688/f1000research.16157.1.

Article

The New Generation *h*DHODH Inhibitor MEDS433 Hinders the In Vitro Replication of SARS-CoV-2 and Other Human Coronaviruses

Arianna Calistri [1,†] , Anna Luganini [2,†] , Barbara Mognetti [2] , Elizabeth Elder [3], Giulia Sibille [2] , Valeria Conciatori [1], Claudia Del Vecchio [1], Stefano Sainas [4] , Donatella Boschi [4] , Nuria Montserrat [5,6,7], Ali Mirazimi [3,8,9], Marco Lucio Lolli [4], Giorgio Gribaudo [2,*,‡] and Cristina Parolin [1,‡]

1   Department of Molecular Medicine, University of Padua, 35121 Padua, Italy; arianna.calistri@unipd.it (A.C.); valeria.conciatori@gmail.com (V.C.); claudia.delvecchio@unipd.it (C.D.V.); cristina.parolin@unipd.it (C.P.)
2   Department of Life Sciences and Systems Biology, University of Turin, 10123 Turin, Italy; anna.luganini@unito.it (A.L.); barbara.mognetti@unito.it (B.M.); giulia.sibille@unito.it (G.S.)
3   Public Health Agency of Sweden, 17182 Solna, Sweden; elizabeth.elder@folkhalsomyndigheten.se (E.E.); ali.mirazimi@folkhalsomyndigheten.se (A.M.)
4   Department of Sciences and Drug Technology, University of Turin, 10125 Turin, Italy; stefano.sainas@unito.it (S.S.); donatella.boschi@unito.it (D.B.); marco.lolli@unito.it (M.L.L.)
5   Pluripotency for Organ Regeneration, Institute for Bioengineering of Catalonia (IBEC), The Barcelona Institute of Technology (BIST), 08028 Barcelona, Spain; nmontserrat@ibecbarcelona.eu
6   Catalan Institution for Research and Advanced Studies (ICREA), 08010 Barcelona, Spain
7   Centro de Investigación Biomédica en Red en Bioingeniería, Biomateriales y Nanomedicina, 28029 Madrid, Spain
8   Karolinska Institute and Karolinska University Hospital, Department of Laboratory Medicine, Unit of Clinical Microbiology, 17177 Stockholm, Sweden
9   National Veterinary Institute, 75189 Uppsala, Sweden
*   Correspondence: giorgio.gribaudo@unito.it; Tel.: +39-011-6704648
†   These authors contributed equally to this work.
‡   Co-senior author.

Abstract: Although coronaviruses (CoVs) have long been predicted to cause zoonotic diseases and pandemics with high probability, the lack of effective anti-pan-CoVs drugs rapidly usable against the emerging SARS-CoV-2 actually prevented a promptly therapeutic intervention for COVID-19. Development of host-targeting antivirals could be an alternative strategy for the control of emerging CoVs infections, as they could be quickly repositioned from one pandemic event to another. To contribute to these pandemic preparedness efforts, here we report on the broad-spectrum CoVs antiviral activity of MEDS433, a new inhibitor of the human dihydroorotate dehydrogenase (*h*DHODH), a key cellular enzyme of the de novo pyrimidine biosynthesis pathway. MEDS433 inhibited the in vitro replication of hCoV-OC43 and hCoV-229E, as well as of SARS-CoV-2, at low nanomolar range. Notably, the anti-SARS-CoV-2 activity of MEDS433 against SARS-CoV-2 was also observed in kidney organoids generated from human embryonic stem cells. Then, the antiviral activity of MEDS433 was reversed by the addition of exogenous uridine or the product of *h*DHODH, the orotate, thus confirming *h*DHODH as the specific target of MEDS433 in hCoVs-infected cells. Taken together, these findings suggest MEDS433 as a potential candidate to develop novel drugs for COVID-19, as well as broad-spectrum antiviral agents exploitable for future CoVs threats.

Keywords: coronavirus; SARS-CoV-2; pyrimidine biosynthesis; *h*DHODH inhibitor; antiviral activity; combination treatment; organoids; broad-spectrum antiviral

1. Introduction

We have been living with COVID-19 for more than a year and a half. One of the most dramatic things this pandemic has taught us is the total unpreparedness to tackle a novel

coronavirus disease by a curative approach. Despite the fact that coronaviruses (CoVs) have long been predicted to cause zoonotic diseases with high probability, as SARS and MERS outbreaks demonstrated, the lack of effective pan-coronavirus (pan-CoVs) antivirals significantly contributed to the vulnerability of our public health systems to the SARS-CoV-2 pandemic, thus making the therapeutic management of COVID-19 mostly supportive, with the only aim to reduce mortality [1–3].

It is reassuring that prevention of COVID-19 is now achievable thanks to the deployment of effective next generation SARS-CoV-2-specific vaccines [4]. However, even in the best scenario possible, we must not fail to consider that: (1) the evolution of SARS-CoV-2 is leading to virus variants that might escape the antibody-mediated immunity and cause reinfections; (2) the durability of protection afforded by the vaccines is not yet known and it may be limited; (3) the large scale-immunization to achieve a global vaccine coverage may not be complete due to unfolding productive and logistical challenges and reluctance to vaccinate; and (4) the value of the current SARS-CoV-2 specific vaccines for effective prevention of new CoVs that might likely may emerge in future from animal reservoir hosts is unknown [5].

For all these reasons, effective broad-spectrum anti-CoVs antivirals can be highly valuable to fill the gap in the control of emerging CoVs diseases given their rapid repositioning from one pandemic event to another. This will allow us to: (1) protect individuals with susceptibility to severe disease from new CoVs and thus save lives; (2) contribute to Public Health measures by slowing down the spread of the new disease; and (3) buy time while waiting for CoV-specific vaccine development [6,7].

To be candidate broad-spectrum anti-CoVs agents, small molecules must interfere with host or viral targets that are: (1) highly conserved among known CoVs; (2) essential to replication or pathogenesis of known hCoVs; and (3) likely to be conserved and essential even in future emerging CoVs [7]. To develop such a molecule, two main strategies can be followed. The first aims to discover broad spectrum Direct Acting Antivirals (DAAs) that target the most conserved proteins among CoVs, such as the RNA-dependent RNA polymerase, the 3C-like protease or main protease (M^{pro}), and the papain-like Protease (PL^{pro}) [8,9]. However, targeting such viral proteins by DAAs is prone to the development of viral resistance, as is well established for other RNA viruses. Therefore, the second drug development strategy works toward the design of broad-spectrum anti-CoVs agents able to interfere with those cellular enzymes and factors utilized by all CoVs during their life cycle. Clearly, these Host-Targeting Antivirals (HTAs) can overcome the potential emergence of drug resistance associated with DAAs, but have the disadvantages of potential off-target effects [8,9].

Pyrimidine availability in infected cells is crucial for CoVs replication and thus compounds targeting the cellular de novo pyrimidine biosynthetic pathway have the potential to be developed as effective broad-spectrum anti-CoV HTA agents. In this biochemical pathway, the dihydroorotate dehydrogenase (DHODH) catalyzes the rate-limiting step of dehydrogenation of dihydroorotate (DHO) to orotate (ORO), ultimately providing uridine monophosphate (UMP), the precursor for all pyrimidine nucleotides for RNA and DNA [10–13]. Therefore, given its critical role, DHODH could be a target of choice for the development of HTAs against SARS-CoV-2 and CoVs and, to validate this antiviral strategy, potent and safe human DHODH (*h*DHODH) inhibitors are urgently required [14]. In this regard, starting from the scaffold of brequinar, one of the most potent *h*DHODH inhibitors so far discovered [15], we have contributed to this need by developing a novel class of potent *h*DHODH inhibitors characterized by an unusual carboxylic bioisostere 2-hydroxypyrazolo [1,5-a] pyridine moiety [16,17].

The aim of this study was thus to investigate the potential of this new class of *h*DHODH inhibitors as broad-spectrum CoVs antivirals. We report that one of these molecules, termed MEDS433, potently inhibits the in vitro replication of SARS-CoV-2 and other hCoVs through the selective block of *h*DHODH enzymatic activity. These results identify MEDS433 as a promising candidate to develop new broad-spectrum anti-CoVs agents.

2. Materials and Methods

2.1. Compounds

The *h*DHODH inhibitors (Figure 1A) were synthesized as described previously [16,17]. Brequinar, uridine, orotic acid (ORO), dihydroorotic acid (DHO), and dipyridamole (DPY) were purchased from Sigma-Aldrich. Remdesivir (RDV) (GS-5734) was obtained by Med-ChemExpress.
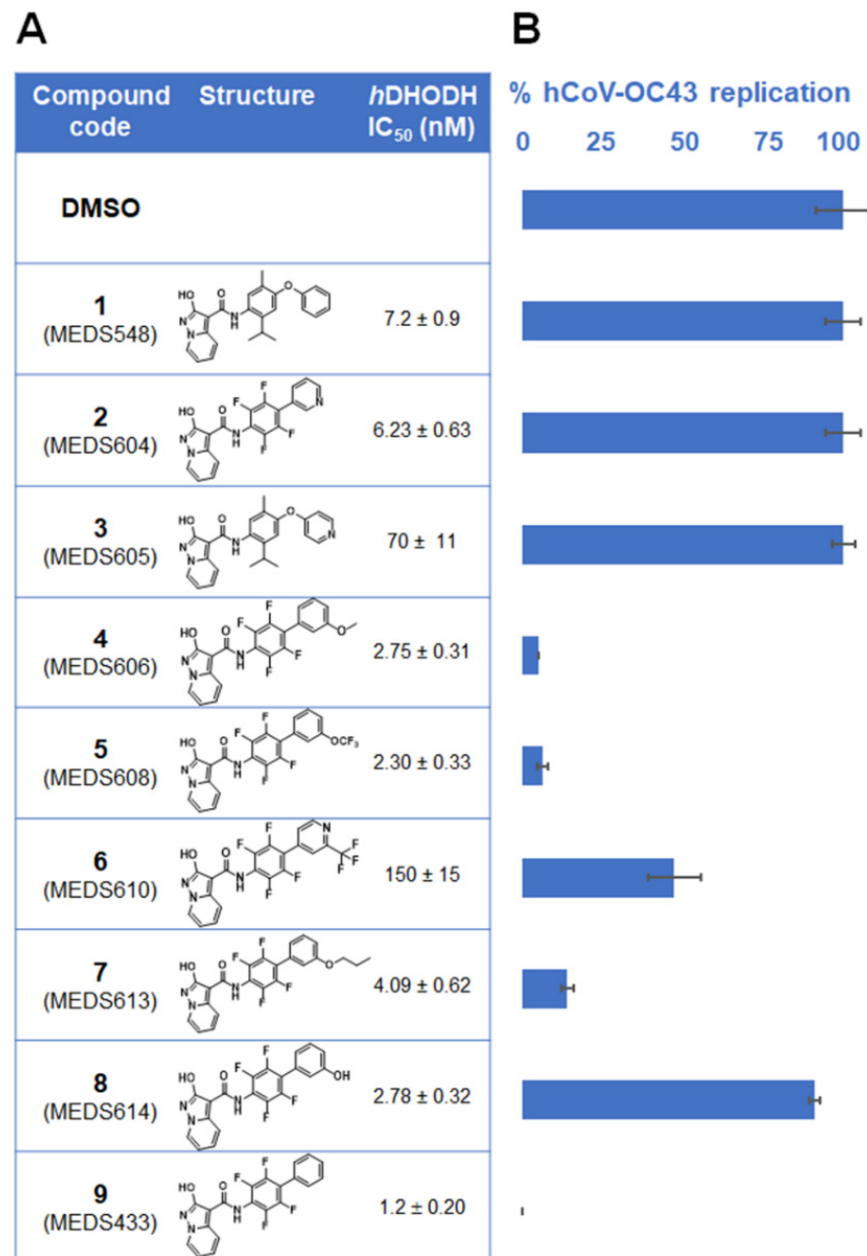

Figure 1. Selection of *h*DHODH inhibitors with anti-hCoV activity. HCT-8 cells were pretreated and treated vehicle (DMSO) or with 0.1 μM of the different *h*DHODH inhibitors showed in (**A**) 1 h prior to, during infection with hCoV-OC43 (100 PFU/well), and throughout the experiment. At 72 h p.i., viral foci were immunostained and the mean foci number in treated culture compared to that of DMSO-treated and hCoV-OC43-infected control HCT-8 cell monolayers. The replication rates shown in (**B**) represent means ± SD (error bars) of three independent experiments performed in triplicate.

2.2. Cells and Viruses

Human lung fibroblasts MRC5 (ATCC CCL-171), the human colorectal carcinoma HCT-8 (ATCC CCL-244), the human lung adenocarcinoma Calu-3 (ATCC HTB-55), and the African green monkey kidney Vero E6 (ATCC CRL-1586) cell lines were purchased from the American Type Culture Collection (ATCC), and maintained in Dulbecco's Modified Eagle Medium (DMEM; Euroclone) supplemented with 10% fetal bovine serum (FBS, Euroclone), 2 mM glutamine, 1 mM sodium pyruvate, 100 U/mL penicillin, and 100 µg/mL streptomycin sulfate (P/S, both from Euroclone).

hCoV-229E (ATCC VR-740) and hCoV-OC43 (ATCC VR-1558) were purchased from ATCC, and propagated and titrated in MRC5 and HCT-8 cells, respectively. SARS-CoV-2 (2019-nCoV/Italy INMI1) was obtained from EVAg, and propagated and titrated in Vero E6 cells. SARS-CoV-2/01/human/2020/SWE was isolated on Vero E6 cells from a nasopharyngeal sample, cultivated and titrated as previously described [18]. All work with SARS-CoV-2 was performed in Biosafety laboratory level 3 (BSL3) facilities either at the University of Padua, Italy, or at the Public Health Agency of Sweden, Sweden.

2.3. Cytotoxicity Assays

Cells were seeded in 96-well plates and, after 24 h, exposed to increasing concentrations of compounds or vehicle (DMSO) as control. After 72 h of incubation, the number of viable cells was determined using either the CellTiter-Glo Luminescent assay (Promega, Madison, WI, USA) according to the specifications of the manufacturer, or the MTT method as previously described [19,20].

2.4. Antiviral Assays

To select the mini-library of *h*DHODH inhibitors, focus forming reduction assays (FFRAs) [21] were performed on HCT-8 cell monolayers treated with the vehicle (DMSO) or with 0.1 µM of the different compounds 1 h prior to and during infection with the hCoV-OC43 (100 PFU/well). At 72 h post-infection (p.i.), cell monolayers were fixed, and subjected to indirect immunoperoxidase staining with a mAb against the hCoV-OC43 N protein (clone.542-D7; Millipore, Burlington, MA, USA) (diluted 1:100). Viral foci were microscopically counted, and the mean counts for each drug concentration were expressed as a percentage of the mean plaque counts of control virus (DMSO). To determine the anti-hCoV-229E activity of MEDS433 or brequinar, MRC5 cell monolayers were treated with different concentrations of the compounds 1 h prior to and during infection with hCoV-229E (100 PFU/well). After 72 h p.i., cell viability was measured using CellTiter-Glo assay as a surrogate measurement of the viral cytopathic effect (CPE), as previously described [22]. To measure the anti-SARS-CoV-2 activity of MEDS433 or brequinar, virus yield reduction assay (VRA) was performed with Vero E6 or Calu-3 cells. Briefly, cell monolayers were treated with the vehicle or increasing concentrations of compounds 1 h before and during infection with SARS-CoV-2 (50 or 100 PFU/well). At 48 h p.i., SARS-CoV-2 in cell supernatants was titrated by plaque assay on Vero E6 cells. Compound concentrations producing 50 and 90% reductions in plaque formation (EC_{50} and EC_{90}) were determined as compared to control treatment (DMSO). To evaluate the effect of uridine, DHO or ORO addition, VRAs were performed with Vero E6 or Calu-3 cells infected with SARS-CoV-2 (50 or 100 PFU/well), and treated with increasing concentrations of uridine, ORO or DHO in presence of 0.3 µM of MEDS433 for Vero E6 cells or 0.5 µM for Calu-3 cells. After 48 h p.i., cell supernatants were harvested and titrated for SARS-CoV-2 infectivity on Vero E6 cells.

To assess the effect of blocking both the de novo biosynthesis and the salvage pathway of pyrimidines, Calu-3 cells were infected with SARS-CoV-2 (100 PFU/well) and treated throughout VRAs with different concentration of MEDS433 in combination with increasing concentrations of DPY in medium supplemented with uridine (20 µM). At 48 h p.i., supernatants were harvested and titrated for SARS-CoV-2 infectivity on Vero E6 cells.

To measure the effect of MEDS433 on SARS-CoV-2 intracellular RNA load, Calu-3 cells were seeded in 24 well-plates and 24 h later were treated with the vehicle or 0.5 μM of compound 1 h before, and during infection with SARS-CoV-2 (100 PFU/well). At 10, 24, and 48 h p.i., total RNA was extracted from cell pellets (PureLink™ RNA Mini Kit-Thermo Fisher Scientific, Waltham, MA, USA) and quantified by Nanodrop 1000 spectrometer (Thermo Scientific). Next, 500 ng RNA were retrotranscribed by means of the High capacity cDNA reverse transcription kit (Applied Biosystem, Waltham, MA, USA) and 50 ng of cDNA were amplified by qPCR by using the following SARS-CoV-2 N gene specific primers/probes [23]:

Forward: CACATTGGCACCCGCAATC;
Reverse: GAGGAACGAGAAGAGGCTTG;
Probe: FAM-ACTTCCTCAAGGAACAACATTGCCA-BBQ.

Data were normalized using GAPDH (ThermoFisher) and analyzed with the $2^{-\Delta\Delta C_t}$ method [24] by adopting the mean of the ΔC_t values obtained for the vehicle treated samples as reference. Finally, data were expressed as the ratio between values calculated for MEDS433 treated samples, and the mean of the ones calculated for vehicle treated samples ± standard deviation.

2.5. Kidney Organoid Generation and SARS-CoV-2 Infection

Kidney organoids were differentiated from human embryonic stem cells as previously described [18,25], and infected with 100 PFU/organoid of SARS-CoV-2/01/human/2020/SWE [18] at day 20–25 of differentiation in advanced RPMI medium (ThermoFisher). Organoids were infected in the presence of DMSO or 0.5 μM MEDS433 in ultra-low attachment plates for 48 h. Organoids were then pooled into groups of four, washed three times with PBS and lysed in Trizol. RNA was extracted using Direct Zol RNA mini kit (Zymo research), and analyzed for the content of SARS-CoV-2 RNA by RT-qPCR using the following primers/probes as previously described [18]:

SARS-CoV-2 E gene:
Forward: ACAGGTACGTTAATAGTTAATAGCGT;
Reverse: ATATTGCAGCAGTACGCACACA;
Probe: FAM-ACACTAGCCATCCTTACTGCGCTTCG-MGB.
Human RNase P:
Forward: AGATTTGGACCTGCGAGCG;
Reverse: GAGCGGCTGTCTCCACAAGT;
Probe: VIC-TTCTGACCTGAAGGCTCTGCGCG-MGB.

Human RNase P was used as an endogenous gene control to normalize the levels of intracellular SARS-CoV-2 RNA.

2.6. Immunofluorescence

Vero E6 cells seeded on coverslip were treated with vehicle or with 0.5 μM MEDS433 1 h prior to infection with SARS-CoV-2 at an MOI of 0.1. At 24 h p.i., cells were fixed, permeabilized, and stained with an anti-SARS-CoV-2 N nucleocapsid protein mAb (Sino Biologicals, Beijing, China) followed by Alexa 488-conjugated rabbit anti-mouse antibody (Life Technologies, Carlsbad, CA, USA). Nuclei were stained with DRAQ5 (InVitrogen, Waltham, MA, USA).

2.7. Statistical Analysis

All statistical analyses were performed using GraphPad Prism version 7.0. Data of antiviral activity are presented as the means ± SDs of at least three experiments performed in triplicate. Differences were considered to be statistically significant for $p < 0.05$.

3. Results

3.1. Identification of a New hDHODH Inhibitor Active against a Human Coronavirus

To investigate the feasibility of targeting *h*DHODH activity to develop broad-spectrum HTA, nine newly designed *h*DHODH inhibitors (Figure 1A) [16,17] were selected for antiviral activity against the prototypical human β-CoV, hCoV-OC43, by using FFRAs in which test compounds were present before, during and after infection (full-treatment). As shown in Figure 1B, when tested at 0.1 μM, five *h*DHODH inhibitors (4, 5, 6, 7, and 9) were able to decrease hCoV-OC43 replication more than 50%, while the remaining four compounds (1, 2, 3 and 8) were ineffective. Notably, compound 9, MEDS433, was the most effective among the tested *h*DHODH inhibitors, since it abrogated hCoV-OC43 replication completely (Figure 1B). MEDS433 was therefore selected for further investigations.

3.2. Inhibition of α- and β-Coronavirus Replication by the hDHODH Inhibitor MEDS433

A significant concentration-dependent inhibition of hCoV-OC43 replication was then confirmed in HCT-8 cells treated with MEDS433 (Figure 2A). MEDS433 was also very effective against another hCoV, the prototypic α-hCoV-229E, whose replication in MRC5 fibroblasts was severely impaired (Figure 2B). As reported in Table 1, the measured EC_{50} and EC_{90} values for both hCoVs were in the low nanomolar range. The comparison with the reference drug RDV, used as a positive control for anti-hCoV antiviral activity [19], highlighted an anti-hCoV-229E potency of MEDS433 comparable to that of RDV (EC_{50} 0.0348 ± 0.005 μM), while the *h*DHODH inhibitor was much more effective than RDV (EC_{50} 0.147 ± 0.034 μM) against hCoV-OC43. To the contrary, MEDS433 was more effective than brequinar against hCOV-229E, as the EC_{50} of the latter was 0.0427 ± 0.003 μM, whereas against hCoV-OC43 the EC_{50} of brequinar (0.022 ± 0.003 μM) was commensurate with that of MEDS433. Finally, the anti-hCoVs activity of MEDS433 was not due to cytotoxicity of target cells themselves, since its cytotoxic concentration (CC_{50}) as determined in uninfected cells was 78.48 ± 4.6 μM for HCT-8 cells, and 104.80 ± 19.75 μM for MRC5 fibroblasts, with a favorable Selective Index (SI) greater than 6300 and 4600 for hCoV-OC43 and hCoV-299E, respectively (Table 1).

Table 1. Antiviral activity of MEDS433 against different human coronaviruses.

hCoV	Cell Line	EC_{50} (μM) [a]	EC_{90} (μM) [b]	CC_{50} (μM) [c]	SI [d]
hCoV-OC43	HCT-8	0.012 ± 0.003	0.044 ± 0.021	78.48 ± 4.60	6329
hCoV-229E	MRC5	0.022 ± 0.003	0.288 ± 0.040	104.80 ± 19.75	4763
SARS-CoV-2	Vero E6	0.063 ± 0.004	0.136 ± 0.007	>500	>7900
SARS-CoV-2	Calu-3	0.076 ± 0.005	0.513 ± 0.016	>125	>1600

[a] EC_{50}, compound concentration that inhibits 50% of replication, as determined by FFRA against hCoV-OC43 in HCT-8 cells, or by measuring MRC5 cell viability as a surrogate of viral CPE against hCoV-229E, or by VRAs against SARS-CoV-2 in Vero E6 or in Calu-3 cells. Reported values represent the means $\pm$ SD of data derived from three experiments in triplicate. [b] EC_{90}, compound concentration that inhibits 90% of viral replication. [c] CC_{50}, compound concentration that produces 50% of cytotoxicity, as determined by cell viability assays in HCT-8, MRC5, Vero E6 or Calu-3 cells. Reported values represent the means $\pm$ SD of data derived from three experiments in triplicate. [d] SI, selectivity index (determined as the ratio between CC_{50} and EC_{50}).
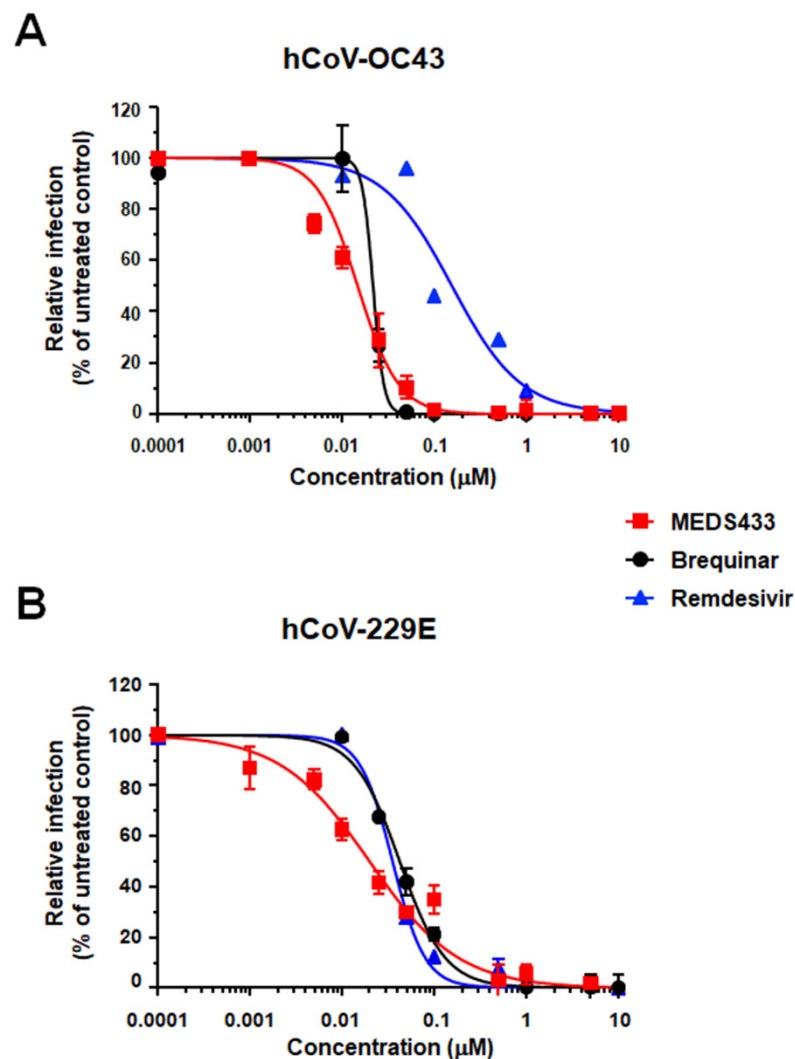
Figure 2. Antiviral activity of MEDS433 against hCoV-OC43 and hCoV-229E. HCT-8 (**A**) or MRC5 (**B**) cell monolayers were infected with the hCoV-OC43 or hCoV-229E (100 PFU/well), and, where indicated, the cells were treated with increasing concentrations of compounds 1 h before, and during virus adsorption. Compounds remained in the culture medium throughout the experiment. hCoV-OC43 replication was quantified at 72 h p.i. by FFRA, while for hCoV-229E, MRC5 cell viability was measured using the CellTiter-Glo luminescent at 72 h p.i. as a surrogate of viral CPE. The compounds concentrations producing 50% and 90% reductions of viral replication (EC_{50} and EC_{90}, respectively) were determined by GraphPad Prism. The data shown represent means $\pm$ SD (error bars) of three independent experiments performed in triplicate.

3.3. MEDS433 Exerts an Antiviral Activity against SARS-CoV-2

To investigate the effect of MEDS433 on SARS-CoV-2 replication, Vero E6 cells were infected with a clinical isolate of SARS-CoV-2, and then treated with 0.5 µM MEDS433. At 24 h p.i., cells were fixed, permeabilized and immunostained for the nucleocapsid N protein expression. As shown in Figure 3A, confocal microscopy revealed that while about 85% of infected control cells expressed the N protein, MEDS433 treatment completely abolished its accumulation, thus indicating that N protein expression could be prevented by targeting the de novo pyrimidine biosynthesis.
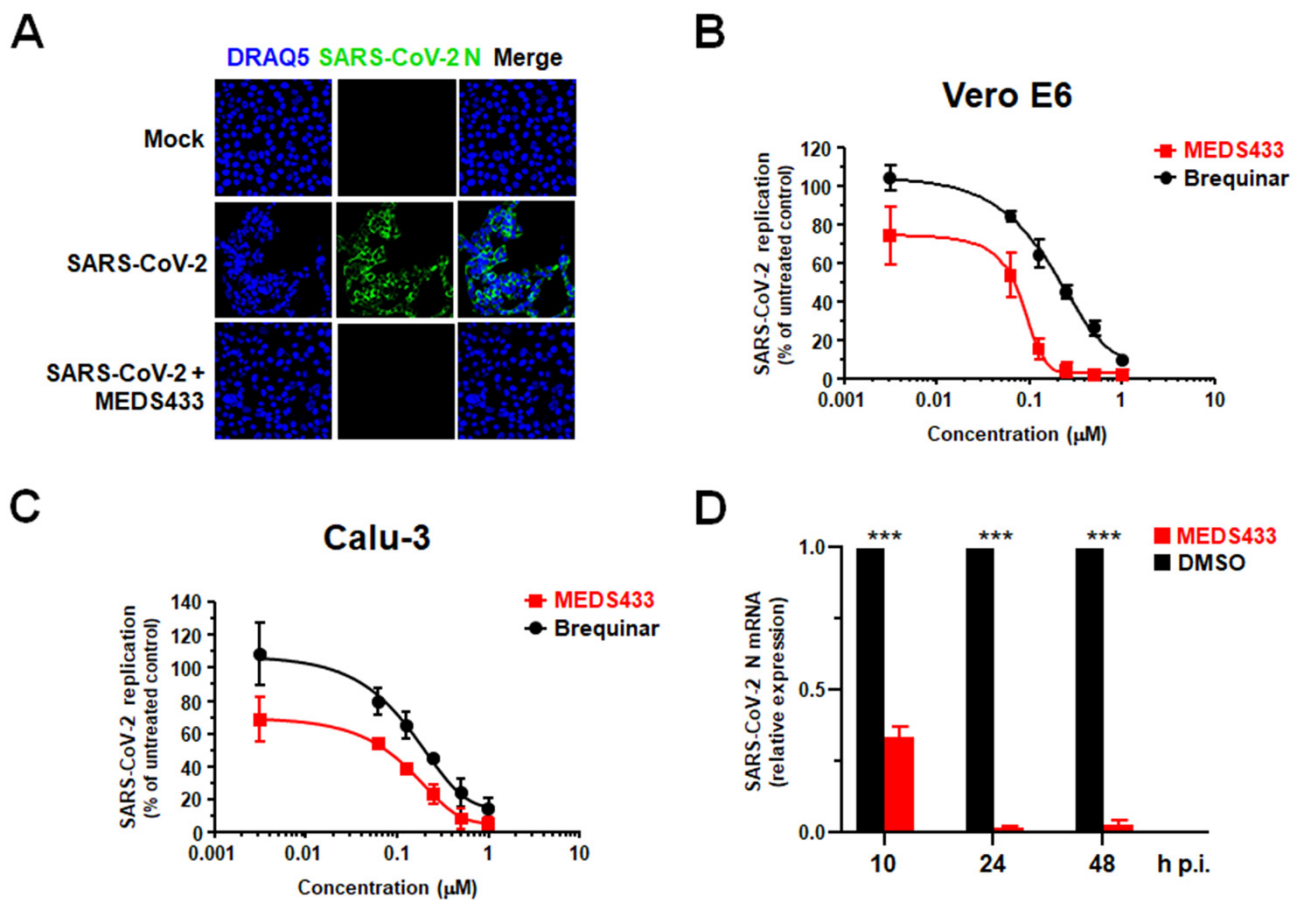
Figure 3. Antiviral activity of MEDS433 against SARS-CoV-2 replication. (**A**) Immunofluorescence analysis of SARS-CoV-2-infected cells. Vero E6 cells were treated with vehicle (DMSO) or with 0.5 μM MEDS433 1 h prior to infection with SARS-CoV-2 at an MOI of 0.1. At 24 h p.i., cells were fixed, permeabilized, and immunostained with an anti-SARS-CoV-2 nucleocapsid protein (N) mAb, followed by Alexa 488-conjugated secondary antibody. Nuclei were stained with DRAQ5. Confocal laser microscopy images acquired in the green (SARS-CoV-2 N) and the blue (DRAQ5) channels are shown, as well as overlaid images (merge). Magnification, ×60. (**B**) Dose dependent inhibition of SARS-CoV-2 replication by MEDS433 in Vero E6 cells. Vero E6 cell monolayers were infected with SARS-CoV-2 (50 PFU/well), and, where indicated, the cells were treated with vehicle (DMSO) or increasing concentrations of MEDS433 or brequinar 1 h before, during virus adsorption, and throughout the experiment. At 48 h p.i., infectious SARS-CoV-2 in cell supernatants was titrated by plaque assay on Vero E6 cells. (**C**) Anti-SARS-CoV-2 activity of MEDS433 in Calu-3 cells. Calu-3 cells were infected with SARS-CoV-2 (100 PFU/well), and, where indicated, the cells were treated with vehicle (DMSO) or increasing concentrations of MEDS433 or brequinar 1 h before, during virus adsorption, and throughout the experiment. At 48 h p.i., infectious SARS-CoV-2 in cell supernatants was titrated by plaque assay on Vero E6 cells. MEDS433 and brequinar concentrations producing 50 and 90% reductions in SARS-CoV-2 yield (EC_{50} and EC_{90}, respectively) were determined as compared to control treatment (DMSO). The data shown represent means $\pm$ SD (error bars) of three independent experiments performed in triplicate. (**D**) Effect of MEDS433 on SARS-CoV-2 intracellular RNA. Calu-3 cells were treated with vehicle (DMSO) or 0.5 μM of MEDS433 1h before and during infection with SARS-CoV-2 (100 PFU/well). At 10, 24, and 48 h p.i., total RNA was extracted and subjected to RT-qPCR by using primers and probe specific for the SARS-CoV-2 N gene. Data were normalized using GAPDH and analyzed with the $2^{-\Delta\Delta C_t}$ method by adopting the mean of the ΔC_t values obtained for the vehicle treated samples as reference. The reported values represent that ratio between data calculated for MEDS433 treated samples and the mean of the ones calculated for vehicle treated samples $\pm$ standard deviation. Statistical significance was calculated by a one-way ANOVA followed by Dunnett's multiple comparison test. *** ($p < 0.0001$) compared to the calibrator sample (DMSO).

VRAs were then performed in SARS-CoV-2-infected Vero E6 cells treated with increasing concentrations of MEDS433 for 48 h and a clear concentration-dependent inhibition of SARS-CoV-2 replication was measured (Figure 3B). Of note, the anti-SARS-CoV-2 activity of MEDS433 was also observed in the more relevant cell model of the human lung adenocarcinoma Calu-3 cells (Figure 3C), in which of 0.076 ± 0.005 μM and 0.513 ± 0.016 μM were measured. Again, the measured EC_{50} and EC_{90} values of MEDS433 in both Vero E6 and Calu-3 cell models were in the low nanomolar range (Table 1). Furthermore, MEDS433 was more effective than brequinar against SARS-CoV-2, since the EC_{50} values of brequinar were of 0.200 ± 0.01 μM in Vero E6 cells, and of 0.214 ± 0.002 μM in Calu-3 cells, respectively (Figure 3B,C). Then, as shown in Table 1, the CC_{50} values of MEDS433 measured in uninfected cells, were >500 μM in Vero E6 cells (SI > 7900) and >125 μM in Calu-3 cells (SI > 1600), thus indicating that its anti-SARS-CoV-2 activity was not due to a reduced cell viability.

Finally, to evaluate a direct effect of *h*DHODH inhibition on the RNA synthesis step of SARS-CoV-2 replicative cycle, the intracellular accumulation of viral N transcript was measured in infected Calu-3 cells treated with 0.5 μM of MEDS433 for 10, 24 or 48 h p.i. As depicted in Figure 3D, RT-qPCR quantification showed a significant reduction in N mRNA levels already at 10 h p.i., and this inhibition became more severe at later times of infection, when MEDS433 almost completely suppressed N mRNA synthesis, thus confirming the importance of the *h*DHODH activity for efficient SARS-CoV-2 replication.

Taken together, the results of the different antiviral assays against SARS-CoV-2, as well as those against hCoV-229E and hCoV-OC43 (Figure 2), highlight a broad-spectrum anti-CoVs activity of MEDS433.

3.4. MEDS433 Affects SARS-CoV-2 Replication in Kidney Organoids

Organoids set a pattern of the physiological conditions of human organs, and therefore they can be suitable infection models for the development of anti-SARS-CoV-2 drugs [26]. Relevant to a suitable organoids model, it is known that, in addition to the lung damage caused by pneumonia, SARS-CoV-2 infection affects several other organs like the kidney. Severe COVID-19 disease is in fact frequently associated with kidney injury produced by both indirect mechanisms and direct damage due to virus replication [27,28]. Actually, SARS-CoV-2 has been found in autopsy specimens and urine samples [29,30], and its cellular receptor, ACE2, is highly expressed in renal tubules [31].

Based on this rationale, to analyze the effect of MEDS433 in a more physiologically and relevant in vitro system, we used kidney organoids as a model of SARS-CoV-2 infection [18]. The organoids used in our model are heterogeneous, and therefore multiple batches of kidney organoids differentiated from human stem cells were employed to perform the antiviral assays. As shown in Figure 4, the average results obtained from infections of three separate batches of organoids indicated that the inhibitory effect of MEDS433 on SARS-CoV-2 replication could be reproduced in kidney organoids, thus suggesting an anti-SARS-CoV-2 activity of MEDS433 even in this complex experimental model.
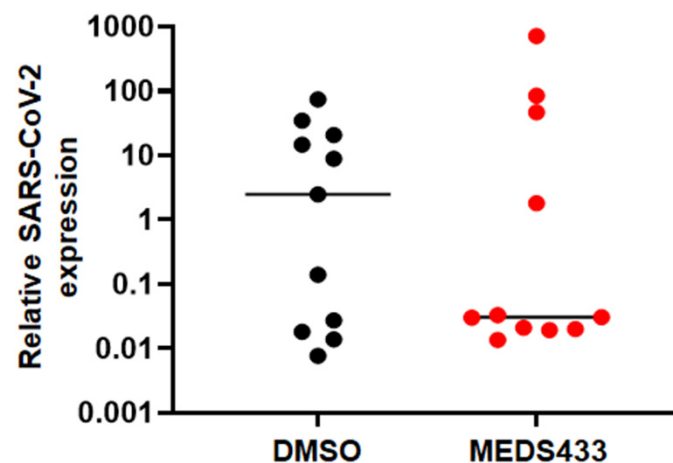
Figure 4. Effects of MEDS433 on SARS-CoV-2 replication in kidney organoids. Kidney organoids were infected with 100 PFU of SARS-CoV-2/01/human/2020/SWE per organoid and simultaneously treated with 0.5 μM MEDS433 or vehicle (DMSO) as a control. After 48 h, kidney organoids were washed, and harvested for analysis of SARS-CoV-2 E RNA levels by RT-qPCR. The results from three independent batches of kidney organoids are shown with line at mean relative to mock-infected controls; batches 1 and 2 contained 3 groups of 4 pooled organoids, batch 3 contained 5 groups of 4 pooled organoids per treatment condition.

3.5. The Antiviral Activity of MEDS433 Is Reversed by Uridine and Orotic Acid

To verify the hypothesis of an interference with the pyrimidine biosynthesis pathway as the mechanism of the anti-hCoVs activity of MEDS433, we investigated in Vero E6 and Calu-3 cells whether the anti-SARS-CoV-2 activity of MEDS433 could be overcome by supplementing cell medium with increasing concentrations of exogenous uridine, thus bypassing the requirement of de novo pyrimidine biosynthesis. As shown in Figure 5, the anti-SARS-CoV-2 activity of 0.3 μM MEDS433 in Vero-E6 (upper panel A) and of 0.5 μM in Calu-3 (upper panel B) cells was significantly reversed by a 100-fold excess of uridine relative to MEDS433 concentration, and completely overturned by greater uridine concentrations, thus confirming that the de novo pyrimidine pathway was inhibited by MEDS433 in SARS-CoV-2-infected cells. Then, to prove that *h*DHODH inhibition was responsible of MEDS433 antiviral effect, increasing concentrations of the *h*DHODH substrate dihydroorotic acid or its product, orotic acid were added to cell medium. In Vero E6 or Calu-3 cells treated with MEDS433 and infected with SARS-CoV-2, the addition of orotic acid reversed in a dose dependent manner the antiviral effect of MEDS433 (Figure 5 lower panels), with complete reversion achieved at the highest concentration (1000× the MEDS433 concentration). In contrast, dihydroorotic acid, even at 1 mM (3333 times more than MEDS433), did not affect MEDS433 antiviral activity (Figure 5, lower panels), thus indicating that MEDS433 inhibited a step in the de novo pyrimidine biosynthesis pathway downstream from dihydroorotic acid.

Altogether, these results confirmed that MEDS433 specifically targets *h*DHODH activity in SARS-CoV-2-infected cells, and that this inhibition is responsible of its overall antiviral activity.
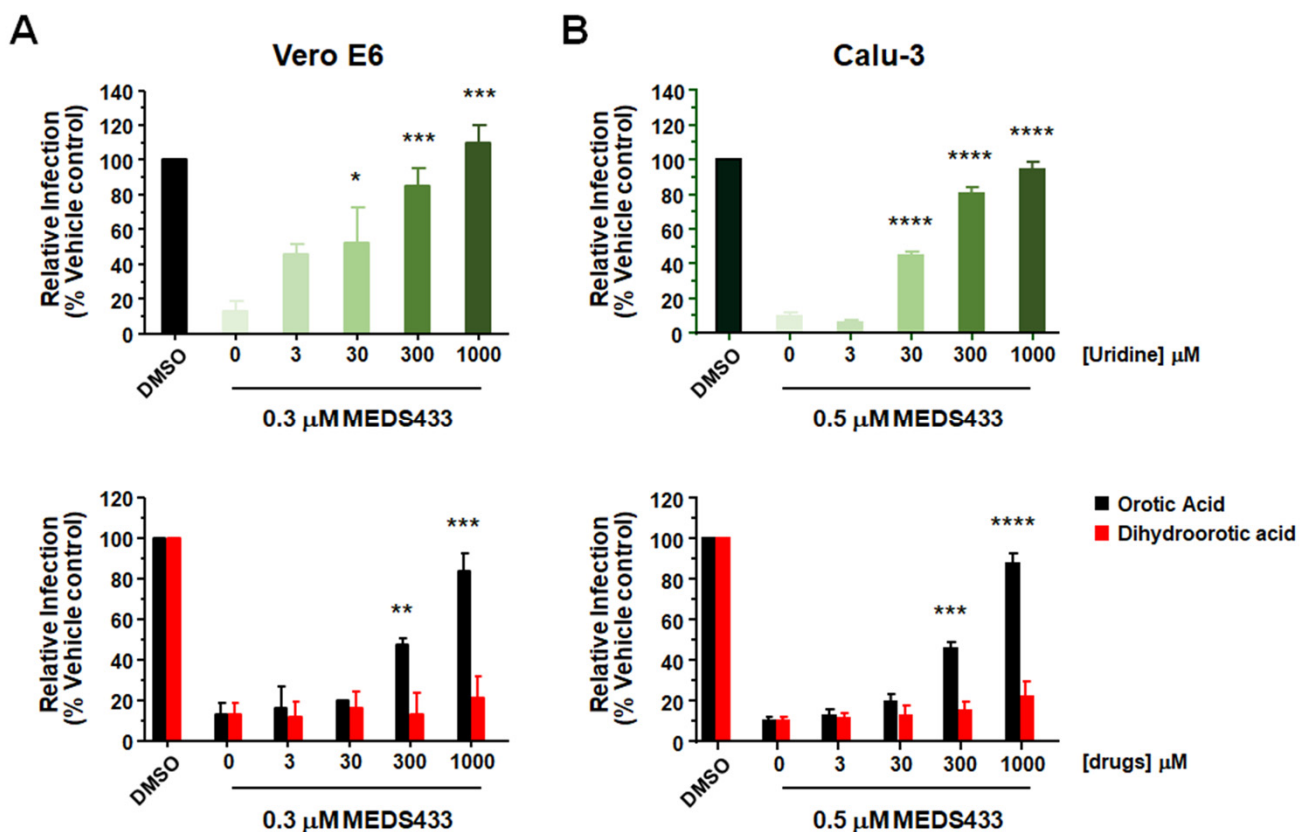
Figure 5. Uridine or orotic acid supplementation counteracts the anti-SARS-CoV-2 activity of MEDS433. Vero E6 (**A**) or Calu-3 (**B**) cells were treated with vehicle (DMSO), or 0.3 µM of MEDS433 for Vero E6 cells, or 0.5 µM of MEDS433 for Calu-3 cells in the absence or presence of increasing concentrations of uridine (upper panel), orotic acid or dihydroorotic acid (lower panel) before and during infection with SARS-CoV-2 (50 PFU/well for Vero E6 cells and 100 PFU for Calu-3 cells). At 48 h p.i. cell supernatants were harvested and titrated on Vero E6 cells. Plaque counts for each drug concentration were expressed as a percent of the mean count of the control cultures treated with DMSO. The data shown represent means ± SD of three independent experiments performed in triplicate. Statistical significance was calculated by a one-way ANOVA followed by Dunnett's multiple comparison test, **** (p) < 0.00001), *** ($p < 0.0001$), ** ($p < 0.001$) and * ($p < 0.05$) compared to the calibrator sample (MEDS433 alone).

3.6. A Combination of MEDS433 with an Inhibitor of the Pyrimidine Salvage Pathway Is Effective against SARS-CoV-2 Replication Even in the Presence of Uridine

The pyrimidine salvage pathway may reduce the antiviral efficacy of a *h*DHODH inhibitor by importing nucleosides from extracellular environment, thus bypassing the block of the de novo biosynthesis [10]. To deal with this problem, the effects of a combination of MEDS433 with an inhibitor of the nucleoside transport, such as dipyridamole (DPY) [32] was investigated. Checkerboard analysis of a MEDS433-DPY combination was therefore carried in Calu-3 cells infected with SARS-CoV-2 in the presence of 20 µM uridine to go beyond its physiological plasma concentrations [33]. As shown in Figure 6, the addition of exogenous uridine reversed the inhibitory effect of 0.25 µM MEDS433 that reduced SARS-CoV-2 replication by more than 80% when tested as single agent (Figure 3C). In contrast, when MEDS433 was examined in the presence of increasing amounts of DPY, the combination of the two molecules restored the antiviral activity of MEDS433 notwithstanding the presence of exogenous uridine (Figure 6). Moreover, the effectiveness of the MEDS433-DPY combination was not due to a reduced Calu-3 cell viability, since none of the tested combinations exerted a cytotoxic effect (data not shown). Together, these results, support the manageability of a combination of a *h*DHODH inhibitor and a pyrimidine salvage inhibitor to inhibit hCoVs replication even in the presence of uridine, thus mimicking in vivo host conditions.
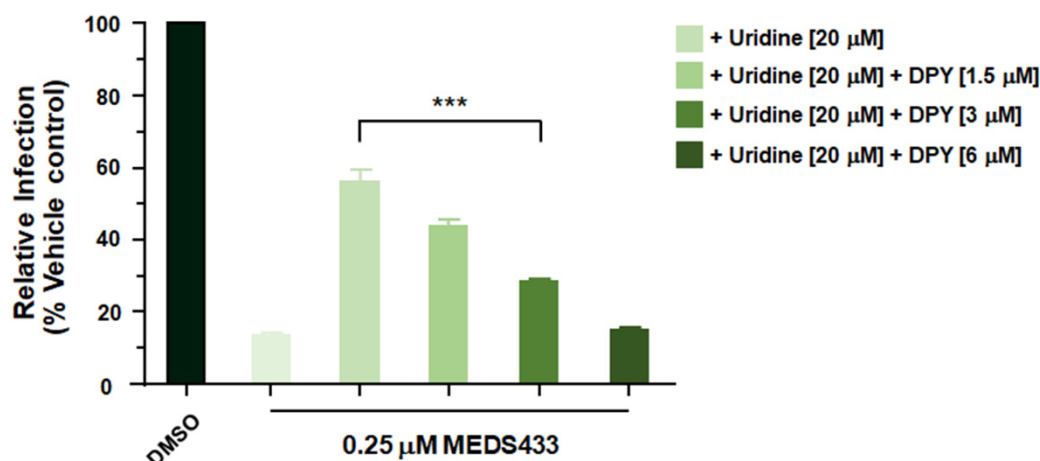
Figure 6. A combination of MEDS433 and dipyridamole hampers SARS-CoV-2 replication even in the presence of uridine. Calu-3 cells were treated with vehicle (DMSO) or 0.25 μM of MEDS433 in the presence of 20 μM uridine alone or in combination with different concentrations of DPY before and during SARS-CoV-2 infection (100 PFU/well). Following virus adsorption, cell monolayers were incubated in the presence of compounds. At 48 h p.i., cell supernatants were harvested and titrated for infectious SARS-CoV-2 on Vero E6 cell monolayers. The data shown represent means ± SD (error bars) of three independent experiments performed in triplicate. Statistical significance was calculated by a one-way ANOVA followed by Dunnett's multiple comparison test. *** ($p < 0.0001$) compared to the calibrator sample (MEDS433 alone).

4. Discussion

In the last few years, the results of several high-throughput screens to discover broad-spectrum antivirals have identified small molecules targeting the host pyrimidine biosynthesis pathway, mostly with the DHODH activity as their major and specific target [34,35]. These findings highlight the potential of targeting DHODH to design and develop antiviral agents endowed with a high genetic barrier to the development of drug resistance, and the ability to target a broad spectrum of viruses, thus enabling a therapeutic approach of newly emerging viruses and contributing to preparedness for unforeseen viral threats [36].

Given these premises, we have investigated the anti-CoVs potential of a series of new small molecules already selected as potent inhibitors of *h*DHODH activity. Among the tested *h*DHODH inhibitors, the one with the greatest potency, MEDS433 (IC$_{50}$ 1.2 nM), was also observed to be the most effective in inhibiting hCoV-OC43 replication (Figure 1). MEDS433 targets the ubiquinone binding site of *h*DHODH with high affinity, thus reducing the possibility of off-target within the cell [16,17]. This high specificity may therefore explain the extremely high SI values of MEDS433 measured against three different hCoVs in four different cells lines, including normal human lung MRC5 fibroblasts (Table 1). The low level of cytotoxicity is undoubtedly a favorable feature of MEDS433 and indeed contributes to making it a promising candidate to develop a new anti-CoVs antiviral. Under normal physiological conditions, the low proliferating airways epithelial cells satisfy their requirement of pyrimidines mainly through the salvage pathway, which recycles pre-existing nucleosides. In contrast, in hCoVs-infected cells, the exceptional need for large pyrimidines pools to cope with rapid viral replication cannot be supplied sufficiently by nucleoside recycling. It is therefore reasonable that de novo pyrimidine biosynthesis rather than the salvage pathway is more critical for hCoVs replication, effectively making the rate-limiting DHODH enzyme activity crucial for maintaining high levels of viral RNA synthesis. Therefore, the observation that hCoVs replication was prevented by MEDS433 is not surprising. However, it is worth noting that our study adds some new pieces of knowledge that may be of interest to be considered towards the validation of *h*DHODH inhibition as a suitable strategy for the therapeutic management of CoVs infections.

The first consists in the observation of the high potency of MEDS433 against SARS-CoV-2. In this regard, given its critical role for viral replication, *h*DHODH has been considered an emerging target of choice for the development of HTA against SARS-CoV-

2 [8,9,14,37]. Thus far, three different *h*DHODH inhibitors have already entered in Phase II/III clinical trials for COVID-19: brequinar (NCT04425252), PTC299 [38] (NCT04439071), and IMU-838 [39] (NCT04379271). The first data available for IMU-838 indicate a clinical activity versus placebo on multiple clinical endpoints (clinical improvement and recovery, reduction of SARS-CoV-2 load in the nasopharynx, systemic anti-inflammatory effects) in hospitalized patients with moderate COVID-19, thus sustaining its further clinical development, as well as the suitability of targeting *h*DHODH for COVID-19 therapeutic intervention [40]. Interestingly, a comparison of the in vitro anti-SARS-CoV-2 efficacy of MEDS433 with that of IMU-838 [31] highlights that MEDS433 is 100-fold more potent than IMU-838 (EC_{50} 7.6 μM, SI 8) with a much more favorable SI (Table 1), thus suggesting for MEDS433 a likely wide therapeutic window of clinical safety and efficacy.

Moreover, the antiviral effect of MEDS433 against SARS-CoV-2 was also observed in the experimental model of kidney organoids (Figure 3D). These organoids are composed of different cell types and model the physiological conditions of the human kidney; thus, they can be used to investigate the effect of SARS-CoV-2 infection on kidney tissues [25,26]. In this regard, we have previously observed that kidney organoids produce infectious SARS-CoV-2 progeny [18]. Although a variability of the effect of MEDS433 on SARS-CoV-2 replication in kidney organoids was measured (Figure 3D), likely reflecting the complexity and heterogeneity of this experimental model [25], the observation of an anti-SARS-CoV-2 activity of MEDS433 even in human organoids is valuable to sustain its preclinical development as a candidate agent for COVID-19.

The second finding that deserves a comment is the antiviral efficacy of MEDS433 against three different hCoVs species. This fact represents an important added value of this new *h*DHODH inhibitor, since in addition to the advantage of overcoming viral drug resistance, it makes MEDS433 of interest for the development of broad-spectrum antiviral agents ready for future emerging CoVs given the independence of its antiviral effects with respect to a specific CoV. We still do not know whether the next emerging CoV may be highly pathogenic as SARS-CoV-1 and MERS, or highly infectious and rapidly spreading as SARS-CoV-2; however, we do know that the possibility exists that novel CoVs will spill-over into human populations, with potentially disastrous consequences [7,36]. Therefore, the need for new broad-spectrum anti-CoVs drugs, effective against both SARS-CoV-2 and CoVs from future zoonoses, is indisputable.

To become a first-line treatment of acute CoV infections, an optimal broad-spectrum CoVs antiviral should, in addition to being highly safe, potent and orally bioavailable, should be suitable for combination treatments that could enhance antiviral efficacy and prevent the emergence of drug resistance [7]. It was therefore pleasing to observe increased efficacy of a combined treatment of MEDS433 with DPY (Figure 6). DPY is a pyrimido-pyrimidine derivative widely used as an oral agent in the prophylaxis of thromboembolism in cardiovascular disease, because of its platelet antiaggregant and vasodilator activities due to the inhibition of the uptake of adenosine into platelets, endothelial cells and erythrocytes [32,41]. DPY is in fact an inhibitor of the equilibrative nucleoside transporters (ENT) 1 and 2, the most effective cell nucleoside/nucleotide transporter involved in the pyrimidine salvage pathway [42]. Indeed, we observed that DPY successfully restored the antiviral activity of MEDS433 concentrations no longer effective against SARS-CoV-2 as a consequence of uridine supplementation mimicking the physiological conditions in the infected host (Figure 6). This finding is relevant for the development of MEDS433 as an antiviral drug candidate, since the failure of some *h*DHODH inhibitors observed in animal models of RNA virus infections is likely due to a systemic compensation of DHODH inhibition by the pyrimidine salvage pathway that flows extracellular uridine into virus-infected cells [43–45]. While the combination of DPY with inhibitors of de novo pyrimidine biosynthesis has been investigated previously to increase the anticancer effects of the latter compounds [46], the potential of this combination against virus infections has not yet been thoroughly explored. To this regard, we have recently observed the efficacy of a synergistic combination of MEDS433 with DPY in suppressing the in vitro

replication of Herpes simplex virus type 1, even in the presence of hyperphysiological concentration of uridine [47]. Importantly, the DPY concentrations observed to be effective in combination with MEDS433 were lower than the DPY C_{max} [48], and therefore clinically achievable in patients treated with DPY. The wide clinical experience of DPY could allow its rapid repositioning against hCoVs to be clinically useful in combination with HTAs and/or DAAs.

Finally, since *h*DHODH inhibitors have been reported to impact the expression of cytokines and chemokines [14,37] and given the importance of the inflammation state in COVID-19 pathogenesis [1,2], it is tempting to speculate that MEDS433 may be also beneficial on the SARS-CoV-2-associated pathogenic inflammation by affecting the production of proinflammatory cytokines and chemokines. It is therefore possible to hypothesize that MEDS433 may exert a dual-action as candidate therapeutics for COVID-19, not only by inhibiting directly SARS-CoV-2 replication through its ability to cause pyrimidine depletion, but also by alleviating the excessive production and release of proinflammatory cytokines and chemokines. In this scenario, *h*DHODH inhibitors, such as MEDS433, could thus give benefit also in the late stages of COVID-19.

5. Conclusions

In conclusion, our study confirms the cellular *h*DHODH activity as a promising target to inhibit SARS-CoV-2 infection [38,39,49], and importantly identifies MEDS433 as an attractive candidate to develop a broad-spectrum anti-CoV HTA that could be rapidly deployable against future novel pathogenic CoVs. For now, the MEDS433′s potent in vitro anti-SARS-CoV-2 activity, and its valuable *drug-like* profile, support further studies to validate its therapeutic efficacy in preclinical animal models of COVID-19.

Author Contributions: Conceptualization, M.L.L. and G.G.; G.G. coordinated the project; methodology, A.C., A.L., N.M., A.M.; formal analysis, A.C., A.L., G.G. and C.P.; investigation, A.C., A.L., B.M., E.E., G.S., V.C., C.D.V., S.S. and C.P.; resources, D.B. and M.L.L.; data curation, A.L. and G.G.; writing—original draft preparation, G.G.; writing—review and editing, A.C., A.L., M.L.L., C.P. and G.G. All authors have read and agreed to the published version of the manuscript.

Institutional Review Board Statement: Not applicable.

Informed Consent Statement: Not applicable.

Data Availability Statement: The data presented in this study are available on request from the corresponding author.

Conflicts of Interest: The authors declare no conflict of interest. The funders had no role in the design of the study; in the collection, analyses, or interpretation of data; in the writing of the manuscript, or in the decision to publish the results.

References

1. Hu, B.; Guo, H.; Zhou, P.; Shi, Z.-L. Characteristics of SARS-CoV-2 and COVID-19. *Nat. Rev. Microbiol.* **2021**, *19*, 141–154. [CrossRef]
2. V'kovski, P.; Kratzel, A.; Steiner, S.; Stalder, H.; Thiel, V. Coronavirus biology and replication: Implications for SARS-CoV-2. *Nat. Rev. Microbiol.* **2021**, *19*, 155–170. [CrossRef] [PubMed]

3. Mishra, S.K.; Tripathi, T. One-year update on the COVID-19 pandemic: Where are we now? *Acta Tropica* **2021**, *214*, 105778. [CrossRef] [PubMed]

4. Forni, G.; Mantovani, A.; on behalf of the COVID-19 Commission of Accademia Nazionale dei Lincei, Rome. COVID-19 vaccines: Where we stand and challenges ahead. *Cell Death Differ.* **2021**, *28*, 626–639. [CrossRef] [PubMed]

5. Richman, D.D. Antiviral drug discovery to address the COVID-19 pandemic. *mBio* **2020**, *11*, e02134-20. [CrossRef]

6. Zumla, A.; Chan, J.F.W.; Azhar, E.I.; Hui, D.S.C.; Yuen, K.-Y. Coronaviruses. Drug discovery and therapeutic options. *Nat. Rev. Drug Discov.* **2016**, *15*, 327–347. [CrossRef]

7. Totura, A.L.; Bavari, S. Broad-spectrum coronavirus antiviral drug discovery. *Expert Opin. Drug Discov.* **2019**, *14*, 397–412. [CrossRef]

8. Li, G.; De Clercq, E. Therapeutic options for the 2019 novel coronavirus (2019-nCoV). *Nat. Rev. Drug Discov.* **2020**, *19*, 149–150. [CrossRef]

9. Tian, D.; Liu, Y.; Liang, C.; Xin, L.; Xie, X.; Zhang, D.; Wang, M.; Li, H.; Fu, X.; Liu, H.; et al. An update review of emerging small-molecule therapeutic options for COVID-19. *Biomed. Pharmacother.* **2021**, *137*, 111313. [CrossRef] [PubMed]

10. Okesli, A.; Khosla, C.; Bassik, M.C. Human pyrimidine nucleotide biosynthesis as a target for antiviral chemotherapy. *Curr. Opin. Biotech.* **2017**, *48*, 127–134. [CrossRef]

11. Reis, R.A.G.; Calil, F.A.; Feliciano, P.R.; Pinheiro, M.P.; Nonato, M.C. The dihydroorotate dehydrogenases: Past and present. *Arch. Biochem. Biophys.* **2017**, *632*, 175–191. [CrossRef]

12. Loeffler, M.; Carrey, E.A.; Knecht, W. The pathway to pyrimidines: The essential focus on dihydroorotate dehydrogenase, the mitochondrial enzyme coupled to the respiratory chain. *Nucleosides Nucleotides Nucleic Acids* **2020**, *39*, 1281–1305. [CrossRef] [PubMed]

13. Boschi, D.; Pippione, A.C.; Sainas, S.; Lolli, M.L. Dihydroorotate dehydrogenase inhibitors in anti-infective drug research. *Eur. J. Med. Chem.* **2019**, *183*, 111681. [CrossRef]

14. Coehlo, A.R.; Oliveira, P.J. Dihydroorotate dehydrogenase inhibitors in SARS-CoV-2 infection. *Eur. J. Clin. Investig.* **2020**, *50*, e13366.

15. Peters, G.J. Re-evaluation of Brequinar sodium, a dihydroorotate dehydrogenase inhibitor. *Nucleosides Nucleotides Nucleic Acids* **2018**, *37*, 666–678. [CrossRef]

16. Sainas, S.; Pippione, A.C.; Lupino, E.; Giorgis, M.; Circosta, P.; Gaidano, V.; Goyal, P.; Bonanni, D.; Rolando, B.; Cignetti, A.; et al. Targeting myeloid differentiation using potent 2-Hydroxypyrazolo [1,5- a] pyridine scaffold-based human dihydroorotate dehydrogenase inhibitors. *J. Med. Chem.* **2018**, *61*, 6034–6055. [CrossRef] [PubMed]

17. Sainas, S.; Giorgis, M.; Circosta, P.; Gaidano, V.; Bonanni, D.; Pippione, A.C.; Bagnati, R.; Passoni, A.; Qiu, Y.; Cojocaru, C.F.; et al. Targeting acute myelogenous leukemia using potent human dihydroorotate dehydrogenase inhibitors based on the 2-hydroxypyrazolo[1,5-a]pyridine scaffold: SAR of the biphenyl moiety. *J. Med. Chem.* **2021**, *64*, 5404–5428. [CrossRef]

18. Monteil, V.; Kwon, H.; Prado, P.; Hagelkruys, A.; Wimmer, R.A.; Stahl, M.; Leopoldi, A.; Garreta, E.; Hurtado del Pozo, C.; Prosper, F.; et al. Inhibition of SARS-CoV-2 infections in engineered human tissues using clinical-grade soluble human ACE2. *Cell* **2020**, *181*, 905–913. [CrossRef] [PubMed]

19. Mosmann, T. Rapid colorimetric assay for cellular growth and survival: Application to proliferation and cytotoxicity assays. *J Immunol. Methods* **1983**, *65*, 55–63. [CrossRef]

20. Gribaudo, G.; Riera, L.; Rudge, T.L.; Caposio, P.; Johnson, L.F.; Landolfo, S. Human cytomegalovirus infection induces cellular thymidylate synthase gene expression in quiescent fibroblasts. *J. Gen. Virol.* **2002**, *83*, 2983–2993. [CrossRef]

21. Brown, A.J.; Wona, J.J.; Graham, R.L.; Dinnon III, K.H.; Sims, A.C.; Feng, J.Y.; Cihlarb, T.; Denison, M.R.; Baric, R.S.; Sheahan, T.P. Broad spectrum antiviral remdesivir inhibits human endemic and zoonotic deltacoronaviruses with a highly divergent RNAdependent RNA polymerase. *Antivir Res.* **2019**, *169*, 104541. [CrossRef]

22. Citarella, A.; Gentile, D.; Rescifina, A.; Piperno, A.; Mognetti, B.; Gribaudo, G.; Sciortino, M.T.; Holzer, W.; Pace, V.; Micale, N. Pseudo-dipeptide bearing α,α-difluoromethyl ketone moiety as electrophilic warhead with activity against coronaviruses. *Int. J. Mol. Sci.* **2021**, *22*, 1398. [CrossRef]

23. Corman, V.M.; Landt, O.; Kaiser, M.; Molenkamp, R.; Meijer, A.; Chu, D.K.; Bleicker, T.; Brünink, S.; Schneider, J.; Schmidt, M.L.; et al. Detection of 2019 novel coronavirus (2019-nCoV) by real-time RT-PCR. *Euro Surveill.* **2020**, *3*, 2000045. [CrossRef]

24. Kenneth, J.; Livak, T.; Schmittgen, D. Analysis of relative gene expression data using real-time quantitative PCR and the $2^{-\Delta\Delta CT}$ method. *Methods* **2001**, *4*, 402–408.

25. Garreta, E.; Prado, P.; Tarantino, C.; Oria, R.; Fanlo, L.; Martì, E.; Zalvidea, D.; Trepat, X.; Roca-Cusachs, P.; Gavalda-Navarro, A.; et al. Fine tuning the extracellular environment accelerates the derivation of kidney organoids from human pluripotent stem cells. *Nat. Mater.* **2019**, *18*, 397–405. [CrossRef] [PubMed]

26. Takayama, K. In vitro and animal models for SARS-CoV-2 research. *Trends Pharmacol. Sci.* **2020**, *41*, 513–516. [CrossRef]

27. Ahmadian, E.; Hosseiniyan Khatibi, S.M.; Razi Soofiyani, S.; Abediazar, S.; Shoja, M.M.; Ardalan, M. Covid-19 and kidney injury: Pathophysiology and molecular mechanisms. *Rev. Med. Virol.* **2021**, *31*, e2176. [CrossRef]

28. Gabarre, P.; Dumas, G.; Dupont, T.; Darmon, M.; Azoulay, E.; Zafrani, L. Acute kidney injury in critically ill patients with COVID-19. *Intensive Care Med.* **2020**, *46*, 1339–1348. [CrossRef]

29. Braun, B.; Lütgehetmann, M.; Pfefferle, S.; Wong, M.N.; Carsten, A.; Lindenmeyer, M.T.; Nörz, D.; Heinrich, F.; Meißner, K.; Wichmann, D.; et al. SARS-CoV-2 renal tropism associates with acute kidney injury. *Lancet* **2020**, *396*, 597–598. [CrossRef]

30. Caceres, P.; Savickas, G.; Murray, S.; Umanath, K.; Uduman, J.; Yee, J.; Liao, T.D.; Bolin, S.; Levin, A.; Khan, M.; et al. High SARS-CoV-2 viral load in urine sediment correlates with acute kidney injury and poor COVID-19 outcome. *J. Am. Soc. Nephrol.* **2021**, SN.2021010059, Online ahead of print. [CrossRef]

31. Danilczyk, U.; Penninger, J.M. Angiotensin-converting enzyme II in the heart and the kidney. *Circ. Res.* **2006**, *98*, 463–471. [CrossRef]

32. Fitzgerald, G.A. Dipyridamole. *N. Engl. J. Med.* **1987**, *316*, 1247–1257.

33. Pizzorno, G.; Cao, D.; Leffert, J.J.; Russell, R.L.; Zhang, D.; Handschumacher, R.E. Homeostatic control of uridine and the role of uridine phosphorylase: A biological and clinical update. *Biochim. Biophys. Acta* **2002**, *1587*, 133–144. [CrossRef]

34. Deans, R.M.; Morgens, D.W.; Okesli, A.; Pillay, S.; Horlbeck, M.A.; Kampmann, M.; Gilbert, L.A.; Li, A.; Mateo, R.; Smith, M.; et al. Parallel shRNA and CRISPR-Cas9 screens enable antiviral drug target identification. *Nat. Chem. Biol.* **2016**, *12*, 361–366. [CrossRef]

35. Yang, Y.; Cao, L.; Gao, H.; Wu, Y.; Wang, Y.; Fang, F.; Lan, T.; Lou, Z.; Rao, Y. Discovery, optimization, and target identification of novel potent broad-spectrum antiviral inhibitors. *J. Med. Chem.* **2019**, *62*, 4056–4073. [CrossRef]

36. Adalja, A.; Inglesby, T. Broad-spectrum antiviral agents: A crucial pandemic tool. *Expert Rev. Anti Infec. Ther.* **2019**, *17*, 467–470. [CrossRef]

37. Xu, Y.; Jiang, H. Potential treatment of COVID-19 by inhibitors of human dihydroorotate dehydrogenase. *Protein Cell* **2020**, *11*, 699–702. [CrossRef]

38. Luban, J.; Sattler, R.; Mühlberger, E.; Graci, J.D.; Cao, L.; Weetall, M.; Trotta, C.; Colacino, J.M.; Bavari, S.; Strambio-De-Castillia, C.; et al. The DHODH inhibitor PTC299 arrests SARS-CoV-2 replication and suppresses induction of inflammatory cytokines. *Virus Res.* **2020**, *292*, 198246. [CrossRef]

39. Hahn, F.; Wangen, C.; Häge, S.; Peter, A.S.; Dobler, G.; Hurst, B.; Julander, J.; Fuchs, J.; Ruzsics, Z.; Überla, K.; et al. IMU-838, a developmental DHODH inhibitor in phase II for autoimmune disease, shows anti-SARS-CoV-2 and broad-spectrum antiviral efficacy in vitro. *Viruses* **2020**, *12*, 1394. [CrossRef]

40. Immunic Therapeutics USA. Main Phase 2 Analysis CALVID-1 Trial of IMU-838 in Moderate COVID-19. Available online: https://www.immunic-therapeutics.com (accessed on 15 July 2021).

41. Schaper, W. Dipyridamole, an underestimated vascular protective drug. *Cardiovasc. Drugs Ther.* **2005**, *19*, 357–363. [CrossRef]

42. Ward, J.L.; Sherali, A.; Mo, Z.P.; Tse, C.M. Kinetic and pharmacological properties of cloned human equilibrative nucleoside transporters, ENT1 and ENT2, stably expressed in nucleoside transporter- deficient PK15 cells: ENT2 exhibits a low affinity for guanosine and cytidine but a high affinity for inosine. *J. Biol. Chem.* **2000**, *275*, 8375–8381. [PubMed]

43. Wang, Q.Y.; Bushell, S.; Qing, M.; Xu, H.Y.; Bonavia, A.; Nunes, S.; Zhou, J.; Poh, M.K.; Florez de Sessions, P.; Niyomrattanakit, P.; et al. Inhibition of dengue virus through suppression of host pyrimidine biosynthesis. *J. Virol.* **2011**, *85*, 6548–6556. [CrossRef]

44. Smee, D.F.; Hurst, B.L.; Day, C.W. D282, a non-nucleoside inhibitor of influenza virus infection that interferes with de novo pyrimidine biosynthesis. *Antivir. Chem. Chemother.* **2012**, *22*, 263–272. [CrossRef]

45. Grandin, C.; Lucas-Hourani, M.; Janin, Y.L.; Dauzonne, D.; Munier-Lehmann, H.; Paturet, A.; Taborik, F.; Vabret, A.; Contamin, H.; Tangy, F.; et al. Respiratory syncytial virus infection in macaques is not suppressed by intranasal sprays of pyrimidine biosynthesis inhibitors. *Antiviral Res.* **2016**, *125*, 58–62. [CrossRef]

46. Gaidano, V.; Houshmand, M.; Vitale, N.; Carrà, G.; Morotti, A.; Tenace, V.; Rapelli, S.; Sainas, S.; Pippione, A.C.; Giorgis, M.; et al. The synergism between DHODH inhibitors and dipyridamole leads to metabolic lethality in acute myeloid leukemia. *Cancers* **2021**, *13*, 1003. [CrossRef]

47. Luganini, A.; Sibille, G.; Mognetti, B.; Sainas, S.; Pippione, A.C.; Giorgis, M.; Boschi, D.; Lolli, M.L.; Gribaudo, G. Effective deploying of a novel DHODH inhibitor against herpes simplex type 1 and type 2 replication. *Antiviral Res.* **2021**, *189*, 105057. [CrossRef]

48. Gregov, D.; Jenkins, A.; Duncan, E.; Sieber, D.; Rodgers, S.; Duncan, B.; Bochner, F.; Lloyd, J. Dipyridamole: Pharmacokinetics and effects on aspects of platelet function in man. *Br. J. Clin. Pharmac.* **1987**, *24*, 425–434. [CrossRef] [PubMed]

49. Xiong, R.; Zhang, L.; Li, S.; Sun, Y.; Ding, M.; Wang, Y.; Zhao, Y.; Wu, Y.; Shang, W.; Jiang, X.; et al. Novel and potent inhibitors targeting DHODH are broad-spectrum antivirals against RNA viruses including newly emerged coronavirus SARS-CoV-2. *Protein Cell* **2020**, *11*, 723–739. [CrossRef] [PubMed]

The Novel *h*DHODH Inhibitor MEDS433 Prevents Influenza Virus Replication by Blocking Pyrimidine Biosynthesis

Giulia Sibille [1] , **Anna Luganini** [1] , **Stefano Sainas** [2] , **Donatella Boschi** [2] , **Marco Lucio Lolli** [2]
and Giorgio Gribaudo [1,*]

1   Department of Life Sciences and Systems Biology, University of Torino, 10123 Torino, Italy
2   Department of Sciences and Drug Technology, University of Torino, 10125 Torino, Italy
*   Correspondence: giorgio.gribaudo@unito.it; Tel.: +39-011-6704648

Abstract: The pharmacological management of influenza virus (IV) infections still poses a series of challenges due to the limited anti-IV drug arsenal. Therefore, the development of new anti-influenza agents effective against antigenically different IVs is therefore an urgent priority. To meet this need, host-targeting antivirals (HTAs) can be evaluated as an alternative or complementary approach to current direct-acting agents (DAAs) for the therapy of IV infections. As a contribution to this antiviral strategy, in this study, we characterized the anti-IV activity of MEDS433, a novel small molecule inhibitor of the human dihydroorotate dehydrogenase (*h*DHODH), a key cellular enzyme of the de novo pyrimidine biosynthesis pathway. MEDS433 exhibited a potent antiviral activity against IAV and IBV replication, which was reversed by the addition of exogenous uridine and cytidine or the *h*DHODH product orotate, thus indicating that MEDS433 targets notably *h*DHODH activity in IV-infected cells. When MEDS433 was used in combination either with dipyridamole (DPY), an inhibitor of the pyrimidine salvage pathway, or with an anti-IV DAA, such as N^4-hydroxycytidine (NHC), synergistic anti-IV activities were observed. As a whole, these results indicate MEDS433 as a potential HTA candidate to develop novel anti-IV intervention approaches, either as a single agent or in combination regimens with DAAs.

Keywords: influenza virus; host-targeting antivirals; de novo pyrimidine biosynthesis; dihydroorotate dehydrogenase; MEDS433; dipyridamole; combination treatment

1. Introduction

Influenza remains a major public health challenge. Every year around the world, influenza viruses (IVs) in fact cause approximately one billion infections, with 3–5 million of severe related respiratory complications, which result in 290,000–650,000 deaths among high-risk groups, with an even greater impact in developing countries [1–4].

Seasonal vaccines represent the most effective measure for the prevention and control of IV infections [5]. Nevertheless, vaccines do not allow sufficient protection to alleviate the annual impact of IVs [6], and thus, the current intervention strategies rely also on antiviral agents to reduce the burden of complications and case fatality rates. In this regard, three classes of direct-acting antiviral (DAA) drugs have been approved: amantadanes, neuraminidase inhibitors (NAIs), and RNA-dependent RNA polymerase (RdRp) complex inhibitors [2–4,7]. Amantadanes act by blocking the IAV M2 ion channel; however, due to resistance by essentially all circulating IVs, they are no longer recommended [8]. Thus, NAIs, such as peramivir, zanamivir, and above all, oseltamivir, represent the standard-of-care for therapeutic management of IV infections [9]. NAIs have been employed successfully for two decades; however, during 2007–2009, resistance to oseltamivir rose drastically among seasonal H1N1 IAV due to the appearance of the NA H275Y amino acid substitution [10]. The subsequent global spread of the 2009 H1N1 IAV pandemic strain, devoid of this mutation when it emerged, reduced the frequency of NAI resistance in seasonal IV to low levels

(<2%), and since then, it has remained low [11]. However, the rapid emergence of IVs with reduced inhibition by oseltamivir between 2007 and 2009 indicated that resistance to NAIs can emerge and spread among circulating IVs [12].

More recently, RdRp inhibitors, such as baloxavir marboxil (baloxavir), which targets the PA subunit of RdRp, and favipiravir, an inhibitor of the PB1 subunit, have been licensed for the treatment of uncomplicated IV infections and those resistant to other antivirals, respectively [13,14]. Globally, IV variants showing reduced susceptibility to baloxavir are detected with low frequency [11].

The available data, however, suggest that the genetic barrier against viral resistance to some approved DAA may be low and pose challenges in the control of IV infections by a curative approach, thus making obvious the need to develop alternative anti-IV agents characterized by new mechanisms of action, with a low propensity to drive the selection of resistant strains, concurrently effective against antigenically different IVs, and thus, promptly deployable against new zoonotic highly pathogenic IVs that may emerge in the future in human populations [12,15].

Taking into consideration these requirements, small molecules able to interfere with those cellular factor and biochemical pathways essential for IV replication may be considered as compelling alternatives to the de novo development of DAAs, inasmuch as such host-targeting antivirals (HTAs) may offer both a broad-spectrum of activity against different IVs and a high genetic barrier against the development of IV resistance [16].

Pyrimidine nucleotides' availability in infected cells is crucial for efficient virus replication, and thus, compounds targeting the cellular pathways responsible for providing adequate supply of pyrimidines have the potential to be developed as effective HTA agents [17]. Especially, in metabolically quiescent uninfected airway epithelial cells, in which productive IV replication occurs, the pyrimidine demands are fulfilled through the salvage pathway from intracellular nucleic acid degradation and from the import of extracellular nucleotides in the bloodstream [17]. In contrast, in virus-infected cells, including those infected with IV, to keep up with the high pyrimidine demands required for viral gene expression and replication, the de novo pyrimidine biosynthesis pathway is upregulated [17–21]. In this biochemical pathway, the human dihydroorotate dehydrogenase (*h*DHODH) catalyzes the oxidation of dihydroorotic acid (DHO) to orotic acid (ORO), a rate-limiting step of in the biosynthesis of uridine and cytidine required to fulfil the cell's pyrimidine nucleotide demand [22,23]. Thus, given its critical role in virus-infected cells, while being dispensable in uninfected cells, *h*DHODH can be considered a druggable target of choice for the development of HTAs [17,22].

To contribute to this antiviral strategy, in the last few years, we synthesized a new class of small molecules, *h*DHODH inhibitors [24–26], which were designed on the scaffold of brequinar, one of the most-potent *h*DHODH inhibitors developed so far [27] and for which an anti-IV activity was recently observed [28]. Among our new *h*DHODH inhibitors, MEDS433 proved be the most effective at inhibiting the in vitro enzymatic activity (IC$_{50}$ 1.2 nM) and at binding in the ubiquinone binding site of *h*DHODH in co-crystallization experiments [24]. Therefore, it was chosen to investigate its suitability as a new HTA [29]. As a confirmation of this hypothesis, recently, we reported the ability of MEDS433 to inhibit the in vitro replication of herpes simplex virus type 1 (HSV-1) and type 2 (HSV-2) [30], as well as of human coronaviruses (CoVs), such as the prototypic α-hCoV-229E and the β-CoVs hCoV-OC43 and SARS-CoV-2 [31].

Based on these premises, the aim of this study was to expand the potential of MEDS433 as a broad-spectrum antiviral by investigating its anti-IV activity. We report the characterization of the ability of MEDS433 to inhibit the in vitro replication of both IAV and IBV as a consequence of a selective block of *h*DHODH enzymatic activity, as well as its suitability for combination treatments with other anti-pyrimidines compounds and with DAAs. These results suggested MEDS433 as a promising HTA candidate, as either a single agent or in combination regimens, to design new therapeutic strategies for the treatment of IV infections.

2. Materials and Methods

2.1. Compounds

MEDS433 was synthesized as described previously [24]. Brequinar, uridine, cytidine, orotic acid (ORO), dihydroorotic acid (DHO), dipyridamole (DPY), and N^4-hydroxycytidine (NHC or EIDD1931) were obtained from Sigma-Aldrich (St. Louis, MO, USA). All compounds were resuspended in DMSO.

2.2. Cells and Viruses

The Madin–Darby canine kidney (MDCK) (ATCC CCL-34), the human adenocarcinoma alveolar basal epithelial A549 (ATCC CCL-185), and the human lung adenocarcinoma Calu-3 (ATCC HTB-55) cell lines were purchased from the American Type Culture Collection (ATCC) and cultured in Dulbecco's modified Eagle medium (DMEM; Euroclone (Milan, Italy)) supplemented with 10% fetal bovine serum (FBS, Euroclone), 2 mM glutamine, 1 mM sodium pyruvate, and 100 U/mL penicillin and 100 µg/mL streptomycin sulfate (P/S, both from Euroclone). All IV infections were performed in the presence of 2 µg/mL of trypsin TPCK treated by bovine pancreas (Sigma-Aldrich) and 0.14% of bovine serum albumin (Sigma-Aldrich).

The Influenza A virus strain A/Puerto Rico/8/34 (PR8) H1N1 (IAV) and influenza B virus strain B/Lee/40 (IBV) were a generous gift from Arianna Loregian (University of Padua, Padua, Italy). IAV and IBV were propagated and titrated by the plaque assay on MDCK cells, as previously described [32,33].

2.3. Cytotoxicity Assay

Cultures of MDCK, A549, or Calu-3 cells, seeded 24 h before in 96-well plates (10,000 cells/well), were exposed to increasing concentrations of the vehicle (DMSO) or of different compounds. After 48 h of incubation, the 3-(4,5-dimethylthiazol-2-yl)-2,5-diphenyltetrazolium bromide (MTT) method [34] was employed to determine the number of viable cells.

2.4. Antiviral Assays

The antiviral activity of MEDS433 or brequinar was determined by the plaque reduction assay (PRA) in MDCK cells or by the virus yield reduction assay (VRA) in A549 cells. For the PRA, MDCK cells were seeded in 24-well plates and, after 24 h, exposed 1 h prior to infection to increasing concentrations of MEDS433 or brequinar and then infected with IAV or IBV (50 PFU/well). Following virus adsorption (1 h at 37 °C), cultures were maintained in medium containing the corresponding compounds, 2 µg/mL of trypsin TPCK, 0.14% of bovine serum albumin, and 0.7% Avicel (FMC BioPolymer (Philadelphia, PA, USA). At 48 h post-infection (h p.i.), the cell monolayers were fixed with 4% formaldehyde-phosphate-buffered saline for 1 h at room temperature (RT) and stained with a solution of crystal violet and 20% ethanol. The viral plaques were microscopically counted, and the mean plaque counts for each drug concentration are expressed as a percentage of the mean plaque counts of control virus (DMSO). The GraphPad Prism software version 8.0 was used to determine the concentration of compounds that produced 50 and 90% reductions in plaque formation (EC_{50} and EC_{90}). For the VRA, A549 or Calu-3 cells seeded in 24-well plates were treated with increasing concentrations of MEDS433 or brequinar and then infected with IAV or IBV at an MOI of 0.001 PFU/cell. After virus adsorption, cells were incubated in medium containing the corresponding compounds, 2 µg/mL of trypsin TPCK and 0.14% of bovine serum albumin. At 48 h p.i., the cell supernatants were harvested and IV yield titrated on MDCK cells.

For time-of-addition experiments, MDCK cells were seeded in 6-well plates and after 24 h exposed to 0.5 µM MEDS433 from −2 to −1 h prior to IAV infection (MOI of 0.1) (pre-treatment, Pre-T); during infection (adsorption stage, from −1 to 0 h; co-treatment, Co-T); after viral adsorption (from 0 to 48 h p.i.; post-treatment, Post-T); or during all

phases (full treatment, Full-T). At 48 h p.i., the cell supernatants were harvested and titrated for IAV infectivity as described above.

To evaluate the effect of uridine, cytidine, DHO, or ORO addition, MDCK and A549 cells were seeded as describe above for the PRA and the VRA, and after 24 h, the cultures were infected with IAV (50 PFU/well or 0.001 PFU/cell) and treated with increasing concentrations of uridine, cytidine, ORO, or DHO in the presence of 0.4 μM of MEDS433. The drugs were maintained throughout the assay, and at 48 h p.i.: for the PRA, the cell monolayers were fixed and viral plaques microscopically counted; for the VRA cells, the supernatants were harvested and IAV yield titrated on MDCK cells.

To investigate the effect of blocking both the de novo biosynthesis and the salvage pathways of pyrimidines, A549 cell monolayers were infected with IAV (0.001 PFU/cell) and treated with 0.4 μM of MEDS433 and increasing concentrations of DPY in the presence of 20 μM uridine, which exceeds the physiological uridine plasma levels [33]. After 48 h p.i., the supernatants were harvested and IAV yield titrated on MDCK cells.

The combination of MEDS433 and DPY was examined by the VRA as describe above. Briefly, MEDS433 was added to A549 cells at $0.25\times$, $0.5\times$, $1\times$, $2\times$, and $4\times$ EC$_{50}$ alone or in combination with 3 μM DPY. The infection was performed with IAV (0.001 PFU/cell), and after 48 h p.i., the supernatants were collected and the influenza virions titrated on MDCK.

To assess the effects of the combination of MEDS433 and NHC on IAV replication, compounds, alone or in combination, were added to A549 cell monolayers at equipotent ratio of $0.25\times$, $0.5\times$, $1\times$, $2\times$, and $4\times$ EC$_{50}$ of each drug. Then, the cells were infected with IAV (0.001 PFU/cell), and after 48 h p.i., the supernatants were harvested and IAV yield titrated on MDCK cells.

The effect of the two-drug combinations was determined by means of the Chou method [35] as computed in the CompuSyn software 1.0 (http://www.combosyn.com (accessed 3 August 2022)) [36]. With this method, a combination index (CI) = 1 represents an additive effect, a CI value > 1 means antagonism, and a CI value < 1 indicates synergism.

2.5. Immunoblotting

Total cell protein extracts were prepared at different times p.i. from MDCK cell monolayers infected with IAV at an MOI of 0.1 PFU/cell and treated with 0.5 μM MEDS433 [37]. Subsequently, equal amounts of protein extracts were fractionated by 8% SDS-PAGE and transferred to PVDF membranes (Bio-Rad (Hercules, CA, USA). Filters were blocked for 2 h at 37 °C in 5% non-fat dry milk in 10 mM Tris-HCl (pH 7.5), 100 mM NaCl, and 0.05% Tween 20 and then immunostained with either the rabbit anti-IAV HA pAb (PA5-34929; Thermo Fisher Scientific (Waltham, MA, USA) (diluted 1:3000) or the rabbit anti-IAV NA pAb (PA5-32238; Thermo Fisher Scientific) (diluted 1:1500). The rabbit anti-GAPDH mAb (D16H11, Cell Signaling) (diluted 1:1000) or the mouse anti-vinculin mAb (V9264; Sigma-Aldrich) (diluted 1:4000) was used as the control for protein loading. Immunocomplexes were detected with a goat anti-rabbit Ig Ab conjugated to horseradish peroxidase (Life Technologies, Carlsbad, CA, USA) or with a goat anti-mouse Ig Ab conjugated to horseradish peroxidase (Life Technologies) and visualized by enhanced chemiluminescence (Western Blotting Luminol Reagent, Santa Cruz, CA, USA).

2.6. hDHODH Gene Silencing

For RNA interference, A549 cells were transfected with a *h*DHODH-targeting small interfering RNA (siRNA) (Origene-SR319917C) or a universal scrambled negative control siRNA (Origene-SR30004) using the siTran 2.0 siRNA Transfection Reagent (Origene, Rockville, MD, USA) and in agreement with the manufacturer's protocol. Expression of the *h*DHODH protein was analyzed at 48 h post-transfection by immunoblotting using the mouse anti-*h*DHODH mAb (SC-166348, Santa Cruz Biotechnology, Santa Cruz, CA, USA) (diluted 1:200). To assess the effect of the *h*DHODH silencing on IAV replication, at 24 h post-transfection, A549 cells were infected with IAV at an MOI of 0.001 PFU/cell, and after 48 h p.i., the cell supernatants were harvested and titrated on MDCK cells.

2.7. Data Analysis

All data were generated from at least three independent experiments performed in triplicate. Statistical analysis was performed using GraphPad Prism version 8.0. Data are presented as the means $\pm$ SDs and considered to be statistically significant for $p < 0.05$.

3. Results

3.1. hDHODH Expression Is Required for Efficient IAV Replication

To evaluate the importance of *h*DHODH in the IV replication cycle, its expression was knocked down by siRNAs in the relevant cell model of human alveolar basal epithelial cells A549 (Figure 1A). As shown in Figure 1B, the reduction of *h*DHODH protein expression significantly affected IAV growth with a 183-fold reduction of the release of infectious virus particles at 48 h p.i., compared to both wild-type A549 cells and cells transfected with a scrambled negative siRNA control. These results therefore sustain the requirement of *h*DHODH for efficient IAV replication.
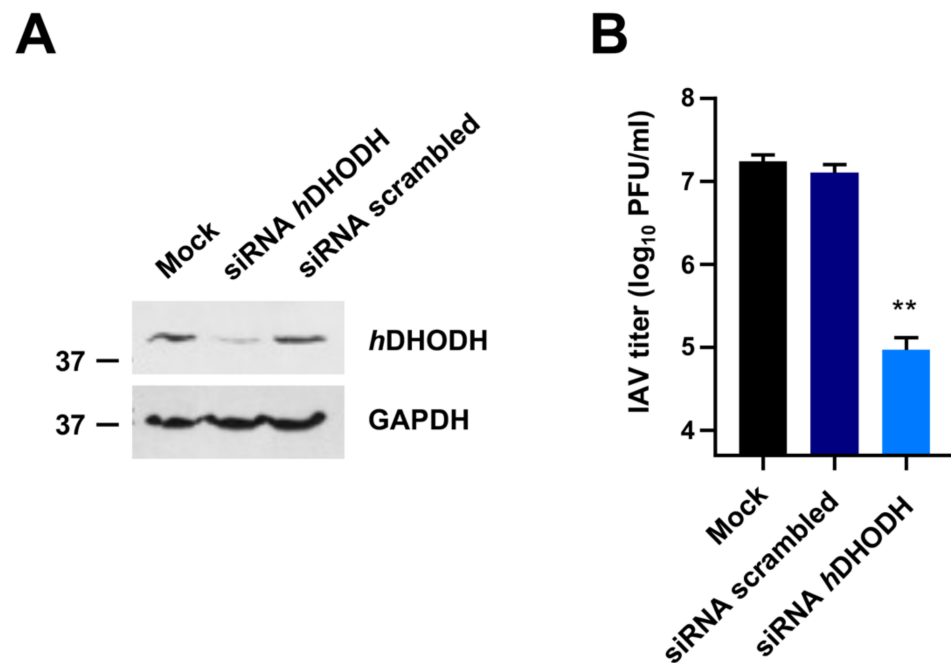
Figure 1. Knockdown of *h*DHODH affects IAV replication. (**A**) Expression of *h*DHODH in A549 cells transfected with *h*DHODH or scrambled negative control siRNAs. At 48 h after of transfection, total protein extracts were prepared, fractionated by 10% SDS-PAGE, and analyzed by immunoblotting with anti-*h*DHODH mAbs. Immunodetection of GAPDH was used as a control for protein loading. Molecular weight markers are shown beside the left side of each panel. (**B**) VRA was performed in A549 cells mock-transfected or transfected with *h*DHODH or scrambled siRNAs. At 24 h after transfection, cells were infected with IAV, and after 48 h p.i., the cell supernatants were harvested and titrated by the plaque assay in MDCK cells. The data shown are the means $\pm$ SDs of two independent experiments performed in triplicate and analyzed by the unpaired *t*-test, corrected at FDR q < 0.05. ** ($p < 0.001$) compared to the calibrator sample (Mock).

3.2. MEDS433 Inhibits IAV and IBV In Vitro Replication

Given the relevance of *h*DHODH for IAV replication, the pharmacological targeting of this enzymatic activity may be exploited to identify anti-IV molecules. Having this in mind, firstly, virus yield reduction assays (VRAs) were performed in A549 cells to investigate the possible anti-IV activity of the new *h*DHODH inhibitor MEDS433 (Figure 2A). As shown in Figure 2B,C, the measurement of the IV yield produced by A549 cells exposed to MEDS433 revealed a remarkable concentration-dependent inhibitory effect on both IAV and IBV replication. As for IAV replication, the EC_{50} and EC_{90} values were 0.064 ± 0.01 µM

and 0.264 ± 0.002 μM, while for IBV, they were 0.065 ± 0.005 μM and 0.365 ± 0.09 μM, respectively (Table 1). It is noteworthy that MEDS433 was more effective than brequinar in inhibiting IV replication, since for this *h*DHODH inhibitor, an EC_{50} of 0.495 ± 0.027 μM and of 0.273 ± 0.014 μM was measured against IAV and IBV, respectively (Figure 2B,C).
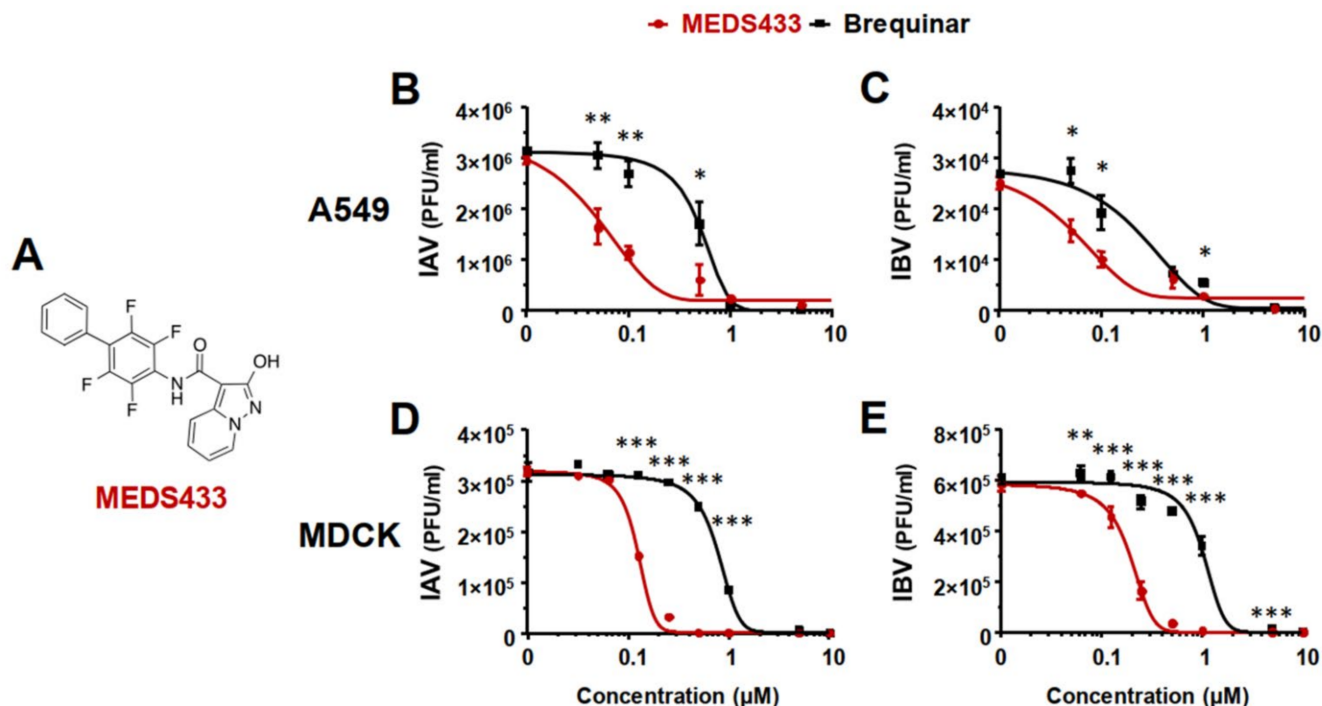

Figure 2. Inhibition of IAV and IBV replication by MEDS433. (**A**) Chemical structure of MEDS433, the *h*DHODH inhibitor investigated as an anti-IV agent in this study. (**B**,**C**) VRAs were performed in A549 cells infected with IAV (**B**) or IBV (**C**) and treated with increasing concentrations of MEDS433 or brequinar 1 h before, during, and post-infection. At 48 h p.i., the cell supernatants were harvested and titrated by the plaque assay in MDCK cells. (**D**,**E**) PRAs were performed in MDCK cell monolayers infected with IAV (**D**) or IBV (**E**) and, where indicated, treated with increasing concentrations of MEDS433 or brequinar. At 48 h p.i., the viral plaques were microscopically counted and converted in viral titer (PFU/mL). The concentrations of MEDS433 or brequinar producing 50% and 90% reductions in plaque formation (EC_{50} and EC_{90}) were then calculated. Data shown are the means ± SDs (error bars) of three independent experiments performed in triplicate and analyzed by a two-way ANOVA, followed by Dunnett's multiple comparison test. Statistical analysis was performed by comparing MEDS433-treated samples with the brequinar-treated samples for each condition. * ($p < 0.01$); ** ($p < 0.001$); *** ($p < 0.0001$).

Table 1. Antiviral activity of MEDS433 against representative influenza viruses.

IV	Cell Line	EC_{50} (μM) [a]	EC_{90} (μM) [b]	CC_{50} (μM) [c]	SI [d]
IAV	A549	0.064 ± 0.01 μM	0.264 ± 0.002 μM	64.25 ± 3.12 μM	1104
	Calu-3	0.055 ± 0.003 μM	0.675 ± 0.05 μM	54.67 ± 3.86 μM	994
	MDCK	0.141 ± 0.021 μM	0.256 ± 0.052 μM	119.8 ± 6.21 μM	850
IBV	A549	0.065 ± 0.005 μM	0.365 ± 0.09 μM	64.25 ± 3.12 μM	988
	Calu-3	0.052 ± 0.006 μM	0.807 ± 0.08 μM	54.67 ± 3.86 μM	1051
	MDCK	0.170 ± 0.019 μM	0.330 ± 0.013 μM	119.8 ± 6.21 μM	705

[a] EC_{50}, compound concentration that inhibits 50% of replication, as determined by the VRAs in A549 and Calu-3 cells, or by the PRAs in MDCK cells. [b] EC_{90}, compound concentration that inhibits 90% of viral replication. [c] CC_{50}, compound concentration that produces 50% cytotoxicity, as determined by the cell viability assays in A549, Calu-3, or MDCK cells. Reported values represent the means ± SDs of data derived from three experiments in triplicate. [d] SI, selectivity index (determined as the ratio between CC_{50} and EC_{50}).

Thereafter, given the HTA feature of MEDS433, a second human airway epithelial cell line was evaluated to investigate its anti-IV activity in a different host cell system. Hence, VRAs were performed in Calu-3 cells. In this cell line, MEDS433 produced EC_{50} and EC_{90} values of 0.055 ± 0.003 µM and 0.675 ± 0.05 µM against IAV and of 0.052 ± 0.006 µM and 0.807 ± 0.08 µM for IBV (Table 1).

To exclude that the anti-IV activity of MEDS433 might be due to the cytotoxicity of target cells, its effect on the viability of uninfected A549 and Calu-3 cells was evaluated by the MTT method, which produced a cytotoxic concentration 50 (CC_{50}) for A549 cells of 64.25 ± 3.12 µM, with a favorable selectively index (SI) of 1104 for IAV and 988 for IBV, and a CC_{50} value of 54.67 ± 3.86 µM for Calu-3 cells, with an SI of 994 for IAV and 1051 for IBV (Table 1). Thus, the anti-IV activity of MEDS433 was not due to the inhibition of cell viability.

Lastly, to rule out the possibility that the antiviral effects of MEDS433 against the IVs was derived from the type of antiviral assay, plaque reduction assays (PRAs) were performed in MDCK cells infected with IAV or IBV. As depicted in Figure 2D,E, a MEDS433-mediated concentration-dependent inhibitory effect on both IAV and IBV replication in MDCK cells was again measured. As reported in Table 1, the EC_{50} and EC_{90} produced by MEDS433 in MDCK cells were 0.141 ± 0.021 µM and 0.256 ± 0.052 µM against IAV, while for IBV, they were 0.170 ± 0.019 µM and 0.330 ± 0.013 µM, respectively. Again, MEDS433 was more potent than brequinar against IAV and IBV even in MDCK cells, since the EC_{50} of the latter were 0.780 ± 0.012 µM against IAV and 1.07 ± 0.07 µM against IBV. Finally, the measurement of the cell viability of uninfected MDCK cells exposed to MEDS433 determined a CC_{50} of 119.8 ± 6.21 µM and an SI of 850 for IAV and 705 for IBV, thus confirming that even in canine cells, the anti-IV activity of MEDS433 was not due to the cytotoxicity of the target cells (Table 1).

Taken together, these results indicated that MEDS433 carried out a potent anti-IV activity that was independent of the type of IV, the cell line, or assay used.

3.3. MEDS433 Affects IAV Protein Expression by Targeting a Post-Entry Phase of the Virus Replicative Cycle

To investigate more in detail the anti-IV activity of MEDS433, cultures of IAV-infected MDCK cells were treated with MEDS433, and at various times p.i., total cell protein extracts were prepared and analyzed by immunoblotting for HA and NA protein content to monitor the levels of these representative IV proteins. As depicted in Figure 3, starting from 16 h p.i., the time point at which both IV glycoproteins became detectable, MEDS433 prevented their accumulation in infected and treated cells, thus indicating its ability to target a synthetic step in the virus replicative cycle.

Subsequently, time-of-addition experiments were carried out to pinpoint which phase of the IV replicative cycle was targeted by MEDS433. To this end, MDCK cells were treated with MEDS433 (0.5 µM) from -2 to -1 h prior to IAV infection (pretreatment (Pre-T)); or during IAV infection (from -1 to 0 h, adsorption stage; cotreatment (Co-T)); or after viral adsorption (from 0 to 48 h p.i.; post treatment (Post-T)); or from -2 to 48 h p.i. (full treatment (Full-T)). Infectious IAV particles released in cell supernatants were harvested at 48 h p.i. and titrated by the plaque assay. As shown in Figure 4A, MEDS433 was ineffective in interfering with the early phases of IAV's replicative cycle. By contrast, it produced a severe reduction of the IAV titer of about three orders of magnitude when added at a post-entry stage (Post-T) or left on the cell from -2 to 48 h p.i. (Full-T), thus in agreement with its ability to block HA and NA protein accumulation at late times of infection (Figure 3).
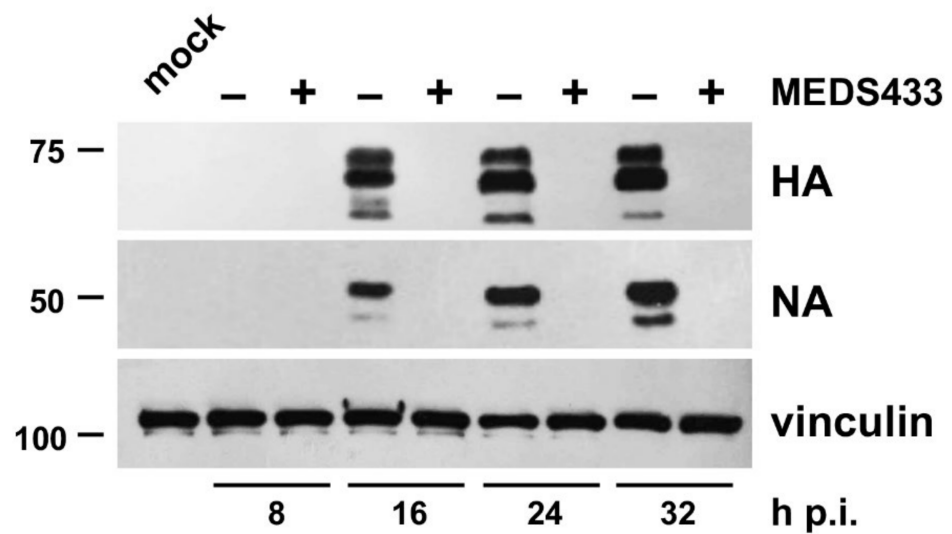
Figure 3. MEDS433 impairs the expression of IAV HA and NA proteins. MDCK cells were infected with IAV at an MOI of 0.1 PFU/cell and, where indicated, treated with 0.5 μM MEDS433 or DMSO as a control. Total cell protein extracts were prepared at the indicated times p.i., fractionated by 8% SDS-PAGE, and analyzed by immunoblotting with anti-IAV HA and anti-IAV NA pAbs. Vinculin immunodetection was used as a control for protein loading. Molecular weight markers are shown at the left side of each panel.
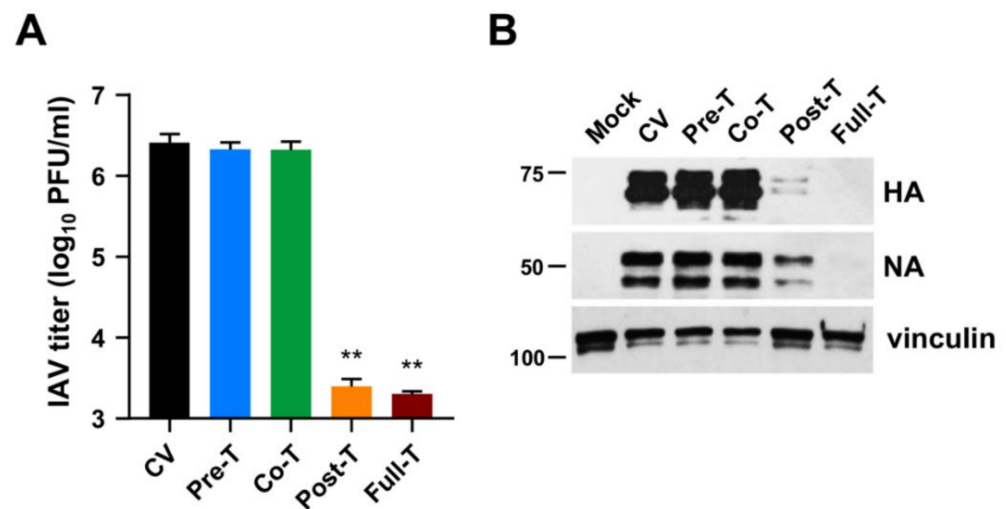

Figure 4. MEDS433 targets a post-entry phase of the IAV replicative cycle. MDCK cell monolayers were infected with IAV at an MOI of 0.1 and, where indicated, treated with 0.5 μM MEDS433 1 h prior to the infection (from −2 to −1 h, **Pre-T**), or during the infection (from −1 to 0 h, **Co-T**), or after infection (from 0 to 48 h p.i., **Post-T**;), or from −2 to 48 h p.i. (**Full-T**). Mock-infected cells (**Mock**) and control IAV-infected cells (**CV**) were exposed to DMSO only. (**A**) Cell supernatants harvested at 48 h p.i. were titrated by the plaque assay, and viral plaques were microscopically counted and plotted as PFU/mL. The data shown are the means ± SD of two independent experiments performed in triplicate and analyzed by a one-way ANOVA followed by Dunnett's multiple comparison test. ** ($p < 0.001$) compared to the calibrator sample (**CV**). (**B**) Total cell extracts were prepared at 48 h p.i., fractionated by 8% SDS-PAGE, and analyzed by immunoblotting with anti-IAV HA and anti-IAV NA pAbs. Vinculin immunodetection was used as a control for protein loading. Molecular weight markers are shown next to the left side of each panel.

Immunoblot analysis of protein extracts prepared from the very same IAV-infected and MEDS433-treated MDCK cells confirmed a severe impairment of HA and NA expression

only by the Post-T and Full-T treatments, while the Pre-T and Co-T were ineffective (Figure 4B).

The results of this section therefore suggested that the antiviral activity of MEDS433 stems from an interference with a biosynthetic step essential for IV replication and that takes places at a post-entry stage. However, as the levels of viral mRNAs were not measured, the effect of MEDS433 on the expression of HA and NA proteins could be due to the inhibition of the synthesis of the corresponding mRNAs or their translation.

3.4. The Pyrimidine Biosynthesis Pathway in Implicated in the Anti-IV Activity of MEDS433

The results of Section 3.3 evoked a mechanism of the anti-IV activity of MEDS433 that is well suited to its ability to inhibit *h*DHODH activity, thus depleting the intracellular pyrimidine pool. To verify this hypothesis, we investigated whether the anti-IV effect of MEDS433 could be reversed by the addition of increasing concentrations of exogenous pyrimidine ribonucleosides, such as uridine or cytidine.

As shown in Figure 5A, IAV replication in MDCK cells was restored more than 50% by the addition of a 100-fold excess of both uridine and cytidine relative to the MEDS433 concentration used (0.4 µM). In human A549 cells, the effect of uridine addition was even more pronounced, since 50% of IAV replication was already achieved at a uridine concentration 50-fold higher relative to MEDS433, while it was completely brought back to the level of untreated control by concentrations of both uridine and cytidine that were 1000-/2000-fold higher (Figure 5C). These results clearly indicated that the de novo pyrimidine synthesis pathway was targeted by MEDS433 in IAV-infected cells.
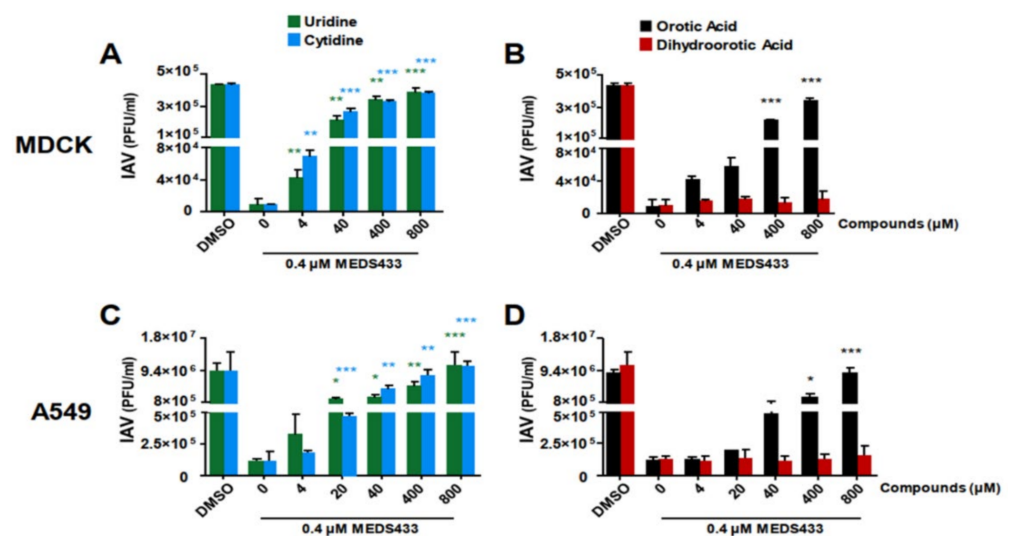

Figure 5. Uridine and orotic acid reversed the inhibitory effect of MEDS433 on IAV replication. (**A**,**B**) PRAs were performed in IAV-infected MDCK cells treated before, during, and post-infection with 0.4 µM MEDS433 in the presence of increasing concentrations of uridine or cytidine (**A**) and dihydroorotic acid or orotic acid (**B**). At 48 h p.i., the viral plaques were stained and microscopically counted. (**C**,**D**) VRAs were performed in A549 cells infected with IAV and treated with 0.4 µM MEDS433 in the presence of increasing concentrations of uridine (**C**) and dihydroorotic acid or orotic acid (**D**). At 48 h p.i., the cell supernatants were harvested and titrated in MDCK cells. Data shown represent means ± SDs of three independent experiments performed in triplicate and analyzed by a one-way ANOVA, followed by Dunnett's multiple comparison test. * ($p < 0.01$); ** ($p < 0.001$); *** ($p < 0.0001$) compared to the calibrator sample (MEDS433 alone).

To further confirm that the inhibition of *h*DHODH enzymatic activity by MEDS433 was effectively responsible for its antiviral activity, IAV-infected MDCK cells were treated with MEDS433 in the presence of increasing concentrations of dihydroorotic acid (DHO), or orotic acid (ORO), inasmuch as they are the *h*DHODH substrate or its product, respectively.

Figure 5B shows that ORO significantly reversed the inhibitory effect of MEDS433 already from a concentration 100-fold that of MEDS433. Conversely, the addition of DHO, even at 800 μM (2000-times more than the MEDS433 concentration used), did not reduce the anti-IAV activity of the *h*DHODH inhibitor (Figure 5B), thus sustaining that, indeed, MEDS433 inhibits a step of the pyrimidine biosynthesis pathway that is downstream from DHO. Similar results were obtained also in A549 cells (Figure 5D).

Together, these results indicated that MEDS433 inhibits IV replication through a specific inhibition of the *h*DHODH enzymatic activity in IV-infected cells, therefore blocking the oxidation of DHO to ORO in the de novo synthesis of pyrimidines.

3.5. The Combination of MEDS433 with an Inhibitor of the Nucleoside Salvage Pathway Enhances the Anti-IAV Activity of the hDHODH Inhibitor

Given that uridine counteracted the anti-IAV activity of MEDS433 (Figure 5), it could be possible that its physiological plasma concentration may limit the antiviral strength of MEDS433 in the host through the salvage pathway.

To address this problem, first, we investigated the effects on IAV replication of the combination of MEDS433 with dipyridamole (DPY), an inhibitor of the nucleoside/nucleotide transport channel hENT1/2 implicated in the pyrimidine salvage pathway [38–40]. For this purpose, VRAs were performed in IAV-infected A549 cells to determine the effect of the combination of a 0.25-, 0.5-, 1-, 2-, or 4-fold of MEDS433 EC_{50} to 3 μM DPY ratio. It is noteworthy that DPY as a single agent did not exert any inhibitory activity on IAV replication up to 10 μM (Figure 6). Nevertheless, when 3 μM DPY was used in combination with the different concentrations of MEDS433, it increased the anti-IAV potency of the *h*DHODH inhibitor (Figure 6); in fact, the EC_{50} of MEDS433 (0.063 ± 0.044 μM) was reduced to 0.011 ± 0.001 μM by the combination with DPY. The computed combination index (CI) values [31,32] corroborated that the combination of MEDS433 with DPY resulted in a synergistic antiviral activity at any of the MEDS433′s concentrations tested, since all the CIs were <0.9 (Table 2).
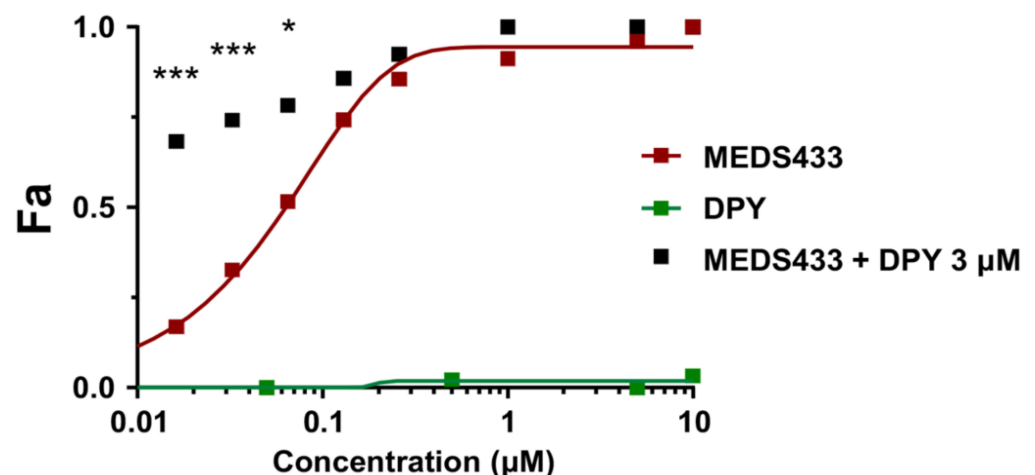

Figure 6. Effects of the combination of MEDS433 and dipyridamole on IAV replication. VRAs were performed in A549 cells treated with MEDS433 alone or in combination with different concentrations of DPY. At 48 h p.i., the cell supernatants were harvested and titrated by the plaque assay in MDCK cells. The effect of the combination was then analyzed by the CompuSyn software [36] and displayed as a fractional effect analysis (Fa) plot in relation to the compound concentrations. The anti-IAV activity of MEDS433 and DPY when used as single agents is depicted by red and green Fa curves, respectively. The effect of the MEDS433-DPY combination is shown with black squares. Results are representative of three independent experiments performed in triplicate and analyzed by a two-way ANOVA, followed by Dunnett's multiple comparison test. Statistical analysis was performed by comparing MEDS433-treated samples with the MEDS433 + DPY-treated samples for each condition. * ($p < 0.01$); *** ($p < 0.0001$).

Table 2. Analysis of the effects of the combination of MEDS433 and DPY against IAV replication.

MEDS433 Concentration (Fold of EC$_{50}$ [a]) + DPY 3 μM	MEDS433/DPY CI [b]	Drug Combination Effect [c] of MEDS433 and DPY
4×	0.824 ± 0.023	Moderate Synergism
2×	0.607 ± 0.116	Synergism
1×	0.341 ± 0.025	Synergism
0.5×	0.203 ± 0.044	Strong Synergism
0.25×	0.126 ± 0.032	Strong Synergism

[a] The EC$_{50}$ values of MEDS433 were determined by VRAs in IAV-infected A549 cells, as described in the Materials and Methods. [b] Combination index (CI), obtained by computational analysis with the CompuSyn software 1.0. Reported values represent means ± SDs of data derived from $n = 3$ independent experiments in triplicate. [c] According to the method of Chou [31], drug combination effects are defined as: strong synergism for $0.1 < CI < 0.3$; synergism for $0.3 < CI < 0.7$; moderate synergism for $0.7 < CI < 0.85$; slight synergism for $0.85 < CI < 0.90$; nearly additive for $0.90 < CI < 1.10$; slight antagonism for $1.10 < CI < 1.20$; moderate antagonism for $1.20 < CI < 1.45$.

Thereafter, we tested the efficacy of the MEDS433-DPY synergistic combination even in the presence of a hyper-physiological concentration of uridine (20 μM), far exceeding its plasma concentrations [41]. As shown in Figure 7, the presence of exogenous uridine reversed, as expected, the inhibitory activity of a MEDS433 concentration (0.4 μM) that remarkable inhibited IAV replication when tested as a single agent (Figure 2B). Conversely, the addition of increasing amounts of DPY restored the antiviral activity of MEDS433, thus sustaining the applicability of this combination to inhibit IAV replication, even in the presence of exogenous uridine (Figure 5A). Furthermore, none of the tested combinations reduced the viability of A549 cells, thus confirming that the DPY-mediated restoration of the MEDS433′s anti-IV activity was not due to a nonspecific cytotoxic effect.
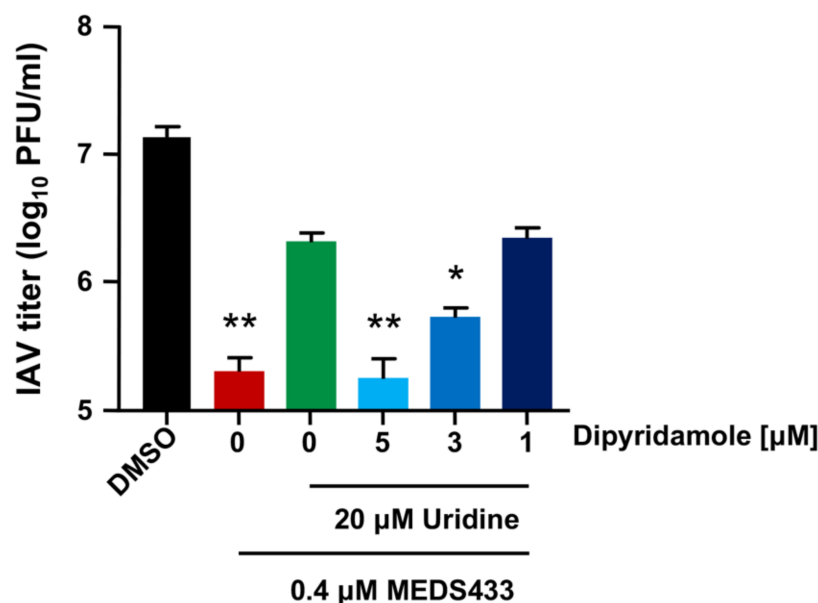

Figure 7. A combination of modulators of pyrimidine metabolism inhibits IAV replication in the presence of exogenous uridine. VRAs were performed in A549 cells treated with MEDS433 alone or in combination with different concentrations of DPY. Where indicated, infected cells were supplemented with 20 μM uridine. At 48 h p.i., the cell supernatants were harvested and titrated by the plaque assay in MDCK cells. The data shown represent means ± SDs of three independent experiments performed in triplicate, and MEDS433-treated samples were analyzed by an unpaired *t*-test, corrected at FDR $q < 0.05$. * ($p < 0.01$); ** ($p < 0.001$) compared to the calibrator sample (MEDS433 + 20 μM uridine, green column).

Taken together, the results of this section suggested that a combination of two modulators of the pyrimidine metabolism, such as a *h*DHODH inhibitor and an inhibitor of the salvage pathway, was effective against IV replication, even in the presence of uridine concentrations that exceed in vivo host conditions.

3.6. MEDS433 and the Ribonucleoside Analogue N^4-Hydroxycytidine Synergistically Act against IAV Replication

Lastly, we investigated whether the combination of MEDS433 with a DAA targeting IV RNA replication could result in a synergistic, additive, or antagonistic effect against IV replication. To this end, first, we measured the EC_{50} of N^4-hydroxycytidine (NHC or EIDD1931), a cytosine analogue that exerts a potent anti-IV antiviral activity as a result of increased viral mutagenesis following its incorporation by IV RdRp [42,43]. The EC_{50} of NHC against IAV, as measured by VRA in A549 cells, was 0.332 ± 0.011 μM. Then, VRAs were performed with different concentrations of both MEDS433 and NHC corresponding to 0.25-, 0.5-, 1-, 2-, or 4-fold their EC_{50} values to obtain equipotent ratios (MEDS433 EC_{50}/NHC EC_{50}). As depicted in Figure 8, the anti-IAV efficacy of NHC was increased by the combination with MEDS433, since the EC_{50} of NHC was decreased to 0.124 ± 0.011 μM by the combination with the *h*DHODH inhibitor. The synergism between MEDS433 and NHC was confirmed by the computed CI values < 0.9 at any of the MEDS433 to NHC combinations tested (Table 3). These results therefore suggested that a combination of MEDS433 with a RdRp-targeting DAA, such as NHC, might be of interest to design new pharmacological approaches for the control of IV infections.
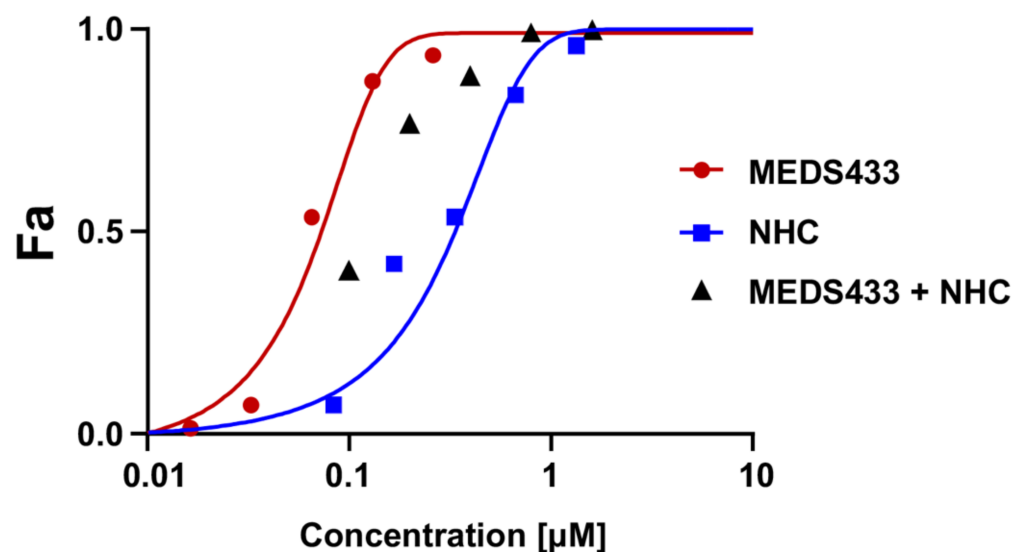

Figure 8. The combination of MEDS433 with NHC is synergistic against IAV replication. A549 cells were treated with different concentrations of MEDS433 alone or in combination with various concentrations of NHC before and during IAV infection. At 48 h p.i., the cell supernatants were harvested and titrated for IAV by the plaque assay in MDCK cells. Viral titers were analyzed by the CompuSyn software 1.0 [36], and the anti-IAV activity is shown as a fractional effect analysis (Fa) plot in relation to the drugs' concentrations. Red and blue Fa curves represent the activity of MEDS433 or NHC on IAV replication when employed as single agents, respectively. The effect of the MEDS433–NHC combination is shown with black triangles. Results are representative of three independent experiments performed in triplicate.

Table 3. Analysis of the effect of the combination of MEDS433 and NHC on IAV replication.

MEDS433/NHC Combination at Equipotent Ratio (fold of EC_{50} [a])	MEDS433/NHC CI [b]	Drug Combination Effect [c] of MEDS433 and NHC
4×	0.075 ± 0.004	Very Strong Synergism
2×	0.484 ± 0.011	Synergism
1×	0.825 ± 0.004	Moderate Synergism
0.5×	0.604 ± 0.028	Synergism
0.25×	0.625 ± 0.019	Synergism

[a] Fold of EC_{50} MEDS433/EC_{50} NHC yielding an equipotent concentration ratio (approximately 1:5.12) between the two combined drugs. The EC_{50} values were determined by VRAs against IAV, as described in the Materials and Methods. [b] Combination index (CI), obtained by computational analysis with the CompuSyn software 1.0. Reported values represent means ± SDs of data derived from n = 3 independent experiments in triplicate. [c] Drug combination effects are defined as: very strong synergism for CI < 0.1; strong synergism for 0.1 < CI < 0.3; synergism for 0.3 < CI < 0.7; moderate synergism for 0.7 < CI < 0.85; slight synergism for 0.85 < CI < 0.90; nearly additive for 0.90 < CI < 1.10; slight antagonism for 1.10 < CI < 1.20; moderate antagonism for 1.20 < CI < 1.45 [31].

4. Discussion

The ongoing COVID-19 pandemic, along with the frequent emergence and re-emergence of human respiratory viruses in recent decades have renewed interest in host-targeting antivirals. Since HTAs target cellular biochemical pathways or factors that can be exploited by many different viruses for their replication, they may exert broad-spectrum antiviral activity and, thus, represent valuable tools in the preparedness against future viral infections [44]. Given the essential role of *h*DHODH in the de novo pyrimidine biosynthesis pathway and its indispensable requirement for efficient viral replication, as we strengthened here for IVs (Figure 1), this host enzymatic activity is considered a reliable HTA target to develop new broad-spectrum antivirals, also against antigenically different IVs [45,46]. To further this prospect sustain, this study reported that the new *h*DHODH inhibitor MEDS433 carries out a potent dose-dependent antiviral activity against IAV and IBV, with a mechanism that derives from a selective inhibition of *h*DHODH activity in IV-infected cells. Our findings corroborate the feasibility of the pharmacological targeting of *h*DHODH to control IV replication, as recently observed also for other *h*DHODH inhibitors, such as brequinar [28], FA-613 [47], and S312 and S416 [48].

MEDS433 is a small molecule belonging to a novel class of *h*DHODH inhibitors that are based on a 2-hydroxypyrazolo [1,5-a]-pyridine scaffold [24–26]. It was designed by applying a bioisosteric approach to brequinar, one of the most-potent *h*DHODH inhibitors [27]. Even though both MEDS433 and brequinar target with high affinity the ubiquinone binding site of *h*DHODH and show a similar potency in inhibiting its enzymatic activity [24], when they were compared for anti-IV activity, MEDS433 resulted in being more effective (Figure 2). The superior activity of MEDS433 against IV replication might depend on its more favorable lipophilicity (logD7.4 value of 2.35) in comparison to the more polar brequinar (logD7.4 value of 1.83) [26]. A value of logD7.4 equal to 2.50 has been suggested as the optimum for the inhibition of mitochondrial *h*DHODH, since inhibitors with a lower logD7.4 may poorly cross the mitochondrial membrane, while those endowed with a higher logD7.4 may display a reduced cellular adsorption [49]. Furthermore, we observed that MEDS433 was less cytotoxic than brequinar; in fact, the CC_{50} measured in A549 cells of brequinar (5.69 μM) was about ten-fold lower than that of MEDS433 (64.25 μM), which determined SI values of 12 for IAV and 21 for IBV, respectively. Again, the optimal lipophilicity of MEDS433 might reduce the possibility of off-targeting effects within host cells, thus explaining the high SI values measured for this *h*DHODH inhibitor. The low cytotoxicity of MEDS433 is undoubtedly a favorable feature and, indeed, contributes to making it a promising HTA candidate.

However, to become a candidate for the treatment of respiratory virus infections, as IVs, an optimal HTA, in addition to being potent and having a low cytotoxicity, as we observed for MEDS433, it should be suitable even for combination treatments to enhance antiviral efficacy and to reduce the risk of the emergence of drug resistance [44]. Keeping

this in mind, it is worth noting that this study adds a couple of new pieces of knowledge that may be of interest to be considered toward the validation of *h*DHODH inhibitors to the design of new therapeutic approaches for the management of IV infections.

The first is related to the limited therapeutic efficacy that has been reported for some *h*DHODH inhibitors in animal models of human viral infections, despite their clear in vitro antiviral activity [50–52]. This failure likely derives from the inadequate antiviral potency and pharmacokinetics performance of the evaluated *h*DHODH inhibitors, as well as from the counteracting effect of the pyrimidine salvage pathway by means of the transport of exogenous uridine into virus-infected cells. Accordingly, the pharmacological targeting of the pyrimidine salvage pathway may be beneficial, inasmuch as it may enhance the in vivo antiviral effect of *h*DHODH inhibitors.

Relevant to this hypothesis is the observations that a combination of MEDS433 with DPY was synergistic against IAV replication (Figure 6), even in the presence of amounts of uridine that exceed the physiological plasma concentration (Figure 7). In fact, notwithstanding that DPY is devoid of anti-IV activity (Figure 6), when used in combination with the *h*DHODH inhibitor, it restored successfully the antiviral activity of a MEDS433 concentration no longer effective as a consequence of uridine supplementation (Figure 7). DPY is a pyrimidopyrimidine derivative that inhibits the equilibrative nucleoside transporters (ENT) 1 and 2, the most effective nucleoside/nucleotide transporters of the pyrimidine salvage pathway [40]. Thanks to its ability to block the uptake of adenosine into platelets, endothelial cells, and erythrocytes, DPY hinders platelet aggregation and vasodilatation. Therefore, DPY is approved as an oral agent in the prophylaxis of thromboembolism in cardiovascular disease [39]. While the combination of DPY with *h*DHODH inhibitors has been proposed to increase the anticancer effects of the latter [53], the potential of this combination against viral infections has been investigated poorly. In this regard, recently, we observed that the combination of MEDS433 with DPY was effective also against HSV-1 and SARS-CoV-2, even in the presence of a hyperphysiological concentration of uridine [30,31]. Importantly, the concentration of DPY (3 µM) that we observed to be synergistic in combination with MEDS433 against IAV replication is lower than the DPY Cmax (2.2 µg/mL, which corresponds to 4.4 µM) [54] and, thus, clinically achievable in patients undergoing DPY therapy. Thus, the wide clinical experience of DPY could allow its rapid repositioning against virus infections, including IVs, to be clinically useful in combination with *h*DHODH inhibitors.

Furthermore, pertinent to the possibility to exploit combinations between compounds targeting the pyrimidine synthesis pathway and DAA against IVs is the observation that several combinations of MEDS433 and N4-hydroxycytidine (NHC) interact in a synergistic manner, each reinforcing the other's antiviral activity against IAV (Figure 8). To our knowledge, this is the first observation of a synergistic effect between NHC and a *h*DHODH inhibitor against IVs.

The ribonucleoside analog NHC is the active metabolite of the prodrug molnupiravir, which was initially developed for IV infections [42,43], then repurposed against SARS-CoV-2, currently approved for use in COVID-19 [55]. NHC, once phosphorylated to the pharmacologically active NHC-triphosphate (NHCTP), is incorporated into nascent RNA by viral RdRps. However, the tautomeric interconversion within NHC then leads to misincorporation of adenine bases instead of guanine bases in the subsequent cycles of viral RNA synthesis, which eventually results in viral mutagenesis, inhibition of viral replication, and antiviral activity [56].

Recently, the combination of NHC with different *h*DHODH inhibitors has been reported to exert a synergistic effect against in vitro replication of SARS-CoV-2 and in reducing viral titers and the pathology in animal models of the infection [57,58]. Since NHCTP competes with cellular CTP for incorporation into nascent RNA, it has been suggested that the impairment of CTP synthesis by *h*DHODH inhibitors reduces this competition and facilitates the incorporation of NHCTP into newly synthetized SARS-CoV-2 RNA. Thereby, *h*DHODH inhibitors potentiate the antiviral effectiveness of NHC. This ribonucleoside ana-

log is in fact imported within cells by the salvage pathway, and therefore, the intracellular NHCTP levels are not affected by the *h*DHODH inhibition [57,58].

Since combinations of different antivirals have proven to be effective in the control of many viral infections, the combination of broad-spectrum nucleoside analogues, such as NHC, with DHODH inhibitors might be suitable to develop therapeutic strategies to control infections of a wide range of viruses.

Lastly, an important added value of MEDS433 is its antiviral effectiveness against a broad range of viruses that cause respiratory tract infections in humans, since, in addition to IAV and IBV, we observed the ability of MEDS433 to prevent the replication of hCOV-229E, hCoV-OC43, and SARS-CoV-2 [31]. This feature and its inherent HTA advantage of the low risk of emergence of drug-resistant strains make MEDS433 of interest for the development of broad-spectrum antiviral agents, even in the preparedness against future emerging human respiratory viruses given the independence of its antiviral effects with respect to a specific virus. The disastrous consequences of COVID-19 are indeed indisputable evidence of the need for new broad-spectrum antiviral drugs known to be effective against respiratory viruses that may emerge from future zoonoses.

5. Conclusions

In conclusion, this study indicated MEDS433 as an attractive novel HTA candidate endowed with advantageous features, such as a potent antiviral activity against both IAV and IBV and rapidly deployable against future novel emerging IVs. Moreover, MEDS433 could also be considered for combination drug treatments with both nucleoside analogues and other anti-pyrimidines, such as NHC and DPY, for the design of new therapeutic approaches to IV infections. Presently, the potent in vitro anti-IV activity of MEDS433 and its valuable drug-like profile support further studies to evaluate its efficacy in preclinical animal models of IV infections.

References

1. *Global Influenza Strategy 2019–2030*; WHO: Geneva, Switzerland, 2019.
2. Peteranderl, C.; Herold, S.; Schmoldt, C. Human influenza virus infections. *Semin. Respir. Crit. Care Med.* **2016**, *37*, 487–500. [CrossRef] [PubMed]
3. Paules, C.; Subbarao, K. Influenza. *Lancet* **2017**, *390*, 687–708. [CrossRef]
4. Krammer, F.; Smith, G.J.D.; Fouchier, R.A.M.; Peiris, M.; Kedzierska, K.; Doherty, P.C.; Palese, P.; Shaw, M.L.; Treanor, J.; Webster, R.G.; et al. Influenza. *Nat. Rev. Dis. Primers* **2018**, *4*, 3. [CrossRef] [PubMed]
5. Yamayoshi, S.; Kawaoka, T. Current and future influenza vaccines. *Nat. Med.* **2019**, *25*, 212–220. [CrossRef]
6. Nachbagauer, R.; Palese, P. Is a universal influenza virus vaccine possible? *Annu. Rev. Med.* **2020**, *71*, 315–327. [CrossRef]
7. Chow, E.J.; Doyle, J.D.; Uyeki, T.M. Influenza virus-related critical illness: Prevention, diagnosis, treatment. *Crit. Care* **2019**, *23*, 214. [CrossRef]
8. Chang, C.; Ramphul, K. *Amantadine*; StatPearls Publishing: Treasure Island, FL, USA, 2022.
9. McKimm-Breschkin, J.L. Influenza neuraminidase inhibitors: Antiviral action and mechanisms of resistance. *Influenza Respir. Viruses* **2013**, *7*, 25–36. [CrossRef]
10. Lampejo, T. Influenza and antiviral resistance: An overview. *Eur. J. Clin. Microbiol. Infect. Dis.* **2020**, *39*, 1201–1208. [CrossRef]
11. Govorkova, E.A.; Takashita, E.; Daniels, R.S.; Fujisaki, S.; Presser, L.D.; Patel, M.C.; Huang, W.; Lackenby, A.; Nguyen, H.T.; Pereyaslov, D.; et al. Global update on the susceptibilities of human influenza viruses to neuraminidase inhibitors and the Cap-dependent endonuclease inhibitor baloxavir, 2018–2020. *Antivir. Res.* **2022**, *200*, 105281. [CrossRef]
12. Davidson, S. Treating influenza infection, from now and into the future. *Front. Immunol.* **2018**, *9*, 1946. [CrossRef]
13. Hayden, F.G.; Sugaya, N.; Hirotsu, N.; Lee, N.; De Jong, M.D.; Hurt, A.C.; Ishida, T.; Sekino, H.; Yamada, K.; Portsmouth, S.; et al. Baloxavir marboxil for uncomplicated influenza in adults and adolescents. *N. Engl. J. Med.* **2018**, *379*, 913–923. [CrossRef]
14. Shiraki, K.; Daikoku, T. Favipiravir, an anti-influenza drug against life-threatening RNA virus infections. *Pharmacol. Ther.* **2020**, *209*, 107512. [CrossRef]
15. Toots, M.; Plemper, R.K. Next-generation direct-acting influenza therapeutics. *Transl. Res.* **2020**, *220*, 33–41. [CrossRef]
16. Van de Wakker, S.I.; Fischer, M.J.E.; Oosting, R.S. New drug strategies to tackle viral-host interactions for the treatment of influenza virus infections. *Eur. J. Pharmacol.* **2017**, *809*, 178–190. [CrossRef]
17. Okesli, A.; Khosla, C.; Bassik, M.C. Human pyrimidine nucleotide biosynthesis as a target for antiviral chemotherapy. *Curr. Op. Biotech.* **2017**, *48*, 127–134. [CrossRef]
18. Gribaudo, G.; Riera, L.; Rudge, T.L.; Caposio, P.; Johnson, L.F.; Landolfo, S. Human cytomegalovirus infection induces cellular thymidylate synthase gene expression in quiescent fibroblasts. *J. Gen. Virol.* **2002**, *83*, 2983–2993. [CrossRef]
19. Gribaudo, G.; Riera, L.; Caposio, P.; Maley, F.; Landolfo, S. Human cytomegalovirus requires cellular deoxycytidylate deaminase for replication in quiescent cells. *J. Gen. Virol.* **2003**, *84*, 1437–1441. [CrossRef]
20. Munger, J.; Bennett, B.; Parikh, A.; Feng, X.-J.; McArdle, J.; Rabitz, H.A.; Shenk, T.; Rabinowitz, J.D. Systems-level metabolic flux profiling identifies fatty acid synthesis as a target for antiviral therapy. *Nat. Biotechnol.* **2008**, *26*, 1179–1186. [CrossRef]
21. Karimi, Z.; Oskouie, A.A.; Rezaie, F.; Ajaminejad, F.; Marashi, S.M.; Azad, T.-M. The effect of influenza virus on the metabolism of peripheral blood mononuclear cells with a metabolomics approach. *J. Med. Virol.* **2022**, *94*, 4383–4392. [CrossRef]
22. Reis, R.A.G.; Calil, F.A.; Feliciano, P.R.; Pinheiro, M.P.; Nonato, M.C. The dihydroorotate dehydrogenases: Past and present. *Arch. Biochem. Biophys.* **2017**, *632*, 75–191. [CrossRef]
23. Loeffler, M.; Carrey, E.A.; Knecht, W. The pathway to pyrimidines: The essential focus on dihydroorotate dehydrogenase, the mitochondrial enzyme coupled to the respiratory chain. *Nucleosides Nucleotides Nucleic Acids* **2020**, *11*, 1–25. [CrossRef]
24. Sainas, S.; Pippione, A.C.; Lupino, E.; Giorgis, M.; Circosta, P.; Gaidano, V.; Goyal, P.; Bonanni, D.; Rolando, B.; Cignetti, A.; et al. Targeting myeloid differentiation using potent 2-Hydroxypyrazolo [1,5-α] pyridine scaffold-based human dihydroorotate dehydrogenase inhibitors. *J. Med. Chem.* **2018**, *61*, 6034–6055. [CrossRef]
25. Sainas, S.; Giorgis, M.; Circosta, P.; Gaidano, V.; Bonanni, D.; Pippione, A.C.; Bagnati, R.; Passoni, A.; Qiu, Y.; Cojocaru, C.F.; et al. Targeting acute myelogenous leukemia using potent human dihydroorotate dehydrogenase inhibitors based on the 2-hydroxypyrazolo[1,5-α] pyridine scaffold: SAR of the biphenyl moiety. *J. Med. Chem.* **2021**, *64*, 5404–5428. [CrossRef]
26. Sainas, S.; Giorgis, M.; Circosta, P.; Poli, G.; Alberti, M.; Passoni, A.; Gaidano, V.; Pippione, A.C.; Vitale, N.; Bonanni, D.; et al. Targeting acute myelogenous leukemia using potent human dihydroorotate dehydrogenase inhibitors based on the 2-hydroxypyrazolo[1,5-α] pyridine scaffold: SAR of the aryloxyaryl moiety. *J. Med. Chem.* **2022**, *64*, 5404–5428. [CrossRef]
27. Peters, G.J. Re-evaluation of Brequinar sodium, a dihydroorotate dehydrogenase inhibitor. *Nucleosides Nucleotides Nucleic Acids* **2018**, *37*, 666–678. [CrossRef]
28. Park, J.-G.; Ávila-Pérez, G.; Nogales, A.; Blanco-Lobo, P.; De la Torre, J.C.; Martínez-Sobrido, L. Identification and characterization of novel compounds with broad-spectrum antiviral activity against influenza A and B viruses. *J. Virol.* **2020**, *94*, e02149-e19. [CrossRef]
29. Boschi, D.; Pippione, A.C.; Sainas, S.; Lolli, M.L. Dihydroorotate dehydrogenase inhibitors in anti-infective drug research. *Eur. J. Med. Chem.* **2019**, *183*, 111681. [CrossRef]
30. Luganini, A.; Sibille, G.; Mognetti, B.; Sainas, S.; Pippione, A.C.; Giorgis, M.; Boschi, D.; Lolli, M.L.; Gribaudo, G. Effective deploying of a novel DHODH inhibitor against herpes simplex type 1 and type 2 replication. *Antivir. Res.* **2021**, *189*, 105057. [CrossRef]

31. Calistri, A.; Luganini, A.; Mognetti, B.; Elder, E.; Sibille, G.; Conciatori, V.; Del Vecchio, C.; Sainas, S.; Boschi, D.; Montserrat, N.; et al. The new generation hDHODH inhibitor MEDS433 hinders the in vitro replication of SARS-CoV-2 and other human coronaviruses. *Microorganisms* **2021**, *9*, 1731. [CrossRef]

32. Luganini, A.; Terlizzi, M.E.; Catucci, G.; Gilardi, G.; Maffei, M.E.; Gribaudo, G. The cranberry extract Oximacro exerts in vitro virucidal activity against influenza virus by interfering with hemagglutinin. *Front. Microbiol.* **2018**, *9*, 1826. [CrossRef]

33. Simon, L.M.; Morandi, E.; Luganini, A.; Gribaudo, G.; Martinez-Sobrido, L.; Turner, D.H.; Oliviero, S.; Incarnato, D. In vivo analysis of influenza A mRNA secondary structures identifies critical regulatory motifs. *Nucleic Acids Res.* **2019**, *47*, 7003–7017. [CrossRef] [PubMed]

34. Pauwels, R.; Balzarini, J.; Baba, M.; Snoeck, R.; Schols, D.; Herdewijn, P.; Desmyter, J.; DeClercq, E. Rapid and automated tetrazolium-based colorimetric assay for the detection of anti-HIV compounds. *J. Virol. Methods* **1988**, *20*, 309–321. [CrossRef]

35. Chou, T.C. Theoretical basis, experimental design, and computerized simulation of synergism and antagonism in drug combination studies. *Pharmacol. Rev.* **2006**, *58*, 621–681. [CrossRef] [PubMed]

36. Chou, T.C.; Martin, N. *CompuSyn for Drug Combinations: PC Software and User's Guide—A Computer Program for Quantitation of Synergism and Antagonism in Drug Combinations, and the Determination of IC50 and ED50 and LD50 Bvalues*; ComboSyn: Paramus, NJ, USA, 2005.

37. Luganini, A.; Caposio, P.; Landolfo, S.; Gribaudo, G. Phosphorothioate-modified oligodeoxynucleotides inhibit human cytomegalovirus replication by blocking virus entry. *Antimicrob. Agents Chemother.* **2008**, *52*, 1111–1120. [CrossRef]

38. Fitzgerald, G.A. Dipyridamole. *N. Engl. J. Med.* **1987**, *316*, 1247–1257. [CrossRef] [PubMed]

39. Schaper, W. Dipyridamole, an underestimated vascular protective drug. *Cardiovasc. Drugs Ther.* **2005**, *19*, 357–363. [CrossRef] [PubMed]

40. Ward, J.L.; Sherali, A.; Mo, Z.P.; Tse, C.M. Kinetic and pharmacological properties of cloned human equilibrative nucleoside transporters, ENT1 and ENT2, stably expressed in nucleoside transporter-deficient PK15 cells: ENT2 exhibits a low affinity for guanosine and cytidine but a high affinity for inosine. *J. Biol. Chem.* **2000**, *275*, 8375–8381. [CrossRef]

41. Pizzorno, G.; Cao, D.; Leffert, J.J.; Russell, R.L.; Zhang, D.; Handschumacher, R.E. Homeostatic control of uridine and the role of uridine phosphorylase: A biological and clinical update. *Biochim. Biophys. Acta* **2002**, *1587*, 133–144. [CrossRef]

42. Yoon, J.-J.; Toots, M.; Lee, S.; Lee, M.-E.; Ludeke, B.; Luczo, J.M.; Ganti, K.; Cox, R.M.; Sticher, Z.M.; Edpuganti, V.; et al. Orally efficacious broad-spectrum ribonucleoside analog inhibitor of influenza and respiratory syncytial viruses. *Antimicrob. Agents Chemother.* **2018**, *62*, e00766-e18. [CrossRef]

43. Toots, M.; Yoon, J.-J.; Cox, R.M.; Hart, M.; Sticher, Z.M.; Makhsous, N.; Plesker, R.; Barrena, A.H.; Reddy, P.G.; Mitchell, D.G.; et al. Characterization of orally efficacious influenza drug with high resistance barrier in ferrets and human airway epithelia. *Sci. Transl. Med.* **2019**, *11*, eaax5866. [CrossRef]

44. Amesh Adalja, A.; Inglesby, T. Broad-spectrum antiviral agents: A crucial pandemic tool. *Exp. Rev. Anti-Infect. Ther.* **2019**, *17*, 467–470. [CrossRef]

45. Coehlo, A.R.; Oliveira, P.J. Dihydroorotate dehydrogenase inhibitors in SARS-CoV-2 infection. *Eur. J. Clin. Investig.* **2020**, *50*, e13366. [CrossRef]

46. Zheng, Y.; Li, S.; Song, K.; Ye, J.; Li, W.; Zhong, Y.; Feng, Z.; Liang, S.; Cai, Z.; Xu, K. A broad antiviral strategy: Inhibitors of human DHODH pave the way for host-targeting antivirals against emerging and re-emerging Viruses. *Viruses* **2022**, *14*, 928. [CrossRef]

47. Cheung, N.N.; Lai, K.K.; Dai, J.; Kok, K.H.; Chen, H.; Chan, K.-H.; Yuen, K.-Y.; Tsun Sao, R.Y. Broad-spectrum inhibition of common respiratory RNA viruses by a pyrimidine synthesis inhibitor with involvement of the host antiviral response. *J. Gen. Virol.* **2017**, *98*, 946–954. [CrossRef]

48. Xiong, R.; Zhang, L.; Li, S.; Sun, Y.; Ding, M.; Wang, Y.; Zhao, Y.; Wu, Y.; Shang, W.; Jiang, X.; et al. Novel and potent inhibitors targeting DHODH are broad-spectrum antivirals against RNA viruses including newly emerged coronavirus SARS-CoV-2. *Protein Cell* **2020**, *11*, 723–739. [CrossRef]

49. Gradl, S.N.; Mueller, T.; Ferrara, S.; Sheikh, S.E.; Janzer, A.; Zhou, H.-J.; Friberg, A.; Guenther, J.; Schaefer, M.; Stellfeld, T.; et al. Discovery of BAY 2402234 by phenotypic screening: A human dihydroorotate dehydrogenase (DHODH) inhibitor in clinical trials for the treatment of myeloid malignancies. In Proceedings of the American Association for Cancer Research Annual Meeting, Atlanta, GA, USA, 29 March–3 April 2019; Volume 79 13 Suppl. Abstract 2.

50. Wang, Q.Y.; Bushell, S.; Qing, M.; Xu, H.Y.; Bonavia, A.; Nunes, S.; Zhou, J.; Poh, M.K.; Florez de Sessions, P.; Niyomrattanakit, P.; et al. Inhibition of dengue virus through suppression of host pyrimidine biosynthesis. *J. Virol.* **2011**, *85*, 6548–6556. [CrossRef]

51. Smee, D.F.; Hurst, B.L.; Day, C.W. D282, a non-nucleoside inhibitor of influenza virus infection that interferes with de novo pyrimidine biosynthesis. *Antivir. Chem. Chemother.* **2012**, *22*, 263–272. [CrossRef]

52. Grandin, C.; Lucas-Hourani, M.; Janin, Y.L.; Dauzonne, D.; Munier-Lehmann, H.; Paturet, A.; Taborik, F.; Vabret, A.; Contamin, H.; Tangy, F.; et al. Respiratory syncytial virus infection in macaques is not suppressed by intranasal sprays of pyrimidine biosynthesis inhibitors. *Antiviral Res.* **2016**, *125*, 58–62. [CrossRef]

53. Gaidano, V.; Houshmand, M.; Vitale, N.; Carr, G.; Morotti, A.; Tenace, V.; Rapelli, S.; Sainas, S.; Pippione, A.C.; Giorgis, M.; et al. The synergism between DHODH inhibitors and dipyridamole leads to metabolic lethality in acute myeloid leukemia. *Cancers* **2021**, *13*, 1003. [CrossRef]

54. Gregov, D.; Jenkins, A.; Duncan, E.; Sieber, D.; Rodgers, S.; Duncan, B.; Bochner, F.; Lloyd, J. Dipyridamole: Pharmacokinetics and effects on aspects of platelet function in man. *Br. J. Clin. Pharmacol. Soc.* **1987**, *24*, 425–434. [CrossRef]

55. Jayk Bernal, A.; Gomes da Silva, M.M.; Musungaie, D.B.; Kovalchuk, E.; Gonzalez, A.; Delos Reyes, V.; Martín-Quirós, A.; Caraco, Y.; Williams-Diaz, A.; Brown, M.L.; et al. Molnupiravir for oral treatment of Covid-19 in nonhospitalized patients. *N. Engl. J. Med.* **2022**, *386*, 509–520. [CrossRef]

56. Kabinger, F.; Stiller, C.; Schmitzová, J.; Dienemann, C.; Kokic, G.; Hillen, H.S.; Hobartner, C.; Cramer, P. Mechanism of molnupiravir-induced SARS-CoV-2 mutagenesis. *Nat. Struct. Mol. Biol.* **2021**, *28*, 740–746. [CrossRef]

57. Stegmann, K.M.; Dickmanns, A.; Heinen, N.; Blaurock, C.; Karrasch, T.; Breithaupt, A.; Klopfleisch, R.; Uhlig, N.; Eberlein, V.; Issmail, L.; et al. Inhibitors of dihydroorotate dehydrogenase cooperate with molnupiravir and N4-hydroxycytidine to suppress SARS-CoV-2 replication. *iScience* **2022**, *25*, 104293. [CrossRef]

58. Schultz, D.C.; Johnson, R.M.; Ayyanathan, K.; Miller, J.; Whig, K.; Kamalia, B.; Dittmar, M.; Weston, S.; Hammond, H.L.; Dillen, C.; et al. Pyrimidine inhibitors synergize with nucleoside analogues to block SARS-CoV-2. *Nature* **2022**, *604*, 134–140. [CrossRef]

Mechanisms of antiviral activity of the new *h*DHODH inhibitor MEDS433 against respiratory syncytial virus replication

Anna Luganini [a,1], Giulia Sibille [a,1], Marta Pavan [a], Maurizia Mello Grand [c], Stefano Sainas [b], Donatella Boschi [b], Marco L. Lolli [b], Giovanna Chiorino [c], Giorgio Gribaudo [a,*]

[a] *Department of Life Sciences and Systems Biology, University of Torino, 10123, Torino, Italy*
[b] *Department of Drug Sciences and Technology, University of Torino, 10125, Torino, Italy*
[c] *Fondazione Edo ed Elvo Tempia, 13900, Biella, Italy*

ARTICLE INFO

ABSTRACT

Human respiratory syncytial virus (RSV) is an important cause of acute lower respiratory infections, for which no effective drugs are currently available. The development of new effective anti-RSV agents is therefore an urgent priority, and Host-Targeting Antivirals (HTAs) can be considered to target RSV infections. As a contribution to this antiviral avenue, we have characterized the molecular mechanisms of the anti-RSV activity of MEDS433, a new inhibitor of human dihydroorotate dehydrogenase (*h*DHODH), a key cellular enzyme of *de novo* pyrimidine biosynthesis. MEDS433 was found to exert a potent antiviral activity against RSV-A and RSV-B in the one-digit nanomolar range. Analysis of the RSV replication cycle in MEDS433-treated cells, revealed that the *h*DHODH inhibitor suppressed the synthesis of viral genome, consistently with its ability to specifically target *h*DHODH enzymatic activity. Then, the capability of MEDS433 to induce the expression of antiviral proteins encoded by Interferon-Stimulated Genes (ISGs) was identified as a second mechanism of its antiviral activity against RSV. Indeed, MEDS433 stimulated secretion of IFN-β and IFN-λ1 that, in turn, induced the expression of some ISG antiviral proteins, such as IFI6, IFITM1 and IRF7. Singly expression of these ISG proteins reduced RSV-A replication, thus likely contributing to the overall anti-RSV activity of MEDS433. Lastly, MEDS433 proved to be effective against RSV-A replication even in a primary human small airway epithelial cell model. Taken as a whole, these observations provide new insights for further development of MEDS433, as a promising candidate to develop new strategies for treatment of RSV infections.

1. Introduction

The Respiratory syncytial virus (RSV) is a leading cause of lower respiratory tract infections (LRTI) that may give rise to severe illnesses, such as bronchiolitis and pneumonia in high-risk groups, including children, adults with a compromised immune system or with comorbidities, and elderly (Jorquera et al., 2016; Jain et al., 2022). Globally, in children aged 0–60 months, RSV infections cause more than 33 million LRTI per year, that lead to an estimated 3.6 million hospitalizations, and around 100,000 in-hospital deaths (Li et al., 2022). RSV infections, however, constitute a substantial disease burden even in adults aged ≥65 years (Nam and Ison, 2019). In fact, it is estimated that 160,000 older adults are hospitalized, and 10,000 of them die due to RSV infection (Hansen et al., 2022). Hence, RSV is a contagious seasonal virus causing significant morbidity and mortality both in pediatric and adult settings.

These days, prevention of RSV infections in adults can be achieved by means of two new RSV prefusion F protein-based vaccines approved in 2023, such as Abrysvo (Pfizer) and Arexvy (GSK) (Soni et al., 2023). However, no RSV vaccine is available yet for infants and young children, for whom the only useable prophylaxis is still based on neutralizing mAbs directed against the F glycoprotein, such as Palivizumab (Garegnani et al., 2021), and the recently approved Nirsevimab (Hammitt et al., 2022; Simões et al., 2023). In contrast, options for treatment of RSV infections are limited to supportive care with bronchodilators and supplemental oxygen (Broadbent et al., 2015), since the only approved antiviral drug against RSV, ribavirin (RBV), is exclusively restricted to hospitalized infants and young children with severe LRTIs (Jain et al., 2022; Tejada et al., 2022). However, concerns about RBV safety and

---

* Corresponding author. Department of Life Sciences and Systems Biology, University of Torino, Via Accademia Albertina 13, 10123, Torino, Italy.
E-mail address: giorgio.gribaudo@unito.it (G. Gribaudo).
[1] Co-first author: A.L. and G.S. contributed equally to this work.

Abbreviations	
HTA	Host-targeting antivirals
DHODH	Dihydroorotate dehydrogenase
ISGs	Interferon Stimulated Genes
RBV	Ribavirin
BSA	Broad-spectrum antivirals
VRA	Virus yield reduction assay
TOA	Time-of-addition
Fa	Fractional effect analysis

efficacy, discourage its clinical use (Beaird et al., 2016). Therefore, given the public health impact of RSV infections on a global scale, as well as the paucity of the current anti-RSV intervention arsenal, the development of new effective antiviral agents to mitigate or reduce the disease burden is an urgent priority.

To meet this need, host-targeting antiviral (HTAs) interfering with cellular biochemical pathways essential for RSV replication may be taken into consideration, as believable alternatives to the *de novo* development of direct-acting antivirals (DAA) targeting specific RSV proteins. In fact, HTAs prevent viral drug resistance and are amenable to be developed as broad-spectrum antivirals (BSA) effective against different viruses (Heylen et al., 2017; Amarelle and Lecuona, 2018).

Considering that the availability of appropriate pyrimidine pools in infected cells is mandatory for efficient viral replication, pharmacological targeting of the pyrimidine biosynthesis pathway is thus a plausible strategy to develop effective HTAs (Okesli et al., 2017; Löffler et al., 2020). Especially, in virus-infected cells, such as those infected with RSV, in which the *de novo* pyrimidine biosynthesis pathway is activated during viral infection to meet the high pyrimidine demand tied to viral gene expression and replication (Gribaudo et al., 2002, 2003; Munger et al., 2008; Martín-Vicente et al., 2020; Karimi et al., 2022). In this regard, the activity of the human dihydroorotate dehydrogenase (*h*DHODH), a mitochondrial enzyme that catalyzes the oxidation of dihydroorotic acid (DHO) to orotic acid (ORO), as a critical step in the biosynthesis of uridine and cytidine (Reis et al., 2017; Löffler et al., 2020), may represent a druggable target of choice to interfere with the replication of RNA viruses (Okesli et al., 2017; Boschi et al., 2019; Coelho and Oliveira, 2020).

To contribute to this intervention avenue, we designed and characterized a small molecule *h*DHODH inhibitor, MEDS433, that is being developed in the perspective of a new HTA. MEDS433 is in fact a potent inhibitor of *h*DHODH (IC$_{50}$ 1.2 nM) that interacts with the enzyme's ubiquinone binding site (Sainas et al., 2018, 2021, 2022). Recently, we have observed that MEDS433 inhibits the *in vitro* replication of herpes simplex virus type 1 (HSV-1) and type 2 (HSV-2) (Luganini et al., 2021), influenza A and B viruses (Sibille et al., 2022), as well as of different human coronaviruses (CoVs), such as the α-hCoV-229E and the β-CoVs hCoV-OC43 and SARS-CoV-2 (Calistri et al., 2021), in the nanomolar range.

Based on these facts, this study intended to expand the potential of MEDS433 as a BSA against respiratory viruses by investigating its activity against RSV. Here, we report on the characterization of the mechanisms by which MEDS433 impairs RSV replication. Especially, MEDS433 was observed to bring about both a direct inhibition of viral RNA genome synthesis, and the induction of antiviral proteins encoded by interferon-stimulated genes (ISG) able to hamper RSV replication. These results confirm once more MEDS433 as a promising HTA and suggest its suitability to design new intervention strategies for RSV infections.

2. Materials and methods

2.1. Compounds

MEDS433 and brequinar were synthesized as previously described (Madak et al., 2017; Sainas et al., 2018). Ribavirin (RBV), uridine (UR), cytidine (CT), orotic acid (OA), dihydroorotic acid (DHO), dipyridamole (DPY), teriflunomide, and human recombinant interferon-alpha-1 (IFN-α) were purchased from Merck. ASLAN003 was obtained from MedChem Express. All compounds were resuspended in 100% DMSO, except IFN-α, which was resuspended in sterile water.

2.2. Cells and viruses

The human adenocarcinoma alveolar basal epithelial A549 (ATCC CCL-185) and the human laryngeal squamous carcinoma HEp-2 (ATCC CCL-23) cell lines were purchased from the American Type Culture Collection (ATCC), the Lenti-X 293T cell line was obtained from Takara. Cells were cultured in Dulbecco's Modified Eagle Medium (DMEM; Euroclone) supplemented with 10% fetal bovine serum (FBS, Euroclone), 2 mM glutamine, 1 mM sodium pyruvate, 100 U/ml penicillin, and 100 μg/ml streptomycin sulfate (Euroclone).

Primary 3D human small airway epithelial tissues (SmallAir™) were obtained from Epithelix, (EP21) and were isolated from the bronchiolar region of healthy donors and cultured on transwell inserts at air-liquid interface (ALI), as ready-formed pseudostratified epithelial layers. ALI cultures were maintained until use according to the manufacturer's protocol.

RSV strain Long A (ATCC VR-26) and RSV strain B (ATCC VR-955) were propagated in HEp-2 cells by infecting 90% confluent monolayers at a virus-to-cell ratio (MOI) of 0.01 and cultured in DMEM supplemented with 2% FBS. Viral stocks were prepared after three rounds of cell freezing and thawing, and centrifugal clarification. Supernatants were then added to equal volumes of 50% sucrose for stabilization. Virus titers were measured by standard plaque assays on HEp-2 cells.

2.3. Antiviral assays

The anti-RSV activity of MEDS433, brequinar, or RBV was measured by the plaque reduction assay (PRA) in HEp-2 cells or by the virus yield reduction assay (VRA) in A549 cells. For PRA, HEp-2 cells (120,000 cells/well) were seeded in 48-well plates, and after 24 h, treated 1 h prior to infection with different compounds concentrations, and then infected with RSV-A or RSV-B (30 PFU/well) in the presence of compounds. After virus adsorption (2 h at 37 °C), viral inocula were removed, and cells incubated in medium containing the corresponding compounds, 0.3% methylcellulose (Sigma-Aldrich) and 2% FBS. At 72 h post-infection (p.i.), cell monolayers were fixed, and stained with crystal violet. Viral plaques were then microscopically counted, and the mean plaque counts for each drug concentration was converted in viral titer (PFU/ml). The GraphPad Prism software version 8.0 was used to determine the concentration of compounds that produced 50 and 90% reductions in plaque formation (EC$_{50}$ and EC$_{90}$).

For the VRA, A549 cells (120,000 cells/well) seeded in 48-well plates were treated with increasing concentrations of compounds, and then infected with RSV-A or RSV-B at an MOI of 0.01 PFU/cell. After virus adsorption, cells were incubated in medium containing the corresponding compounds. At 72 h p.i., the cell supernatants were harvested, and the RSV yield titrated by plaque assay on HEp-2 cells.

To evaluate the effect of UR, CT, ORO, or DHO addition, PRAs were performed with HEp-2 cells infected with RSV-A, and treated with increasing concentrations of UR, CT, ORO or DHO in presence of 0.05 μM of MEDS433. Compounds were maintained throughout the assay, and at 72 h p.i., cell monolayers were fixed, stained with crystal violet, and viral plaques microscopically counted.

To investigate the effect of blocking both the *de novo* biosynthesis and the salvage pathway of pyrimidines, in the absence or presence of UR, PRAs were performed in HEp-2 cells infected with RSV-A, and exposed throughout the assay to different concentration of MEDS433 in combination with increasing concentrations of DPY (1, 3, 5 μM) in medium supplemented with a hyper-physiological concentration of uridine (20 μM). At 72 h p.i., cell monolayers were fixed, stained and viral plaques microscopically counted.

For time-of-addition (TOA) studies, HEp-2 cells were seeded at a density of 240,000 cells/well in 24-well plates. The following day, cells monolayers were treated with 0.05 μM MEDS433 from −3 to −2 h prior to infection before infection with RSV-A (MOI of 0.1 PFU/cell) (pre-treatment, PRE-T); or during infection (adsorption stage, from −2 to 0 h, co-treatment, CO-T); or after virus adsorption (from 0 to 48 h p.i., post-treatment, POST-T); or throughout the experiment (full treatment, Full-T). At 48 h p.i., cell supernatants were harvested, and titrated for RSV-A infectivity on HEp-2 cells as described above.

The effects of two- (MEDS433 and RBV), or three-drug combination (MEDS433, RBV, and DPY) were assessed by PRAs as described above. MEDS433 and RBV, alone or in combination, were added on HEp-2 cell monolayers at equipotent ratio of at $0.25 \times$, $0.5 \times$, $1 \times$, $2 \times$, and $4 \times$ EC_{50} of each drug. For the three-drug combination, DPY (3 μM) was added to the MEDS433 and RBV concentrations used in the two-drug combination. The effect of the two- or three-drug combination was then assessed by the Chou-Talalay method (Chou, 2006), based on the median-effect principle of the mass-action law computed in the CompuSyn software (Chou and Martin, 2005) (http://www.combosyn.com). With the Chou-Talalay method, a Combination Index (CI) = 1 represents an additive effect, a CI value > 1 means antagonism, and a CI value < 1 indicates synergism.

Primary small air epithelial cultures were treated basally 1 h before infection with 1, 5, or 10 μM MEDS433. Afterwards, epithelia cultures were infected apically with RSV-A at an MOI of 0.02 PFU/cell (input, time = 0 h), and incubated at 37 °C for 3 h in presence of compound. Viral inocula were then removed, and epithelia cultures washed twice with culture medium, then 200 μl of medium was added apically for 20 min to collect any residual viral particle (time = 3 h). Basal medium containing MEDS433 was changed daily, and apical washes were performed as above to harvest RSV virus particles release at 24, 48, 72, and 96 h p.i. time-points. Supernatants were then titrated for RSV infectivity on HEp-2 cell monolayers as described above, while epithelium cultures were formalin-fixed at 96 h p.i., paraffin-embedded, sectioned at a thickness of 4 μm, and stained with hematoxylin-eosin for microscopic analysis.

2.4. Cytotoxicity assay

Cytotoxicity was evaluated at 72 h post-treatment on A549 or HEp-2 cells using the CellTiter-Glo assay (Promega). To determine the cytotoxic effect of MEDS433 on primary small air epithelial cells, at each time-point the basal medium was harvested, and the LDH-Glo Cytotoxicity Assay (Promega) was performed following the manufacturer's instructions.

2.5. Quantitative real time PCR

HEp-2 cells were seeded in a 6-well plate (600,000 cells/well) and, after 24 h, treated with 0.05 μM MEDS433 1h prior to and during infection with RSV-A at an MOI of 0.1 PFU/cell. At different times p.i., cells were harvested, and RNA was extracted and purified by using an RNA purification kit (Macherey-Nagel). The levels of RSV-A RNA were then assessed by quantitative real time PCR using a GENESIG standard kit (Primerdesign). RSV genomic copy numbers were expressed as the normalized RNA copy number per nanogram of total RNA.

2.6. Gene expression profiling

Cultures of HEp-2 cells seeded in 6-well plates (1,000,000 cells/well) were left untreated or exposed to 1 μM of MEDS433 for 16 h. Thereafter, a culture of both untreated or MEDS433-treated cell monolayers was infected with RSV-A at an MOI of 1 PFU/cell. For the MEDS433-treated and RSV-infected cells, the compound was maintained during viral infection. At 24 h p.i., all cell samples were harvested, and total RNA was isolated by means of miRNeasy Mini kit (Qiagen). TURBO DNA Free kit (Thermo Fisher Scientific) was used to remove contaminating DNA. RNA quality and quantity were assessed using Agilent 2100 bioanalyzer (Agilent Technologies) and NanoDrop ND-1000 Spectro-photometer (Thermo Fisher Scientific), respectively. Gene expression profiling was carried out using the Agilent one-color labelling method. Labeling, hybridization, washing, and slide scanning were performed following the manufacturer's protocols. Briefly, mRNA from 100 ng of tot RNA was amplified, labeled with Cy3 and purified. Six-hundred ng of labeled specimens were then hybridized on Agilent Human Gene Expression v3 $8 \times 60K$ microarrays. After 17 h of hybridization, slides were washed and scanned using the Agilent Scanner (G2505C, Agilent Technologies).

Images were analyzed using the Feature Extraction software version 10.7.3.1 (Agilent Technologies). Raw data elaboration was carried out with Bioconductor (www.bioconductor.org), using LIMMA (LInear Models for Microarray Analysis) R package. Background correction was performed with the *normexp* method with an offset of 50, and *quantile* was used for the between-array normalization. The empirical Bayes method was used to compute a moderated t-statistics for two-class comparisons. MeV version 4.9.0 was used for unsupervised hierarchical clustering, and heatmap generation was performed on selected groups of genes and experimental conditions.

2.7. hDHODH gene knockdown

For RNA interference, A549 cells were transfected with a universal scrambled negative control siRNA (SR30004, Origene), or a *h*DHODH-targeting small interfering RNA (siRNA) (SR319917C, Origene) using the siTran 2.0 siRNA Transfection Reagent (TT320002, Origene). The content of the *h*DHODH protein was then measured at 72 h post-transfection by immunoblotting with a mouse anti-*h*DHODH mAb (SC-166348, Santa Cruz Biotechnology). To assess the effect of the *h*DHODH knockdown on RSV-A replication, at 24 h post-transfection, A549 cells were infected with RSV-A at an MOI of 0.01 PFU/cell, and after 72 h p.i., cell supernatants were harvested, and titrated on HEp-2 cells.

2.8. Analysis of proteins

For immunoblotting, HEp-2 cell monolayers were left untreated or treated with 1 μM of MEDS433, or with 100 ng/ml of IFNα for 24 or 48 h. Protein extracts were then prepared as previously described (Luganini et al., 2008), and equal amounts were fractionated by 4–15% SDS-PAGE and then transferred to PVDF membranes (BioRad). Filters were blocked for 2 h at 37 °C in EveryBlot Blocking Buffer (BioRad), and immuno-stained with either the mouse anti-*h*DHODH mAb (E−8, Santa Cruz Biotechnology), or the rabbit anti-IFI6 pAb (54355, Cell Signaling Technology, CST), or the rabbit anti-IFITM1 pAb (13126, CST), or the rabbit anti-IRF-7 mAb (D2A1J, CST), or the rabbit anti-IRF-1 mAb (D5E4, CST), or the rabbit anti-OAS2 pAb (54155, CST), or the rabbit anti-IRF3 mAb (D6I4C, CST), or the rabbit anti-phospho IRF3 (Ser 386) (E7J8G, CST). A rabbit anti-vinculin mAb (E1E9V, CST) or a rabbit anti-GAPDH mAb (D16H11, CST) were used as controls for protein loading. Immunocomplexes were then detected with goat anti-mouse Ig Ab or goat anti-rabbit Ig Ab conjugated to horseradish peroxidase (Life Technologies) and visualized by enhanced chemiluminescence (Clarity Western ECL Substrate, BioRad).

IFN-α IFN-β, IFN-λ1, or IFN-λ2 were quantified in cell supernatants using VeriKine-HS Human IFN-α All Subtype and IFN-β TCM ELISA Kits

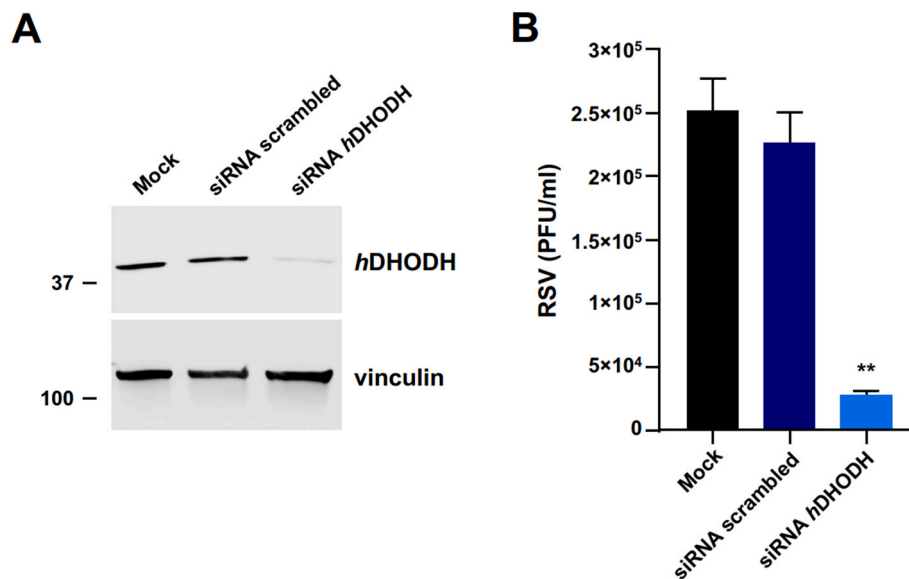**Fig. 1. Knockdown of *h*DHODH affects RSV replication.** (**A**) *h*DHODH protein content in A549 cells mock-transfected or transfected with a scrambled negative control or *h*DHODH siRNAs. At 72 h after transfection, total protein extracts were analyzed by immunoblotting with an anti-*h*DHODH mAb. Immunodetection of vinculin was used as a control for protein loading. Molecular weight markers are indicated at the left side of each panel. (**B**) RSV yield from A549 cells mock-transfected or transfected with scrambled or *h*DHODH siRNAs. At 24 h after transfection, cells were infected with RSV-A at an MOI of 0.01 PFU/cell, and after 72 h p.i., cell supernatants were recovered, and titrated by plaque assay in HEp-2 cells. Data shown are the means ± SD (error bars) of $n = 2$ independent experiments performed in triplicate and analyzed by Kruskal-Wallis Dunn's multiple comparison test compared to the calibrator sample (Mock). **, $p < 0.005$.
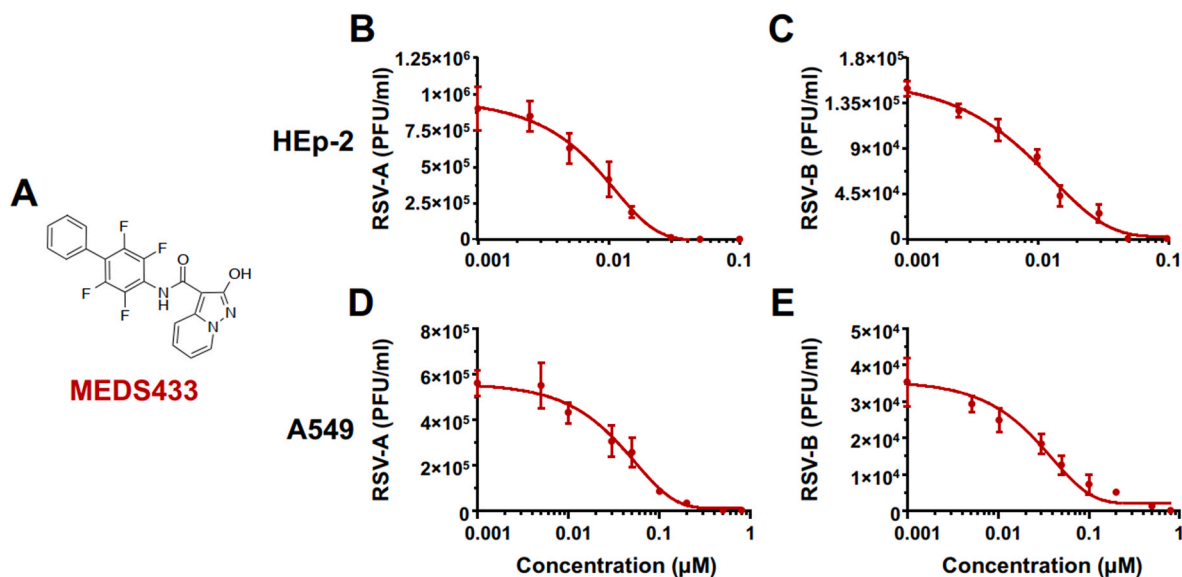

Fig. 2. MEDS433 inhibits the replication of RSV-A and RSV-B. (**A**) Chemical structure of MEDS433. (**B, C**) PRAs were performed in HEp-2 cells infected with RSV-A (**B**) or RSV-B (**C**) and treated with increasing concentrations of MEDS433 1 h before, during, and post-infection. At 72 h p.i., the viral plaques were microscopically counted and converted in viral titer (PFU/ml). (**D, E**) VRAs were performed in A549 cell monolayers infected with RSV-A (**D**) or RSV-B (**E**) and treated with increasing concentrations of MEDS433 throughout the experiment. At 72 h p.i., cell supernatants were harvested, and titrated by the plaque assay in HEp-2 cells. Data shown are the means ± SD of $n = 3$ independent experiments performed in triplicate.

(PBL Assay Science), or Human IFN-λ1 and IFN-λ2 ELISA kits (Innovative Research, Inc.), according to the manufacturers' instructions.

To neutralize IFN-β and IFN-λ1 in cell supernatants, murine neutralizing mAbs against IFN-β and IFN-λ1 (InvivoGen) were added to untreated or MEDS433-treated HEp-2 cell cultures at a concentration of 10 μg/ml.

2.9. Lentiviral vectors

Human IFI6, IFITM1, and IRF7 cDNAs purchased from Origene

(SC112388, SC117830 and SC126916, respectively) were cloned into the pLVX-TetOne vector (Takara). Lentiviral vectors (LV) for doxycycline-inducible expression of IFI6, IFITM1 and IRF-7 proteins were generated in Lenti-X 293T cells by transfection of pLVX-TetOne containing IFI6, IFITM1, or IRF7 cDNAs, and the Lenti-X™ Tet-One™ Inducible Expression System (Takara) according to the manufacturer's instructions. At 48 h after transfection, LV-containing supernatants were collected and titrated using the Lenti-X™ qRT-PCR Titration kit (Takara). LV-transduced HEp-2 cell lines were then generated by infecting HEp-2 cell monolayers with LV-empty, or LV-IFI6, or LV-

Table 1
Antiviral activity of *h*DHODH inhibitors and ribavirin against RSV strains.

Compound	Cell line	RSV	EC$_{50}$ (µM)[a]	EC$_{90}$ (µM)[b]	CC$_{50}$ (µM)[c]	SI[d]
MEDS433	HEp-2	RSV-A	0.0078 ± 0.00006	0.020 ± 0.00009	84.30 ± 0.574	10808
		RSV-B	0.0083 ± 0.00004	0.025 ± 0.00021		10157
	A549	RSV-A	0.0381 ± 0.00022	0.136 ± 0.00089	64.25 ± 3.125	1686
		RSV-B	0.0277 ± 0.00018	0.120 ± 0.00102		2319
Brequinar	HEp-2	RSV-A	0.0113 ± 0.00005	0.0311 ± 0.00016	71.70 ± 0.341	6345
		RSV-B	0.0190 ± 0.00012	0.0322 ± 0.00021		3774
Teriflunomide	HEp-2	RSV-A	8.58 ± 0.309	21.91 ± 0.187	109.22 ± 0.742	13
		RSV-B	6.54 ± 0.278	18.94 ± 0.611		17
ASLAN003	HEp-2	RSV-A	0.59 ± 0.088	2.41 ± 0.204	>400	>678
		RSV-B	0.64 ± 0.029	2.47 ± 0.125		>625
Ribavirin	HEp-2	RSV-A	2.3760 ± 0.0117	>10	240.46 ± 5.691	101
		RSV-B	1.3264 ± 0.0105	6.0315 ± 0.03949		181

[a] EC$_{50}$, compound concentration that inhibits 50% of virus replication, as determined against RSV-A and RSV-B by PRAs in HEp-2 cells, and by VRAs in A549 cells.

[b] EC$_{90}$, compound concentration that inhibits 90% of RSV-A or RSV-B replication, as determined by PRAs in HEp-2 cells, and by VRAs in A549 cells.

[c] CC$_{50}$, compound concentration that produces 50% of cytotoxicity, as determined by cell viability assays in HEp-2 and A549 cells. Reported values represent the means ± SD of data derived from three experiments in triplicate.

[d] SI, selectivity index determined as the ratio between CC$_{50}$ and EC$_{50}$.

IFITM1, or LV-IRF7, at an MOI of 1, in the presence of 4 µg/ml of polybrene. Stable LV-transduced HEp-2-derived cell lines were obtained by selection in medium containing 2.5 µg/ml puromycin. The inducible expression of IFI6, IFITM1, or IRF7 proteins was achieved by stimulating the corresponding LV-derived cell line with doxycycline (100 ng/ml).

2.10. Statistical analysis

All statistical tests were performed using GraphPad Prism version 8.0 (GraphPad Software). Antiviral assays data are presented as the means ± SD of at least three experiments performed in triplicate. P values ≤ 0.05 were considered significant.

3. Results

3.1. Efficient RSV replication needs hDHODH expression

To appreciate the relevance of *h*DHODH for the completion of RSV productive replication, its expression was knocked down by means of siRNAs in the relevant cell model of human alveolar basal epithelial cells A549 (Fig. 1A). In comparison with mock-transfected A549 cells or cells transfected with a scrambled negative siRNA, the reduced level of *h*DHODH protein content significantly affected RSV-A replication with about 10-fold reduction of released infectious virus at 72 h post infection (h p.i.) (Fig. 1B). This observation thus indicated that optimal RSV replication necessitates *h*DHODH expression.
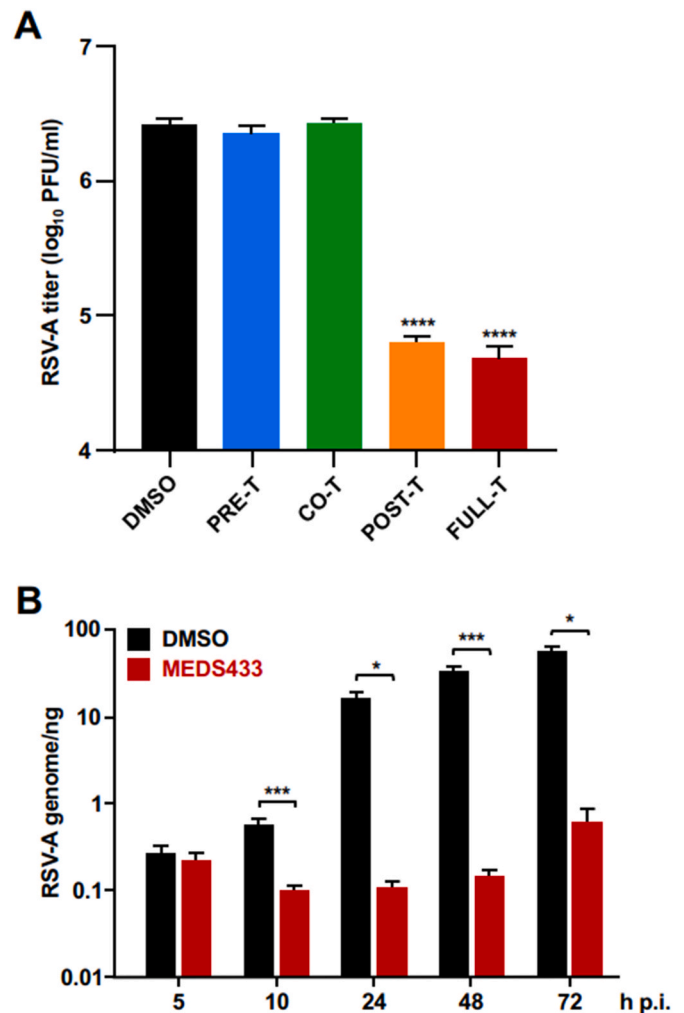

Fig. 3. MEDS433 abolishes RSV genome synthesis. (**A**) MEDS433 acts a post-entry stage of the RSV replication cycle. HEp-2 cells monolayers were infected with RSV-A at an MOI of 0.1 and where indicated, treated with 0.05 µM MEDS433 prior to infection (from −3 to −2 h prior, PRE-T), or during the infection (from −2 to 0 h p.i., CO-T); or after virus infection (from 0 to 48 h p.i., POST-T); or from −3 to 48 h p.i. (FULL-T). Control RSV-A-infected cells were exposed to vehicle DMSO only. At 48 h p.i., infectious RSV particles released in cell supernatants were titrated by plaque assay in HEp-2 cells. The data shown are the mean ± SD of *n* = 2 independent experiments performed in triplicate and analyzed by a one-way ANOVA followed by Dunnett's multiple comparison test. ****, p < 0.0001 compared to the calibrator sample (DMSO). (**B**) MEDS433 inhibits RSV RNA replication. HEp-2 cell monolayers were infected with RSV-A at an MOI of 0.1, and, where indicated, the infected cells were exposed to 0.05 µM MEDS433 or 0.02% DMSO. At 5, 10, 24, 48, and 72 h p.i., total RNA was isolated, and qPCR performed with appropriate RSV-A primers and probe. RSV-A RNA genomic copies were normalized per nanogram of RNA. The data shown are the means ± SD of *n* = 2 independent experiments performed in triplicate and analyzed by unpaired *t*-test compared to the calibrator sample (DMSO). *, p < 0.05; ***, p < 0.001.

3.2. The hDHODH inhibitor MEDS433 restricts RSV replication

Seeing that *h*DHODH expression is required for RSV replication, the pharmacological targeting of its enzymatic activity may represent a strategy to develop new anti-RSV agents. To this end, the anti-RSV activity of the new *h*DHODH inhibitor MEDS433 (Fig. 2A) was investigated by plaque reduction assay (PRA) in HEp-2 cells infected with RSV-A or RSV-B. Fig. 2 (panels B and C) shows that MEDS433 inhibited RSV-A and RSV-B plaque formation in a dose-dependent manner. The EC$_{50}$ and EC$_{90}$ were 0.0078 ± 0.00006 µM and 0.020 ± 0.00009 µM for RSV-
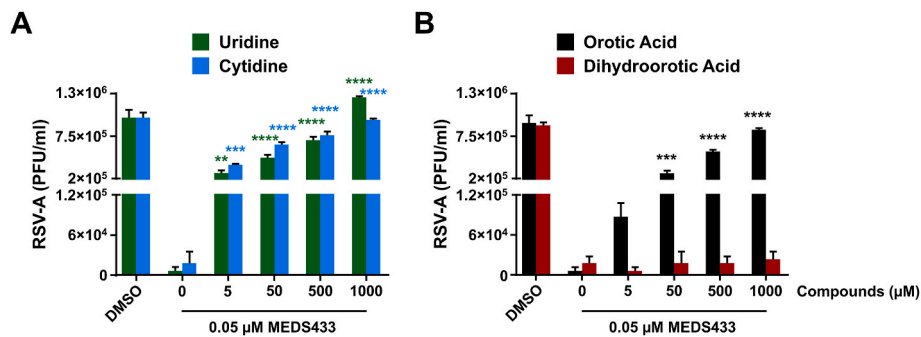
A

B

Fig. 4. The anti-RSV activity of MEDS433 is reversed by uridine, cytidine and orotic acid. HEp-2 cell monolayers were exposed to 0.05 μM of MEDS433 in the presence or absence of increasing concentrations of uridine and cytidine (**A**), dihydroorotic acid and orotic acid (**B**) before and during infection with RSV-A (30 PFU/well). Following virus adsorption, cells were incubated in the presence of compounds and, at 72 h.p.i., viral plaques were stained, microscopically counted, and plotted as PFU/ml. Control RSV-A-infected cells were exposed to vehicle DMSO only (DMSO). The data shown represent means ± SDs of $n = 3$ independent experiments performed in triplicate and analyzed by a two-way ANOVA, followed by Dunnett's multiple comparison test, versus to the calibrator sample (MEDS433 alone). **, $p < 0.005$; ***, $p < 0.001$; ****, $p < 0.0001$.

A

B
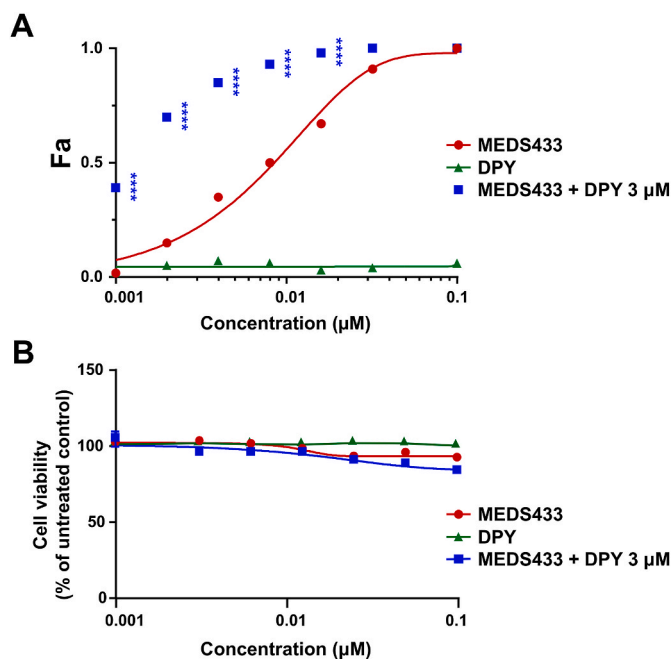
Fig. 5. The combination of MEDS433 and DPY is synergistic against RSV replication. (**A**) PRAs were performed in HEp-2 cells exposed to different concentrations of MEDS433 alone, or in combination with different amounts of DPY. At 72 h after RSV-A infection (30 PFU/well), viral plaques were stained, and microscopically counted. The effect of the combination was then analyzed by the CompuSyn software and displayed as a fractional effect analysis (Fa) plot in relation to the compound concentrations. The antiviral activity of MEDS433 and DPY, when used as single agents is depicted by red and green Fa curves, respectively. The effect of the MEDS433-DPY combination is shown with blue squares. Results are representative of $n = 3$ independent experiments performed in triplicate and analyzed by a two-way ANOVA, followed by Sidak's multiple comparison test. Statistical analysis was performed by comparing MEDS433-treated samples with the MEDS433 + DPY-treated samples for each condition. **** ($p < 0.0001$). (**B**) To determine cell viability, HEp-2 cell monolayers were exposed to different concentrations of MEDS433 alone or in combination with different amounts of DPY, or vehicle (DMSO) as control. After 72 h of incubation, the number of viable cells was determined by the CellTiter-Glo Luminescent assay. Results are shown as means ± SD (error bars) of three independent experiments performed in triplicate.

A, and 0.0083 ± 0.00004 μM and 0.025 ± 0.00021 μM for RSV-B, respectively (Table 1). This potent anti-RSV activity was not due to non-specific MEDS433 cytotoxicity since its cytotoxic concentration 50

Table 2
Analysis of the combination of MEDS433 and DPY against RSV-A replication.

MEDS433 concentration (fold of EC_{50}[a]) + 3 μM DPY	MEDS433 + DPY CI[b]	Drug combination effect of MEDS433 + DPY[c]
4x	0.192 ± 0.026	**Strong synergism**
2x	0.698 ± 0.034	**Synergism**
1x	0.657 ± 0.075	**Synergism**
0.5x	0.551 ± 0.042	**Synergism**
0.25x	0.493 ± 0.055	**Synergism**

[a] The EC_{50} values of MEDS433 were determined by PRAs in RSV-A-infected HEp-2 cells.

[b] Combination Index (CI), obtained by computational analysis with the CompuSyn software 1.0. Reported values represent means ± SD of data derived from $n = 3$ independent experiments in triplicate.

[c] Following the method of Chou (2006), drug combination effects are defined as: strong synergism for $0.1 < CI < 0.3$; synergism for $0.3 < CI < 0.7$.
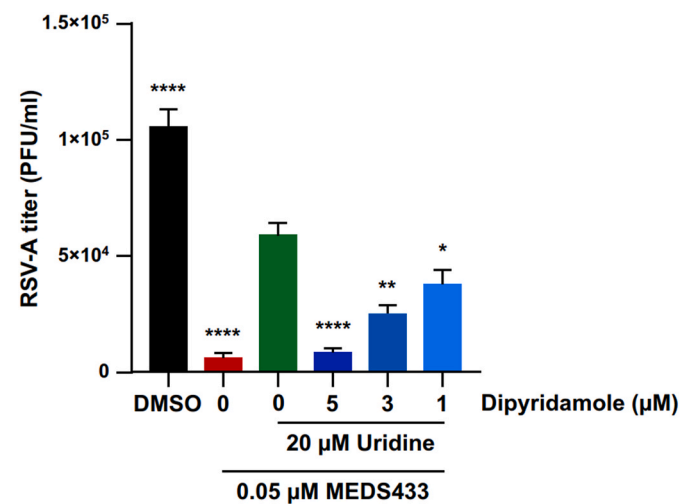

Fig. 6. A combination of modulators of pyrimidine metabolism inhibits RSV replication in the presence of exogenous uridine. PRAs were performed in HEp-2 cells treated with 0.05 μM MEDS433 alone, or in combination with different concentrations of DPY and 20 μM uridine prior to and during RSV-A infection (30 PFU/well). After virus adsorption, cells were incubated in the presence of compounds and at 72 h p.i., viral plaques were stained, and microscopically counted. Data shown are the means ± SD of $n = 3$ independent experiments performed in triplicate. Samples were analyzed by one-way ANOVA Dunnett's multiple comparison test. *, $p < 0.05$; **, $p < 0.005$; ****, $p < 0.0001$ compared to the calibrator sample (MEDS433 + 20 μM uridine, green column).
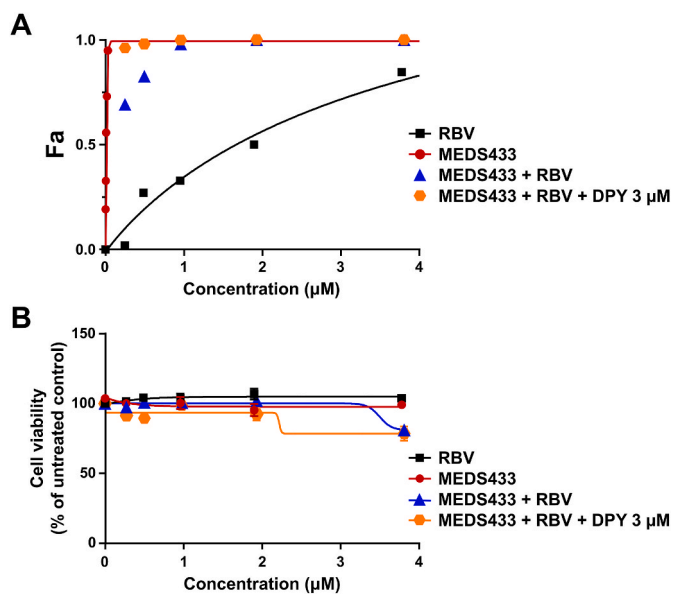
6

Fig. 7. Effects of the combination of MEDS433, RBV and DPY on RSV replication. (**A**) PRAs were performed in HEp-2 cell monolayers treated with different concentrations of MEDS433 and RBV as single agents, or in combination each other. Then, cells treated with MEDS433-RBV combination were also exposed to 3 μM of DPY prior to and during RSV-A infection (30 PFU/well). After virus adsorption, cells were incubated in the presence of compounds and, at 72 h p.i., viral plaques were stained and counted. Plaque numbers were analyzed by the CompuSyn software. The effects on RSV-A replication of MEDS433 or RBV used as single agents are depicted by red and black Fa curve, respectively. The effect of MEDS433-RBV or MEDS433-RBV-DPY combinations are indicated by blue triangles and orange hexagons, respectively. The results are representative of $n = 3$ independent experiments performed in triplicate. (**B**) To determine the cytotoxic effect of combinations, HEp-2 cells were treated with vehicle (DMSO), or with different concentrations of MEDS433 alone or in combination with different concentrations of RBV, and in the absence or presence of 3 μM of DPY. At 72 h, HEp-2 cell viability was assessed by the CellTiter-Glo Luminescent assay. Results are shown as means ± SD (error bars) of three independent experiments performed in triplicate.

(CC$_{50}$) for HEp-2 cells was of 84.30 ± 0.574 μM that produced positive Selectivity Index (SI) values of 10808 and 10157 for RSV-A and RSV-B, respectively (Table 1). Moreover, when compared with other *h*DHODH inhibitors, MEDS433 was slightly more effective than brequinar, a potent *h*DHODH inhibitor (Peters, 2018) endowed with a BSA activity against several human respiratory viruses (Sepúlveda et al., 2022; Zheng et al., 2022), inasmuch the EC$_{50}$ of brequinar was 0.0113 ± 0.00005 μM and 0.0190 ± 0.00012 μM for RSV-A and RSV-B, respectively (Table 1). MEDS433, however, proved to be superior both to teriflunomide, the active metabolite of the clinically approved *h*DHODH inhibitor

leflunomide endowed with an anti-RSV activity (Dunn et al., 2011), and to ASLAN003, a potent *h*DHODH inhibitor for which an antiviral activity against SARS-CoV-2 has recently been observed (Stegmann et al., 2022). In fact, the measured EC$_{50}$ value of teriflunomide was 8.58 ± 0.309 μM against RSV-A and 6.54 ± 0.278 μM against RSV-B, while that of ASLAN003 was 0.59 ± 0.088 μM and 0.64 ± 0.029 μM for RSV-A and RSV-B, respectively (Table 1). Furthermore, it is noteworthy that MEDS433 was much more effective than RBV, because the measured EC$_{50}$ for RBV was 2.3760 ± 0.0117 μM against RSV-A and 1.3264 ± 0.0105 μM against RSV-B (Table 1).

Then, to confirm the suitability of MEDS433 as an HTA candidate against RSV, the A549 cell line, as a second human airway epithelial cell model, was adopted to verify the anti-RSV activity in a different host cell system. Moreover, to leave aside the possibility that the inhibitory effect of MEDS433 stemmed from the type of antiviral assay, virus yield reduction assays (VRAs) were performed in A459 cells. As shown in Fig. 2 (panels D and E), even in A549 cells, MEDS433 exerted a potent anti-RSV activity with EC$_{50}$ and EC$_{90}$ values of 0.0381 ± 0.00022 μM and 0.136 ± 0.00089 μM for RSV-A, and of 0.0277 ± 0.00018 μM and 0.120 ± 0.00102 μM for RSV-B. Again, SI values were positive since in A549 cells the MEDS433 CC$_{50}$ value was of 64.25 ± 3.125 μM, thus resulting in a SI of 1686 and 2319 for RSV-A and RSV-B, respectively (Table 1).

Overall, the results of these antiviral assays suggest a potent anti-RSV activity of MEDS433 in the low nanomolar range that was independent of the RSV strain used, the cell line, or the assay used.

3.3. MEDS433 acts at a post-entry stage of RSV replicative cycle through the inhibition of viral RNA genome synthesis

To identify the phase of the RSV replicative cycle targeted by MEDS433, time-of-addition (TOA) experiments were carried out by treating HEp-2 cells with MEDS433 (0.05 μM, 2 x EC$_{90}$) from −3 to −2 h prior to RSV-A infection (pretreatment, PRE-T); or during the infection (from −2 to 0 h p.i.; cotreatment, CO-T); or after virus adsorption (from 0 to 48 h p.i.; post-treatment, POST-T); or from −3 to 48 h p.i. (full-treatment, FULL-T). At 48 h p.i., infectious RSV-A particles released in cell supernatants were titrated by plaque assay. As depicted in Fig. 3A, MEDS433 did not affect neither the adsorption phase, nor the entry phase of RSV replication cycle. Conversely, it reduced significantly the production of infectious RSV particles of about two orders of magnitude, when added at a post-entry stage (POST-T) or left on cells from - 3 to 48 h p.i. (FULL-T). These results therefore indicated that the antiviral activity of MEDS433 derived from an interference with a synthetic stage of the RSV replication cycle that occurs after virus entry.

Thereafter, to further investigate the ability of MEDS433 to interfere with RSV replication, the effect of the *h*DHODH inhibitor on the synthesis of RSV genome was investigated at various times p.i. by qRT-PCR. Fig. 3B shows that in comparison to DMSO-treated cells, the addition of

Table 3
Analysis of the effects of the combination of MEDS433, RBV and DPY against RSV-A replication.

MEDS433+RBV combination at equipotent ratio (fold of EC$_{50}$[a])	MEDS433+RBV CI[b]	Drug combination effect of MEDS433+RBV[c]	MEDS433+RBV + 3 μM DPY CI[d]	Drug combination effect of MEDS433+RBV+3 μM DPY[c]
4x	0.435 ± 0.053	**Synergism**	0.425 ± 0.072	**Synergism**
2x	0.214 ± 0.027	**Strong synergism**	0.213 ± 0.036	**Strong synergism**
1x	0.573 ± 0.042	**Synergism**	0.106 ± 0.018	**Strong synergism**
0.5x	0.646 ± 0.118	**Synergism**	0.287 ± 0.373	**Strong synergism**
0.25x	0.424 ± 0.045	**Synergism**	0.182 ± 0.032	**Strong synergism**

[a] Fold of EC$_{50}$ MEDS433/EC$_{50}$ RBV yielding an equipotent concentration ratio (approximately 1:0.008) between the two combined drugs. The EC$_{50}$ values was determined by PRAs against RSV-A in HEp-2 cells.

[b] Combination Index (CI), extrapolated by computational analysis with the CompuSyn software. Reported values represent means ± SD of data derived from $n = 3$ independent experiments in triplicate using MEDS433+RBV concentration ratio as showed in[a].

[c] Drug combination effect defined as: strong synergism for 0.1 < CI < 0.3; synergism for 0.3 < CI < 0.7, according to the method of Chou (2006).

[d] Combination Index (CI), extrapolated by computational analysis with the CompuSyn software. Reported values represent means ± SD of data derived from $n = 3$ independent experiments in triplicate using MEDS433+RBV concentration ratio showed in[a] and added with 3 μM of DPY for each combination.
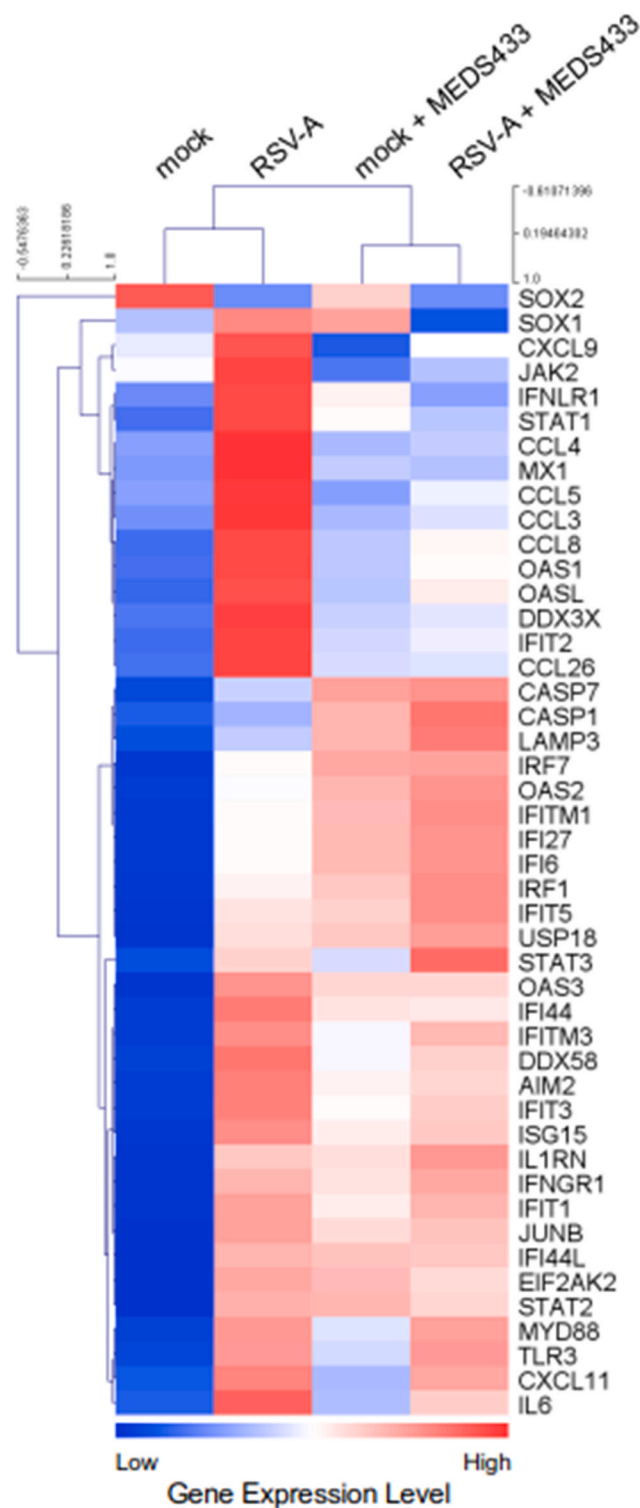
Fig. 8. MEDS433 and RSV infection upregulate the expression of Interferon-Stimulated Genes (ISGs). HEp-2 cell monolayers were treated with 1 μM MEDS433 or DMSO for 16 h, and then, where indicated, cells were infected with RSV-A at an MOI of 1 in presence of the compound for 24 h. Thereafter, mRNA was purified, labeled and hybridized to human gene expression microarrays. After hybridization, slide scanning, and image analysis, expression values, reported as log2 intensities, were normalized and replicated measurements averaged. Unsupervised hierarchical clustering, with Pearson's correlation as distance metrics, was applied to the expression profiles of ISGs and innate immune genes in the 4 experimental conditions, using standardized log2 intensities.

MEDS433 (0.05 μM) almost suppressed completely the accumulation of RSV genomes throughout the entire timeframe of RSV replication that was evaluated, thus suggesting that indeed it hindered the synthesis of new viral RNA genomes. Similar results were obtained in HEp-2 cells infected with RSV-B (data not shown).

These results thus identify inhibition of viral RNA replication as a mechanism of antiviral activity of MEDS433 against RSV, and allow to hypothesize that it may stem from depletion or imbalance of pyrimidine pools caused by the inhibition of *h*DHODH activity.

3.4. The anti-RSV activity of MEDS433 derives from specific inhibition of the novo pyrimidine biosynthesis

To verify the above hypothesis, we investigated whether the antiviral activity of MEDS433 against RSV could be affected by the addition of increasing concentrations of exogenous uridine or cytidine, as final products of the *de novo* pyrimidine pathway. As shown in Fig. 4A, RSV-A replication in HEp-2 cells was gradually rescued by the addition of increasing amounts of both uridine and cytidine, thus indicating that the *de novo* pyrimidine biosynthesis pathway was inhibited by MEDS433 in RSV-infected cells.

To further confirm that MEDS433 antiviral activity derived from its ability to block *h*DHODH enzymatic function, RSV-A-infected HEp-2 cells were exposed to MEDS433 in the presence of increasing concentrations of orotic acid (ORO) or dihydroorotic acid (DHO), as the specific *h*DHODH product or substrate, respectively. As depicted in Fig. 4B, only the addition of ORO reversed the antiviral activity of MEDS433, while that of DHO, even at 20,000-fold excess the MEDS433 concentration used (0.05 μM), did not affect the inhibitory effect of MEDS433.

Taken together, these results clearly indicated that the MEDS433-mediated suppression of RSV genome replication (Fig. 3B), derived from a specific inhibition of the *h*DHODH enzymatic activity in RSV-infected cells that prevents the oxidation of DHO to ORO in the *de novo* biosynthesis of pyrimidines.

3.5. The combination of MEDS433 with an inhibitor of the pyrimidine salvage pathway is effective against RSV even in the presence of uridine

Since we observed that addition of exogenous uridine reversed the anti-RSV activity of MEDS433, it could be possible that its physiological plasma concentration in the host reduces the antiviral activity of MEDS433 through the salvage pathway. To consider this problem, we investigated the effect of the combination of MEDS433 with dipyridamole (DPY), an inhibitor of the nucleoside transporters hENT1 and 2 implicated in the pyrimidine salvage pathway (Fitzgerald, 1987; Ward et al., 2000; Schaper, 2005). For this purpose, PRAs were performed in RSV-A-infected HEp-2 cells to assess the effect of the combination of a 0.25-, 0.5-, 1-, 2-, or 4-fold of MEDS433 EC_{50} to 3 μM DPY. Fig. 5A shows the consequence of MEDS433-DPY combination as a fractional effect analysis (Fa) plot relative to the compound concentrations, where Fa values closer to 1 indicate greater antiviral activity. It's to be noted that DPY did not exert any inhibitory activity on RSV-A replication when used as a single agent, even tested up to 12 μM (Fig. 5 and data not shown). Nevertheless, when 3 μM DPY was used in combination with different concentrations of MEDS433, it increased the anti-RSV activity of the *h*DHODH inhibitor (Fig. 5A, blue squares); in fact, the EC_{50} of MEDS433 (0.0085 ± 0.00003 μM) was reduced to 0.0013 ± 0.000004 μM by the combination with DPY. As reported in Table 2, values of the computed combination index (CI) (Chou and Martin, 2005; Chou, 2006) confirmed that the combination of MEDS433 with DPY resulted in a synergistic antiviral activity at any of the MEDS433 concentrations tested, since all the CIs were <0.7. Moreover, the DPY-mediated increase of MEDS433 antiviral activity was not due to an aspecific cytotoxic effect, since none of the combinations examined affected HEp-2 cell viability (Fig. 5B).

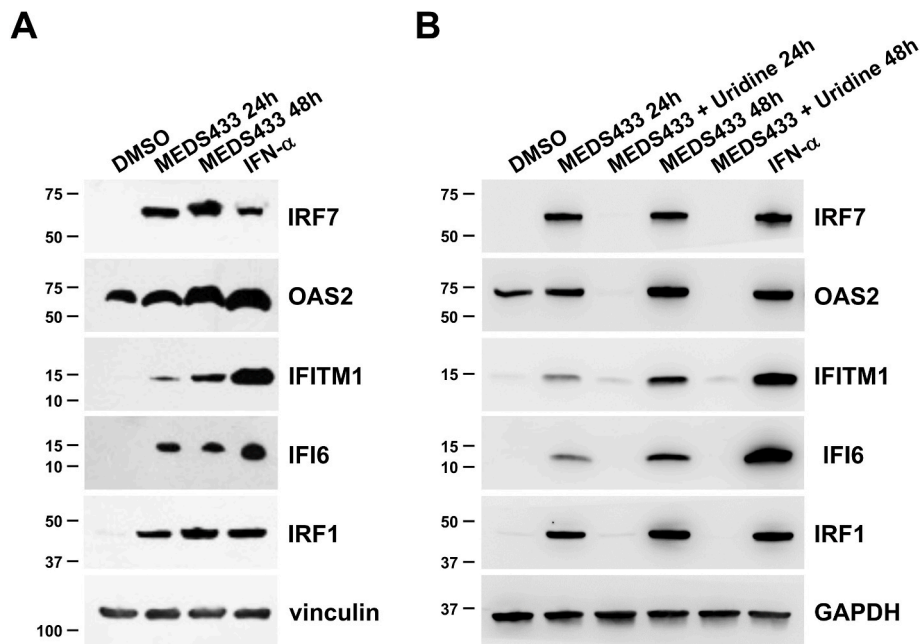Then, we examined whether the MEDS433-DPY synergistic

Fig. 9. MEDS433-induced ISG proteins expression depends on pyrimidine depletion. HEp-2 cells were treated with DMSO or with 1 μM MEDS433 for 24 or 48 h in the absence (**A**) or presence of uridine (1 mM) (**B**). Cells treated with IFN-α (100 ng/ml) for 24 h served as a positive control for ISG proteins expression. Then, total cell protein extracts were prepared, fractionated by 4–15% SDS-PAGE, and analyzed by immunoblotting with anti-IRF7, anti-OAS2, anti-IFITM1, anti-IFI6, or anti-IRF1 Abs. Vinculin or GAPDH immunodetection was used as a control for protein loading. Molecular weight markers are shown at the left side of each panel.

combination could be effective even in the presence of a hyper-physiological concentration of uridine (20 μM), far exceeding the plasma concentrations (Pizzorno et al., 2002). As shown in Fig. 6, the presence of exogenous uridine reversed, as expected, the inhibitory activity of 0.05 μM MEDS433 that suppressed RSV-A replication when tested as a single agent (Fig. 2B). To the contrary, addition of increasing amounts of DPY renovated the inhibitory activity of MEDS433, therefore suggesting the suitability of this combination to inhibit RSV replication, even in the presence of exogenous uridine, as occurring in the host.

3.6. MEDS433 and RBV act synergistically against RSV replication

Next, we investigated whether the anti-RSV activity of MEDS433 and RBV, to date the only drug approved for the treatment of severe RSV infections, could produce additive, synergistic, or antagonistic effect when examined in combination. For this purpose, PRAs were performed with different concentrations of both MEDS433 and RBV corresponding to 0.25-, 0.5-, 1-, 2-, or 4-fold of their EC_{50} values to obtain equipotent ratios (MEDS433 EC_{50}/RBV EC_{50}). Fig. 7A shows that the anti-RSV effectiveness of RBV was clearly increased by the combination with MEDS433 as shown by FA values (blue triangles) closer to 1 than those of RBV when used as a single agent. Accordingly, the EC_{50} of RBV (1.6652 ± 0.0034 μM when used as a single agent) was reduced to < 0.235 μM by the addition of the *h*DHODH inhibitor. The synergism between RBV and MEDS433 was confirmed by the computed CI values < 0.7 at any of the MEDS433 to RBV combination tested (Table 3).

Then, to evaluate the efficacy of the MEDS433-RBV combination in the background of a DPY treatment able to hamper the pyrimidine salvage pathway, the combination of different MEDS433 EC_{50} to RBV EC_{50} was measured in the presence of 3 μM DPY. As reported in Fig. 7A and Table 3, the anti-RSV activity of the MEDS433-RBV combination was further enhanced by the addition of DPY, since the FA values of the triple combination (orange hexagons) were even more close to 1 than those of the MEDS433-RBV combination, and the EC_{50} of RBV further reduced to < 0.235 μM.

Furthermore, excluding concentrations of MEDS433-RBV higher than 2 μM for which weak cytotoxicity was observed, none of the other

MEDS433-RBV-DPY combinations exhibited significant cytotoxic effects against HEp-2 cells (Fig. 7B), thus indicating that their synergistic anti-RSV activity was not the result of an increased cytotoxicity, which would have prevented the virus from replicating, but that it derived from the combined interference of different targets and mechanisms of action.

Together, these results suggest that the combination of MEDS433 with RBV and that of MEDS433, RBV and DPY might be of interest to design a new pharmacological strategy to be considered for the control of RSV infections.

3.7. MEDS433 stimulates the expression of ISG proteins that contribute to the antiviral activity against RSV

Since a link between inhibition of pyrimidine biosynthesis and enhanced expression of Interferon-Stimulated Genes (ISGs) has been observed for some *h*DHODH inhibitors (Lucas-Hourani et al., 2013; Cheung et al., 2017; Zheng et al., 2022), we investigated whether MEDS433 was able to regulate ISGs expression that, in turn, may contribute to the overall anti-RSV activity of the *h*DHODH inhibitor. To this end, gene expression profiling by microarray was performed to detect changes in a set of ISGs and host innate immune genes after RSV-A infection and/or MEDS433 treatment of HEp-2 cells. As shown in Fig. 8, host genes involved in the Interferon (IFN) pathway were clearly upregulated by RSV infection, including STAT1, MX1 and OAS1, as well as some inflammatory chemokines, such as CCL3 (MIP-1α), CCL4 (MIP-1β), and CCL5 (RANTES). Noteworthy, expression of these virus-induced inflammatory chemokines, as well as of IL6, was reduced by MEDS433 treatment of RSV-infected cells. However, the most intriguing finding was the ability of MEDS433 to stimulate the expression of some ISGs that were not upregulated by RSV infection, such as IRF7, OAS2, IFITM1, IFI27, IFI6, and IRF1. Interestingly, the expression of these MEDS433-induced ISG remained elevated even in MEDS433-treated and RSV-infected cells (Fig. 8). This finding was then validated at the protein level (Fig. 9A), thus confirming that MEDS433 induced these antiviral ISG proteins independently of RSV infection. Moreover, supplementation with exogenous uridine reversed extensively the induction of the ISG proteins by MEDS433 (Fig. 9B), hence sustaining a functional
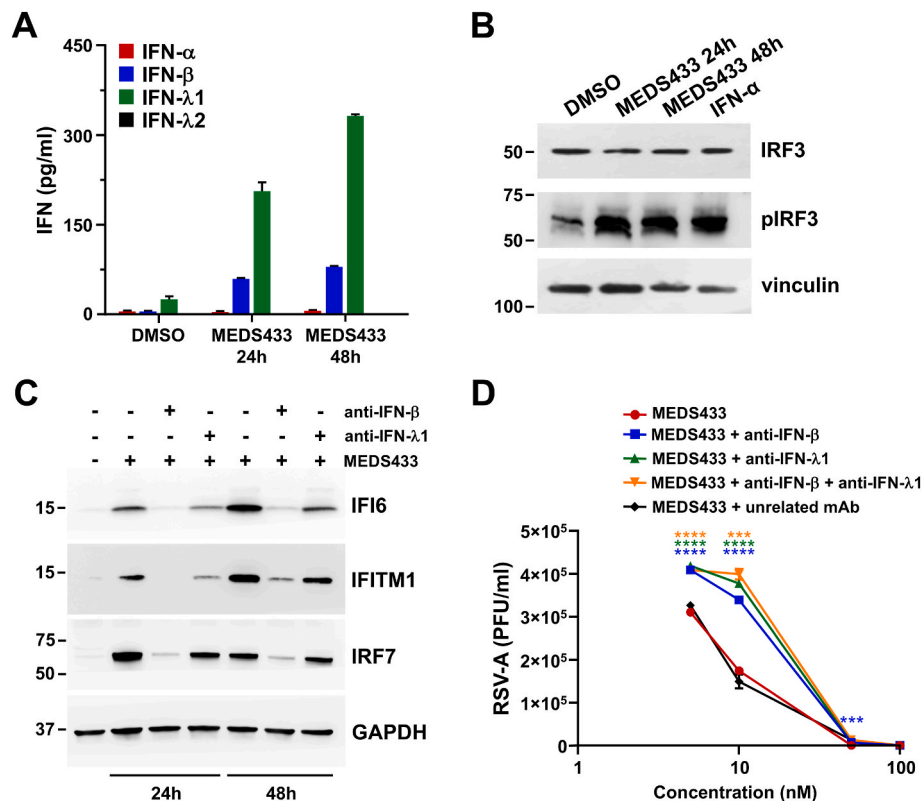
Fig. 10. The MEDS433-induced secretion of IFN-β and IFN-λ1 is required for the stimulation of ISG proteins and the anti-RSV activity. (**A**) MEDS433 treatment induces the production of type-I and type-III IFNs. HEp-2 cells were exposed to DMSO or 1 μM MEDS433 for 24 or 48 h. Cell culture medium was subjected to either IFN-α and IFN-β, IFN-λ1, or IFN-λ2 ELISA to measure IFNs. Data shown are the means ± SD (error bars) of two independent experiments performed in triplicate. (**B**) MEDS433 stimulates the phosphorylation of IRF3. HEp-2 cells were treated with DMSO, or with 1 μM MEDS433 for 24 or 48 h, or with IFN-α (100 ng/ml) for 24 h. Total cell protein extracts were then prepared and analyzed by immunoblotting with anti-IRF3 or anti-phospho-IRF3 mAbs. Vinculin immunodetection was used as a control for protein loading. Molecular weight markers are shown at the left side of each panel. (**C**) Neutralization of IFN-β or IFN-λ1 reduces the accumulation of MEDS433-induced ISG proteins. HEp-2 cells were left untreated or treated with 1 μM MEDS433 for 24 or 48 h in the absence or presence of neutralizing mAbs against IFN-β (10 μg/ml) or IFN-λ1 (10 μg/ml). Then, total cell protein extracts were prepared, and analyzed by immunoblotting with anti-IFI6, IFITM1, or IRF7 Abs. GAPDH immunodetection was used as a control for protein loading. Molecular weight markers are shown at the left side of each panel. (**D**) Neutralization of IFN-β or IFN-λ1 decreases the strength of the antiviral activity of MEDS433 against RSV. VRAs were performed in HEp-2 cell monolayers infected with RSV-A and treated with increasing concentrations of MEDS433 1 h before, during, and post-infection, and in the presence or absence of neutralizing mAbs against IFN-β (10 μg/ml) or IFN-λ1 (10 μg/ml), or an unrelated murine mAb (10 μg/ml). At 72 h p.i., cell supernatants were harvested, and titrated by the plaque assay in HEp-2 cells. Data shown are the means ± SD of $n = 2$ independent experiments performed in triplicate and analyzed by two-way ANOVA Dunnett's multiple comparison test. ***, p < 0.001; ****, p < 0.0001 compared to the calibrator sample (MEDS433 alone).

relationship existing between stimulation of ISGs expression and inhibition of pyrimidine biosynthesis.

To investigate the mechanism by which MEDS433 upregulated the expression of ISG proteins in the absence of an external interferon inducer, such as RSV infection, we examined whether the *h*DHODH inhibitor could directly induce type I and/or type III Interferons (IFNs) production. To this end, ELISA were performed to detect IFNs in the supernatants of HEp-2 cells stimulated with MEDS433. As shown in Fig. 10A, MEDS433 induced the secretion of large amounts of IFN-λ1 and, to a lesser extent, of IFN-β, while neither any of the human IFN-α subtypes, nor IFN-λ2 were detected by ELISA in the supernatants of MEDS433-treated cells. In this regard, transcription of the IFN-β gene requires the activation of the constitutive transcription factor IRF3, while that of IFN-λ1 gene requires activated IRF3-IRF7 heterodimers (Negishi et al., 2018). Since we observed that IRF7 is induced by MEDS433 (Fig. 9), we hypothesized that the *h*DHODH inhibitor could induced the activation of the early regulator IRF3 and thus IFN-β gene transcription; then, secreted IFN-β, in an autocrine manner, could induce IRF7 and, as a consequence, activated the expression of IFN-λ1. Indeed, MEDS433 proved able to stimulate IRF3 phosphorylation (Fig. 10B), thus sustaining its ability to directly induce IFN-β gene transcription.

Then, to evaluate the contribution of secreted IFN-β and IFN-λ1 in the upregulation of ISG proteins expression, the content of IF6, IFITM1 and IRF7 proteins was measured in HEp-2 cells exposed to MEDS433 in the presence of neutralizing mAbs directed against IFN-β or IFN-λ1. As depicted in Fig. 10C, the presence of neutralizing antibodies reduced the levels of all examined ISG proteins, thus confirming that stimulation of ISG proteins expression was a consequence of MEDS433-induced secretion of IFN-β and IFN-λ1.

To further confirm the importance of secreted type I IFNs in the overall anti-RSV activity of MEDS433, VRAs were performed in HEp-2 cells infected with RSV-A in the absence or presence of neutralizing mAbs against IFN-β or IFN-λ1. Fig. 10D shows that the neutralization of IFN-β, IFN-λ1, or both decreased significantly the inhibitory activity of MEDS433. In fact, its EC_{50} value (0.0086 ± 0.00003 μM) was raised to 0.0189 ± 0.00052 μM by the anti-IFN-β mAb, 0.0214 ± 0.00077 μM by the anti-IFN-λ1 mAb, and 0.0233 ± 0.00038 by the addition of both mAbs. These results therefore sustain a contribution of the activated IFN pathway in the overall antiviral activity of MEDS433 against RSV.

Then, to investigate the relevance of these MEDS433-induced ISG proteins in the overall anti-RSV activity of the *h*DHODH inhibitor, a doxycycline-regulated expression system was developed for efficient expression of IFI6, IFITM1, or IRF7 in HEp-2 cells through their
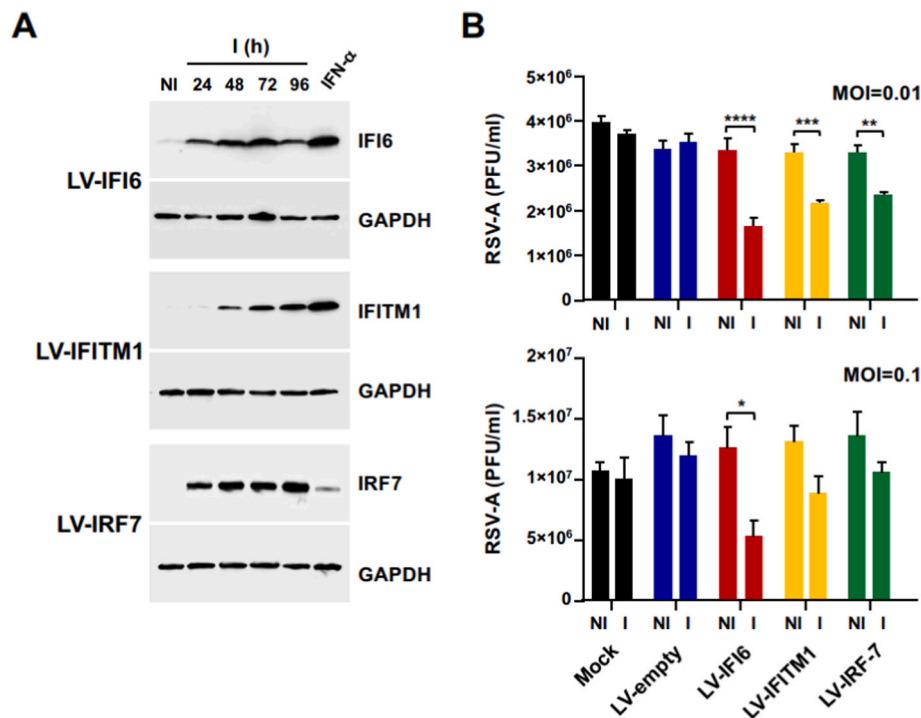
Fig. 11. Inducible expression of IFI6, IFITM1 or IRF7 proteins hampers RSV-A replication. (**A**) Doxycycline-inducible expression of IFI6, IFITM1 and IRF7 in HEp-2-derived cells lines LV-IFI6, LV-IFITM1, and LV-IRF7. Protein extracts were from not-induced (NI) cells, or from cells exposed to doxycycline (100 ng/ml) for 24, 48, 72, or 96 h. Extracts from NI cells exposed to IFN-α (100 ng/ml) for 24 h were used as a positive control for ISG protein expression. GAPDH immunodetection was used as a control for protein loading. (**B**) Replication of RSV-A is affected by the inducible expression of IFI6, IFITM1, or IRF7. LV-empty, LV-IF6, LV-IFITM1, and LV-IRF7 cells were left untreated or treated with doxycycline (100 ng/ml) 24 h prior to infection with RSV-A at MOI of 0.01 or 0.1. At 72 h p.i., supernatants were harvested, and titrated for RSV infectivity in HEp-2 cells. The data shown are the means ± SD of $n = 2$ independent experiments performed in triplicate and analyzed by a two-way ANOVA followed by Sidak's multiple comparison test compared to the corresponding NI sample. *, $p < 0.05$; **, $p < 0.005$; ***, $p < 0.001$; ****, $p < 0.0001$.

transduction with Tet-One lentiviral vectors (LV) containing the corresponding ISG ORFs. As reported in Fig. 11A, the doxycycline-inducible expression of IFI6, IFITM1, and IRF7, was confirmed by immunoblotting in LV-transduced cell lines up to 96 h of antibiotic stimulation. RSV-A replication was then examined in these cell lines, in the absence of MEDS433 treatment; in comparison to mock-transduced HEp-2 cells or cells transduced with an empty LV (LV-empty), the doxycycline-induced expression of all ISG proteins affected RSV-A yield, with a maximum reduction rate of more than 2-fold for cells expressing IFI6 (Fig. 11B).

Taken as a whole, the results of this section indicate as a second mechanism of the antiviral activity of MEDS433 against RSV, its ability to stimulate the activation of the IFN pathway, through induction of IFN-β and IFN-λ1 secretion that, in turn, upregulates the expression of antiviral ISG proteins able to exert a functional role in hindering RSV replication.

3.8. MEDS433 inhibits RSV-A replication in a mucociliated human small airway epithelium model

Lastly, the anti-RSV activity of MEDS433 was investigate in primary human bronchiolar epithelial tissues maintained at the air-liquid interface. This cell system represents a valuable model to assess both toxicity and efficacy of candidate antiviral agents in an *ex vivo* system that recapitulates the lining of human lung small airway, including ciliated and goblet cells that produce cilia movement and mucus (Hasan et al., 2018). As shown in Fig. 12A, treatment of the small airway epithelium with 1 μM MEDS433 after RSV-A infection, already at 24 h p.i., caused a significant reduction of the RSV yield released compared to untreated and RSV-infected cultures (RSV-A). The extent of the inhibitory effect of MEDS433 was more pronounced from 48 h p.i. and up to 96 h p.i. Indeed, when epithelia were exposed to higher concentrations of

MEDS433 (5 or 10 μM), the inhibition of the release of RSV infectious particles was even more severe and quantified as more than 2 orders of magnitude (Fig. 12A). The antiviral activity of MEDS433 in this *ex vivo* respiratory epithelium model was not due to non-specific cytotoxicity, since LDH levels measured in the basal medium of MEDS433-treated cultures were comparable to that of untreated mock-infected epithelium (Mock) (Fig. 12B). These results were further confirmed by histological analysis. In fact, as depicted in Fig. 12C, mock-infected MEDS433-treated epithelia (*Middle and Lower left* panels) showed a healthy appearance, with intact cilia and an unaltered histological structure compared to the untreated mock-infected epithelium (Mock) (Fig. 12C, *Upper left*). RSV infection, as expected, caused severe tissue damages characterized by cilia disappearance and thinning of the epithelial layer (RSV-A) (Fig. 12C, *Upper right*). However, when small airway epithelia were treated with MEDS433 after RSV infection, their histological structure was protected, and tissues appeared healthy at 96 h p.i. (Fig. 12C, *Middle and Lower right* panels).

Together, these results confirm that MEDS433 exerted an anti-RSV activity even in an *ex vivo* model of human respiratory epithelium.

4. Discussion

To replicate efficiently in human cells, viruses requires the contribution of host cell *h*DHODH, as we reaffirmed here for RSV (Fig. 1). Therefore, its enzymatic activity is a reliable HTA target to develop new broad-spectrum antivirals (Zheng et al., 2022). To further support such perspective, in this study, we have characterized the anti-RSV activity of MEDS433, a novel *h*DHODH inhibitor. The observed results suggest that the overall antiviral activity of MEDS433 against RSV derives from both the selective inhibition of *h*DHODH activity in RSV-infected cells that causes pyrimidine depletion and the consequent suppression of RSV
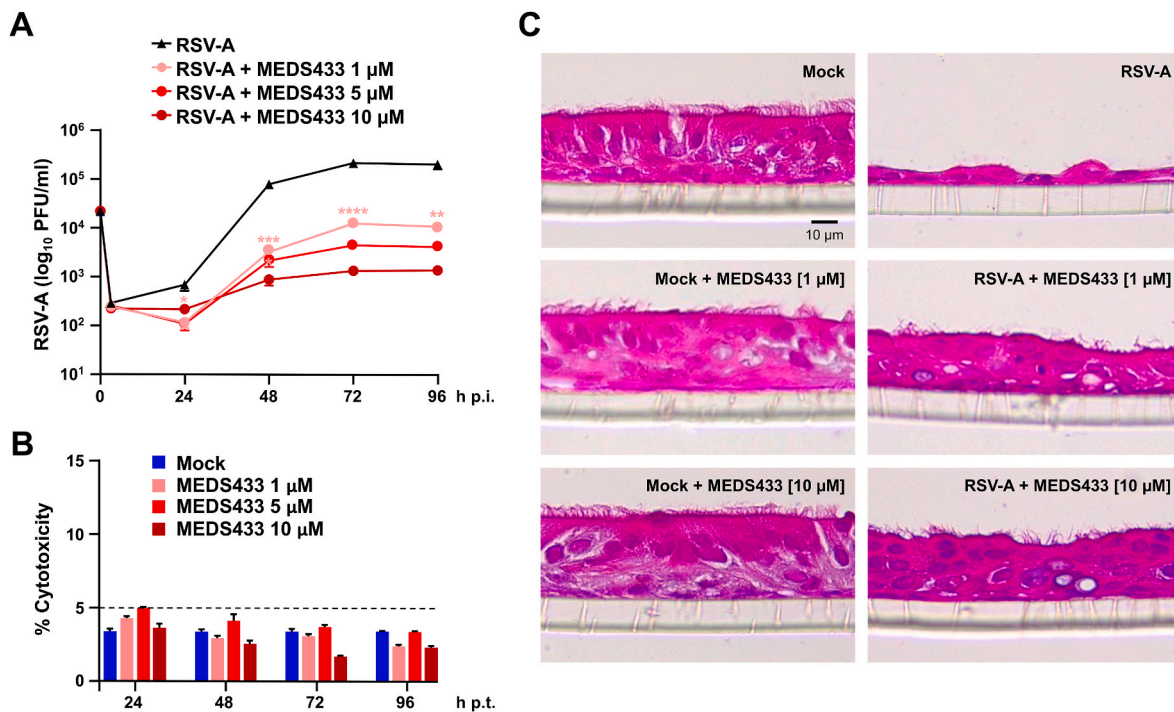
Fig. 12. MEDS433 inhibit RSV replication in a human mucociliated small airway epithelium model (A) Bronchiolar epithelia were treated with different concentrations of MEDS433 (1, 5 and 10 μM) in the basolateral (BL) medium for 1 h at 37 °C before infection. Then, small airway epithelia were infected apically with RSV-A at an MOI of 0.02 in presence of MEDS433 for 3h at 37 °C. After viral absorption, the inoculum was removed, and MEDS433 was applied in the BL medium. Viral progeny was harvested from the apical surface at 24, 48, 72, and 96 h p.i. and titrated by the plaque assay in HEp-2 cells. The data shown are the means ± SD of $n = 2$ independent experiments performed in duplicate and analyzed by a two-way ANOVA, followed by Dunnett's multiple comparison test. Statistical analysis was performed by comparing the RSV-A-infected sample (RSV-A) with the MEDS433-treated and RSV-infected tissues for each time. Statistical significance is shown only for RSV-A+MEDS433 1 μM samples. *, $p < 0.05$; **, $p < 0.005$; ****, $p < 0.0001$. (B) To determine the cytotoxic effect of the different concentrations of MEDS433, at each time-point post-treatment (p.t.) the basal medium was harvested and the released LDH was measured by the LDH-Glo Cytotoxicity assay. Results are expressed as % cytotoxicity and as means ± SD (error bars) of two independent experiments performed in duplicate. The threshold limit 5% of the toxicity index indicates the physiological cell turnover in this airway epithelium model. (C) Transversal cross sections of small airway epithelia stained at 96 h p.i. Representative histological images of mock-infected (Mock, *Left*), MEDS433-treated and mock-infected (Mock+MEDS433, *Left*), RSV-infected (RSV-A, *Right*), or MEDS433-treated and RSV-infected epithelia (RSV-A+MEDS433, *Right*) are shown. Slides were prepared from epithelia stained with hematoxylin-eosin. Magnification: 40 × . Scale bar for each image: 10 μm.

genome synthesis, as well as the activation of antiviral ISG proteins that hamper RSV replication.

These results confirm the viability of *h*DHODH pharmacological targeting to develop anti-RSV agents, as previously reported for other *h*DHODH inhibitors, such as leflunomide (Dunn et al., 2011), FA-613 (Cheung et al., 2017), and RYL-634 (Yang et al., 2019). However, it is worth noting that our study adds a couple of new pieces of knowledge that may be relevant to develop further pyrimidine synthesis inhibitors against RSV infections.

The first pertains to the observation that a combination between MEDS433 and DPY, an inhibitor of the pyrimidine salvage pathway, was synergistic against RSV replication (Fig. 5A), even in the presence of uridine concentration higher than physiological plasma concentration (Fig. 6). In fact, despite that DPY is lacking anti-RSV activity (Fig. 5), when combined with MEDS433, it restored the antiviral activity of a concentration of MEDS433 no longer effective in presence of uridine (Fig. 6). This observation is relevant, inasmuch poor effectiveness has been reported for some *h*DHODH inhibitors in the treatment of infections by RNA viruses in both rodents and non-human primate models, despite their *in vitro* efficacy (Wang et al., 2011; Smee et al., 2012; Grandin et al., 2016). It has been speculated that this failure could depend on an insufficient antiviral potency or poor pharmacokinetics of the evaluated DHODH inhibitor, and/or on the compensating effect of the host pyrimidine salvage pathway through the import of exogenous uridine into virus-infected cells (Zheng et al., 2022). Accordingly, the pharmacological targeting of the pyrimidine salvage pathway may be

beneficial, as it may enhance the *in vivo* antiviral efficacy of DHODH inhibitors.

DPY is a pyrimidopyrimidine derivative that inhibits ENT 1 and 2, the most effective nucleoside transporters of the pyrimidine salvage pathway (Fitzgerald, 1987; Ward et al., 2000), and an antiplatelet agent approved for the prophylaxis of thromboembolism in cardiovascular diseases (Schaper, 2005). However, the combination of DPY and *h*DHODH inhibitors against viral infections is at a very early stage and is still understudied. In this regard, we have observed that the combination of DPY with MEDS433 was effective against HSV-1, SARS-CoV-2, and influenza A virus, even in the presence of a hyper-physiological concentration of uridine (Luganini et al., 2021; Calistri et al., 2021; Sibille et al., 2022). Importantly, the concentration of DPY (3 μM) synergic with MEDS433 against RSV replication (Fig. 6) is lower than the DPY Cmax (2.2 μg/mL, which corresponds to 4.4 μM) (Gregov et al., 1987) and, thus, clinically achievable in patients undergoing DPY therapy. The wide clinical experience of DPY could allow its rapid repositioning even against respiratory virus infections, including RSV, to be clinically advantageous in combination with *h*DHODH inhibitors.

A second point worth discussing concerns the ability of MEDS433 to stimulate the expression of ISG proteins that hamper RSV replication (Fig. 11). Although it has been previously reported that *h*DHODH inhibitors induce ISGs expression (Lucas-Hourani et al., 2013; Cheung et al., 2017; Luthra et al., 2018), this is the first observation, to our knowledge, that a *h*DHODH inhibitor stimulates the expression of antiviral ISG proteins, such as IFI6, IFITM1 I and IRF7, which reduce

RSV replication when expressed in isolation (Fig. 11B), and previously observed to affect the virus (McDonald et al., 2016; Smith et al., 2019). Our results therefore functionally sustain the view that the antiviral activity of *h*DHODH inhibitors depends on both the pyrimidine depletion that halts the activity of viral polymerases, and the induction of protein effectors of the innate antiviral response (Lucas-Hourani et al., 2013). Although the mechanisms underlying the activation of ISGs following inhibition of pyrimidine biosynthesis remain to be well-defined, it has been hypothesized that the cellular stress associated to nucleoside deprivation fosters expression of ISGs that, in turn, contribute to the establishment of an antiviral state to infections by RNA viruses (Zheng et al., 2022). In this regard, we observed that the induction of ISG proteins by MEDS433 is linked to depletion of pyrimidines, as uridine supplementation prevented their expression in cells exposed to the *h*DHODH inhibitor (Fig. 9B). Moreover, different pathways of ISGs activation have been suggested for different *h*DHODH inhibitors (Zheng et al., 2022), since the dependency from type I IFNs production has been reported for FA613 (Cheung et al., 2017), while an IFN-independent mechanism has been observed for DD264, brequinar, and SW835 (Lucas-Hourani et al., 2013; Luthra et al., 2018). Here, we have observed that the MEDS433-mediated induction of IFI6, IFITM1, and IRF7 proteins requires secretion of IFN-β and IFN-λ1, as their neutralization reduces the accumulation of these ISG proteins in MEDS433-treated cells (Fig. 10C). Since neutralization of IFN-β and IFN-λ1 reduced the anti-RSV activity of MEDS433 as well (Fig. 10D), activation of the IFN pathway and ISG proteins expression indeed contribute to the overall anti-RSV activity of MEDS433.

Interestingly, activation of IRF1, through the DNA damage response kinase ATM, has been observed to occur in HEK293T cells for the SW835-mediated and IFN-independent ISGs stimulation (Luthra et al., 2018). Although IRF1 was induced even by MEDS433 in HEp-2 cells (Fig. 9), a role of this transcription factor in the ISGs stimulation, in the context of the IFN-dependent mechanism triggered by MEDS433, remains to be defined. In this study, we have observed the ability of MEDS433 to stimulate the phosphorylation of constitutive IRF3 (Fig. 10B), as an essential step in its activation that leads up to IFN-β gene transcription (Negishi et al., 2018). Although further investigations are required to fully elucidate the mechanism(s) of the IFN-dependent ISGs stimulation by MEDS433 (i.e., activation of the transduction pathways upstream from IRF3 phosphorylation), our observations provide novel insights toward the development of pyrimidine synthesis inhibitors to modulate the innate antiviral response.

Moreover, it should be emphasized, as an important added value of MEDS433, its broad-spectrum antiviral efficacy against different human viruses that cause RTIs. In fact, in addition to RSV, we have observed the ability of MEDS433 to inhibit the replication of influenza A and B viruses (Sibille et al., 2022), as well as of coronaviruses, such as hCoV-229E, hCoV-OC43, and SARS-CoV-2 (Calistri et al., 2021). Indeed, this trait and the inherent HTA advantage of the low risk of emergence of drug resistance, make MEDS433 of interest for the development of new BSA agents, even in the preparedness against future emerging human respiratory viruses, given the independence of its antiviral effects with respect to a specific virus.

5. Conclusions

In conclusion, this study suggests MEDS433 as an attractive novel anti-RSV HTA candidate endowed with advantageous features, such as a very potent antiviral activity, its amenability to combination regimens with both nucleoside analogues and other anti-pyrimidines, such as RBV and DPY, as well as its ability to trigger protein effectors of the innate antiviral response. The potent *in vitro* anti-RSV activity of MEDS433 and its valuable drug-like profile now ensure further studies to evaluate its efficacy in preclinical animal models of RSV infection.

Declaration of competing interest

The authors declare that they have no known competing financial interests or personal relationships that could have appeared to influence the work reported in this paper.

Data availability

Data will be made available on request.

References

Amarelle, L., Lecuona, E.A., 2018. Nonhospitable host: targeting cellular factors as an antiviral strategy for respiratory viruses. Am. J. Respir. Cell Mol. Biol. 59, 666–667. https://doi.org/10.1165/rcmb.2018-0268ED.

Beaird, O.E., Freifeld, A., Ison, M.G., Lawrence, S.J., Theodoropoulos, N., Clark, N.M., Razonable, R.R., Alangaden, G., Miller, R., Smith, J., Young, J.A.H., Hawkinson, D., Pursell, K., Kaul, D.R., 2016. Current practices for treatment of respiratory syncytial virus and other non-influenza respiratory viruses in high-risk patient populations: a survey of institutions in the Midwestern Respiratory Virus Collaborative. Transpl. Infect. Dis. 18, 210–215. https://doi.org/10.1111/tid.12510.

Boschi, D., Pippione, A.C., Sainas, S., Lolli, M.L., 2019. Dihydroorotate dehydrogenase inhibitors in anti-infective drug research. Eur. J. Med. Chem. 183, 111681 https://doi.org/10.1016/j.ejmech.2019.111681.

Broadbent, L., Groves, H., Shields, M.D., Power, U.F., 2015. Respiratory syncytial virus, an ongoing medical dilemma: an expert commentary on respiratory syncytial virus prophylactic and therapeutic pharmaceuticals currently in clinical trials. Influenza Other Resp. Viruses. 9, 169–178. https://doi.org/10.1111/irv.12313.

Calistri, A., Luganini, A., Mognetti, B., Elder, E., Sibille, G., Conciatori, V., Del Vecchio, C., Sainas, S., Boschi, D., Montserrat, N., Mirazimi, A., Lolli, M.L., Gribaudo, G., Parolin, C., 2021. The new generation hDHODH inhibitor MEDS433 hinders the in vitro replication of SARS-CoV-2 and other human coronaviruses. Microorganisms 9, 1731. https://doi.org/10.3390/microorganisms9081731.

Cheung, N.N., Lai, K.K., Dai, J., Kok, K.H., Chen, H., Chan, K.H., Yuen, K.Y., Kao, R.Y.T., 2017. Broad-spectrum inhibition of common respiratory RNA viruses by a pyrimidine synthesis inhibitor with involvement of the host antiviral response. J. Gen. Virol. 98, 946–954. https://doi.org/10.1099/jgv.0.000758.

Chou, T.C., 2006. Theoretical basis, experimental design, and computerized simulation of synergism and antagonism in drug combination studies. Pharmacol. Rev. 58, 621–681. https://doi.org/10.1124/pr.58.3.10.

Chou, T.C., Martin, N., 2005. CompuSyn for Drug Combinations: PC Software and User's Guide: a Computer Program for Quantitation of Synergism and Antagonism in Drug Combinations, and the Determination of IC$_{50}$ and ED$_{50}$ and LD$_{50}$ Values. ComboSyn Inc., Paramus, NJ. https://www.combosyn.com.

Coelho, A.R., Oliveira, P.J., 2020. Dihydroorotate dehydrogenase inhibitors in SARS-CoV-2 infection. Eur. J. Clin. Invest. 50, e13366 https://doi.org/10.1111/eci.13366.

Dunn, M.C.C., Knight, D.A., Waldman, W.J., 2011. Inhibition of respiratory syncytial virus in vitro and in vivo by the immunosuppressive agent leflunomide. Antivir. Ther. 16, 309–317. https://doi.org/10.3851/IMP1763.

Fitzgerald, G.A., 1987. Dipyridamole. N. Engl. J. Med. 316, 1247–1257. https://doi.org/10.1056/NEJM198705143162005.

Garegnani, L., Styrmisdóttir, L., Roson Rodriguez, P., Escobar Liquitay, C.M., Esteban, I., Franco, J.V., 2021. Palivizumab for preventing severe respiratory syncytial virus (RSV) infection in children. Cochrane Database Syst. Rev. 11 https://doi.org/10.1002/14651858.CD013757.pub2. CD013757.

Grandin, C., Hourani, M.L., Janin, Y.L., Dauzonne, D., Munier-Lehmann, H., Paturet, A., Taborik, F., Vabret, A., Contamin, H., Tangy, F., Vidalain, P.O., 2016. Respiratory syncytial virus infection in macaques is not suppressed by intranasal sprays of pyrimidine biosynthesis inhibitors. Antivir. Res. 125, 58–62. https://doi.org/10.1016/j.antiviral.2015.11.006, 2016.

Gregov, D., Jenkins, A., Duncan, E., Sieber, D., Rodgers, S., Duncan, B., Bochner, F., Lloyd, J., 1987. Dipyridamole: pharmacokinetics and effects on aspects of platelet function in man. Br. J. Clin. Pharmacol. 24, 425–434. https://doi.org/10.1111/j.1365-2125.1987.tb03194.x.

Gribaudo, G., Riera, L., Rudge, T.L., Caposio, P., Johnson, L.F., Landolfo, S., 2002. Human cytomegalovirus infection induces cellular thymidylate synthase gene expression in quiescent fibroblasts. J. Gen. Virol. 83, 2983–2993. https://doi.org/10.1099/0022-1317-83-12-2983.

Gribaudo, G., Riera, L., Caposio, P., Maley, F., Landolfo, S., 2003. Human cytomegalovirus requires cellular deoxycytidylate deaminase for replication in quiescent cells. J. Gen. Virol. 84, 1437–1441. https://doi.org/10.1099/vir.0.18979-0.

Hammitt, L.L., Dagan, R., Yuan, Y., Baca Cots, M., Bosheva, M., Madhi, S.A., Muller, W. J., Zar, H.J., Brooks, D., Grenham, A., Wählby Hamrén, U., Mankad, V.S., Ren, P., Takas, T., Abram, M.E., Leach, A., Griffin, M.P., Villafana, T., MELODY Study Group, 2022. Nirsevimab for prevention of RSV in healthy late-preterm and term infants. N. Engl. J. Med. 386, 837–846. https://doi.org/10.1056/NEJMoa2110275.

Hansen, C.L., Chaves, S.S., Demont, C., Viboud, C., 2022. Mortality associated with influenza and respiratory syncytial virus in the US, 1999-2018. JAMA Netw. Open 5, e220527. https://doi.org/10.1001/jamanetworkopen.2022.0527.

Hasan, S., Sebo, P., Osicka, R., 2018. A guide to polarized airway epithelial models for studies of host-pathogen interactions. FEBS J. 285, 4343–4358. https://doi.org/10.1111/febs.14582.

Heylen, E., Neyts, J., Jochmans, D., 2017. Drug candidates and model systems in respiratory syncytial virus antiviral drug discovery. Biochem. Pharmacol. 127, 1–12. https://doi.org/10.1016/j.bcp.2016.09.014.

Jain, H., Schweitzer, J.W., Justice, N.A., 2022. Respiratory syncytial virus infection. In: StatPearls [Internet], Treasure Island (FL). StatPearls Publishing.

Jorquera, P.A., Anderson, L., Tripp, R.A., 2016. Human respiratory syncytial virus: an introduction. Methods Mol. Biol. 1442, 1–12. https://doi.org/10.1007/978-1-4939-3687-8_1.

Karimi, Z., Oskouie, A.A., Rezaei, F., Ajaminejad, F., Marashi, S.M., Azad, T.-M., 2022. The effect of influenza virus on the metabolism of peripheral blood mononuclear cells with a metabolomics approach. J. Med. Virol. 94, 4383–4392. https://doi.org/10.1002/jmv.27843.

Li, Y., Wang, X., Blau, D.M., Caballero, M.T., Feikin, D.R., Gill, C.J., Madhi, S.A., Omer, S. B., Simões, E.A.F., Campbell, H., Pariente, A.B., Bardach, D., Bassat, Q., Casalegno, J.-S., Chakhunashvili, G., Crawford, N., Danilenko, D., Do, L.A.H., Echavarria, M., Gentile, A., Gordon, A., Heikkinen, T., Huang, Q.S., Jullien, S., Krishnan, A., Lopez, E.L., Markić, J., Mira-Iglesias, A., Moore, H.C., Moyes, J., Mwananyanda, L., Nokes, D.J., Noordeen, F., Obodai, E., Palani, N., Romero, C., Salimi, V., Satav, A., Seo, E., Shchomak, Z., Singleton, R., Stolyarov, K., Stoszek, S.K., Von Gottberg, A., Wurzel, D., Yoshida, L.M., Yung, C.F., Zar, H.J., Respiratory Virus Global Epidemiology Network, Nair, H., RESCEU Investigators, 2022. Global, regional, and national disease burden estimates of acute lower respiratory infections due to respiratory syncytial virus in children younger than 5 years in 2019: a systematic analysis. Lancet 399, 2047–2064. https://doi.org/10.1016/S0140-6736(22)00478-0.

Löffler, M., Carrey, E.A., Knecht, W., 2020. The pathway to pyrimidines: the essential focus on dihydroorotate dehydrogenase, the mitochondrial enzyme coupled to the respiratory chain. Nucleos Nucleot. Nucleic Acids 39, 1281–1305. https://doi.org/10.1080/15257770.2020.1723625.

Lucas-Hourani, M., Dauzonne, D., Jorda, P., Cousin, G., Lupan, A., Helynck, O., Caignard, G., Janvier, G., André-Leroux, G., Khiar, S., Escriou, N., Desprès, P., Jacob, Y., Munier-Lehmann, H., Tangy, F., Vidalain, P.-O., 2013. Inhibition of pyrimidine biosynthesis pathway suppresses viral growth through innate immunity. PLoS Pathog. 9, e1003678 https://doi.org/10.1371/journal.ppat.1003678.

Luganini, A., Caposio, P., Landolfo, S., Gribaudo, G., 2008. Phosphorothioate-modified oligodeoxynucleotides inhibit human cytomegalovirus replication by blocking virus entry. Antimicrob. Agents Chemother. 52, 1111–1120. https://doi.org/10.1128/AAC.00987-07.

Luganini, A., Sibille, G., Mognetti, B., Sainas, S., Pippione, A.C., Giorgis, M., Boschi, D., Lolli, M.L., Gribaudo, G., 2021. Effective deploying of a novel DHODH inhibitor against herpes simplex type 1 and type 2 replication. Antivir. Res. 189, 105057 https://doi.org/10.1016/j.antiviral.2021.105057.

Luthra, P., Naidoo, J., Pietzsch, C.A., De, S., Khadka, S., Anantpadma, M., Williams, C.G., Edwards, M.R., Davey, R.A., Bukreyev, A., Ready, J.M., Basler, C.F., 2018. Inhibiting pyrimidine biosynthesis impairs Ebola virus replication through depletion of nucleoside pools and activation of innate immune responses. Antivir. Res. 158, 288–302. https://doi.org/10.1016/j.antiviral.2018.08.012.

Madak, J.T., Cuthbertson, C.R., Chen, W., Showalter, H.D., Neamati, N., 2017. Design, synthesis, and characterization of brequinar conjugates as probes to study DHODH inhibition. Chemistry 23, 13875–13878. https://doi.org/10.1002/chem.201702999.

Martín-Vicente, M., González-Riaño, C., Barbas, C., Jiménez-Sousa, M.Á., Brochado-Kith, O., Resino, S., Martínez, I., 2020. Metabolic changes during respiratory syncytial virus infection of epithelial cells. PLoS One 15, e0230844. https://doi.org/10.1371/journal.pone.0230844.

McDonald, J.U., Kaforou, M., Clare, S., Hale, C., Ivanova, M., Huntley, D., Dorner, M., Wright, V.J., Levin, M., Martinon-Torres, F., Herberg, J.A., Tregoning, J.S., 2016. A simple screening approach to prioritize genes for functional analysis identifies a role for Interferon Regulatory Factor 7 in the control of respiratory syncytial virus disease. mSystems 1, e00051-16. https://doi.org/10.1128/mSystems.00051-16.

Munger, J., Bennett, B.D., Parikh, A., Feng, X.-J., McArdle, J., Rabitz, H.A., Shenk, T., Rabinowitz, J.D., 2008. Systems-level metabolic flux profiling identifies fatty acid synthesis as a target for antiviral therapy. Nat. Biotechnol. 26, 1179–1186. https://doi.org/10.1038/nbt.1500.

Nam, H.H., Ison, M.G., 2019. Respiratory syncytial virus infection in adults. BMJ 366, l5021. https://doi.org/10.1136/bmj.l5021.

Negishi, H., Taniguchi, T., Yanai, H., 2018. The interferon (IFN) class of cytokines and the IFN Regulatory Factor (IRF) transcription factor family. Cold Spring Harbor Perspect. Biol. 10, a028423. https://doi.org/10.1101/cshperspect.a028423.

Okesli, A., Khosla, C., Bassik, M.C., 2017. Human pyrimidine nucleotide biosynthesis as a target for antiviral chemotherapy. Curr. Opin. Biotechnol. 48, 127–134. https://doi.org/10.1016/j.copbio.2017.03.010.

Peters, G.J., 2018. Re-evaluation of Brequinar sodium, a dihydroorotate dehydrogenase inhibitor. Nucleos Nucleot. Nucleic Acids 37, 666–678. https://doi.org/10.1080/15257770.2018.1508692.

Pizzorno, G., Cao, D., Leffert, J.J., Russell, R.L., Zhang, D., Handschumacher, R.E., 2002. Homeostatic control of uridine and the role of uridine phosphorylase: a biological and clinical update. Biochim. Biophys. Acta 1587, 133–144. https://doi.org/10.1016/s0925-4439(02)00076-5.

Reis, R.A.G., Calil, F.A., Feliciano, P.R., Pinheiro, M.P., Nonato, M.C., 2017. The dihydroorotate dehydrogenases: past and present. Arch. Biochem. Biophys. 632, 175–191. https://doi.org/10.1016/j.abb.2017.06.019.

Sainas, S., Pippione, A.C., Lupino, E., Giorgis, M., Circosta, P., Gaidano, V., Goyal, P., Bonanni, D., Rolando, B., Cignetti, A., Ducime, A., Andersson, M., Järvå, M., Friemann, R., Piccinini, M., Ramondetti, C., Buccinnà, B., Al-Karadaghi, S., Boschi, D., Saglio, G., Lolli, M.L., 2018. Targeting myeloid differentiation using potent 2-hydroxypyrazolo[1,5- a]pyridine scaffold-based human dihydroorotate dehydrogenase inhibitors. J. Med. Chem. 61, 6034–6055. https://doi.org/10.1021/acs.jmedchem.8b00373.

Sainas, S., Giorgis, M., Circosta, P., Gaidano, V., Bonanni, D., Pippione, A.C., Bagnati, R., Passoni, A., Qiu, Y., Cojocaru, C.F., Canepa, B., Bona, A., Rolando, B., Mishina, M., Ramondetti, C., Buccinnà, B., Piccinini, M., Houshmand, M., Cignetti, A., Giraudo, E., Al-Karadaghi, S., Boschi, D., Saglio, G., Lolli, M.L., 2021. Targeting acute myelogenous leukemia using potent human dihydroorotate dehydrogenase inhibitors based on the 2-hydroxypyrazolo[1,5- *a*]pyridine scaffold: SAR of the biphenyl moiety. J. Med. Chem. 64, 5404–5428. https://doi.org/10.1021/acs.jmedchem.0c01549.

Sainas, S., Giorgis, M., Circosta, P., Poli, G., Alberti, M., Passoni, A., Gaidano, V., Pippione, A.C., Vitale, N., Bonanni, D., Rolando, B., Cignetti, A., Ramondetti, C., Lanno, A., Ferraris, D.M., Canepa, B., Buccinnà, B., Piccinini, M., Rizzi, M., Saglio, G., Al-Karadaghi, S., Boschi, D., Miggiano, R., Tuccinardi, T., Lolli, M.L., 2022. Targeting acute myelogenous leukemia using potent human dihydroorotate dehydrogenase inhibitors based on the 2-hydroxypyrazolo[1,5-a]pyridine scaffold: SAR of the aryloxyaryl moiety. J. Med. Chem. 65, 12701–12724. https://doi.org/10.1021/acs.jmedchem.2c00496.

Schaper, W., 2005. Dipyridamole, an underestimated vascular protective drug. Cardiovasc. Drugs Ther. 19, 357–363. https://doi.org/10.1007/s10557-005-4659-6.

Sepúlveda, C.S., García, C.C., Damonte, E.B., 2022. Inhibitors of nucleotide biosynthesis as candidates for a wide spectrum of antiviral chemotherapy. Microorganisms 10, 1631. https://doi.org/10.3390/microorganisms10081631.

Sibille, G., Luganini, A., Sainas, S., Boschi, D., Lolli, M.L., Gribaudo, G., 2022. The novel hDHODH inhibitor MEDS433 prevents Influenza virus replication by blocking pyrimidine biosynthesis. Viruses 14, 2281. https://doi.org/10.3390/v14102281.

Simões, E.A.F., Madhi, S.A., Muller, W.J., Atanasova, V., Bosheva, M., Cabañas, F., Baca Cots, M., Domachowske, J.B., Garcia-Garcia, M.L., Grantina, I., Nguyen, K.A., Zar, H. J., Berglind, A., Cummings, C., Griffin, M.P., Takas, T., Yuan, Y., Wählby Hamrén, U., Leach, A., Villafana, T., 2023. Efficacy of nirsevimab against respiratory syncytial virus lower respiratory tract infections in preterm and term infants, and pharmacokinetic extrapolation to infants with congenital heart disease and chronic lung disease: a pooled analysis of randomised controlled trials. Lancet Child Adolesc. Health 7, 180–189. https://doi.org/10.1016/S2352-4642(22)00321-2.

Smee, D.F., Hurst, B.L., Day, C.W., 2012. D282, a non-nucleoside inhibitor of influenza virus infection that interferes with de novo pyrimidine biosynthesis. Antivir. Chem. Chemother. 22, 263–272. https://doi.org/10.3851/IMP2105.

Smith, S.E., Busse, D.C., Binter, S., Weston, S., Diaz Soria, C., Laksono, B.M., Clare, S., Van Nieuwkoop, S., Van den Hoogen, B.G., Clement, M., Marsden, M., Humphreys, I. R., Marsh, M., de Swart, R.L., Wash, R.S., Tregoning, J.S., Kellam, P., 2019. Interferon-Induced Transmembrane Protein 1 restricts replication of viruses that enter cells via the plasma membrane. J. Virol. 93, e02003-e02018 https://doi.org/10.1128/JVI.02003-18.

Soni, A., Kabra, S.K., Lodha, R., 2023. Respiratory syncytial virus infection: an update. Indian J. Pediatr. https://doi.org/10.1007/s12098-023-04613-w.

Stegmann, K.M., Dickmanns, A., Heinen, N., Blaurock, C., Karrasch, T., Breithaupt, A., Klopfleisch, R., Uhlig, N., Eberlein, V., Issmail, L., Herrmann, S.T., Schreieck, A., Peelen, E., Kohlhof, H., Sadeghi, B., Riek, A., Speakman, J.R., Groß, U., Görlich, D., Vitt, D., Müller, T., Grunwald, T., Pfaender, S., Balkema-Buschmann, A., Dobbelstein, M., 2022. Inhibitors of dihydroorotate dehydrogenase cooperate with molnupiravir and N4-hydroxycytidine to suppress SARS-CoV-2 replication. iScience 25, 104293. https://doi.org/10.1016/j.isci.2022.104293.

Tejada, S., Martinez-Reviejo, R., Karakoc, H.N., Peña-López, Y., Manuel, O., Rello, J., 2022. Ribavirin for treatment of subjects with respiratory syncytial virus-related infection: a systematic review and meta-analysis. Adv. Ther. 39, 4037–4051. https://doi.org/10.1007/s12325-022-02256-5.

Wang, Q.-Y., Bushell, S., Qing, M., Xu, H.Y., Bonavia, A., Nunes, S., Zhou, J., Poh, M.K., Florez de Sessions, P., Niyomrattanakit, P., Dong, H., Hoffmaster, K., Goh, A., Nilar, S., Schul, W., Jones, S., Kramer, L., Compton, T., Shi, P.-Y., 2011. Inhibition of dengue virus through suppression of host pyrimidine biosynthesis. J. Virol. 85, 6548–6556. https://doi.org/10.1128/JVI.02510-10.

Ward, J.L., Sherali, A., Mo, Z.P., Tse, C.M., 2000. Kinetic and pharmacological properties of cloned human equilibrative nucleoside transporters, ENT1 and ENT2, stably expressed in nucleoside transporter-deficient PK15 cells. Ent2 exhibits a low affinity

for guanosine and cytidine but a high affinity for inosine. J. Biol. Chem. 275, 8375–8381. https://doi.org/10.1074/jbc.275.12.8375.

Yang, Y., Cao, L., Gao, H., Wu, Y., Wang, Y., Fang, F., Lan, T., Lou, Z., Rao, Y., 2019. Discovery, optimization, and target identification of novel potent broad-spectrum antiviral inhibitors. J. Med. Chem. 62, 4056–4073. https://doi.org/10.1021/acs.jmedchem.9b00091.

Zheng, Y., Li, S., Song, K., Ye, J., Li, W., Zhong, Y., Feng, Z., Liang, S., Cai, Z., Xu, K., 2022. A broad antiviral strategy: inhibitors of human DHODH pave the way for host-targeting antivirals against emerging and re-emerging viruses. Viruses 14, 928. https://doi.org/10.3390/v14050928.

4. DISCUSSION

Infections caused by RNA and DNA viruses are responsible for millions of deaths worldwide every year. Specific prophylactic and direct-acting antiviral agents (DAAs) have been developed against individual viruses, however the efficiency of the treatments has decreased significantly due to the onset of resistances and, moreover, they have proved useless against other viruses (Coelho *et al.* 2020).

The COVID-19 pandemic and the frequent appearance of new human respiratory viruses in recent decades have exacerbated the situation.

For these reasons, it was necessary to focus on the discovery of new antiviral drugs depicted as host-targeting antiviral agents (HTA): they directly target host pathway that the virus exploits for the replication and, in doing so, the problem of resistances is eliminated as the virus mutation cannot bypass these cellular processes. This is an efficient therapeutic approach for a wide range of viruses and its important in the event of the emergence of new epidemics, in case of a new outbreaks, such as SARS-CoV-2: the reuse of FDA-approved drugs is critical to reducing the time to find an effective treatment (Boschi *et al.* 2019; Coelho *et al.* 2020).

In the last few years, the results of several high-throughput screens to discover broad-spectrum antivirals have identified small molecules targeting the host *de novo* pyrimidine biosynthesis pathway, mostly with the DHODH activity as their major and specific target. For example, Xiong et al. tested a library of DHODH inhibitors against several viruses, such as SARS-CoV-2, Influenza A Virus, Zika Virus, and Ebola Virus. Among these, two inhibitors were selected, S416 and S312: the antiviral activity exerted from DHODHi S312 is approximately 15 times more potent and S416 is approximately 574 times more potent than antiviral activity of Teriflunomide (Xiong *et al.* 2020). Sainas and colleagues have also created a library of compounds inhibitors of the DHODH enzyme; among these, the compound number 4 stands out, the MEDS433, with an extremely low IC50 (1.5 nM) compared to that of brequinar (1.8 nM) and that of teriflunomide (388 nM), both inhibitors of DHODH (Sainas *et al.* 2018).

These findings highlight the potential of targeting DHODH to design and develop antiviral agents endowed with a high genetic barrier to the development of drug resistance, and the ability to target a broad spectrum of viruses, thus enabling a therapeutic approach of newly emerging viruses and contributing to preparedness for unforeseen viral threats (Xiong *et al.* 2020; Sainas *et al.* 2018).

Under normal physiological conditions, cells fulfill their requirement of pyrimidines mainly through the salvage pathways, therefore recycling pre-existing nucleosides from both degradation of intracellular nucleic acids and uptake of extracellular nucleosides. In contrast, in highly metabolically active virus-infected cells, the exceptional need for large pyrimidines pools associated to rapid viral replication cannot be supply sufficiently by nucleotide recycling (Sainas *et al.* 2018; Hahn *et al.* 2020). To keep up with the pyrimidine demand in infected cells, in fact, herpesviruses activate both the *de novo* pyrimidine biosynthetic gene expression and the metabolic flux to UTP (Gribaudo *et al.* 2002). It is therefore reasonable that *de novo* pyrimidine biosynthesis rather than its salvage pathway is more critical for herpesvirus replication, effectively making the rate limiting DHODH enzyme activity crucial for maintaining high levels of viral genome synthesis, and thus ensure efficient viral replication. This data was also confirmed in our lab, since the silencing of DHODH through the use of specific *h*DHODH- siRNA significantly reduced the viral replication of both the Influenza A virus and the Respiratory Syncytial Virus. So, the results above described support the idea that mitochondrial *h*DHODH enzymatic activity is considered a reliable HTA target to develop new broad-spectrum antivirals, also against antigenically different viruses.

Given these premises, we were able to confirm the efficacy of pyrimidines biosynthetic pathway inhibitors by analyzing the antiviral activity of MEDS433, a novel small molecule, representative of a novel class of *h*DHODH inhibitors based on a hydroxypyrazole-pyrimidine scaffold (Sainas *et al.* 2018; Sainas *et al.* 2021).

To further this prospect, we tested a library of DHODH inhibitors against HSV and hCoV-OC43, and, among these compounds, the new *h*DHODH inhibitor MEDS433 carries out a potent dose-dependent antiviral activity. In particular this activity was confirmed against a wide range of DNA viruses (such as HSV-1 and -2) and RNA viruses (such as RSV-A and -B, IAV and IBV, hCoV-OC43, hCoV-229E and SARS-CoV-2), with a mechanism that derives from a selective inhibition of *h*DHODH activity in infected cells. MEDS433 is characterized by the highest inhibitory potency against *h*DHODH (IC50 1.2 nM) and a favorable lipophilicity with a logD7.4 value of 2.35. To this regard, a logD7.4 value of 2.50 has been suggested for optimal inhibition of mitochondrial DHODH, since inhibitors with lower logD7.4 are disadvantaged in reaching the mitochondrial membrane, while higher logD7.4 values may reduce their cellular adsorption (Gradl *et al.* 2019).

Furthermore, this molecule was previously validated as a therapeutic agent against Acute Myeloid Leukemia (AML), acting as a *h*DHODH inhibitor able to restore myeloid differentiation at lower cytotoxic concentrations respectively to those exhibited by

brequinar, the most potent hDHODH inhibitor and, therefore, taken as reference (Sainas *et al.* 2018). Crystallographic studies of MEDS433 in complex with hDHODH then showed that it has a binding mode similar to that of brequinar, inside the ubiquinone binding site of the enzyme (Sainas *et al.* 2018).

Our findings corroborate the feasibility of the pharmacological targeting of hDHODH to control virus replication, as recently observed also for other hDHODH inhibitors, such as brequinar, FA-613, and S312 and S416.

It was proved to directly bind the ubiquinone binding site of the hDHODH enzyme with high specificity, thus reducing the possible off-targeting issues inside the host-cells (Sainas *et al.* 2018). It's probably due to this high affinity, that MEDS433 shows much higher SI values than brequinar against nine It's probably due to this high affinity, that MEDS433 shows much higher SI values than brequinar against nine different viruses in nine different cells lines, including normal human lung MRC5 fibroblasts.

Again, also the optimal lipophilicity of MEDS433 might reduce the possibility of off-targeting effects within host cells, other motivation that could explain the high SI values measured for this hDHODH inhibitor.

All these features of MEDS433 are undoubtedly favorable and contribute to making it a promising candidate for HTA.

However, we were able to add additional awareness to the activity of the compound in perspective of its possible validation as a therapeutic agent. We therefore highlight below several essential points that validate this claim of ours.

As described above, the first point is the high potency of MEDS433 against different viruses, such as Herpesviruses, Coronaviruses, Influenza Viruses, Respiratory Syncytial Viruses, that is not dependent on the cell lines that we used for the experiments. In fact, we performed the antiviral assays of our study with a lot of different cell lines: Madin-Darby Canine Kidney (MDCK), Human Adenocarcinoma Alveolar Basal Epithelial (A549), the Human Lung Adenocarcinoma (Calu-3), the Human lung fibroblasts (MRC5), the Human Colorectal Carcinoma (HCT-8), the African green monkey kidney (Vero), the human Laryngeal Squamous Carcinoma (HEp-2) cells. In addition to the high antiviral activity of MEDS433, also a low level of cytotoxicity is undoubtedly a favorable characteristic of this molecule which, in fact, contributes to making it a promising candidate for the development of a new anti-IV antiviral.

The second important point is that MEDS433 inhibits the replication of several viruses, both DNA (HSV) and RNA (CoV, RSV, IV), and not only within each of these virus families, MEDS433 inhibits the replication of different strains. This fact represents an important

added value of this new *h*DHODH inhibitor, as, in addition to the advantage of overcoming viral drug resistance, it makes MEDS433 interesting for the development of broad-spectrum antiviral agents, as its high antiviral action is not virus/strain dependent.

A new drug, to become a first-line treatment of viral infections, should be suitable for combination treatments that could improve antiviral efficacy and prevent the emergence of drug resistance. In our study, we pleasantly observed an increase in the virus replication reduction in the cells treated with a synergistic combination of MEDS433 and dipyridamole. DPY is a synthetic phosphodiesterase (PDE) inhibitor derivative of pyrimido-pyrimidine, used as antiplatelet aggregation for the prophylaxis of thromboembolism in cardiovascular disease, because inhibit the uptake of adenosine into platelets, endothelial cells and erythrocytes (Liu *et al.* 2020). We used DPY because is able to inhibit the equilibrative nucleoside transporters (ENT) 1 and 2, the most effective cell nucleoside/nucleotide transporter involved in the pyrimidine salvage pathway (Boschi *et al.* 2019). In fact, we demonstrated that the same combination was necessary to protect the antiviral efficacy of DHODH inhibitor following activation of pyrimidine salvage pathway caused by the presence of uridine. The addition of the nucleotide reduced the beneficial effects achieved by MEDS433 and it's important to remember that the circulating levels of uridine in humans are between 2 and 9 µM, so we used a concentration a little bit higher of uridine (20 µM) than the physiological one (Coelho *et al.* 2020). Knowing that the C_{max} of dipyridamole clinically achievable in patient treated with this molecule cannot overcome the 4.6 µM, we tested the combination of increasing MEDS433 concentrations together with a fixed of DPY concentration (3 µM) and we demonstrated that this combination restored the antiviral effect of MEDS433, despite the presence of uridine in the medium to mimic the physiological condition. Additionally, at 5 µM DPY, the compounds showed an even greater action in slowing down the viral replicative rescue. This discovery was relevant, as uridine is present in physiological conditions in human plasma and it could have reduced the action of MEDS433 making it unusable as an antiviral drug *in vivo*. Accordingly to results obtained from HSV, Coronaviruses, IV and RSV studies, we confirmed that dipyridamole, at human tolerated doses, could synergistically work with MEDS433 in order to increase the potential antiviral action of the inhibitor and to decrease the replicative rescue entailed by uridine addition in the cell medium in experiment *in vitro*.

Another discovery that deserves further comment is the observation that different combinations of MEDS433 and DAA currently in clinical use against the viruses we tested, such as Acyclovir, Ribavirin, Remdesivir, EIDD1931, interact synergistically, strengthening each other's antiviral activity against viruses. In the case of HSV, to our knowledge, this was

one of the first observations of a synergistic effect between a direct-acting antiviral agent used to treat infections caused by DNA viruses and a DHODH inhibitor. While, in the case of RNA viruses it had already been observed, such as the Junín arenavirus causing Argentine hemorrhagic fever, it was reported that the combination of A771726, the active metabolite of the *h*DHODH inhibitor leflunomide approved by the FDA for the treatment of rheumatoid arthritis and autoimmune diseases (Sanders *et al.* 2002) and ribavirin showed significantly more potent antiviral activity than either single drug treatment (Sepulveda *et al.* 2018).

The possibility of exploiting combinations between DAA and agents that act on the pyrimidine pathway against viral infections is relevant, it is possible to have in mind a regimen based on three different molecules: the direct-acting agent, the DHODH inhibitor and DPY. As we observed in our studies, in fact DPY not only restores the antiviral efficacy of the DHODH inhibitor which could be abolished by the absorption of exogenous pyrimidines from the bloodstream, but also strengthens the synergism between the DAA tested (ACV-RBV-EIDD1931) and MEDS433 against the HSV, RSV and Coronaviruses, respectively.

Obviously, to validate our hypothesis, future investigations on animal models will be needed, as our data are based exclusively on tests carried out *in vitro*, but this combination could represent a therapeutic plan to reduce the onset of resistance against DAAs and to reduce side effects caused by individual drugs administered at higher doses.

A noteworthy point from our latest study on MEDS433 against RSV concerns the ability of MEDS433 to stimulate the expression of ISG proteins that hinder RSV replication. Although it has been previously reported that DHODH inhibitors induce the expression of ISGs (Lucas-Hourani *et al.* 2013; Cheung *et al.* 2017; Luthra et al. 2018), this is the first observation, to our knowledge, that an inhibitor of *h*DHODH stimulates the expression of antiviral ISG proteins, such as IFI6, IFITM1, and RF7, which has been observed to reduce RSV replication when expressed in isolation (McDonald *et al.* 2016; Smith *et al.* 2019). Our results therefore functionally support the hypothesis that the antiviral activity of DHODH inhibitors is based both on pyrimidine depletion which arrests the activity of viral polymerases, and on the induction of protein effectors of the innate antiviral response (Lucas-Hourani *et al.* 2013). Although the mechanisms underlying the activation of ISGs following inhibition of pyrimidine biosynthesis remain well defined, it has been hypothesized that cellular stress associated with nucleoside deprivation favors the expression of ISGs which, in turn, contribute to the establishment of an antiviral state towards RNA virus infections (Zheng *et al.* 2022). In this regard, different ISG activation pathways have been suggested for different DHODH inhibitors (Zheng *et al.* 2022), as dependence on type

I IFN production has been reported for FA613 (Cheung *et al.* 2017), while an IFN-independent mechanism was observed for DD264, brequinar, and SW385 (Lucas-Hourani *et al.* 2013; Luthra *et al.* 2018). Here, we observed that MEDS433-mediated induction of IFI6, IFITM1, and IRF7 proteins requires the secretion of IFN-β and IFN-λ1, as their neutralization reduces the accumulation of these ISG proteins in MEDS433-treated cells. Interestingly, activation of IRF1, through the DNA damage response kinase ATM, was observed in HEK293T cells for SW385-mediated, IFN-independent stimulation of ISGs (Luthra *et al.* 2018). Although IRF1 was also induced by MEDS433 in HEp-2 cells, the role of this transcription factor in the stimulation of ISGs, in the context of the IFN-dependent mechanism triggered by MEDS433, remains to be defined. However, we observed the ability of MEDS443 to stimulate IRF3 phosphorylation, as an essential step in its activation pathway leading to IFN-β gene transcription and synthesis (Negishi *et al.* 2018). Although further investigations are needed to fully elucidate the mechanisms of IFN-dependent ISG activation by MEDS433 (i.e., activation of transduction pathways upstream of IRF3 phosphorylation), our observations provide new insights towards the development of inhibitors of pyrimidine synthesis to modulate the innate antiviral response.

Moreover, the antiviral effect of MEDS433 against SARS-CoV-2 was also observed not only *in vitro* in a cell culture system, but also in the experimental model of kidney organoids. These organoids are composed of different cell types and model the physiological conditions of the human kidney; thus, they can be used to investigate the effect of SARS-CoV-2 infection on kidney tissues (Garreta *et al.* 2019; Takayama 2020). In this regard, we have previously observed that kidney organoids produce infectious SARS-CoV-2 progeny (Monteil *et al.* 2020). Although a variability of the effect of MEDS433 on SARS-CoV-2 replication in kidney organoids was measured, likely reflecting the complexity and heterogeneity of this experimental model (Garreta *et al.* 2019), the observation of an anti-SARS-CoV-2 activity of MEDS433 even in human organoids is valuable to sustain its preclinical development as a candidate agent for COVID-19.

In addition, MEDS433 was also tested against RSV-A on human pseudostratified mucociliated small airway epithelium model with excellent results already after 48 hours of treatment, underlining that this molecule exerts antiviral activity even in an *ex vivo* model of human respiratory epithelium without shows cytotoxicity.

In conclusion, MEDS433 seems like an excellent candidate as a Broad-Spectrum Antiviral Agent. Its antiviral efficacy against several human viruses and the intrinsic advantage of HTA deriving from the low risk of emergence of drug resistance, make this DHODH inhibitor interesting for the development of new BSAAs, also in the preparation against

future emerging human respiratory viruses, given the independence of its antiviral effects with respect to a specific virus.

5. CONCLUSIONS

In conclusion, this PhD thesis suggests MEDS433 as a new interesting BSAA candidate against several RNA respiratory viruses (Influenza Virus, Respiratory Syncytial Virus, Coronavirus), but also against DNA viruses, such as HSV. This molecule not only exerts a very potent antiviral activity with low cytotoxicity, but is also predisposed to combination regimens with both nucleoside analogues and other anti-pyrimidines, such as RBV and DPY. Furthermore, its mechanism of action is not only linked to blocking the synthesis of pyrimidines, but is capable of triggering the protein effectors of the innate antiviral response. MEDS433 also exerts potent antiviral activity in ex vivo systems, not just *in vitro*. These characteristics of MEDS433, combined with its valuable drug-like profile, now warrant further studies to evaluate its efficacy in preclinical animal models of virus infection.

6. REFERENCES

6.1   Bibliography

Ambrosio F.A., Costa G., Romeo I., Esposito F., Alkhatib M. et al. Targeting SARS-CoV-2 main protease: a successful story guided by an *in silico* drug repurposing approach.

Andersen P.I., Ianevski A., Lysvand H., Vitkauskiene A., Oksenych V. et al. Discovery and development of safe-in-man broad-spectrum antiviral agents. *International Journal of Infectious Disease* 2020, 93: 268-276. https://doi.org/10.1016/j.ijid.2020.02.018

Bekker L.G., Beyrer C., Mgodi N., Lewin S.R., Delany-Moretlwe S. et al. HIV infection. *Nature Reviews disease primers* 2023, 9:42. https://doi.org/10.1038/s41572-023-00452-3

Boschi D., Pippione A.C., Sainas S., Lolli M.L. Dihydroorotate dehydrogenase inhibitors in anti-infective drug research. *European Journal of Medicinal Chemistry* 2019, 183: 111681. https://doi.org/10.1016/j.ejmech.2019.111681

Cachay E.R. Antiretroviral Treatment of Human Immunodeficiency Virus (HIV) Infection. *MSD Manual* 2023.

Cheung N.N., Lai K.K., Dai J., Kok K.H., Chen H. et al. Broad-spectrum inhibition of common respiratory RNA viruses by a pyrimidine synthesis inhibitor with involvement of the host antiviral response. *Journal of General Virology* 2017, 98: 946-954. https://doi.org/10.1099/jgv.0.000758

Chitalia V.C., Munawar A.H. A painful lesson from the COVID-19 pandemic: the need for broad-spectrum, host-directed antivirals. *Journal of Translational Medicine* 2020, 18: 390. https://doi.org/10.1186/s12967-020-02476-9

Coelho A.R., Oliveira P.J. Dihydroorotate dehydrogenase inhibitors in SARS-CoV-2 infection. *European Journal of Clinical Investigation* 2020, 50 (10): 13366. https://doi.org/10.1111/eci.13366

Debing Y., Neyts J., Delang L. The future of antivirals: broad-spectrum inhibitors. *Current Opinion in Infectious Diseases* 2015, 28: 596-602. https://doi.org/10.1097/QCO.0000000000000212

El Sayed K.A. Natural products as antiviral agents. *Studies in Natural Products Chemistry* 2000, 24: 473-572. https://doi.org/10.1016%2FS1572-5995(00)80051-4

Esposito F., Sechi M., Pala N., Sanna A., Koneru P.C. at al. Discovery of dihydroxyindole-2-carboxylic acid derivatives as dual allosteric HIV-1 Integrase and Reverse Transcriptase associated Ribonuclease H inhibitors. *Antiviral Research* 2020, 174: 104671. https://doi.org/10.1016/j.antiviral.2019.104671

Garreta E., Prado P., Tarantino C., Oria R., Fanlo L. et al. Fine tuning the extracellular environment accelerates the derivation of kidney organoids from human pluripotent stem cells. *Nature Materials* 2019, 18: 397-405. https://doi.org/10.1038/s41563-019-0287-6

GBD 2017 Disease and Injury Incidence and Prevalence Collaborators. Global, regional, and national incidence, prevalence, and years lived with disability for 354 diseases and injuries for 195 countries and territories, 1990–2017: a systematic analysis for the Global Burden of Disease Study 2017. *Lancet* 2018, 392: 1789–858. https://doi.org/10.1016/S0140-6736(18)32279-7

Geraghty R.J., Aliota M.T., Bonnac L.F. Broad-Spectrum Antiviral Strategies and Nucleoside Analogues. *Viruses* 2021, 13: 667. https://doi.org/10.3390/v13040667

Gradl S.N., Mueller T., Ferrara S., El Sheikh S., Janzer A. et al. Discovery of BAY 2402234 by phenotypic screening: A human Dihydroorotate Dehydrogenase (DHODH) inhibitor in clinical trials for the treatment of myeloid malignancies. *Cancer Research* 2019, 79: 2. https://doi.org/10.1158/1538-7445.AM2019-2

Gribaudo G., Riera L., Rudge T.L., Caposio P., Johnson L.F. et al. Human cytomegalovirus infection induces cellular thymidylate synthase gene expression in quiescent fibroblasts. *Journal of General Virology* 2002, 83: 2983-2993. https://doi.org/10.1099/vir.0.18979-0

Haake C., Cook S., Pusterla N., Murphy B. Coronavirus Infections in Companion Animals: Virology, Epidemiology, Clinical and Pathologic Features. *Viruses* 2020, 12:1023. https://doi.org/10.3390/v12091023

Hahn F., Wangen C., Hage S., Peter A.S., Dobler G. IMU-838, a Developmental DHODH Inhibitor in Phase II for Autoimmune Disease, Shows Anti-SARS-CoV-2 and Broad-Spectrum Antiviral Efficacy In Vitro. *Viruses* 2020, 12(12): 1394. https://doi.org/10.3390/v12121394

Hodinka R.L. Respiratory RNA Viruses. *Microbiology Spectrum* 2016, 4(4): DMIH2-0028-2016. https://doi.org/10.1128/microbiolspec.dmih2-0028-2016

Hoffmann H.H., Kunz A., Simon V.A., Palese P., Shaw M.L. Broad-spectrum antiviral that interferes with de novo pyrimidine biosynthesis. *PNAS* 2011, 108 (14): 5777-5782. https://doi.org/10.1073/pnas.110114310

Ianevski A., Zusinaite E., Kuivanen S., Strand M., Lysvand H. et al. Novel activities of safe-in-human broad-spectrum antiviral agents. *Antiviral Research* 2018, 154: 174-182. https://doi.org/10.1016/j.antiviral.2018.04.016

Jain H., Schweitzer J.W., Justice N.A. Respiratory syncytial virus infection. *StatPearls [Internet]* 2023, Treasure Island (FL). StatPearls Publishing. Bookshelf ID: NBK459215

Ji X., Li Z. Medicinal chemistry strategies toward host targeting antiviral agents. *Medicinal Research Reviews* 2020, 40: 1519-1557. https://doi.org/10.1002/med.21664

Krammer F., Smith G.J.D., Fouchier R.A.M., Peiris M., Kedzierska K. et al. Influenza. *Nature Reviews disease primers* 2018, 4: 3. https://doi.org/10.1038/s41572-018-0002-y

Liu Q., Gupta A., Okesli-Armlovich A., Qiao W., Fischer C.R. Enhancing the Antiviral Efficacy of RNA-Dependent RNA Polymerase Inhibition by Combination with Modulators of Pyrimidine Metabolism. *Cell Chemical Biology* 2020, 27(6): 668-677. https://doi.org/10.1016/j.chembiol.2020.05.002

Luban J., Sattler R.A., Muhlberger E., Graci J.D., Cao L. The DHODH inhibitor PTC299 arrests SARS-CoV-2 replication and suppresses induction of inflammatory cytokines. *Virus Research* 2021, 292: 15. https://doi.org/10.1016/j.virusres.2020.198246

Lucas-Hourani M., Dauzonne D., Jorda P., Cousin G., Lupan A. et al. Inhibition of Pyrimidine Biosynthesis Pathway Suppresses Viral Growth through Innate Immunity. *Plos Pathogens* 2013, 9: e1003678. https://doi.org/10.1371/journal.ppat.1003678

Luthra P., Naidoo J., Pietzsch C.A., De S., Khadka, S. et al. Inhibiting pyrimidine biosynthesis impairs Ebola virus replication through depletion of nucleoside pools and activation of innate immune responses. *Antiviral Research* 2018, 158: 288–302. https://doi.org/10.1016/j.antiviral.2018.08.012

Maffei M., Salata C., Gribaudo G. Tackling the Future Pandemics: Broad-Spectrum Antiviral Agents (BSAAs) Based on A-Type Proanthocyanidins. *Molecules* 2022, 27:8353. https://doi.org/10.3390/ molecules27238353

McDonald J.U., Kaforou M., Clare S., Hale C., Ivanova M. et al. A simple screening approach to prioritize genes for functional analysis identifies a role for Interferon Regulatory Factor 7 in the control of respiratory syncytial virus disease. *mSystems* 2016, 1: e00051-16. https://doi.org/10.1128/mSystems.00051-16.

Mercorelli B., Luganini A., Nannetti G., Tabarrini O., Palù G. et al. Drug Repurposing Approach Identifies Inhibitors of the Prototypic Viral Transcription Factor IE2 that Block Human Cytomegalovirus Replication. *Cell Chemical Biology* 2016, 23: 340-351. http://dx.doi.org/10.1016/j.chembiol.2015.12.012

Mercorelli B., Palù G., Loregian A. Drug Repurposing for Viral Infectious Diseases: How Far Are We? *Trends in Microbiology* 2018, 26: 865. https://doi.org/10.1016/j.tim.2018.04.004

Monteil V., Kwon H., Prado P., Hagelkrüys A., Wimmer R.A. et al. Inhibition of SARS-CoV-2 Infections in Engineered Human Tissues Using Clinical-Grade Soluble Human ACE2. *Cell* 2020, 181 (4): P905-913. https://doi.org/10.1016/j.cell.2020.04.004

Negishi H., Taniguchi T., Yanai H. The interferon (IFN) class of cytokines and the IFN Regulatory Factor (IRF) transcription factor family. *Cold Spring Harbor Perspectives in Biology* 2018, 10: a028423. https://doi.org/10.1101/cshperspect.a028423.

Okesli A., Khosla C., Bassik M.C. Human pyrimidine nucleotide biosynthesis as a target for antiviral chemotherapy. *Current Opinion in Biotechnology* 2017, 48: 127-134. http://dx.doi.org/10.1016/j.copbio.2017.03.010

Pavan M., Bolcato G., Bassani D., Sturlese M., Moro S. Supervised Molecular Dynamics (SuMD) Insights into the mechanism of action of SARS-CoV-2 main protease inhibitor PF-07321332. Journal of Enzyme Inhibition and Medical Chemistry 2021, 36: 1645-1649. https://doi.org/10.1080/14756366.2021.1954919

Reis R.A.G., Calil F.A., Feliciano P.R., Pinheiro M.P., Nonato M.C. The dihydroorotate dehydrogenases: Past and present. *Archives of Biochemistry and Biophysics* 2017, 632: 175-191. http://dx.doi.org/10.1016/j.abb.2017.06.019

Sainas S., Pippione A.C., Lupino E., Giorgis M., Circosta P. et al. Targeting Myeloid Differentiation Using Potent 2-Hydroxypyrazolo[1,5-a]pyridine Scaffold-Based Human Dihydroorotate Dehydrogenase Inhibitors. *Journal of Medicinal Chemistry* 2018, 61: 6034-6055. https://doi.org/10.1021/acs.jmedchem.8b00373

Sainas, S., Giorgis, M., Circosta, P., Gaidano, V., Bonanni, D. et al. Targeting Acute Myelogenous Leukemia Using Potent Human Dihydroorotate Dehydrogenase Inhibitors Based on the 2-Hydroxypyrazolo[1,5-a]pyridine Scaffold: SAR of the Biphenyl Moiety. *Journal of Medicinal Chemistry* 2021, 64: 5404-5428. https://doi.org/10.1021/acs.jmedchem.0c01549

Sanders S., Harisdangkul V. Leflunomide for the Treatment of Rheumatoid Arthritis and Autoimmunity. *The American Journal of the Medical Sciences* 2002, 323 (4): 190-193. https://doi.org/10.1097/00000441-200204000-00004

Sepùlveda C.S., Garcìa C.C., Damonte E.B. Antiviral activity of A771726, the active metabolite of leflunomide, against Junín virus. *Journal of Medical Virology* 2018, 90: 819-827. https://doi.org/10.1002/jmv.25024

Sepùlveda C.S., Garcìa C.C., Damonte E.B. Inhibitors of Nucleotide Biosynthesis as Candidates for a Wide Spectrum of Antiviral Chemotherapy. *Microorganisms* 2022, 10: 1631. https://doi.org/10.3390/ microorganisms10081631

Simoes, E.A.F., Madhi, S.A., Muller, W.J., Atanasova, V., Bosheva, M. et al. Efficacy of nirsevimab against respiratory syncytial virus lower respiratory tract infections in preterm and term infants, and pharmacokinetic extrapolation to infants with congenital heart disease and chronic lung disease: a pooled analysis of randomised controlled trials. *Lancet Child Adolescent Health* 2023, 7: 180–189. https://doi.org/10.1016/S2352-4642(22)00321-2

Smith S.E., Busse D.C., Binter S., Weston S., Diaz Soria C. et al. Interferon-Induced Transmembrane Protein 1 restricts replication of viruses that enter cells via the plasma membrane. *Journal of Virology* 2019, 93: e02003-e02018 https://doi.org/10.1128/JVI.02003-18

Soni A., Kabra S.K., Lodha R. Respiratory Syncytial Virus infection: an update. *Indian Journal of Pediatrics* 2023, 90: 1245:1253. https://doi.org/10.1007/s12098-023-04613-w

Takayama K. *In Vitro* and Animal Models for SARS-CoV-2 research. *Trends in Pharmacological Sciences* 2020, 41(8): p513-517. https://doi.org/10.1016/j.tips.2020.05.005

Taveira N. Antivirals and Vaccines. *International Journal of Molecular Sciences* 2023, 24: 10315. https://doi.org/10.3390/ ijms241210315

Tripp R.A., Jorquera P.A. Human Respiratory Syncytial Virus: Methods and Protocols. *Methods in Molecular Biology*, 2016. http://dx.doi.org/10.1007/978-1-4939-3687-8

Whitley R.J., Roizman B. Herpes Simplex Virus Infections. *Lancet* 2001, 9267:1513-1518. https://doi.org/10.1016/S0140-6736(00)04638-9

Xiong R., Zhang L., Li S., Sun Y., Ding M. et al. Novel and potent inhibitors targeting DHODH are broad-spectrum antivirals against RNA viruses including newly-emerged coronavirus SARS-CoV-2. *Protein & Cell* 2020. https://doi.org/10.1007/s13238-020-00768-w

Yamauchi Y. Influenza Virus: Methods and Protocols. *Methods in Molecular Biology* 2018. https://doi.org/10.1007/978-1-4939-8678-1

Yamayoshi S., Kawaoka Y. Current and future influenza vaccines. *Nature Medicine* 2019, 25: 212-220. https://doi.org/10.1038/s41591-018-0340-z

Zhang Y., Xu C., Zhang H., Liu G.D., Xue C. et al. Targeting Hemagglutinin: Approaches for Broad Protection against the Influenza A Virus. *Viruses* 2019, 11: 405. https://doi.org/10.3390/v11050405

Zheng Y., Li S., Song K., Ye J., Li W. et al. A Broad Antiviral Strategy: Inhibitors of Human DHODH Pave the Way for Host-Targeting Antivirals against Emerging and Re-Emerging Viruses. *Viruses* 2022, 14: 928. https:// doi.org/10.3390/v14050928

6.2   Sitography

AIFA. Updates on drugs compared to the articles cited. https://www.aifa.gov.it/documents/20142/1123276/remdesivir_18.09.2020.pdf (accessed 10 December 2023).

CDC. RSV Surveillance & Research. https://www.cdc.gov/rsv/research/index.html (accessed 10 December 2023).

ECDC. European Centre for Disease Prevention and Control. https://www.ecdc.europa.eu/en (accessed 10 December 2023).

EMA. European Medicines Agency, Science Medicines Health. https://www.ema.europa.eu/en/human-regulatory-overview/public-health-threats/coronavirus-disease-covid-19/covid-19-medicines (accessed 31 January 2024).

FDA. Food and Drug Administration. https://www.fda.gov/consumers/consumer-updates/know-your-treatment-options-covid-19 (accessed 31 January 2024).

US AID. Avian Influenza and its Global Implications. https://web.archive.org/web/20080815071811/http://www.usaid.gov/about_usaid/acvfa/intro_ai.pdf (accessed 10 December 2023).

White House Archive. National Strategy for Pandemic Influenza. https://web.archive.org/web/20090111210653/http://www.whitehouse.gov/homeland/nspi.pdf (accessed 10 December 2023).

WHO. Informations on viruses: health topics, surveillance program and trends in the spread of viruses. https://www.who.int (accessed 10 December 2023).

7. ACKNOWLEDGMENTS